Investigating the functions of the c-Jun and JunB transcription factors in classical Hodgkin Lymphoma

by

Jing Xi Zhang

A thesis submitted in partial fulfillment of the requirements for the degree of

Master of Science
in
Immunology

Department of Medical Microbiology and Immunology
University of Alberta

ABSTRACT

Classical Hodgkin lymphoma (cHL) is characterized by the presence of abnormal mononuclear Hodgkin and multinuclear Reed-Sternberg (HRS) cells, which are thought to be derived from clonally expanded germinal center B cells. The tumour cells have been demonstrated to have various signalling pathways being dysregulated to promote cell proliferation and survival. Among the deregulated pathways, the activator protein-1 (AP-1) signalling pathway, which consists of a family of transcription factors has been implicated in promoting cell proliferation and is involved in regulating immune evasion in cHL. However, very few studies have been conducted on the specific role of each AP-1 member, particularly the two aberrantly expressed AP-1 proteins, c-Jun and JunB, in the pathogenesis of cHL.

We used a shRNA-mediated gene silencing approach to specifically knock down c-Jun and JunB protein in cHL cell lines and examined the effect on proliferation and apoptosis. We found that knocking down either protein reduced proliferation rate and resulted in a prolonged G_0/G_1 phase compared to control shRNA-expressing cells. Moreover, knocking down c-Jun or JunB did not significantly affect the apoptosis rate in cHL cell lines. We further examined their function in tumour growth *in vivo* and observed a similar smaller tumour formed with cells expressing either c-Jun or JunB shRNA compared to control group. Interestingly, the c-Jun and JunB knockdown cells within cell lines shared similarities in proliferation and cell cycle defect suggesting the two AP-1 proteins may have some similar functions in cHL. In addition, we examined the transcriptional profile of the two AP-1 proteins by doing microarrays in order to understand the cellular function

of c-Jun and JunB in cHL. We found the two proteins shared many common targets within each cell line and they influenced many genes involved in inflammatory response, proliferation, and apoptosis. The results of this study provide insight into the genes and cellular functions regulated by c-Jun and JunB in cHL and the increased knowledge of the roles of these proteins may eventually lead to the development of novel targets for treatment.

PREFACE

The project in this thesis was undertaken under the supervision of Dr. Robert J. Ingham

Chapter 3

All experiments in this chapter were performed by J.X. Zhang. Joyce Wu assisted with the mice experiments (Figure 3.9). Anton Savin repeated some of the growth curve experiments (Figure 3.2F & H) and the restoration experiment (Figure 3.11). A portion of this chapter is part of a manuscript in preparation (written together with Dr. Robert J. Ingham and Joyce Wu). All mouse experiments were approved by the University of Alberta Animal Care and Use Committee and followed protocol (AUP# 393).

Chapter 4

All experiments in this chapter were performed by J.X. Zhang. Joyce Wu and Dr. Robert J. Ingham assisted with c-Jun#4 validation experiments (Figure 4.6). Joyce Wu and Anton Savin also repeated some targets validation experiments (Figures 4.4-4.5). Dr. Konrad Famulski assisted with the microarray analysis.

ACKNOWLEDGMENTS

Firstly, I would like to thank my supervisor, Dr. Robert Ingham, for mentoring me over the past 3.5 years. He had made a welcoming and comforting training environmental since I started my project. Especially I would like to thank his generosity and understanding during the time I had family issues. Next, I would like to thank my supervisory committee, Drs. Troy Baldwin and Jim Smiley for all of their inputs and suggestions on my research.

I would also like to thank the past and present Ingham lab members. Particularly Dr. Joel Pearson who taught me many skills when I first started in the lab. I would also like to thank Joyce Wu who had been a great labmate during these years and had helped with my project, particularly during the time I was away for family matters. I am also thankful to many professional staffs who have helped with various aspects of my project, in particular Dr. Julinor Bacani for helping with analyzing tumours from xenograft experiments, Dr. Andrea Holmes for helping with flow cytometry, Dr. Konrad Famulski for his technical supports on microarray analysis and HSLAS staff for helping with mice work, as well as members of the Baldwin lab for providing suggestions and comments during lab meetings.

Finally, I want to thank all of my family. My mom and dad have devoted a lot of effort and time during my education years and showed great support when I decided to come to University of Alberta for graduate study. I would also like to thank my relatives and friends for giving a lot of happiness over these years.

Table of Contents

ABSTRACT ii
PREFACE iv
ACKNOWLEDGMENTS v
LIST OF TABLES x
LIST OF FIGURES xi
LIST OF ABBERATIONS xiii
CHAPTER 1: INTRODUCTION 1
1.1: Classical Hodgkin Lymphoma (cHL) 2
1.1.1 Identification and clinical features of cHL 2
1.1.2 Cellular Morphology and phenotype 3
1.1.3 Reprogramming of gene expression 4
1.1.4 classical Hodgkin lymphoma microenvironment 6
1.1.5 Dysregulated transcription network in cHL 12
1.2: c-Jun and JunB transcriptional factors 18
1.2.1 AP-1 family transcriptional factors 18
1.2.3 c-Jun in cell proliferation, apoptosis and transformation 22
1.2.4 JunB in cell proliferation, apoptosis and transformation 24
1.2.5 Regulation and function of c-Jun and JunB in cHL 25
1.3: Hypothesis and Thesis objectives 31
CHAPTER 2: MATERIALS AND METHODS 33
2.1: Cell lines 34
2.2: Generating stable shRNA-expressing cell lines using lentiviral transduction 35
2.2.1 Generating lentiviral particles 35
2.2.2 Lentiviral titration 37
2.2.3 Infecting cHL cell lines with lentiviral particles 37
2.3: Protein methods 38
2.3.1 Cell lysis 38
2.3.2 Protein quantification and normalization using the bicinchoninic acid (BCA) assay 38

2.3.3 Western blotting 39
2.3.4 Analysis of CD48 protein expression by flow cytometry 40
2.4: RNA methods 41
2.4.1 RNA isolation 41
2.4.2 DNA digestion and reverse transcription 42
2.4.3 PCR analysis of cDNA 43
2.4.4 qRT-PCR 43
2.5: DNA methods 47
2.5.1 DNA isolation 47
2.5.2 PCR analysis of DNA 47
2.5.3 PCR purification and sequencing 47
2.5.4 Short Tandem Repeats (STR) profiling 48
2.6: Growth assays 48
2.6.1 Growth curves 48
2.6.2 Resazurin assays 49
2.6.3 Cell cycle analysis 49
2.6.4 Nocodazole experiments 50
2.7: Estimation of cell cycle stage duration 50
2.7.1 Calculation of doubling time 50
2.7.2 Calculation of time spent in each cell cycle stage 51
2.8: Apoptosis analysis using terminal deoxynucleotidyl transferase dUTP nick end labeling (TUNEL) 51
2.9: Xenograft experiments 52
2.10: Microarray experiments and analyses 52
2.10.1 Microarray experiments 52
2.10.2 Gene ontology analysis using DAVID 53
2.11: Statistical analyses 54
CHAPTER 3: C-JUN AND JUNB REGULATE PROLIFERATION BY INFLUENCING CELL CYCLE PROGRESSION PRIMARILY AT THE G_0/G_1 PHASE IN CHL CELL LINES 55
3.1: Introduction 56
3.2 c-Jun and JunB protein levels are significantly elevated in cHL cell lines compared to Burkitt lymphoma. 56

3.3 Knocking down c-Jun or JunB expression reduces cHL cell growth rate... 59
3.4 Knocking down c-Jun or JunB expression with a second shRNA resulted a similar slow growth phenotype in cHL cell lines. ... 62
3.5. c-Jun and JunB knockdown minimally affects spontaneous apoptosis rate in cHL ... 64
3.6 Knocking down c-Jun or JunB altered the cell cycle status of cHL cell lines. ... 67
3.7 Knocking down c-Jun or JunB with a second shRNA showed a similar defect in the cell cycle distribution ... 71
3.8 Comparing the two L-428 cell lines ... 73
3.9 Knockdown cells require longer time to progress through G_0/G_1 to enter S phase after nocodazole block at G_2/M. ... 77
3.10 Knocking down c-Jun or JunB impaired L-428 tumour cell growth *in vivo* ... 80
3.11 c-Jun and JunB double knockdown cells had a similar slow growth rate as single knockdown cells ... 83
3.12 c-Jun was up-regulated in JunB knockdown cells over time ... 86
3.13 Discussion ... 88
3.13.1 Summary of findings ... 88
3.13.2 Comparing our cell cycle results with published data and future directions for unveiling the cell cycle defect associated with c-Jun/JunB knockdown. ... 89
3.13.3 Limitations of study and unresolved issues ... 90
5.13.4 Conclusions ... 94
CHAPTER 4: EXAMINING CHANGES IN TRANSCRIPTIONAL PROFILE IN C-JUN AND JUNB KNOCKDOWN CHL CELL LINES BY MICROARRAY STUDIES ... 95
4.1 Introduction ... 96
4.2 c-Jun/JunB-dependent gene profiling in L-428 (Amin) and KM-H2 cells . 97
4.3 c-Jun and JunB share many common dysregulated genes within each cell line ... 102
4.4 Functional analysis of differentially expressed genes ... 104
4.5 Examining selected down-regulated genes ... 108
4.6 Examining selected up-regulated genes ... 111
4.7 Examining c-Jun-regulated genes in c-Jun#4 knockdown cells ... 116

4.8 L-428 (Amin) targets were similarly regulated in L-428 (DSMZ) cells ... 118
4.9 Discussion ... 120
4.9.1 Summary of findings ... 120
4.9.2 Inconsistency of $p21^{Cip1}$ regulation with different c-Jun shRNAs ... 121
4.9.3 GO annotation reveals many important c-Jun/JunB function in cHL pathogenesis ... 121
4.9.4 Limitations of GO annotation and microarray approaches ... 124
4.9.4 Some previously known c-Jun/JunB targets are missing from our microarray results ... 125
4.9.5 Conclusion ... 126
CHAPTER 5: GENERAL DISCUSSION AND FUTURE DIRECTIONS ... 127
5.1 Summary of findings ... 128
5.2 Potential targets involved in the delay in G_0/G_1 progression in cHL knockdown cells ... 128
5.3 Comparing the function of c-Jun and JunB in regulating proliferation and apoptosis amongst other CD30 positive lymphomas ... 130
5.4 Future work to solve the shRNA problems ... 132
5.5 Redundancy between c-Jun and JunB in cHL cell lines ... 134
5.6 Future directions for examining c-Jun/JunB-regulated candidate genes identified by microarray and their application to clinical studies ... 138
5.7 Conclusions ... 140
REFERENCES ... 141
APPENDICES ... 166
Appendix 1: c-Jun and JunB shRNA targeting sequence ... 167
Appendix 2: Additional shRNA tested ... 170
Appendix 3: STR report ... 172
Appendix 4: Complete list of differentially expressed genes (>1.5-fold change) ... 174
Appendix 5: Common regulated genes ... 192
Appendix 6: Gene Ontology analysis of differentially expressed genes ... 197
Appendix 7: Knockdown of c-Jun and JunB by siRNAs ... 214

LIST OF TABLES

Table 2.1: shRNA used in transduction 36
Table 2.2: Primary antibodies used in western blotting and flow cytometry 41
Table 2.3: List of primer sequences used in PCR 45
Table 2.4: List of primer sequences used in qRT-PCR..... 46
Table 4.1: Gene ontology analysis of differentially expressed genes..... 105
Table 4.2: Summary of fold change of selected genes from microarray and qRT-PCR experiments. 114
Appendix 4: Complete list of differentially expressed genes (>1.5-fold change)……174
Appendix 5: Common regulated genes……192
Appendix 6: List of genes in the top 10 Annotation clusters……...197

LIST OF FIGURES

Figure 1.1 - Microenvironment of cHL 10
Figure 1.2 - Dysregulated signalling pathways in HRS cells 16
Figure 1.3 - Structure of c-Jun and JunB 21
Figure 1.4 - Regulation of c-Jun and JunB transcription in cHL..... 28
Figure 3.1 - Expression of c-Jun and JunB amongst different lymphoma cell lines. 58
Figure 3.2 - Effect of knocking down c-Jun or JunB on cHL cell growth..... 61
Figure 3.3 - Knockdown of c-Jun or JunB with a second shRNAs resulted in reduced growth rate..... 63
Figure 3.4 - Knocking down c-Jun or JunB has minimal effect on spontaneous apoptosis rate. 65
Figure 3.5 - c-Jun or JunB knockdown cells have a deregulated cell cycle with a common prolonged G_0/G_1 phase..... 69
Figure 3.6 – Knocking down c-Jun or JunB with another shRNA resulted in a similar cell cycle profile as the first shRNAs 72
Figure 3.7 - L-428 (Amin) and (DSMZ) cell lines comparison..... 75
Figure 3.8 - Cell cycle dysregulation in c-Jun and JunB knockdown L-428 (Amin) cells following nocodozole block at G_2/M..... 79
Figure 3.9 - c-Jun and JunB knockdown impairs the ability of the L-428 (Amin) cHL cell line to form tumours in immunocompromised mice..... 81
Figure 3.10 - Examining the growth defect in L-428 (Amin) double knockdown cells 84
Figure 3.11 - Up-regulation of c-Jun in JunB shRNA-expressing cells. 87
Figure 4.1 – Microarray analysis procedure 99
Figure 4.2 – Identification of genes with altered expression in c-Jun and JunB shRNA–expressing cHL cell lines. 101
Figure 4.3 – Analyzing common targets with Venn diagrams 103
Figure 4.4 - Validation of selected down-regulated genes. 110
Figure 4.5 - Validation of up-regulated genes. 113
Figure 4.6 – Examining c-Jun targets in c-Jun shRNA #4 knockdown cells..... 117

Figure 4.7 – Examining targets in L-428 (DSMZ) cells 119
Figure 5.1 - Possible Models for how c-Jun and JunB could regulate cHL proliferation..... 137
Appendix 1 – Targeting sequence map of shRNA used……. 167
Appendix 2 – Additional JunB shRNA tested…… 170
Appendix 7 – Knockdown of c-Jun and JunB by siRNAs……...214

LIST OF ABBERATIONS

7-AAD	7-amino-actinomycin D
ALCL	Anaplastic Large Cell Lymphoma
AP-1	activator protein 1
aRNA	amplified RNA
BCMA	B cell maturation antigen
BCR	B cell receptor
BrdU	Bromodeoxyuridine
bZIP	basic leucine zipper
CD95L	Fas ligand
CDK	cyclin dependent kinases
ChIP	Chromatin Immunoprecipitation
cHL	classical Hodgkin lymphoma
CML	chronic myeloid leukemia
CRE	cAMP response elements
CTL	Cytotoxic T lymphocyte
DLBCL	diffuse large B cell lymphoma
EBV	Epstein-Barr virus
EMSA	Electrophoretic Mobility Shift Assay
ERK	extracellular signal-related kinase
Gal-1	galectin-1
HRS	Hodgkin and Reed-Sternberg
HL	Hodgkin Lymphoma

IgV	immunoglobulin variable
IKK	inhibitor kappa B kinase
JAK	Janus kinase
LMP1	latent membrane protein 1
LMP2A	latent membrane protein 2A
LTA	lymphotoxin α
MAPK	mitogen activated protein kinase
MEF	mouse embryo fibroblasts
MEK	MAPK/extracellular signal-related kinase
MICA	MHC class I related chain A
NEMO	nuclear factor-kappa B essential modulator
NF-κB	nuclear factor-kappa B
NIK	nuclear factor-kappa B-inducing kinase
NK	Natural killer
NLPHL	nodular lymphocyte-predominate Hodgkin lymphoma
$p21^{Cip1}$	cyclin dependent kinase inhibitor
PD-L1	program death receptor ligand-1
PI3K/AKT	Phosphatidylinositol-3 kinases/AKT
RS	Reed-Sternberg
RTK	receptor tyrosine kinases
SAPE	Streptavidin-Phycoerythrin
shRNA	short-hairpin RNA
STAT	signal transducer and activator of transcription

SOCS	suppressor of cytokine signalling
TACI	transmembrane activator and CAML interactor
TAD	transactivation domain
TAM	tumour associated macrophage
Th2	T helper 2
TNF	tumour necrosis factor
TNFAIP3	TNFα-induced protein 3
TNFR	tumour necrosis factor receptor
TPA	12-O-tetradecanoylphorbol-13-acetate
Treg	regulatory T cells
TUNEL	terminal deoxynucleotidyl transferase dUTP nick end labelling
WHO	World Health Organization
XIAP	X-linked inhibitor of apoptosis

CHAPTER 1: INTRODUCTION

1.1: Classical Hodgkin Lymphoma (cHL)

1.1.1 Identification and clinical features of cHL

Hodgkin lymphoma was first described by Thomas Hodgkin in 1832 as a disease associated with enormous lymph node swelling (1). However, it was not until the beginning of the 1900 when Dorothy Reed and Carl Sternberg independently identified the hallmark cells, which Reed called "peculiar giant cells", that the characteristic of Hodgkin's disease was recognized (2). These "giant cells" were later named Hodgkin cells when they had only one nucleus and Reed-Sternberg (RS) cells when they had multiple nuclei. Because these Hodgkin and Reed-Sternberg (HRS) cells show a distinct morphology and immunophenotype, they are used as a requisite for diagnosis of Hodgkin lymphoma (3). Over the next several decades, people tried to discover the origin of these HRS cells. It is now established that HRS cells are lymphocyte-derived and Hodgkin's disease was renamed Hodgkin lymphoma (HL) by the World Health Organization (WHO) (4). Today, HL is one of the most frequently occurring lymphomas in the Western world, and accounts for 30% of all lymphomas diagnosed with an incidence rate of 3 per 100,000 people in the Western world per year (5). In 2014, there were 990 new cases of HL diagnosed in Canada (6). It has been observed to be more frequent in males than females and has a bimodal age distribution with the first peak incidence occurring in adolescents and young adults, and a second incidence peak in late adulthood (age over 55) (7, 8). HL is currently treated with multi-agent chemotherapy, radiation therapy and/or in combination with hematopoietic stem cell transplantation, and monoclonal antibodies (3). In general, the cure rates for

HL are high, with an overall five year survival rate of 80-85%; however, there is still a 10-30% relapse rate and 5-10% refractory cases (8-10). In addition, patients who achieve long-term survival with conventional treatments have risks of developing heart diseases and secondary neoplasms, including lung cancer and leukemia (11-13). Therefore, there is still a demand for research in developing new treatments in order to avoid long-term side effects.

HL is subdivided into classical Hodgkin lymphoma (cHL) and nodular lymphocyte-predominate Hodgkin lymphoma (NLPHL) based on differences in the morphology of the tumour cells and the composition of the surrounding infiltrates (9). cHL represents 95% of HL and 15% of all lymphomas in developed countries (4, 8, 14) and is further subdivided into nodular sclerosis (~80%), mixed cellularity (~15%), and the less common lymphocyte deplete and lymphocyte-rich Hodgkin lymphoma (9, 15). The percentage and composition of the infiltrates varies between subtypes but in general, the neoplastic cells only accounts for a small percentage of the entire tumour tissue (3, 16).

1.1.2 Cellular Morphology and phenotype

HRS cells are characterized by large horseshoe shaped nuclei with visible nucleolus and moderate amount of cytoplasm (17). HRS cells consistently express the tumour necrosis factor (TNF) family CD30, which is used as a molecular marker for HRS cells (17); however, HRS cells variably express many other markers including markers from dendritic cells, T cell, and B cells (18-21). Due to the highly variable expression patterns of cellular proteins and co-expression of markers of several cell lineages, people had struggled to determine the origin of those tumour

cells. Early immunohistological studies revealed HRS cells might either be related to B cells (more frequently) or T cells (less frequently) (17, 22). By isolating single HRS cells from cHL tissue sections and a subsequent PCR amplification, it is now known that majority of HRS cells are derived from mature germinal center B cells due to the presence of clonally rearranged immunoglobulin variable (IgV) genes and signs of somatic hypermutation (23-26). Only in rare cases (<5%), HRS cells are derived from T cells (27-29). For a long time, people thought the multinucleated RS cells were derived from cell fusions of two different cells (30) due to the presence of other lineage molecules (19, 20) and frequent chromosomal abnormalities (31, 32). However, molecular analysis on primary HRS cells revealed these cells do not carry germline IgH configuration, which argues against the notion of cell fusion with a non-B cell (33). Recently, a time-lapse microscopy analysis and nuclear fluorescence labelling revealed that the RS cells come from mononucleated Hodgkin cells which undergo incomplete cytokinesis and the daughter cells re-fuse together to give rise to the multinucleated cells (34).

In about 40% of cHL cases, the HRS cells are latently infected by Epstein-Barr virus (EBV) and express viral proteins such as EBV latent membrane proteins 1 (LMP1) and 2A (LMP2A) which are thought to increase the risk of disease development and contribute to the pathogenesis of EBV+ cHL (35-38).

1.1.3 Reprogramming of gene expression

Despite their germinal center B cell origin, HRS cells have undergone reprogramming of gene expression which makes them unique among other B cell lymphomas that usually retain B cell phenotypes (39). Many B cell specific genes

are not expressed in HRS cells and some are further inactivated by epigenetic mechanisms (3, 23, 40-42). For example, although the tumour cells possess rearranged IgV, they do not express functional B cell receptor (BCR) on cell surface due to acquisition of deleterious IgV mutations, such as nonsense or frameshift mutations that make the BCR nonfunctional (24). They also show no or reduced expression of multiple B cell transcriptional factors that activate B cell specific genes (43). For example, the transcriptional factor PU.1, which is necessary for B cell development, is repressed in cHL (44) and B cell specific markers including Oct2 and Bob1 are also not expressed in HRS cells (45, 46). Moreover, markers that are usually associated with other hematopoietic lineages are often observed in these cells such as the T cell transcription factor Notch 1 which reduces the expression of many B cell differentiation factors (47, 48). Collectively, the HRS cells show a global loss of B cell phenotype, especially they lack a functional BCR which is necessary for the survival of mature B cells (49). Intriguingly, in contrast to normal mature B cells, HRS cells do not undergo apoptosis in periphery but they proliferate, which raises the question of how HRS cells escape apoptosis and retain proliferation and survive. There are two ways these HRS cells can gain pro-survival and anti-apoptotic signals: 1) interaction with the microenvironment and 2) mutations and alterations of genes and cellular pathways. I will discuss these two mechanisms in more detail below.

1.1.4 classical Hodgkin lymphoma microenvironment

As mentioned above, one of the mechanisms by which HRS cells escape apoptosis and obtain proliferative and survival signals is through interaction with their surrounding non-neoplastic cells in the tumour microenvironment. These cells include lymphocytes, granulocytes, macrophages, mesenchymal stromal cells and fibroblasts (50). They are very important for their two major roles in the pathogenesis of cHL: provision of 1) immune suppression and evasion and 2) growth and survival signals. I will discuss these two aspects below in detail.

1.1.4.1 Immune suppression and evasion

One important mechanism HRS cells use to evade host immune response is to establish a T helper 2 (Th2) polarized immunosuppressive environment by inducing regulatory T (Treg) and Th2 cells and inhibiting cytotoxic T lymphocytes (CTLs) and natural killer (NK) cells. For example, HRS cells specifically recruit Th2 cells and Treg cells by producing chemokines such as CCL17 (19, 51), CCL5, CCL22 (52) and IL-7 (53). In vitro co-culture experiment showed cHL cell lines alone can induce the differentiation of naïve T cells to Treg cells (54). Treg cells are important for abrogating CTLs or NK cells by secreting inhibitory cytokines IL10 and TGF-β (55) and expressing CD137 (56). IL10 (57) and TGF-β (58, 59) produced by Tregs and HRS cells can inhibit CTL activation, down modulate Th1 responses and induce differentiation of naïve $CD4^+$ T cells into Tregs that further supports the immunosuppressive environment (50, 60). CD137 is ectopically expressed on HRS cells and can down-regulate CD137 ligand in the target cells (eg. CTLs) to reduce T cell activation (56). Besides Tregs, another cell type that has drawn researchers'

attention recently in the process of immune evasion, is the macrophage. Gene profiling and immunohistochemistry studies demonstrated a tumour promoting role of the tumour associated macrophage (TAM) in the cHL microenvironment (61, 62). Recently, Tudor *et al* demonstrated supernatants of cHL cell lines can induce macrophages to a immunomodulatory M2 phenotype (63) which secretes the MIF cytokine to block the CTL-mediated anti-tumour response (64, 65).

Although there is a significant amount of evidence supporting a Th2 dominate phenotype in cHL (55, 66), new evidence has emerged that showed a Th1 dominant environment with a central memory T cell phenotype and capable of producing Th1 cytokines such as IFN-γ and TNF-α (67). Thus the composition of the cHL microenvironment still needs further investigation. Clinical studies allude to a correlation of EBV infection with a Th1 proinflammatory profile (68), suggesting the nature of the cHL microenvironment may depend on the EBV state of disease. Nonetheless, both EBV+ and EBV- tumour cells have several mechanisms to suppress cytotoxic effectors cells.

One of the mechanisms to escape immune surveillance is by downregulation of antigen presentation. HRS cells down-regulate HLA class I molecules to evade immune recognition and attack (69-72). In contrast, the non-classical HLA class I molecule, HLA-G, is up-regulated to inhibit NK cell activation by engaging with the inhibitory receptor KIR2DL4 on NK cells (73). Another way to escape immune recognition is the release of soluble ligands such as MHC class I related chain A (MICA) and BAG6 to shed the activating receptor NKG2D and NKp30 respectively. NKG2D and NKp30 are found on CTLs and NK cells and by shedding

these receptors, HRS cells can impair cytolytic activity of CTLs and NK cells (71, 74, 75). Moreover, TGF-β produced by HRS cells at tumour sites can down-regulate expression of the NKG2D receptor and further impair the recognition and anti-tumour activity of cytotoxic effector cells (75-77).

HRS cells have been shown to overexpress several surface molecules to either induce apoptosis of CTLs or inactivate immune cells. For example, they express high levels of Fas ligand (CD95L) that when engaged with CD95 on CTLs, can induce apoptosis of CTLs (78-80). Similarly, HRS cells also express immunosuppressive molecules such as program death receptor ligand-1 (PD-L1) and Galectin-1 (Gal-1) to inhibit cytotoxic immune cells. Galectin-1 can promote the secretion of Th2 cytokines and increase abundance of Treg cells (81-83). Whereas PD-L1, when interacting with the PD-1 receptor on T cells, can recruit phosphatases to PD-1 to dephosphorylate proximal TCR signaling molecules thereby preventing T cell activation or inducing T cell exhaustion (84-86). Mouse studies further showed PD-L1 expression on tumour cells increases apoptosis of anti-tumoural T cells (87). In the case of cHL, disruption of PD-L1/PD1 pathway with blocking antibody can inhibit dephosphorylation of TCR signaling molecules and restore T cell activity (IFN-γ production) in vitro (88) Blockage of PD1 with monoclonal antibody drug, nivolumab, further demonstrates clinical efficacy in relapsed cHL patients (89). These studies support the importance of PD-L1 in cHL tumour evasion. Collectively, HRS cells employ multiple mechanisms to shape an immunosuppressive environment in order to evade anti-tumour attack by the host immune system.

1.1.4.2 Growth and survival factors

Another component of the microenvironment is granuolocytes and stromal cells which are thought to provide tumour cells with growth and survival signals (**Figure 1.1**). The inflammatory cells recruited to tumour tissue can activate proliferative signal in HRS cells by either direct receptor ligand interaction or via cytokine induction. For example, HRS cells express several members of the tumour necrosis factor receptor (TNFR) superfamily including CD30 and CD40. CD30 has been used as a marker for cHL and its ligand (CD30L) is expressed on eosinophils and mast cells in the infiltrates (90, 91); whereas CD40 ligand is expressed on CD4+ T cells (92-94). Eosinophils and mast cells are attracted by CCL5 (19, 95, 96) and CCL28 (97), whereas CD4+ T cells are attracted by CCL17 (19). Eosinophils can be further recruited by CCL11 from fibroblasts in the milieu (98). Engagement of CD30 (91, 99) or CD40 (79, 94, 100) with their ligands triggers activation of several cellular signaling pathways that promote tumour proliferation and survival as well as production of cytokines. Secondly, cells such as neutrophils, fibroblasts and DCs which are recruited by IL-8 (101), FGF (102) and CCL22 (103) respectively can produce growth factors that bind to receptor tyrosine kinases (RTKs) found on HRS cells to activate growth signals (104-106). In addition, several cytokines have been shown to support HRS cell growth and survival such as IL-7 (53, 107), IL9 (108), IL15 (109) and IL13 (110, 111). In summary, cellular interactions in the microenvironment not only support immune evasion but also provide growth and survival signals to HRS cells.

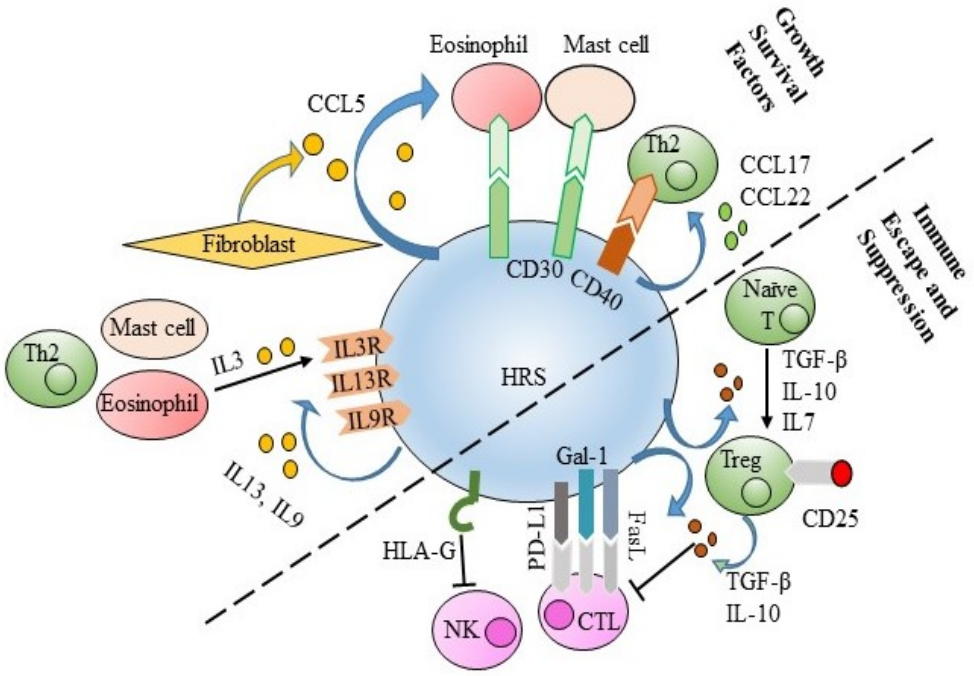

Figure 1.1 - Microenvironment of cHL

HRS cells interact with other cells in their environment to acquire growth and survival signals. HRS cells attract eosinophils and mast cells via direct chemokine secretion (CCL5) or indirect fibroblast recruitment into the lymphoma tissue to provide CD30L signal for growth and survival. HRS cells also secret chemokines (CCL17 and CCL22) to recruit Th2 cells to obtain additional survival signals via CD40L interaction. Cytokines such as IL3, IL9 and IL13 are secreted either by HRS cells or surrounding non-neoplastic cells to provide additional growth and survival signals. HRS cells can evade anti-tumour immune attack by CTL and NK cells via both direct and indirect mechanisms. Direct mechanisms include induction of

cytotoxic cell apoptosis by expressing PD-L1, FasL or secretion of Gal-1, and inhibition of NK cell activation by expressing HLA-G. Indirect mechanisms include recruitment of Th2 and Treg cells which inhibit cytotoxic cell proliferation by either expressing IL-2 receptor alpha chain CD25, or secreting anti-inflammatory cytokines TGF-β and IL-10. (Figure adapted from (9))

1.1.5 Dysregulated transcription network in cHL

Besides their dependency on the microenvironment for proliferation and survival, HRS cells have intrinsic mechanisms such as mutations in apoptosis pathways and deregulation of multiple signaling pathways that contribute to the abnormal proliferation and characteristic HRS cell phenotype **(Figure 1.2)**. First of all, HRS cells use several mechanisms to escape from apoptosis. There are two main apoptosis pathways: the extrinsic (death receptor) pathway and the intrinsic (mitochondrial) pathway. Analysis on the death receptor CD95 and the members of CD95 signalling pathway (eg. FADD, caspase 8) revealed infrequent mutations (112-114). Later, HRS cells were found to have strong expression c-FLIP which impairs the CD95-mediated extrinsic apoptosis pathway (115, 116). Inhibition of the intrinsic pathway is mediated through strong expression of the anti-apoptotic factors bcl-xl, c-IAP2, X-linked inhibitor of apoptosis protein (XIAP) and down-regulation of pro-apoptotic factor BIK (117-120). Moreover, cHL cell lines have been shown to have mutations in the functional domains of the tumour suppressor *TP53* gene, which leads to an inactive p53 protein and impaired transcriptional activity of its downstream targets (121). In addition to gene aberrations, p53 activity is further suppressed by its inhibitor protein Hdm2, which is highly expressed in HRS cells (117, 122). Inhibition of Hdm2 by its antagonist nutlin-3A restores p53 activity and increases HRS cell sensitivity to apoptosis inducers (123, 124). In summary, mutations in many regulator genes contribute to the apoptosis-resistance phenotype in HRS cells.

Secondly, HRS cells have mutations in many signaling pathways that regulate proliferation (125). These include the nuclear factor-kappa B (NF-κB) pathway (126), Janus kinase/signal transducer and activator of transcription (JAK/STAT) pathway (127), the mitogen activated protein kinase/ extracellular signal-regulated kinase (MAPK/ERK) pathway (100), Phosphatidylinositol-3 kinases/AKT (PI3K/AKT) pathway (128, 129), and Activator protein-1 (AP-1) pathway (130). Among them, the genetic lesions most frequently found in HRS cells involve members of two signaling pathways: NF-κB and JAK/STAT pathway, which I will discuss separately next.

1.1.5.1 NF-κB signalling pathway

The NF-κB pathway plays an important role in regulating various cellular functions including proliferation, apoptosis, immunity, inflammation, development and stress (131). In HRS cells, constitutive activation of the NF-κB pathway is one of the hallmarks of tumour cells and it has been shown to be important for HRS cell proliferation and survival (125, 126, 132).

The NF-κB pathway can be activated via RTKs and members of TNFRSF such as CD30 (99), CD40 (92). In EBV+ cHL, NF-κB is activated by LMP1 which mimics an active CD40 receptor (133-135). Once these receptors are engaged with their ligands from infiltrating cells, a signaling cascade triggers activation of IκKinase (IKK) which phosphorylate the inhibitor IκB members. Phosphorylated IκB will undergo ubiquitination and degradation, thereby releasing the active form of NF-κB heterodimers, which normally is sequestered as inactive form in the cytosol (136). Free NF-κB heterodimer can translocate to nucleus, where they

induce target gene expression associated with cell proliferation and survival (**Figure 1.2**).

In cHL tumour cells, several genetic lesions in this pathway results in the constitutive activation of NF-κB. For example, frequent (40%) genomic gains of *REL*, which encode one of NF-κB family member c-Rel is observed in cHL (137, 138), and mutations in the gene of NF-κB inhibitor IκBα are also found in 20% cHL cases (139, 140). In addition, the gene TNFα-induced protein 3 (*TNFAIP3*) which encode the tumour suppressor A20 is found to have somatic mutations in cHL cell lines and primary HRS cells (141, 142). A20 is a ubiquitin-modifying enzyme that negative regulates NF-κB pathway by adding ubiquitin to RIP and promote its degradation (143, 144), This event can inhibit the ubiquitination of the IκB complex, thereby preventing the release of NF-κB dimers and down-regulating signalling (144). However, in cHL, A20 is often mutated thus leading to constitutive NF-κB activation.

1.1.5.2 JAK-STAT signalling

Another dysregulated pathway commonly observed in cHL is the JAK-STAT pathway which is usually activated by cytokines (145). Dimerization or oligomerization of the cytokine receptor such as IL receptors allows JAKs to come in proximity and become activated. Activated JAKs can phosphorylate STAT proteins and induce STATs to homodimerize and translocate to nucleus, where they act as transcription factors to induce the expression of various genes involved in proliferation, differentiation, inhibiting apoptosis, and immune response (146).

In cHL, the JAK-STAT pathway is constitutively active due to several genetic alterations in this pathway. For example, the JAK2 locus is amplified in 30% cases and translocation of the JAK2 gene that produces oncogenic fusion protein JAK2-SEC31A was also reported in 3% cHL patients (147-149). Moreover, patient survival in cHL has been correlated with the expression of a microRNA, miR-135a, which targets JAK2 (150) and chemical inhibition of JAK2 with clinical inhibitor decreased tumour growth in vitro and in vivo, and prolonged the mouse survival in vivo (151). Besides the activation of JAK2, many downstream signaling molecules of this pathway are also dysregulated. For example, many STAT proteins such as STAT3, 5 and 6 are constitutively activated in HRS cells (152-155) and some such as STAT3 and STAT6 have been demonstrated to promote proliferation and survival of HRS cells (110, 127, 156, 157). The constitutive STAT activation are dependent on the constitutively active JAKs upstream (153) or high levels of cytokines in the microenvironment (154). Furthermore, mutations of suppressor of cytokine signalling (SOCS-1), a negative regulator of STAT activity (158), has also been identified in HRS cells, and the mutated SOCS-1 correlated with high nuclear phopho-STAT5 in HRS cells from cHL tumour tissue (159). In addition, PTPN2, a protein tyrosine phosphatase that is capable of dephosphorylate JAKs, is also inactivated in cHL cell lines (160). In summary, constitutively activation of JAK-STAT pathway in cHL is attributed to gain-of-function mutations in the JAKs and inactivation of negative regulators.

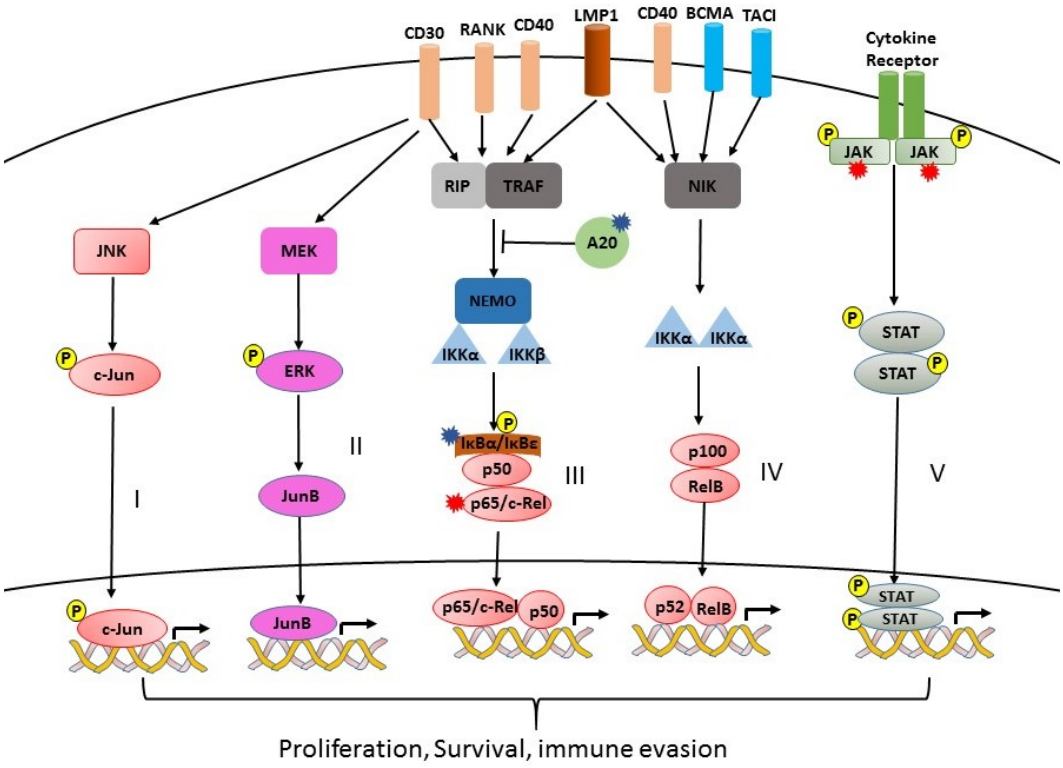

Figure 1.2 - Dysregulated signalling pathways in HRS cells

Dysregulation of signalling pathways can induce various gene expressions that are beneficial to tumour cells. Figure showed five major signalling pathways in HRS cells are shown. I: JNK/c-Jun pathway and II: MAPK/ERK/JunB pathway that are activated by CD30. These signaling cascades leads to aberrant expression of c-Jun and JunB and constitutive AP-1 activity, which can induce target gene expression. III: canonical and IV: alternative NFκB pathway. Various receptor-ligand interaction stimulate cellular proteins (TRAF/RIP) or kinase NIK to activate the IKK complexes. In the canonical pathway, IKKα and IKKβ phosphorylate the

inhibitors IκBα/IκBε which signals them for proteasome degradation and release of active form of NFκB dimers. In the alternative pathway, NIK activate IKKα complex which processes the precursor protein p100 into mature p52 subunit. p52 forms dimer with RelB and translocate to nucleus to regulate gene expression. The negative regulator A20 can inhibit the signal transduction from receptor to the IKK complex by adding ubiquitins to RIP to trigger degradation of RIP (143). V: JAK/STAT pathway. Stimulation of cytokine receptors lead to activation of JAKs and subsequent phosphorylation of STATs, which act as transcriptional factors in nucleus. All these pathways contribute to the proliferation, survival of HRS cells. Proteins with gain of function mutations or alterations are indicated by the red star and proteins with inactivating mutations are indicated with blue star. Abbreviations: BCMA, B cell maturation antigen; ERK, extracellular signal-related kinase; IKK, inhibitor kappa B kinase; MEK, MAPK/extracellular signal-related kinase; NEMO, nuclear factor-kappa B essential modulator; NIK, nuclear factor-kappa B-inducing kinase; TACI, transmembrane activator and CAML interactor. (Figure adapted from (161))

1.2: c-Jun and JunB transcriptional factors

1.2.1 AP-1 family transcriptional factors

Besides the NFκB and JAK/STAT pathways, another signalling pathway found to be dysregulated in cHL is the activator protein 1 (AP-1) family. AP-1 proteins are a collection of transcription factors that consists of the Jun, Fos/Fra, ATF, and Maf subfamilies (162). They are transiently and rapidly activated by mitogenic or stress signals and function to regulate various cellular processes such as proliferation, apoptosis, differentiation and immunity (162-164). AP-1 proteins belong to the basic leucine zipper (bZip) group of DNA binding transcription factors. This bZip motif is located in the C-terminal region and consists of a basic domain for DNA binding and a leucine zipper (Zip) region for dimerization (**Figure 1.3**). The dimerized transcriptional complex can then bind to consensus DNA sequences (AP-1 sites) of their targets genes and regulate their transcription (162). AP-1 sites include 12-O-tetradecanoylphorbol-13-acetate (TPA) responsive elements (TRE, 5'-TGA(G/C)TCA-3') (165) and cAMP response elements (CRE, 5'-TGACTGCA-3') (166) as well as some variant sites (167, 168). The composition of the AP-1 dimers determines the specificity of the binding of AP-1 site on the promoter and consequently the genes they regulate (169, 170). The relative binding affinity of each AP-1 dimer depends on the specific sequence in the DNA binding domain and the promoter region of the target gene (171, 172). AP-1 proteins also contain a transactivation domain (TAD) which is required for transcriptional activation. The region of TAD varies among the different subfamilies (173, 174). In this thesis, I will focus on two members of the Jun subfamily, c-Jun and JunB.

c-Jun and JunB are encoded by the single exon genes *JUN* and *JUNB,* respectively. Both c-Jun and JunB can form either homodimers or a more stable heterodimers with members of Fos subfamily that have a higher affinity and transcriptional activity for the target TRE DNA sequence (170-172, 175). JunB in general is considered a weaker transcriptional activator than c-Jun due to two main structural differences. Firstly, the DNA binding domain in JunB has a few amino acid changes leading to a 10-fold decrease in DNA binding ability and this is thought to contribute to the lower transactivation potential and transforming activity as compared to c-Jun (176). Secondly, their transactivation domains are slightly different such that c-Jun contains serine residues (Ser63/73) that can undergo JNK phosphorylation (177-180), which increases its affinity for DNA and transcriptional activity through recruitment of a histone acetylase coactivator CBP (181-184). JunB on the other hand, lacks these serine residues. Although it can be phosphorylated by JNK on other residues, phosphorylation does not increase its transactivation potential to the same extent as c-Jun (176, 182, 185). Consequently, JunB has a much weaker transactivation potential. Sometimes JunB can even antagonize c-Jun by forming less effective heterodimers with c-Jun or competing for AP-1 sites or binding on target promoter (176, 186). However, JunB is also a transcriptional activator of genes such as IL-4 or aromatase (187, 188) and its transactivation potential can be enhanced by sumoylation (189) or JNK mediated phosphorylation at threonine residues (187).

Transcription of c-Jun and JunB is rapidly and transiently stimulated by a number of extracellular signals such as growth factors, cytokines, hormones, cell-

matrix interactions, bacterial and viral infections as well as other physical and chemical stresses (162). These extracellular signals trigger activation of multiple MAPKs, which include JNK, ERK and p38 MAP kinase family, that regulate the expression and activity of c-Jun and JunB. In CD30+ lymphomas, c-Jun transcription is controlled by an auto-regulatory loop involving JNK phosphorylation (190). JunB, on the other hand, is transcriptionally regulated by MEK/ERK/ETS-1 pathway (191-194). Its translation is controlled via mTOR in Anaplastic Large Cell Lymphoma (ALCL) (195). In regulating their protein stability, several E3 ligases have been implicated in c-Jun degradation such as Fbw7 (196, 197), Itch (198, 199) and Cop1 (200, 201). JunB protein turnover is regulated by Itch- (199, 202, 203) and Smurf1- (204) mediated ubiquitination and proteasomal degradation.

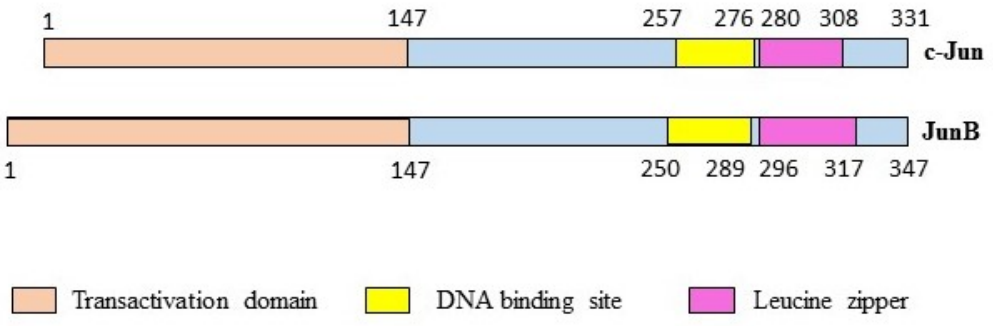

Figure 1.3 - Structure of c-Jun and JunB

Figure shows the protein structures of two of Jun proteins. The numbers indicate the amino acids representing the location of each domain. Structures adapted from (173, 176, 205)

One important function of AP-1 signalling is to transmit proliferative signals in response to mitogenic stimuli. In the next two sections, I will specifically discuss the role of c-Jun and JunB in regulating cell proliferation, apoptosis, and transformation.

1.2.3 c-Jun in cell proliferation, apoptosis and transformation

c-Jun is considered a positive regulator of proliferation and an oncogene in many cancers. Early studies among different AP-1 deficient mouse embryos revealed that c-Jun$^{-/-}$ embryos showed severe development defect as mouse embryo with a c-jun null mutation is embryonic lethal (206). Also, mouse embryo fibroblasts (MEFs) derived from c-Jun$^{-/-}$ embryos showed slower growth rate with reduced expression of cyclin D1 (162, 206). Studies on fibroblasts further revealed c-Jun is important at the G_1 to S checkpoint as inhibition of c-Jun using blocking antibodies or antisense RNAs resulted in a G_1/S block and a partial G_0 arrest (207, 208). Moreover, overexpression of c-Jun in NIH 3T3 fibroblasts leads to increased proportion of S and G_2/M cell populations further supporting its role in G_1/S transition (209). Additional studies revealed that c-Jun is also required for progression through the G_0/G_1 phase of the cell cycle as c-Jun null MEFs exhibited increased G_0/G_1 arrest (210). The underlying mechanism has been attributed to two cell cycle regulators, cyclin D1 and cyclin dependent kinase inhibitor ($p21^{Cip1}$). Cyclin D1 interacts with cyclin dependent kinases (CDK) 4 and 6 to regulate the G_1/S transition (211-213). c-Jun was shown to have transactivation potential on the cyclin D1 promoter as ectopic expression of c-Jun induces cyclin D1 promoter activity (185, 214). $p21^{Cip1}$ on the other hand, is a negative regulator of the G_1 phase

and G_1/S transition by binding to cyclinD-CDK4/6, as well as cyclinA-CDK1 and cyclinB-CDK2, thereby inhibiting their activity and resulting in G_1 and G_2 arrest (211, 215-218). There is much literature suggesting c-Jun negatively regulates the $p21^{Cip1}$ promoter (219, 220). For example when cells are transfected with a dominant negative c-Jun construct, $p21^{Cip1}$ is greatly up-regulated suggesting c-Jun functions to repress $p21^{Cip1}$ expression in regulating G_1 progression (221). In addition, c-Jun has also been implicated in negative regulation of $p21^{Cip1}$ in an indirect pathway through direct repression of the tumour suppressor p53 (222, 223), a known transcriptional regulator of $p21^{Cip1}$ (224, 225). However, one group reported c-Jun can positively regulate $p21^{Cip1}$ (226). Collectively, c-Jun can stimulate cell cycle progression through induction of cyclin D1 transcription and repression of p53 and $p21^{Cip1}$ transcription.

Different from its role in proliferation, c-Jun function in apoptosis is complex and is cell type dependent. For example, c-Jun is anti-apoptotic as it can protect fibroblast cells from UV-induced apoptosis and the mechanism requires phosphorylation of c-Jun at JNK sites (210). Moreover, conditional knockout of c-Jun in hepatocytes led to increased apoptosis associated with elevated p53 levels, further supporting the anti-apoptotic function of c-Jun (227). In contrast, there is some evidence suggesting c-Jun is pro-apoptotic. For example, c-Jun has been shown to regulate stress-induced apoptosis via a mechanism that requires phosphorylation by JNK (228).

In the area of transformation and cancer, c-Jun is considered a proto-oncogene because of its ability to transform immortal rat fibroblast cell lines (229). This is

further supported by loss-of-function and gene knockout experiments which revealed c-Jun is required for Ras-mediated transformation of primary rat embryo cells or fibroblasts (229-232). Moreover, c-Jun is required for initiation of skin tumours in pre-neoplastic cells as expression of a dominate negative mutant of c-Jun or complete gene deletion blocked tumour formation in mice (233-235). Mouse model experiments further showed c-Jun/AP-1 is involved in the development of skin tumours as conditional inactivating c-Jun in epidermis resulted in smaller tumour (236). Consistent with its cell cycle promoting function, c-Jun is frequently overexpressed in many human cancers and has been demonstrated to be involved in tumour growth or resistance to apoptosis as in the case of colorectal cancer (237), breast cancer (238, 239), hepatocellular carcinoma (227) and diffuse large B cell lymphoma (DLBCL) (240, 241).

1.2.4 JunB in cell proliferation, apoptosis and transformation

In contrast to c-Jun, JunB function in cell proliferation is context dependent. For a long time, JunB was best known as a negative regulator of proliferation (242-244), antagonist of c-Jun (218), and inducer of senescence (244, 245). Molecular mechanisms underlying the growth inhibitory function of JunB include repression of cyclin D1 (185) and up-regulation of cyclin dependent kinase inhibitor $p16^{INK4A}$ expression (245), which together exert a cell cycle inhibitory effect in G_0/G_1 phase. Later JunB was shown to have growth promoting activity such as induction of cyclin A2 which is required for S phase progression (246) and inhibition of $p21^{Cip1}$ expression in Hela cells to facilitate cell progression through G_1/S (247). During embryonic development, JunB can substitute for c-Jun to regulate the survival of c-

Jun deficient embryos but not fully rescue c-Jun deficient mice after birth (248). In addition, JunB knockout mice have multiple defects in extraembryonic tissues and results in embryonic lethality (249) suggesting JunB, like c-Jun, is necessary for development and the two are not fully redundant.

Similar to its role in proliferation, in the context of transformation and cancer, JunB can be both oncogene and tumour suppressor depending on cell context. For example, JunB has been shown to be involved in tumour proliferation in other lymphomas such as ALK+ ALCL (250, 251). In contrast, it can also function as a tumour suppressor in B-lymphoid malignancies and acts as a negative regulator of B cell proliferation and transformation (252). JunB deficient mice exhibited a higher potential for Abelson-induced proliferation and transformation (253). Moreover, JunB expression is silenced in advanced stage chronic myeloid leukemia (CML) by promoter methylation and silencing *JunB* in mice is associated with myeloid hyperproliferation which progresses into a myeloproliferative disorder similar to human CML (243, 254). Other evidences suggesting JunB may function as a tumour suppressor can be found in other types of cancer. For example, mice with genetic inactivation of JunB in the prostate epithelium developed invasive prostate cancer (244). Collectively, JunB is suggested to have the ability to either promote or inhibit proliferation and cancer progression depending on cell context.

1.2.5 Regulation and function of c-Jun and JunB in cHL

CD30+ lymphomas represent a group of lymphoproliferative disorders of T- or B-cell lineages including cHL, ALK+ and ALK- ALCL, primary cutaneous ALCL,

lymphomatoid papulosis and CD30+ DLBCL. They shared many cellular features such as expression of CD30 molecule and display higher than normal levels of c-Jun and JunB, with cHL tumour cells having the highest level of these two proteins (130, 250, 255). Moreover, immunohistochemistry using primary HRS cells from patient samples demonstrated that not only are they abundantly expressed, c-Jun in particular is active as it is phosphorylated by JNK at Ser73 (250, 256). As mentioned above, AP-1 signalling is dysregulated in cHL in such a way that it is constitutively active in HRS cells whereas in primary B cells, AP-1 is transiently induced by mitogenic or stress signals (16, 163). The mechanism responsible for the high c-Jun and JunB expression in cHL is in part due to the CD30 signalling pathway which activates JNK and MEK/ERK (257). In HRS cells c-Jun regulates its own expression (130) and c-Jun activity is enhanced by JNK phosphorylation at Ser73 (256). JunB on the other hand, has been shown to have increased copy number in primary HRS cells (258) and its transcription is regulated by the CD30/MEK/ERK/ETS-1 pathway as demonstrated using chromatin immunoprecipitation (ChIP) assay, in vitro DNA binding assay and promoter driven luciferase assay (193, 194). Specifically, ETS-1 was found to be the key factor in regulating JunB transcription in cHL as demonstrated by a 50% reduction in JunB promoter activity when the ETS-1 binding site on JunB promoter was mutated (193). Besides the ERK/ETS-1 pathway, some studies suggested JunB is also regulated by the constitutively active NF-κB signaling pathway as JunB protein was reduced following forced expression of NF-κB repressor IκB (130). However, Watanabe *et al.* later demonstrated JunB expression is NF-κB independent using

NF-κB inhibitor drug DHMEQ (194). Whether NF-κB is involved in JunB transcription regulation requires further investigation. In addition, JunB, but not c-Jun, can positively feedback to CD30 signaling (**Figure 1.4**). This is achieved by JunB binding to the AP-1 site in the microsatellite sequence (MSs) of the CD30 promoter and thereby promote the transcription of *CD30* (259, 260).

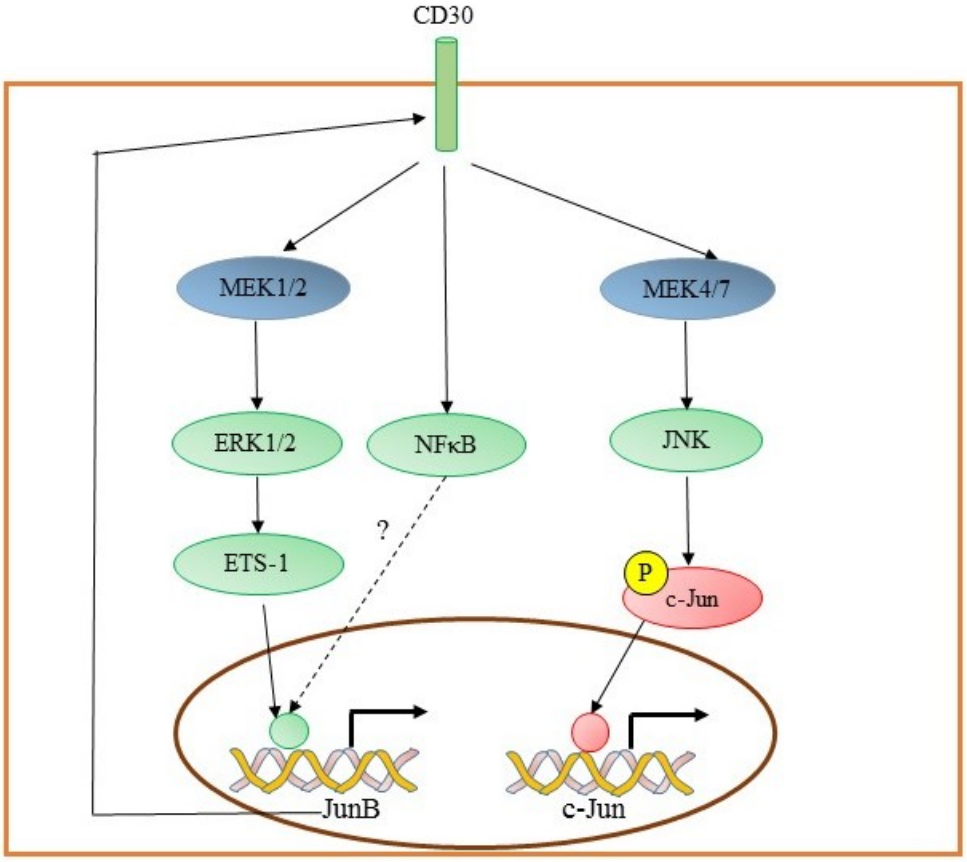

Figure 1.4 - Regulation of c-Jun and JunB transcription in cHL

Figure shows the transcriptional regulation of c-Jun and JunB in HRS cells. c-Jun is regulated by JNK phosphorylation at Ser 73 which activate its transcriptional activity and can further bind to the promoter of *c-Jun* gene and form a positive auto-regulatory loop. JunB is transcriptionally regulated by a MAPK ERK1/2-ETS-1and perhaps by the NFκB transcriptional factor.

AP-1 activity has been shown by some groups to play an important function in cHL pathogenesis, including proliferation and immunosuppression. Evidence supporting its role in HRS cell proliferation comes from studies using a dominant negative mutant of the c-Fos protein, A-Fos, which specifically forms inactive heterodimers with Jun subfamily members and reduces AP-1 DNA binding activity (130, 261). When A-Fos was transfected into L-428 cHL cell line, it resulted in a marked reduction of AP-1 activity accompanied by a decrease in cell growth and in the cell cycle regulator cyclin D2 at the mRNA level (130). However, because A-Fos inhibits AP-1 activity indiscriminately (261), no evidence for the involvement of distinct AP-1 proteins can be drawn from this study, especially the two aberrantly expressed AP-1 proteins, c-Jun and JunB. Later, Watanabe *et al.* used siRNA to knockdown ETS-1 which led to reduced JunB levels and reduced proliferation of the KM-H2 cHL cell line, suggesting a potential role for JunB in cHL proliferation (193). Moreover, Leventaki *et al.* demonstrated that c-Jun/JNK may also promote HRS cell proliferation by using a JNK inhibitor which resulted in cell cycle arrest at G_2/M with inactivation of c-Jun and up-regulation of $p21^{Cip1}$ (256). However, the above two studies all used methods to inhibit the upstream regulator of c-Jun or JunB, which do not definitively prove the defects are attributed to c-Jun or JunB. For example, both JNK and ETS-1 have multiple targets that may contribute to the reduced proliferation and cell cycle dysregulation (262, 263). Thus, investigation of the specific role of each c-Jun and JunB in cHL proliferation is still required.

In addition to their function in cHL proliferation, other roles of c-Jun and JunB in cHL pathogenesis have been described as well. For example, overexpression of c-Jun and JunB and elevated AP-1 activity in HRS cells resulted in the induction of target genes to suppress anti-tumour T cell activity and promote the immunosuppressive environment. Some of the important targets identified so far includes Galectin 1, PD-L1 and lymphotoxin α (LTA). Galectin 1 is an immunomodulatory glycan-binding protein that is highly expressed in cHL cell lines and primary HRS cells compared to other B cell lymphomas or normal lymphocytes (83, 264). Its transcription is regulated by a c-Jun/AP-1 complex as demonstrated by supershift Electrophoretic Mobility Shift Assay (EMSA) and luciferase-reporter assay (83). In vitro co-culture experiments and transcriptional factor profiling revealed Galectin 1 favours a Th2/Treg skewed immunosuppressive environment by promoting Th2 cell survival and the secretion of Th2 cytokines, as well as increasing the relative abundance of the Treg population (82, 83).

Another AP-1 regulated immunosuppressive molecule is PD-L1, which when bound to PD-1 found on activated T cells, can lead to inhibition of activation and proliferation of T cells (84). Expression of PD-L1 on HRS cells is AP-1 dependent as demonstrated by promoter-driven luciferase activity. Moreover, ChIP revealed the regulation is mediated by c-Jun and JunB; inhibiting AP-1 activity with a dominant negative c-Jun construct reduced PD-L1 transcription, further confirming the AP-1-dependent transcriptional regulation (265). Moreover, PD-L1 expression was found to correlate with c-Jun expression in patient samples (264). Given the function of PD-L1 in T cell tolerance and that its expression is markedly elevated

in cHL cell lines and patient samples (88, 265, 266), it is postulated c-Jun/JunB-driven PD-L1 can inhibit Th1/CTL mediated anti-tumour attack. This is supported by functional studies using PD-L1 blocking antibody on primary HRS cells which restored IFN-γ production and T cell activation (88).

Recently, Fhu *et al* identified another microenvironment modulating molecule LTA, which is secreted by HRS cells and functions to activate endothelial cells to enhance naïve CD4 T cell recruitment which provides proliferation and survival signals. Its transcription is partially dependent on AP-1 activity (267). However, based on this study, it is inconclusive of the involvement of c-Jun and JunB in promoter regulation because they used a JNK inhibitor to show AP-1-dependent LTA production. JNK inhibitor may inhibit multiple targets (262) and the inhibitor concentration used in the assay was quite high (100μM) which could lead to off-targeting effects (268-270). Thus, the relationship between AP-1 and LTA still needs investigation.

1.3: Hypothesis and Thesis objectives

Based on previous reports (130, 256) and c-Jun/JunB function in tumour proliferation in other CD30+ lymphomas (240, 251), we hypothesize both these proteins are important for promoting cHL cell line proliferation and preventing apoptosis. Moreover, we hypothesize c-Jun and JunB are also involved in tumour growth. In particular, we wanted to examine their role in regulating cHL cell line growth and survival individually and more specifically using a short-hairpin RNA (shRNA)-mediated gene silencing technique because previous studies, as discussed above, employ methods that either inhibit total AP-1 activity (130) or JNK activity

(256). Furthermore, given that AP-1 sites are common in the human genome, there are likely still many more genes that could be regulated by c-Jun and JunB that are not identified and could contribute to the pathogenesis of this lymphoma. Therefore, we wanted to know what genes whose expression is altered when c-Jun/JunB was knocked down in order to identify new transcription targets (direct or indirect) of c-Jun and JunB in cHL. The specific objectives of my thesis project were to:

1. Examine whether c-Jun and JunB are important in cHL cell line proliferation, apoptosis and tumour formation.
2. Identify genes that are transcriptionally influenced (directly or indirectly) by c-Jun and JunB knock-down in cHL using microarrays.

CHAPTER 2: MATERIALS AND METHODS

2.1: Cell lines

The cHL cell lines L-428 (DSMZ), and L-540 were obtained from Leibniz Institute DSMZ-German Collection of Microorganisms and Cell Cultures (Braunschweig, Germany). KM-H2 and L-428 (Amin) was obtained from Dr Hesham Amin (M.D. Anderson Cancer Center, Houston, TX). All cHL cell lines are EBV negative cell lines established from Hodgkin lymphoma. L-428 and the T cell derived L-540 cell line are derived from nodular sclerosis subtype, whereas KM-H2 cells are from mixed cellularity subtype (29, 271). The ALK+ ALCL cell lines Karpas299 and SUP-M2 were obtained from Leibniz Institute DSMZ-German Collection of Microorganisms and Cell Cultures (Braunschweig, Germany). The ALK+ ALCL cell lines SR (also known as SR-786) and UCONN were obtained from the American Type Culture Collection (ATCC; Manassas, USA) and Dr. Raymond Lai (University of Alberta, Edmonton, AB), respectively. The Burkitt lymphoma cell line, Ramos, was from Dr. Michael Gold (University of British Columbia, Vancouver, BC) and the BJAB Burkitt Lymphoma cell line was from Dr. Tony Pawson (University of Toronto, Toronto, ON). All cells were cultured in Roswell Park Memorial Institute (RPMI) 1640 media (Gibco; Burlington, ON, Canada) supplemented with 1 mM sodium pyruvate (Sigma-Aldrich; St Louis, MO), 2 mM L-glutamine (Gibco), and 50 μM 2-mercaptoethanol (BioShop; Burlington, ON, Canada). L-428, Ramos, BJAB and ALK+ALCL cell lines were supplemented with 10% heat-inactivated fetal bovine serum (FBS), and KM-H2 and L-540 cell lines were supplemented with 20% heat-inactivated fetal bovine serum (FBS). HEK 293T cells were from Dr. Maya Schmulevitz (University of Alberta), and were

cultured in Dulbecco's Modified Eagle's Medium (DMEM) supplemented with 10% heat-inactivated FBS, 1 mM sodium pyruvate and 2 mM L-glutamine. All cells were maintained at 37°C in a 5% CO_2 atmosphere.

2.2: Generating stable shRNA-expressing cell lines using lentiviral transduction

2.2.1 Generating lentiviral particles

HEK 293T cells were used to generate lentiviral particles using the MISSION short hairpin RNA (shRNA) lentiviral system (Sigma-Aldrich). 2 ml of HEK 293T cells were seeded at 30% confluence in a 6 well plate 24 hours before transfection. On the day of transfection, media was removed and replaced with 3ml fresh media. Transfection cocktail was made with a plasmid mixture consisting of 1.13 µg of shRNA vector and 10 µl of lentiviral packaging mix (SHP001; Sigma-Aldrich), and 86 µl DMEM/FuGENE HD mix which consists of 79 µl of serum free DMEM and 7 µl FuGene HD (Promega; Madison, WI). The shRNA vectors used in this study are listed in **Table 2.1**. The entire transfection cocktail was added to each well of HEK 293T cells which were then incubated at 37°C overnight. Approximately 16 hours post-transfection, media was discarded and replaced with 3ml fresh media. At 48 hours post-transfection, the media was collected and replaced with 3ml fresh media, which was collected again at 72 hours post-transfection. The collected media was passed through 0.45 µm low protein-binding syringe filter (EMD Millipore; Billerica, Massachusetts) to generate lentivirus-containing supernatants, which were aliquoted into 1ml aliquots and stored at -80°C for use**.**

Table 2.1: shRNA used in transduction

Name	Vector	TRC identifier/ catalogue number	shRNA Sequence
control (non-targeting) shRNA	pLKO.1-Neo	SHC002	CCG G**CA ACA AGA TGA AGA GCA CCA** ACT CGA G**TT GGT GCT CTT CAT CTT GTT G**TT TTT
JunB shRNA#1	pLKO.1-Neo	TRCN0000014943	CCG G**CA GAC TCG ATT CAT ATT GAA** TCT CGA G**AT TCA ATA TGA ATC GAG TCT G**TT TTT
c-Jun shRNA#1	pLKO.1-Neo	TRCN0000010366	CCG G**TA GTA CTC CTT AAG AAC ACA** ACT CGA G**TT GTG TTC TTA AGG AGT ACT A**TT TTT G
control (non-targeting) shRNA	pLKO.5-puro	SHC216	CCG G**GC GCG ATA GCG CTA ATA ATT** TCT CGA G**AA ATT ATT AGC GCT ATC GCG C**TT TTT
JunB shRNA#1	pLKO.1-puro	TRCN0000014943	CCG G**CA GAC TCG ATT CAT ATT GAA** TCT CGA G**AT TCA ATA TGA ATC GAG TCT G**TT TTT
JunB shRNA#6	pLKO.1-puro	TRCN0000232087	CCG G**GG AAA CAG ACT CGA TTC ATA** TCT CGA G**AT ATG AAT CGA GTC TGT TTC C**TT TTT G
c-Jun shRNA#1	pLKO.1-puro	TRCN0000010366	CCG G**TA GTA CTC CTT AAG AAC ACA** ACT CGA G**TT GTG TTC TTA AGG AGT ACT A**TT TTT G
c-Jun shRNA#4	pLKO.1-puro	TRCN0000039590	CCG G**CG CAA ACC TCA GCA ACT TCA** ACT CGA G**TT GAA GTT GCT GAG GTT TGC G**TT TTT G

GFP shRNA	pLKO.1-puro	SHC005	CCG G**TA CAA CAG CCA CAA CGT CTA T**CT CGA G**AT AGA CGT TGT GGC TGT TGT A**TT TTT

Table 2.1 - Information on the shRNAs used in generating stable knockdown cell lines are listed. Neo: G418 resistance. Puro: puromycin resistance. shRNA sequence is listed with targeting sequences bolded and underlined.

2.2.2 Lentiviral titration

Each viral supernatant stock was tittered to give equal amount of viral particles that will be used in subsequent infection and the procedure is described as follows. Each of control, c-Jun, JunB shRNA-containing lentiviral supernatant was diluted in 10% RPMI media to give 1, 1/3, 1/9 and 1/27 dilutions. Then the supernatant at each concentration was used to infect HEK 293T cells. 48 hours post infection, 1 μg/ml puromycin was added to each cell culture and cells were incubated at 37°C for two to three days. Cells were examined under the microscope to determine the optimal concentration of viral supernatant. The concentration that gave the highest viability was used in subsequent cHL cell line infection. Titration was performed by Joyce Wu (graduate student).

2.2.3 Infecting cHL cell lines with lentiviral particles

Before infection, cHL cell lines were counted and resuspended to $5x10^5$ cells/ml and 1 ml was transferred to each well of 6 well plate. 1ml of lentiviral supernatants

was added to each well of cells and 4 µl (8 µg/ml) polybrene (Sigma-Aldrich) was added to the mixture. Cells were incubated at 37°C for 24 hours. 24 hours post-infection, cells were spun down and washed twice with 10 ml RPMI media. Cells were then resuspended in 5 ml fresh RPMI media and incubated at 37°C. After 24 hours, puromycin (Sigma-Aldrich) or G418 disulphate salt solution (Sigma-Aldrich) were added to a final concentration of 0.5 µg/ml or 750 µg/ml respectively to select for successfully infected cells.

2.3: Protein methods

2.3.1 Cell lysis

Cells were collected by centrifuging at 1,800 x*g* for 5 min, washed once with PBS and lysed in 1% Nonidet P-40 (NP-40) lysis buffer for 10 min on ice. The lysis buffer contained 1% NP-40 , 50 mM Tris pH 7.4, 150 mM NaCl, 2 mM EDTA, 10% glycerol, 1 mM phenylmethyl sulfonyl fluoride (PMSF; BioShop, Burlington, ON), 1 mM sodium orthovanadate (Sigma-Aldrich), and 1:100 dilution of protease inhibitor cocktail (PIC; Sigma-Aldrich). Cleared cell lysates were obtained by centrifuging at 20,817 x*g* for 15 min at 4°C.

2.3.2 Protein quantification and normalization using the bicinchoninic acid (BCA) assay

Protein concentration of lysates were quantified using the Pierce BCA protein assay kit (Thermo Scientific; Rockford, Illinois). Lysates were pre-diluted 1:1 with ddH_2O and 10 µl of diluted lysates or lysis buffer alone (blank) were loaded in triplicate to wells of a 96 well plate. A standard BSA stock with a range of known protein concentrations was loaded the same way. BCA reagent mixture was

prepared by mixing Reagent A with Reagent B at 1:50 ratio. 90 µl of BCA reagent mixture was added to each sample and standard. The plate was incubated at 37°C for 30 min and the absorbance was measured at 562 nm wavelength using a FLUOstar OPTIMA microplate reader (BMG Labtech; Ortenberg, Germany). Absorbance of blank was subtracted from the samples and the protein concentration was calculated from the standard curve generated by the BSA standards. Samples were stored in 5X sodium dodecyl sulfate-polyacrylamide gel electrophoresis (SDS-PAGE) sample buffer (312.5 mM Tris pH 6.8, 10% glycerol, 11.5% SDS, 500 mM DTT, 0.1% bromophenol blue, pH 6.8) and normalized with 1X SDS-PAGE sample buffer.

2.3.3 Western blotting

Samples were boiled for 5 min on a heating block prior to loading. Proteins were separated on SDS-PAGE gels at a constant current of 25 mA/gel with maximum voltage of 215 V for 1.5-2 hours. Afterwards, proteins were transferred from resolving gels onto nitrocellulose membranes (Bio-Rad) in transfer buffer (25 mM Tris pH 8.5, 20% methanol, 192 mM glycine) using a Bio-Rad Trans-Blot SD Semi-Dry transfer cell at a constant voltage of 15 V for 30-60 min.

Membranes were blocked in 5% milk in 1X TBS for 30 min at room temperature or 4°C overnight, washed with 0.05% TBST and incubated with primary antibodies for 30 min – 1hr at room temperature or 4°C overnight. The primary antibodies used are listed in **Table 2.2**. Afterwards, blots were washed 3 times for 10 min using 0.05% or 0.1% TBST. Membranes were then incubated in horseradish-peroxidase (HRP)-conjugated secondary antibodies (Bio-Rad) at

1:10,000 dilution for 30-60 min at room temperature, washed 3 times for 10 min with 0.05% or 0.1% TBST and bands were visualized after addition of Enhanced SuperSignal® West Pico Chemiluminescent solution (Thermo Scientific).

After films were developed, membranes were stripped 3 times for 10 min with stripping solution (0.1% TBST, pH 2), washed and re-probed with different antibodies as described above.

2.3.4 Analysis of CD48 protein expression by flow cytometry

Cells were collected by centrifuging at 688 x*g* for 5 min, washed with PBS and blocked with 2% BSA in PBS for 30 min on a shaker at room temperature. Cells were then washed twice with PBS and incubated with anti-CD48 primary antibody (MEM-102) (1:20 dilution) for 1 hour at room temperature and washed twice again with PBS to remove non-specific binding. Afterwards, cells were incubated with Fluorescein isothiocyanate (FITC)-conjugated secondary antibody (1:500 dilution) (Life Technologies) for 40 min at room temperature and washed twice with PBS before analyzing on a BD LSR Fortessa (BD Biosciences; San Jose, CA). For negative controls, cells were treated the same way without primary antibody incubation.

Table 2.2: Primary antibodies used in western blotting and flow cytometry

Antibody	Species	Dilution	Source
β-actin (AC15)	mouse	1:5000	Santa Cruz
Annexin A1 (EH17a)	mouse	1:200	Santa Cruz
CD48 (MEM-102)	mouse	1:20	Santa Cruz
CDKN1A/p21 (12D1)	rabbit	1:1000	Cell Signalling
c-Jun (60A8)	rabbit	1:1000	Cell Signalling
eIF3J (#3261)	rabbit	1:1000	Cell Signalling
GBP1 (1B1)	rat	1:600	Santa Cruz
JunB (C-11)	mouse	1:200	Santa Cruz
PDGFRα (D13C6)	rabbit	1:1000	Cell Signalling
STAT1 (42H3)	rabbit	1:1000	Cell Signalling
α-tubulin (DM1A)	mouse	1:500	Santa Cruz

Table 2.2 – List of antibodies used with the clone name or catalogue number shown beside. Antibodies were diluted according to the indicated dilution factor in 1X TBS and 0.02% NaN_3.

2.4: RNA methods

2.4.1 RNA isolation

Total RNA was extracted and purified from approximately $5x10^6$ L-428 or KM-H2 cells expressing control, c-Jun or JunB shRNA using the RNeasy® mini kit (QIAGEN, Germany). The procedure was revised from that outlined in the manufacturer's protocol. Cells were spun down at 688 x*g* for 5 min and lysed in 350 µl RLT buffer for 5 min on ice to allow for complete lysis before centrifugation as described in protocol. Supernatant was transferred to an Eppendorf tube and an equal volume of 70% ethanol was added. The entire sample was transferred to a RNeasy spin column and incubated at room temperature for 2 min to allow RNA

binding before centrifugation as described in the manufacturer's protocol. Afterward, RNA was washed with RW1 and RPE buffers as described in the protocol and RNA was eluted in RNase free H_2O. The concentration and purity of RNA was determined by nanodrop using a NanoDrop ND-1000 spectrometer (Thermo Scientific).

2.4.2 DNA digestion and reverse transcription

DNA digestion was performed prior to reverse transcription to remove any genomic DNA. In a PCR tube, 2 µg of RNA was added along with 1 µl 10X DNase reaction buffer, 1 µl DNase I amplification grade (Invitrogen) and UtraPure™ DNase/RNase free ddH_2O (Invitrogen) for a total volume of 10 µl. Digestion was carried out at room temperature for 15 min, then 1 µl of 25 mM EDTA was added to the mixture and heated at 65°C for 10 min to stop digestion. The reaction was then cooled down on ice for 2 min.

For reverse transcription, Superscript II reverse transcriptase (Life Technologies) was used to generate cDNA using 2 µg RNA and Oligo dT primer. Briefly, to 2 µg RNA, 1 µl of 10 mM dNTPs (Thermo Scientific) and 1 µl (1 µg) random primers (Invitrogen) was added and the mixture was heated at 65°C for 5 min and cooled down on ice for 2 min. In a separate tube, phase II mix was prepared as follows, for each RNA sample, 4 µl of 5X First strand buffer (Invitrogen), 1 µl each of the 0.1 m DTT, 40 U/µl RNaseOUT ribonuclease inhibitor (Invitrogen) and 200 U/µl Superscript II reverse transcriptase (Invitrogen) were added to the mix. 7 µl of the phase II mix was added to each RNA/dNTP/primer mixture. The reaction was carried out as follows: 25 °C for 5 min, 50°C for 1 hr and 70°C for 15 min.

cDNA was diluted with ddH_2O to 1/4 for polymerase chain reaction (PCR) analysis and 1/64 for quantitative real time polymerase chain reaction (qRT-PCR).

2.4.3 PCR analysis of cDNA

The quality of cDNA generated was tested using *GAPDH* primers. The reaction was performed as follows: in PCR tube I, 1 µl of 1/4 cDNA or ddH_2O (blank) was added along with 7.5 µl of each 100 pmol/µl forward and reverse primer (0.3 µM each). In tube II, PCR mix was made with 1 µl of 10 mM dNTP, 5 µl 10X Taq buffer (+KCl), 6 µl 25 mM $MgCl_2$, 1 µl low fidelity *Taq* polymerase (Biological Sciences Fermentation Unit, University of Alberta) and 21 µl H_2O. The PCR reaction was started by adding tube I to tube II for a total volume of 50 µl and cycling was performed on a Biometra T-gradient thermal cycler (Biometra; Goettingen Germany). The program started with an initial denaturing step at 95°C for 5 min followed by 40 cycles of denaturing at 95°C for 30 sec, annealing at 48-56°C (depending on primer set) for 30 sec, and extension at 72°C for 30 sec, followed by a final extension step at 72°C for 5 min. A list of primers used for PCR can be found in **Table 2.3**. The products were run on 1% or 2% agarose gels containing 1:10,000 SYBR Safe stain at constant voltage of 130 V for 30 min and was visualized on a Molecular Imager® Gel Doc™ XR^+ Imaging system (Bio-Rad).

2.4.4 qRT-PCR

cDNA samples were diluted with water to 1:64 to be used in qRT-PCR which was performed using PerfeCTa SYBR Green FastMix (Quanta Biosciences; Gaithersburg, MD). 2.5 µl of 1:64 cDNA samples (or water alone as blank control) were plated in 96-well real time PCR plate (VWR; Mississauga, ON) in triplicate

along with 2.5 µl of 1.2 µM forward and reverse primer mix and 5 µl of 2X PerfeCTa SYBR Green FastMix. Reactions were kept on ice before being run on a Bio-Rad CFX96 Real-Time PCR Detection System (Bio-Rad). The conditions used included an initial denaturing step at 95°C for 2 min followed by 40 cycles of denaturing at 95°C for 15 sec, annealing at 50-53°C depending on the primers for 20 sec, and extension at 68°C for 30 sec. A list of primers used in qRT-PCR can be found in **Table 2.4**. Expression level of the gene of interest was normalized to *β-actin* and averaged within the triplicates. A melting curve was analyzed to exclude any impure product or faulty readings. The relative expression level was determined using $\Delta\Delta^{-CT}$ method (272).

Table 2.3: List of primer sequences used in PCR

Target gene	Forward primer sequence	Reverse primer sequence	Annealing Temp (°C)
ELMO-SLCO3A1 #1	CGT CAA GGT GGC CAT AGA AT	TGT GGA AAC CCA AAC ATC AA	50
ELMO-SLCO3A1 #2	CGT CAA GGT GGC CAT AGA AT	TAA TGA ACT TCT GGA GCT GG	49
ELMO-SLCO3A1 #3	TGG CCG TTT ACG CTG T	GTC TTC ACA GAG GTC ACA TT	49
GAPDH	GAC AGT CAG CCG CAT CTT CT	TTA AAA GCA GCC CTG GTG AC	50
p53 (4-4)	CCT GGT CCT CTG ACT GCT CT	GGC ATT GAA GTC TCA TGG AAG	56
p53 (4-6)	CCG TCC CAA GCA ATG GAT G	CAC TCG GAT AAG ATG CTG AG	56
SLC-ELMO#1	GTT CTT TGC TAG AAC CCA CA	TTG TGA ACA GGT GTA TGT GA	48
TNRC18B-MYLPF	CAT CCG CTC GCT CAA G	ATG CAG AAA CTG ACA TAC C	47

Table 2.3 - Primer sequences and annealing temperatures used in PCR reactions. p53 (4-4) and SLC-ELMO#1 sets were used on genomic DNA. All the others were used on cDNA.

Table 2.4: List of primer sequences used in qRT-PCR

Target gene	Forward primer sequence	Reverse primer sequence	Annealing Temp (°C)
ANXA1	GCA GGC CTG GTT TAT TGA AA	GCT GTG CAT TGT TTC GCT TA	50
CD24	AGG GGA CAT GGG CAG AGC	CCT TGG TGG TGG CAT TAG TTG	53
CD52	AAT GCC ATA ATC CAC CTC TTC TG	TGC TTG GCC CCT ACA TCA TTA	53
CDKN1A ($p21^{C1P}$)	GGG ACA GCA GAG GAA GAC CAT	CGG CGT TTG GAG TGG TAG A	53
CFI	CTG GGG ACG AGA AAA AGA TAA C	CCC CCA ACT CAC AAC ACC	53
DCBLD2	ACA ACC TCG CAG TAG CAA TGA AT	GCC CGG TCC CAG TAA GGT A	50
eIF3J	GTG AAG ATA CTG CGG CTG AAA A	TCC CTC CCC CAC CTG AAG	53
GBP1	GCC CAC AGA AAC CCT CCA G	ATA AAT TCC CGC CTT CAC TTC TT	53
IL-7	GTC GCG GCG TGG GTA AG	AAC AAG GAT CAG GGG AGG AAG T	53
PDGFRA	GCA CGC CGC TTC CTG AT	GCA CGG CGA TGG TCT CC	50
PTPN3	CGA GGA CGC CAG CCA GTA CTA C	CTC CTG ATC ACC AGG GCC AG	52
SELL	GAG CCC AAC AAC AAG AAG AAC A	GGC CCA TAG TAC CCC ACA TC	53
STAT1	ATT ACA AAG TCA TGG CTG CT	ATA TCC AGT TCC TTT AGG GC	50
β-actin	AGA AAA TCT GGC ACC ACA CC	TAG CAC AGC CTG GAT AGC AA	50-53

Table 2.4- primer sequences and annealing temperatures used in qRT-PCR. Note: the annealing temperature for β-actin in each experiment was the same as the annealing temperature of the target genes checked in each reaction.

2.5: DNA methods

2.5.1 DNA isolation

Total genomic DNA was extracted and purified from approximately $3x10^6$ L-428 KM-H2, L-540, Karpas 299 or SUP-M2 cells using the QIAamp® DNA mini kit (QIAGEN, Germany). The procedure was revised from that outlined in the manufacturer's protocol. Cells were spun down at 688 x*g* for 5 min and resuspended in 200 µl of PBS. 20 µl of Proteinase K solution was added to remove protein contamination and inactivate nucleases. Cells were lysed in 200 µl AL buffer by vortexing for 15 seconds and incubating at 56°C for 10 min followed by short spin for 7 seconds at 6000 x*g*. An equal volume (200 µl) of 100% ethanol was added to entire mixture and mixed by vortexing for 15 seconds followed by a short spin for 7 seconds at 6000 x*g*. The entire sample was transferred to the QIAamp Mini spin column and centrifuged at 6000 x*g* for 1 min. Afterwards, the DNA was washed with AW1 and AW2 buffers as described in the manufacturer's protocol and DNA was eluted in AE buffer. The concentration and purity of DNA was determined by nanodrop using a NanoDrop ND-1000 spectrometer (Thermo Scientific). DNA was later diluted to 500 ng/µl in AE buffer.

2.5.2 PCR analysis of DNA

The reaction was performed as described in section **2.4.3** except for template, 1 µl of genomic DNA (500 ng) was used. The primers used were listed in **Table 2.3.**

2.5.3 PCR purification and sequencing

PCR products were purified using the QIAquick® PCR purification kit (QIAGEN Science; Maryland, USA). The procedure was based on the manufacturer's protocol.

Briefly, to 40 µl of PCR product, 200 µl (5X volume) PB buffer was added and the entire sample was transferred to a QIAquick spin column and spun for 1 min at 14,549 x*g*. DNA was washed with 750 µl PE buffer by centrifugation at 14,549 x*g* for 1 min. To elute DNA, 30 µl EB buffer was added and incubated for 2 min before elution by centrifuging at 14,549 x*g* for 1 min.

For sequencing, 10 µl of purified PCR product (2 ng/µl) and 1 µl of primer (3.2 µM) were added to sequencing tube. Samples were sent to the Alberta Transplant Applied Genomics Centre Applied Genomics Core (University of Alberta, Edmonton, AB, Canada) for Sanger sequencing.

2.5.4 Short Tandem Repeats (STR) profiling

Genomic DNA extracted from KM-H2 and L-428 (Amin and DSMZ) cells was sent to The Centre for Applied Genomics (TCAG; The Hospital for Sick Children; Toronto, Ontario) for STR profiling. The GenePrint® 10 System (Promega) was used for cell line authentication. The analysis was performed by a TCAG technician.

2.6: Growth assays

2.6.1 Growth curves

Cells were resuspended to $4x10^4$ cells/ml (KM-H2), $5x10^4$ cells/ml (L-428-Amin, L-540) or $8x10^4$ cells/ml (L-428-DSMZ) in 5 ml fresh media. Samples were mixed with Trypan blue (Gibco) at a 1:1 ratio and triplicate measurements were obtained daily by counting the number of viable cells using a hemocytometer. Daily counting was carried out until control shRNA-expressing cells reached saturation and less than 60% viability. Results were expressed as the total number of viable cells. All

growth curve experiments were performed on knock-down cells derived from at least two independent infections.

2.6.2 Resazurin assays

Growth curves were set up as described above. On days 4, 5, and 6, Resazurin. (Sigma Aldrich) is used to assess cell viability. 100 µl of control or c-Jun/JunB shRNA-expressing cells or media alone (blank) were plated in a 96 well plate in triplicate along with 11 µl of 10X Resazurin solution (final concentration of 44 µM). The plate was incubated at 37°C for 4 hours and the resulting fluorescence was read on a FLUOstar OPTIMA microplate reader at 545 nm emission and 590 nm excitation wavelength. The sample measurement was subtracted from the average of the media alone fluorescence and triplicate measurements were averaged and normalized to control shRNA-expressing cells which were arbitrarily set at 100%.

2.6.3 Cell cycle analysis

Cells were maintained at 3-4x10^5 cells/ml before labelling. Bromodeoxyuridine (BrdU) and 7-amino-actinomycin D (7-AAD) staining was performed using the BD Pharmingen^{TM} FITC-BrdU Flow kit (BD Biosciences, San Jose, CA) as outlined in the manufacturer's protocol. Briefly, cells were incubated at 37°C in the presence of 10 µM BrdU for 30 minutes (KM-H2) or 1 hour (L-428, L-540,), collected and washed with PBS. Cells were fixed and permeabilized with BD Cytofix/Cytoperm buffer for 15 min on ice and washed once. Cells were then permeabilized with BD Cytoperm Permeabilization Buffer Plus for 10 min on ice and washed once followed by re-fixing the cells with BD Cytofix/Cytoperm Buffer for 5 min on ice and washed once. Cells were then treated with DNase (300 µg/ml in PBS) to expose

incorporated BrdU by incubating the cells at 37°C for 1-1.5 hours. Cells were then stained for anti-BrdU antibody (1:50 dilution) for 20 min at room temperature in the dark. Afterwards, total DNA was stained with 10-20 µl of 50 µg/ml 7-AAD solution for 3-4 min at room temperature in the dark. Cells were then washed and resuspended in FACS buffer (Dulbecco's PBS containing 1% FBS, 0.02% NaN_3) for analysis on a BD LSR Fortessa flow cytometer (BD Biosciences). All the washing was performed by centrifuging at 6800 x*g* for 3 min at 4°C with 1X Perm/Wash buffer. Compensation controls and set up were performed as in the manufacturer's protocol. All data were analysed using FlowJo software (Ashland, OR).

2.6.4 Nocodazole experiments

L-428 (Amin) cells were maintained at density of 4-5x10^5 cells/ml and blocked at G_2/M by incubating in the presence of nocodazole at 37 °C. For this experiment only, L-428 cells were grown in 20% FBS and incubated with 400 ng/ml nocodazole for 24 hours. At the end of blocking stage, nocodazole was removed by centrifuging cells at 688 x*g* for 5 min and washed with fresh RPMI twice. Cells were resuspended in fresh media to release from G_2/M. At 0, 12, 18, 24 and 36 hours post release, cells were BrdU pulse-labelled for 1.5 hours for cell cycle analysis as described in section **2.6.3**.

2.7: Estimation of cell cycle stage duration

2.7.1 Calculation of doubling time

Doubling times were calculated using the formula T_{2x} (hr) = $(t_2\text{-}t_1) \times \frac{ln2}{ln(N2/N1)}$, where t_1, t_2, N_1, N_2 refer to the time and cell number, respectively at two different

time points within the log phase of the growth curve. The equation was adapted from Korzynska et al (273). For the growth curves associated with knockdown cells, the last three days were used for the calculation.

2.7.2 Calculation of time spent in each cell cycle stage

The time for the cells to progress through each cell cycle was calculated using the formula $T\ (G_N)\ (hr) = T_{2x} \times \%\ (G_N)$, where $T(G_N)$ refers to the time duration in each specific stage of cell cycle, T_{2x} refers to doubling time and $\%\ (G_N)$ refers to the percentage of cells in that particular stage from the cell cycle analysis (274).

2.8: Apoptosis analysis using terminal deoxynucleotidyl transferase dUTP nick end labeling (TUNEL)

Apoptosis was analyzed by terminal deoxynucleotidyl transferase dUTP nick end labelling (TUNEL) using the In Situ Cell Death Detection Kit, Fluorescein (Roche Applied Science; Laval, QC, Canada). $2x10^7$ cells at density of $3\text{-}4x10^5$ cells/ml were collected and washed three times in PBS, fixed, permeabilized and labelled as described in the manufacturer's protocol. Briefly, cells were fixed in 2% Paraformaldehyde for 1 hour at room temperature with shaking, washed twice with PBS and permeabilized with permeabilization solution (0.1% Triton X-100 in 0.1% sodium citrate) for 2 min on ice. Cells were then washed twice with PBS and incubated in 50 µl TUNEL reaction mixture (1:10 enzyme solution in label solution) at 37°C for 1 hour in the dark. Afterwards, cells were washed twice with PBS and resuspended in FACS buffer. All washing steps were carried out by centrifuging at 1,500 x*g* for 5 min. As a positive control, cells were pre-treated with DNase (300 µg/ml in PBS; BD Pharmingen™, BD Biosciences, San Jose, CA) for 10 minutes

(KM-H2) or 30 minutes (L-428) at room temperature and washed once with PBS before incubation with TUNEL reaction mixture. As a negative control, cells were incubated in label solution without enzyme solution. The percentage of dUTP-positive cells were analyzed using a BD LSR Fortessa flow cyctometer (BD Biosciences).

2.9: Xenograft experiments

All mouse experiments were approved by the University of Alberta Animal Care and Use Committee and followed protocol (AUP# 393). 5×10^5 L-428 cells expressing either control, c-Jun, or JunB shRNA were resuspended in 50 µl of PBS and mixed with an equal volume of BD Matrigel® Matrix (BD Bioscience). The cell/matrigel mixture was then injected subcutaneously into the neck of isofluorane-anesthetized two month old female NOD.CB17-*Prkdc*^{scid}/J mice (Charles River; Wilmington, Massachusetts). Mice were monitored, weighed and scored as described in our approved animal protocol. When any tumour was observed to have a size >1cm in any dimension, all mice were euthanized by CO_2 and tumours were harvested. Tumours were then weighed and the length and width were measured. The volume was calculated using the equation volume= ½ × (length × width^2) as previously described (275-277).

2.10: Microarray experiments and analyses

2.10.1 Microarray experiments

Four sets of mRNA were isolated from control, c-Jun, or JunB shRNA-expressing cell lines as described in RNA methods (Section **2.4.1**). The KM-H2 sets were from two independent infections and the L-428 (Amin) sets were from three independent

infections, and each set included infections with shRNA-containing vectors conferring resistance to puromycin and G418. Samples were sent to the Alberta Transplant Applied Genomics Centre (University of Alberta, Edmonton, AB, Canada) where mRNAs were converted into amplified RNAs (aRNAs) as described in GeneChip® 3' IVT Express Protocol (Cat # 901229) (Affymetrix, Santa Clara, CA). aRNAs were then probed on GeneChip® PrimeView™ human gene expression arrays (Affymetrix). Data were analyzed by Dr. Konrad Famulski (University of Alberta) using GeneSpring GX software (Agilent Technologies, Mississauga, ON) and the values from the c-Jun/JunB shRNA-expressing cells were normalized to control shRNA-expressing cells. Candidate genes were selected based on their corrected p value (<0.05) and a fold change (>1.5) between c-Jun/JunB and control shRNA-expressing cells.

2.10.2 Gene ontology analysis using DAVID

Differentially expressed genes with > 1.5 fold change in c-Jun or JunB shRNA-expressing cells in both cell lines were combined and analyzed using Database for Annotation, Visualization, and Integrated Discovery (DAVID) bioinformatics resources 6.7 (National Institute of Allergy and Infectious Diseases NIAID, NIH) for functional annotation (278, 279). Functional annotation clustering and gene-annotation enrichment analysis were used for analysis of biological pathways and molecular functions. The top ten clusters with two representative categories in each cluster were selected based on enrichment scores and corrected p-values.

2.11: Statistical analyses

Statistical analyses comparing knockdown cells with control cells was performed using either paired or two-tailed independent *t* test as indicated in the figure legends.

CHAPTER 3: C-JUN AND JUNB REGULATE PROLIFERATION BY INFLUENCING CELL CYCLE PROGRESSION PRIMARILY AT THE G_0/G_1 PHASE IN CHL CELL LINES

3.1: Introduction

Previous studies had suggested a role for AP-1 proteins in promoting cHL proliferation (130, 256). However, the distinct role and functional contribution of specific AP-1 transcription factors, particularly the two aberrantly expressed AP-1 proteins, c-Jun and JunB, has not been fully addressed in cHL. Therefore, we used a shRNA-mediated gene silencing approach to discriminate the relative contributions of c-JunB and JunB in HRS cell proliferation, apoptosis and tumour formation.

3.2 c-Jun and JunB protein levels are significantly elevated in cHL cell lines compared to Burkitt lymphoma.

Aberrant expression of the AP-1 proteins, c-Jun and JunB, is a common theme in CD30+ lymphomas (250, 255). We first wanted to show this in our cHL cell lines and compare the expression level of c-Jun and JunB between different cHL cell lines and with other lymphomas. We had four cHL cell lines: L-540, KM-H2 and two L-428 cells obtained from two different sources, the Amin lab and DSMZ. We also used cells from another CD30+ lymphoma (ALK+ ALCL) which is known to have abundant c-Jun and JunB (251, 280), and a CD30- B cell lymphoma (Burkitt lymphoma) which expresses little c-Jun or JunB (130). Protein expression of c-Jun and JunB was analyzed amongst three cHL cell lines (L-428 (Amin), KM-H2, L-540), four ALK+ ALCL cell lines (Karpas 299, SUP-M2, SR, UCONN) and two Burkitt lymphoma cell lines (BJAB, Ramos). As expected, we observed significantly higher expression of c-Jun and JunB in cHL and ALK+ ALCL cell lines compared to the CD30- Burkitt lymphoma cell lines (**Figure 3.1A**). Also, the

relative expression levels of c-Jun and JunB were different amongst the three cHL cell lines. While JunB was more abundantly expressed in KM-H2 and L-540, c-Jun levels were higher in L-428 (Amin) and L-540. In addition, we compared c-Jun and JunB protein level between the two L-428 cell lines. As expected, the two L-428 cells showed similar c-Jun and JunB protein expression (**Figure 3.1B**). We choose to use all four cell lines for our study because they represent two different cHL subtypes and lineages. While L-428 (Amin and DSMZ) and L-540 are from nodular sclerosis subtype, KM-H2 is from mixed cellularity subtype (271). In addition, L-428 (Amin and DSMZ) and KM-H2 are B cell-derived whereas L-540 is a T cell-derived cell line (271). Therefore, using cells derived from two different histological subtypes and two different cell types will give us a more complete understanding of c-Jun and JunB function in cHL growth and survival.

Figure 3.1

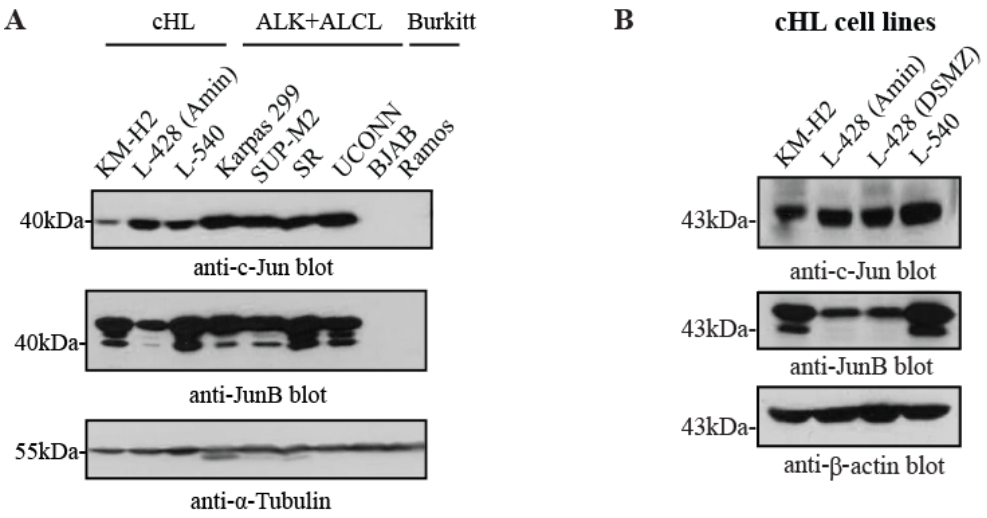

Figure 3.1 - Expression of c-Jun and JunB amongst different lymphoma cell lines.

A. Expression levels of c-Jun and JunB amongst cell lines derived from different types of lymphomas. Molecular mass markers are shown on the left of the blots and the anti-α-tubulin blot serves as loading control. **B**. Western blots showing the relative c-Jun and JunB protein level amongst four cHL cell lines. Molecular mass markers are shown on the left of the blots and the anti-β-actin blot serves as loading control.

3.3 Knocking down c-Jun or JunB expression reduces cHL cell growth rate

In order to investigate the functional contribution of c-Jun and JunB in HRS cell proliferation, we first generated c-Jun and JunB stable knockdown cell lines in L-428 (Amin), L-428 (DSMZ), L-540 and KM-H2 cells using shRNAs. Western blotting analysis demonstrated a significant reduction in c-Jun and JunB protein levels in the corresponding shRNA-expressing cells in all four cell lines (**Figure 3.2A-D**). Thus, using a shRNA-mediated gene silencing approach, we were able to considerably reduce c-Jun and JunB protein expression.

To investigate the function of c-Jun and JunB in cHL cell line growth, we generated growth curves using our stable cell lines. We observed a significantly reduced growth rate in both c-Jun and JunB knockdown cells, compared to control shRNA-expressing cells. The phenotype was consistent in both L-428 (DSMZ) and (Amin) (**Figure 3.2E & F**), L-540 (**Figure 3.2G**) and KM-H2 cells (**Figure 3.2H**). Next, we approximated the doubling time of the control and knockdown cell lines using the method adapted from Korzynska et al (273). We found that in all four cell lines, c-Jun and JunB shRNA-expressing cells exhibited a significantly longer doubling time (approximately 1.5- to 2-fold) compared to control shRNA-expressing cells. Importantly, we observed that knocking down c-Jun or JunB resulted a similar reduced growth phenotype in each cell line. The two L-428 cells exhibited similar slow growth rate when c-Jun or JunB were knocked-down; however, the doubling times were different for the two L-428 cells. L-428 (Amin) grew faster and had a higher saturation density than the L-428 (DSMZ).

Figure 3.2

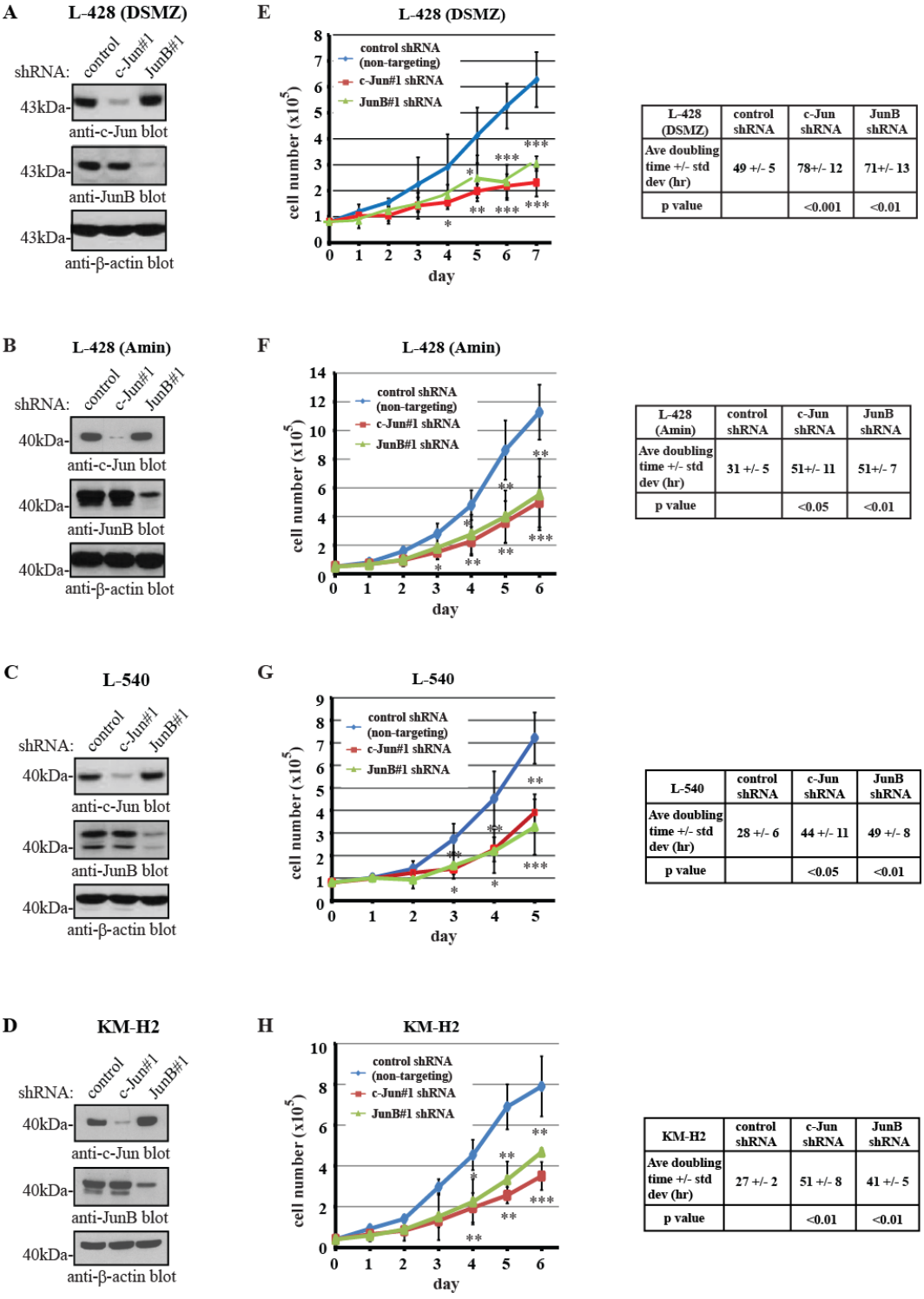

L-428 (DSMZ)	control shRNA	c-Jun shRNA	JunB shRNA
Ave doubling time +/- std dev (hr)	49 +/- 5	78+/- 12	71+/- 13
p value		<0.001	<0.01

L-428 (Amin)	control shRNA	c-Jun shRNA	JunB shRNA
Ave doubling time +/- std dev (hr)	31 +/- 5	51+/- 11	51+/- 7
p value		<0.05	<0.01

L-540	control shRNA	c-Jun shRNA	JunB shRNA
Ave doubling time +/- std dev (hr)	28 +/- 6	44 +/- 11	49 +/- 8
p value		<0.05	<0.01

KM-H2	control shRNA	c-Jun shRNA	JunB shRNA
Ave doubling time +/- std dev (hr)	27 +/- 2	51 +/- 8	41 +/- 5
p value		<0.01	<0.01

Figure 3.2 - Effect of knocking down c-Jun or JunB on cHL cell growth.

Four cHL cell lines L-428 (DSMZ) (**A**), L-428 (Amin) (**B**), L-540 (**C**) and KM-H2 (**D**) cells stably expressing the indicated shRNA were examined for the degree of silencing of c-Jun or JunB at the protein level. The chosen blots correspond to lysates obtained from days 0 or 1 of the growth curve. Molecular mass markers are shown on the left of the blots and the anti-β-actin blot serves as a loading control. **E-H** Growth curves (left) associated with the indicated shRNA-expressing cells were obtained by live cell counting by Trypan blue exclusion. The average and standard deviation of the doubling times (right) were estimated as described in the Materials and Methods using the last three days of each independent growth curve experiment. The data are the average and standard deviation of five (L-428 (DSMZ) & L-540) or three (L-428 (Amin) & KM-H2) independent experiments from at least two different infections. *p* values represent independent, two-tailed *t* tests comparing the c-Jun or JunB knockdown to control shRNA-expressing cells. Note *p* values in **E-H** above are for JunB and below are for c-Jun. * $p<0.05$, ** $p<0.01$, *** $p<0.001$.

3.4 Knocking down c-Jun or JunB expression with a second shRNA resulted a similar slow growth phenotype in cHL cell lines.

In order to confirm the observed growth defect was due to reduced c-Jun and JunB protein level and not the off-targeting of the shRNAs, we used a second shRNA that targets different sequence of the *c-Jun* and *JunB* genes. While c-Jun#4 shRNA targets a completely different region from c-Jun#1 shRNA, JunB#6 shRNA partially overlaps with JunB#1 shRNA (**Appendix 1**). We used this shRNA because we could not find a second JunB shRNA that targets a different region of the gene and efficiently silences JunB expression (**Appendix 2**). We performed growth curve experiments on two cHL cell lines, L-428 (Amin) and KM-H2 cells. Western blotting experiment showed a considerable reduction in c-Jun and JunB protein level in c-Jun#4 and JunB#6 shRNA-expressing cells (**Figure 3.3A).** Similar to results observed with the first shRNAs (**Figure 3.2F & H**), we observed a slow growth phenotype in cells expressing the second shRNAs (**Figure 3.3B**). However, KM-H2 c-Jun#4 shRNA-expressing cells reached saturation at a lower density (~$4x10^5$ cells/ml) than c-Jun#1 shRNA-expressing cells (compare **Figure 3.2H** with **Figure 3.3B**). Also, the degree of c-Jun protein reduction with c-Jun#4 shRNA was variable amongst different infections and the restoration rate of c-Jun protein with this shRNA also varied amongst different experiments, which made the experiment difficult to perform. Thus the growth curves were done on cells from one single infection which had a significant knockdown level over the experiment. Nonetheless, using two separate shRNAs, we observed a similar slow growth phenotype in c-Jun and JunB shRNA-expressing cells.

Figure 3.3

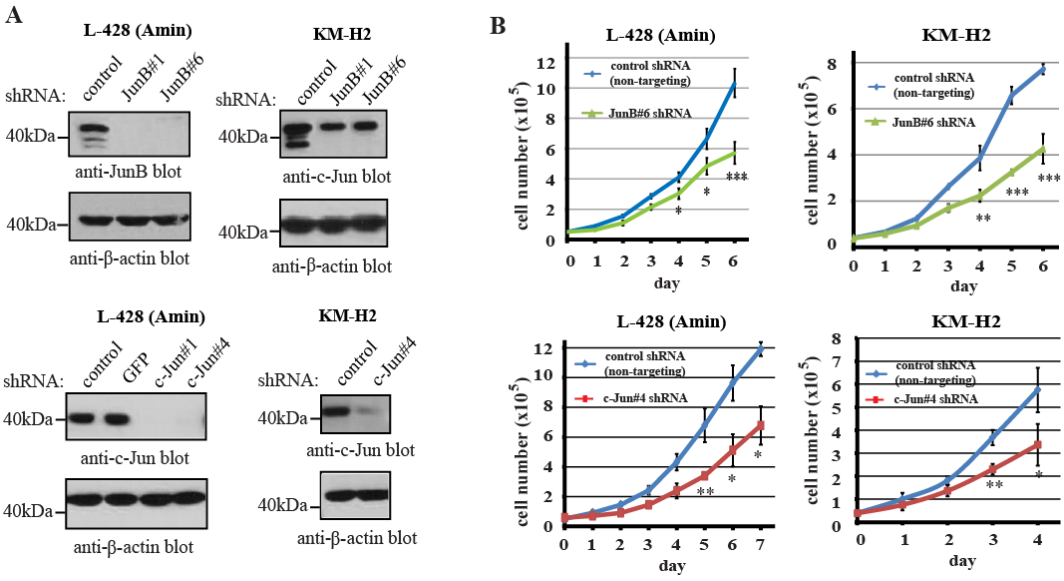

Figure 3.3 - Knockdown of c-Jun or JunB with a second shRNAs resulted in reduced growth rate.

(A) Western blots showing the level of c-Jun or JunB protein expression in the indicated shRNA-expressing cells. (**B**) Growth curves associated with the indicated shRNA-expressing cells in **A**. For western blots in **A**, the anti-β-actin blot serves as a loading control and the molecular mass markers are indicated to the left of the blots. *GFP* refers to a shRNA targeting GFP (green fluorescent protein) mRNA which is normally not expressed in human cell lines and it serves as another non-targeting control. For the growth curve in **B**, the data are the average and standard deviation of 3 independent experiments. *p* values represent independent, two-tailed *t* tests. * $p<0.05$, ** $p<0.01$, *** $p<0.001$.

3.5. c-Jun and JunB knockdown minimally affects spontaneous apoptosis rate in cHL

The slow growth phenotype could be due to a reduced proliferation rate, increased spontaneous apoptosis, or both these events. To further investigate the cause of the growth defect, we performed Terminal deoxynucleotidyl transferase mediated dUTP Nick End Labeling (TUNEL) to specifically look at the spontaneous apoptosis rate in our knockdown cells. Both L-428 (DSMZ) and L-428 (Amin) (**Figure 3.4A & B**) and KM-H2 (**Figure 3.4D**) knockdown cells did not undergo significant spontaneous apoptosis compared to control shRNA-expressing cells (**Figure 3.4**). Thus, reducing c-Jun or JunB expression does not significantly affect cell survival in L-428 and KM-H2 cell lines growing in stable culture. Interestingly, we observed a small population of apoptotic cells (10%) in L-540 c-Jun and JunB knockdown cells (**Figure 3.4C**). This suggests that apoptosis may be partly contributing to the slow growth phenotype (**Figure 3.2G**) in these cells. In addition, although the apoptosis rates associated with c-Jun/JunB knockdown were different amongst the four cell lines, the phenotype was similar between the two knockdowns within each cell line.

Figure 3.4

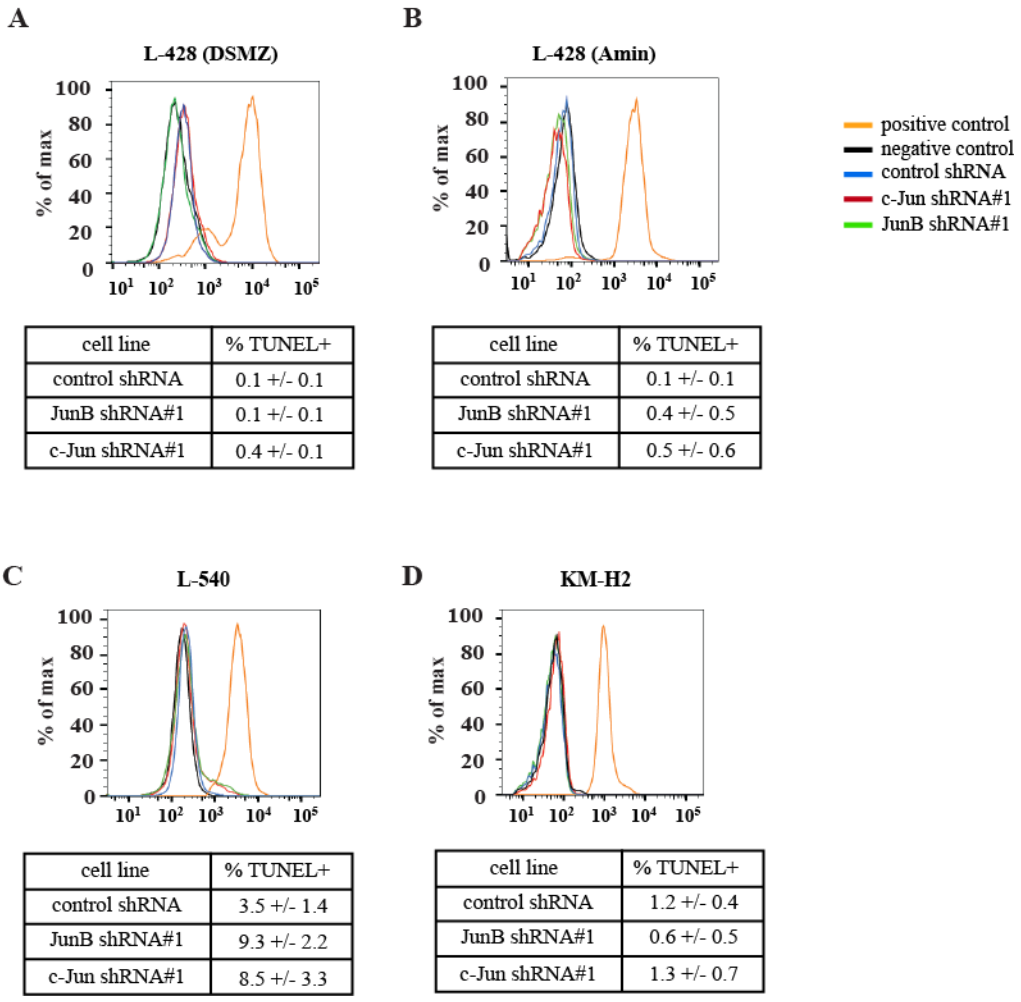

cell line	% TUNEL+
control shRNA	0.1 +/- 0.1
JunB shRNA#1	0.1 +/- 0.1
c-Jun shRNA#1	0.4 +/- 0.1

cell line	% TUNEL+
control shRNA	0.1 +/- 0.1
JunB shRNA#1	0.4 +/- 0.5
c-Jun shRNA#1	0.5 +/- 0.6

cell line	% TUNEL+
control shRNA	3.5 +/- 1.4
JunB shRNA#1	9.3 +/- 2.2
c-Jun shRNA#1	8.5 +/- 3.3

cell line	% TUNEL+
control shRNA	1.2 +/- 0.4
JunB shRNA#1	0.6 +/- 0.5
c-Jun shRNA#1	1.3 +/- 0.7

Figure 3.4 - Knocking down c-Jun or JunB has minimal effect on spontaneous apoptosis rate.

Apoptosis was examined in L-428 (DSMZ) (**A**), L-428 (Amin) (**B**), L-540 (**C**) or KM-H2 (**D**) cells expressing control, c-Jun, or JunB shRNAs. The percent TUNEL positive cells was determined by comparing the shRNA-expressing cells to the negative control which was control shRNA-expressing cells treated without

terminal transferase. DNase-treated cells were used as the positive control. Histogram plots are representative of two (L-428 (DSMZ) & L-540) or four (L-428 (Amin) & KM-H2) independent experiments from two infections. The table below shows the percentage of apoptotic cells (% TUNEL positive). These data represent the average and standard deviation of four (**B&D**) or two independent experiments (**A&C**).

3.6 Knocking down c-Jun or JunB altered the cell cycle status of cHL cell lines.

We next examined whether the growth defect was due to deregulation of the cell cycle by performing 5-bromo-2'-deoxyuridine (BrdU) labelling and 7-aminoactinomycin D (7-AAD) staining to discriminate the percentage of cells in the different stages of cell cycle. We found all knockdown cells showed a significant reduction in the proportion of cells in S phase (**Figure 3.5**). Other stages of cell cycle were also changed in the knockdowns, but this varied amongst different cell lines. While L-428 (DSMZ) knockdowns showed a 2-fold increase in the proportion of cells in G_2/M (**Figure 3.5A**), L-428 (Amin) and L-540 knockdown cells demonstrated a 1.3- to 2-fold increase in percentage of cells in G_0/G_1 (**Figure 3.5B & C**). In addition, consistent with previously observations (**Figures 3.2E-H and 3.4**), knocking down c-Jun or JunB resulted in a similar disruption of the cell cycle within each cHL cell line. Surprisingly, we observed that the two L-428 cells had different cell cycle distributions. Amin cells exhibited a much smaller number of cells in G_0/G_1 (20% vs 55%) and larger proportion of cells in G_2/M (37% vs 5%) than the DSMZ L-428 cells (compare **Figure 3.5A and B**).

Next, we wanted to know the time required for the cells to progress through each cell cycle stage in order to get a better appreciation of the defect in the cell cycle. Since the relative length of time required for the completion of cell cycle is directly correlated with the percentage of cells observed in the various stages (281), we calculated the time spent in each stage from the estimated doubling times listed in **Figure 3.2E-H** and cell cycle data in **Figure 3.5**. In all three cell lines investigated, except L-428 (Amin), knocking down c-Jun or JunB resulted in a

significant extension in G_0/G_1 (2- to 2.5-fold) and G_2/M (2- to 4-fold) (**Figure 3.5A, C-D**). L-428 (Amin) showed a prolonged G_0/G_1, but the G_2/M phase was constant between the knockdown and control cells (**Figure 3.5B**). Furthermore, although the percentage of cells in S phase was less in the knockdown cells, the time spent in S phase was similar in the control and c-Jun/JunB shRNA-expressing cells (**Figure 3.5A-C**). One exception was KM-H2 cells in which c-Jun and JunB knockdown cells exhibited a 1.4-fold increase in the duration of S phase (**Figure 3.5D**). Although the cell cycle distributions of the two L-428 cells were different (**Figure 3.5A & B**), the knockdowns exhibited a similar trend of a prolonged G_0/G_1 phase in both cells. The difference was that the Amin cells showed a much greater defect (6- to 7-fold) (**Figure 3.5B**) compared to the DSMZ cells (2-fold) (**Figure 3.5A**). Taken together, knocking down c-Jun or JunB resulted in a similar alteration in cell cycle profile within each cell line and the primary defect associated with c-Jun/JunB knockdown in all four cHL cell lines was a prolonged G_0/G_1 phase.

Figure 3.5

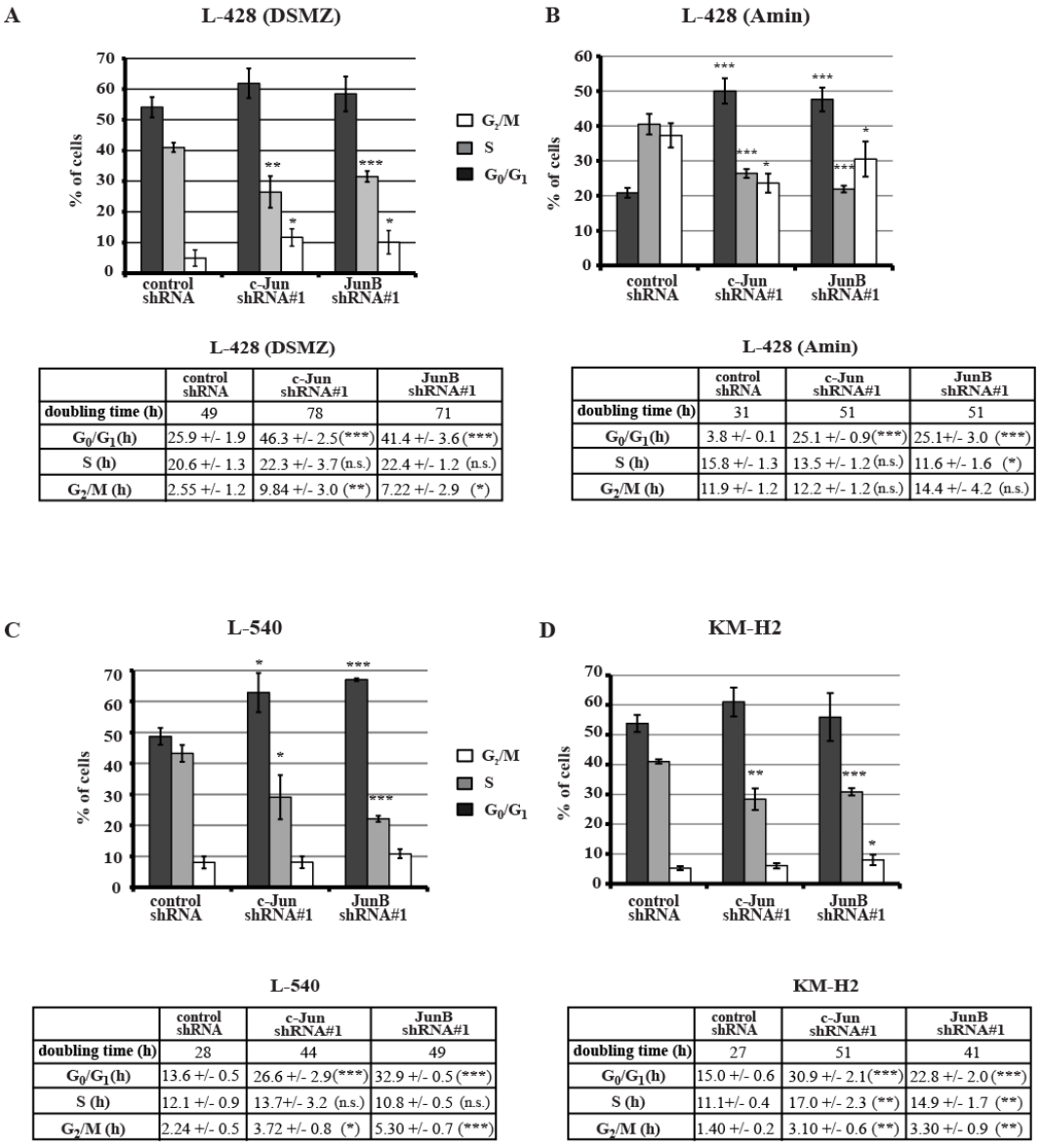

L-428 (DSMZ)

	control shRNA	c-Jun shRNA#1	JunB shRNA#1
doubling time (h)	49	78	71
G_0/G_1 (h)	25.9 +/- 1.9	46.3 +/- 2.5(***)	41.4 +/- 3.6(***)
S (h)	20.6 +/- 1.3	22.3 +/- 3.7 (n.s.)	22.4 +/- 1.2 (n.s.)
G_2/M (h)	2.55 +/- 1.2	9.84 +/- 3.0 (**)	7.22 +/- 2.9 (*)

L-428 (Amin)

	control shRNA	c-Jun shRNA#1	JunB shRNA#1
doubling time (h)	31	51	51
G_0/G_1 (h)	3.8 +/- 0.1	25.1 +/- 0.9(***)	25.1+/- 3.0 (***)
S (h)	15.8 +/- 1.3	13.5 +/- 1.2 (n.s.)	11.6 +/- 1.6 (*)
G_2/M (h)	11.9 +/- 1.2	12.2 +/- 1.2 (n.s.)	14.4 +/- 4.2 (n.s.)

L-540

	control shRNA	c-Jun shRNA#1	JunB shRNA#1
doubling time (h)	28	44	49
G_0/G_1 (h)	13.6 +/- 0.5	26.6 +/- 2.9(***)	32.9 +/- 0.5 (***)
S (h)	12.1 +/- 0.9	13.7+/- 3.2 (n.s.)	10.8 +/- 0.5 (n.s.)
G_2/M (h)	2.24 +/- 0.5	3.72 +/- 0.8 (*)	5.30 +/- 0.7 (***)

KM-H2

	control shRNA	c-Jun shRNA#1	JunB shRNA#1
doubling time (h)	27	51	41
G_0/G_1 (h)	15.0 +/- 0.6	30.9 +/- 2.1(***)	22.8 +/- 2.0 (***)
S (h)	11.1+/- 0.4	17.0 +/- 2.3 (**)	14.9 +/- 1.7 (**)
G_2/M (h)	1.40 +/- 0.2	3.10 +/- 0.6 (**)	3.30 +/- 0.9 (**)

Figure 3.5 - c-Jun or JunB knockdown cells have a deregulated cell cycle with a common prolonged G_0/G_1 phase

Figure shows the summary of four (L-428 (DSMZ) (**A**) & L-540 (**C**)) or three (L-428 (Amin) (**B**) & KM-H2 (**D**)) independent experiments analyzing the cell cycle distribution for cells labelled with BrdU and 7-AAD. The table below each graph

represents the length of each stage of cell cycle that was calculated using the percentages of cells in each stage of the cell cycle above and the doubling time in **Figure 3.2E-H**. Data represents the average and standard deviation of four (**A&C**) or three (**B&D**) independent experiments. The (*) beside each number indicates the *p* value. Note: results are derived from four independent infections for L-428 (DSMZ) and L-540, and one infection for L-428 (Amin) and KM-H2 cells. *p* values represent independent, two-tailed *t* tests.* $p<0.05$, ** $p<0.01$, *** $p<0.001$, n.s. not significant.

3.7 Knocking down c-Jun or JunB with a second shRNA showed a similar defect in the cell cycle distribution.

Similar to growth curve experiments, we also examined the cell cycle status in cHL cells expressing additional shRNAs. Consistent with the first shRNAs (**Figure 3.5B**), knocking down c-Jun or JunB in L-428 (Amin) cells with another shRNA led to a 2.5-fold increase of the proportion of cells in G_0/G_1 phase accompanied by a 2-fold decrease in the percentage of cells in S phase (**Figure 3.6A & B**). We also observed a moderate but statistically insignificant decrease in the proportion of cells in G_2/M in the knockdown cells. Nonetheless, our c-Jun#4 and JunB#6 shRNA-expressing cells demonstrated a cell cycle distribution profile that was similar to the c-Jun and JunB #1 shRNA-expressing L-428 (Amin) cells. Moreover, we also examined the cell cycle status in JunB#6 shRNA-expressing L-428 (DSMZ) (**Figure 3.6C**) and KM-H2 cells (**Figure 3.6D**). While KM-H2 cells showed a consistent profile between the two JunB shRNAs, which all resulted in a significant decrease in S phase proportion (**compare Figure 3.5D** and **3.6D**), L-428 (DSMZ) did not reach statistical significance (**Figure 3.6C**), probably because the experiment was only performed twice. Nonetheless we saw a similar trend of a decrease in S phase accompanied by an increase in G_2/M phase (**compare Figure 3.5C and 3.6C**). Overall, using another shRNA to decrease c-Jun or JunB expression, we observed similar trend of dysregulated cell cycle profile in three cHL cell lines.

Figure 3.6

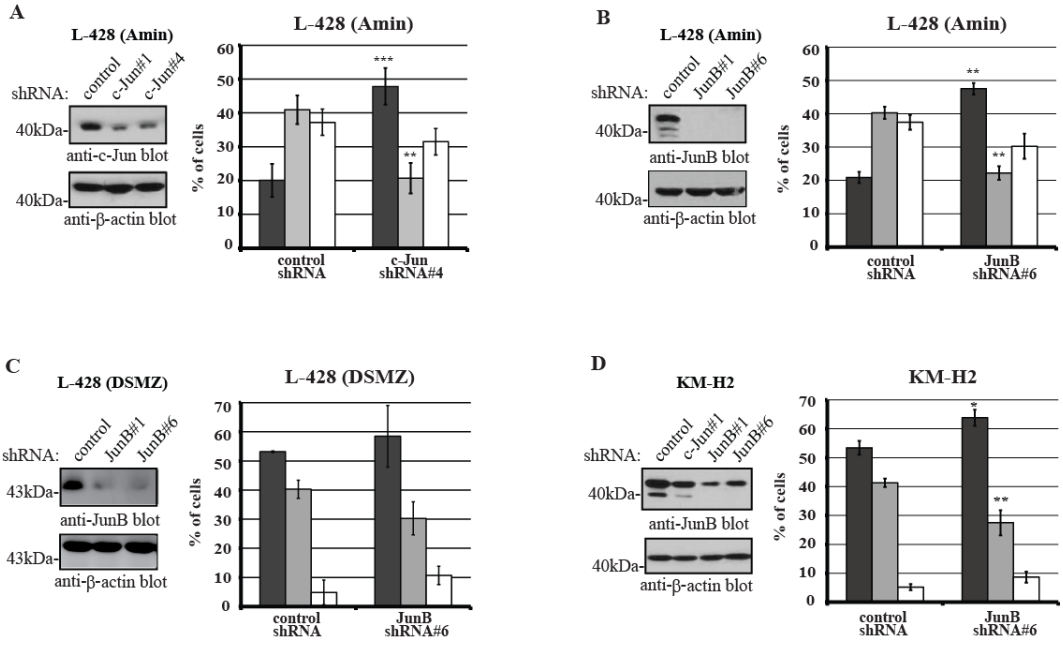

Figure 3.6 – Knocking down c-Jun or JunB with another shRNA resulted in a similar cell cycle profile as the first shRNAs

Three cHL cell lines L-428 (Amin) (**A&B**)**,** L-428 (DSMZ) (**C**) and KM-H2 (**D**) cells expressing a different shRNA were examined for cell cycle status. The western blots (left) indicates the level of c-Jun/JunB protein expression in the corresponding shRNA-expressing cells. The anti-β-actin blot serves as a loading control and the molecular mass markers are indicated to the left of the blots. The cell cycle distribution (right) represents the summary of four (**A**), two (**B&C**) or three (**D**) independent experiments analyzing the cell cycle distribution for cells labelled with BrdU and 7-AAD. Note: results are derived from one independent infections for L-428 (Amin) and L-428 (DSMZ), and two infections for KM-H2 cells. *p* values represent independent, two-tailed *t* tests.* $p<0.05$, ** $p<0.01$, *** $p<0.001$,

3.8 Comparing the two L-428 cell lines

Since we observed a phenotypic difference between the DSMZ and the Amin L-428 cells in their growth rate (**Figure 3.2E & F)** and cell cycle status **(Figure 3.5A & B**), we wanted to further compare these cell lines. One of the molecular signatures published for the DSMZ L-428 cells is the expression of two fusion transcripts, *ELMO1-SLCO3A1* and *TNRC18B-MYLPF* (70). As expected, our L-428 (DSMZ) cells expressed both fusion transcripts; and they were not detected in ALK+ ALCL cell lines and other cHL cell lines (KM-H2 and L-540) (**Figures 3.7A and B**). To our surprise, the L-428 (Amin) cells expressed *TNRC18B-MYLPF* but not the *ELMO1-SLCO3A1* fusion transcript (**Figures 3.7A and B**). We further showed we could not amplify the ELMO1-SLCO3A1 fusion gene by PCR on genomic DNA (**Figure 3.7C**). Our inability to detect the *ELMO1-SLCO3A1* fusion transcript in the L-428 (Amin) cells led us to further investigate other molecular signatures of these cells. First, L-428 cells have been demonstrated to have a distinct *TP53* mutation in exon 4, which causes a premature stop codon and results in a truncated form of *p53* (121). PCR of genomic DNA showed both Amin and DSMZ L-428 cells were heterozygous at the *TP53* locus with one wild-type allele and the other allele associated with a small deletion in exon 4 (**Figure 3.7D**) as previously reported (121). RT-PCR on mRNA further confirmed the small deletion in *p53* in both the Amin and DSMZ L-428 cells and this deletion was distinct to L-428 cells because all other cell lines tested showed full length *p53* in exon 4 (**Figure 3.7E**). Thus our data were similar to published results (121), suggested both Amin and DSMZ cells are L-428 cells because they only expressed the truncated allele. To

further investigate the Amin cell identity, we performed short tandem repeat (STR) profiling to authenticate the cell line. Based on the report (**Figure 3.7F**, **Appendix 3**), the DSMZ cells had a complete match with the repository reference but the Amin cells showed three loci with loss of heterozygosity (LOH). Nonetheless, the Amin cells showed 7 out of 10 loci matched with reference data. This strongly suggests that the Amin cell is derived from the same origin as the DSMZ L-428 cells but may have incurred some mutations. KM-H2, which was used as a negative control, demonstrated a completely different profile from these two L-428 cells. Therefore, the two L-428 cells are likely derived from the same original cell but they have undergone changes that affect their growth rate and cell cycle profile.

Figure 3.7

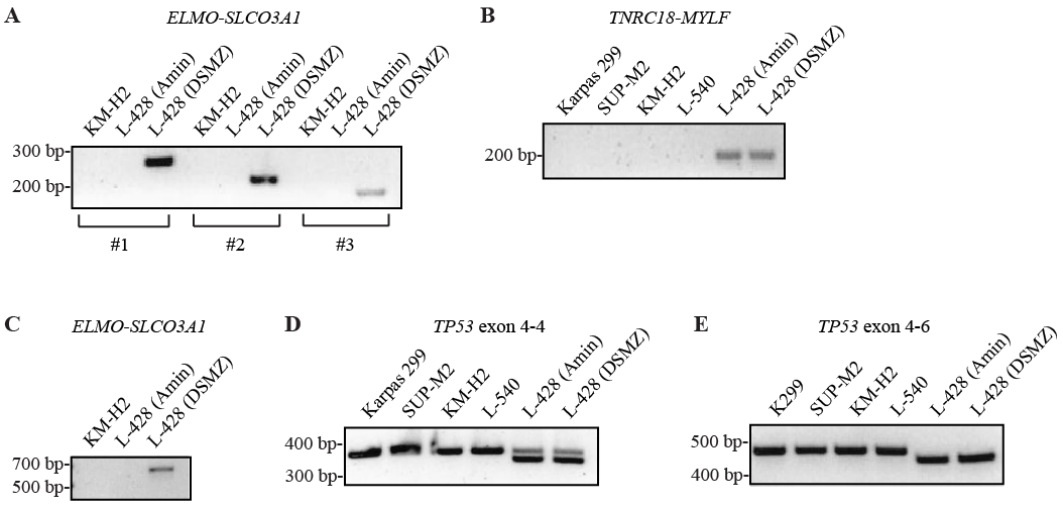

F **Short Tandem Repeats (STR) Profile**

	L-428 (ref)	L-428 (DSMZ)	L-428 (Amin)	KM-H2
AMEL	X / X	X / X	X / X	X / X
CFS1PO	10 / 13	10 / 13	10 / 10	10 / 14
D13S317	14 / 14	14 / 14	14 / 14	10 / 11
D16S539	11 / 12	11 / 12	11 / 11	9 / 9
D21S11	31.2 / 31.2	31.2 / 31.2	31.2 / 31.2	30 / 31.2 / 32.2
D5S818	11 / 12	11 / 12	11 / 11	11 / 13
D7S820	11 / 11	11 / 11	11 / 11	11 / 12
TH01	7 / 9.3	7 / 9.3	7 / 9.3	7 / 9
TPOX	8 / 9	8 / 9	8 / 9	8 / 10 / 11 / 12
vWA	15 / 15	15 / 15	15 / 15	17 / 18

Figure 3.7 - L-428 (Amin) and (DSMZ) cell lines comparison

RT-PCR analysis of *ELMO-SLCO3A1* (**A**) and *TNRC18-MYLF* (**B**) for detection of the indicated fusion transcripts. Three different primer sets were used in **A** to identify the *ELMO-SLCO3A1* transcript. **C** PCR analysis of genomic DNA with primers spanning the breakpoint of *ELMO-SLCO3A1*. **D-E** Analysis of *TP53* deletion in L-428 cells. **D** PCR analysis of genomic DNA with exon 4 specific primers spanning the deletion point. The doublet represents the heterozygous mutation in L-428 cells, which have one wild type and one mutant allele. **E** RT-

PCR analysis using primers spanning exons 4 to exon 6. KM-H2, L-540 and the ALK+ ALCL cell lines Karpas 299 and SUP-M2 were used as negative controls. For **A-C** and **D-E,** L-428 data was a representative of two independent experiments from two different samples. The sizes of PCR products are shown to the left of each gel. **F** STR profiling using GenePrint 10 system. The ten markers examined are listed to the left and the values of each allele are separated by a dashed line. L-428 (ref) refers to the reference value obtained from the database of DSMZ for the L-428 (DSMZ) cell line.

3.9 Knockdown cells require longer time to progress through G_0/G_1 to enter S phase after nocodazole block at G_2/M.

In all four cHL cell lines we examined, the primary reason for the decreased proliferation rate of c-Jun and JunB knockdown cells was a delay in G_0/G_1 phase. While the L-428 (Amin) cells showed a 5- to 6-fold increase in G_0/G_1 phase in knockdown cells (**Figure 3.5B**), KM-H2, L-428 (DSMZ) and L-540 showed similar trend with a 2- to 2.5-fold increase (**Figure 3.5A, C & D**). To further investigate the delay in G_0/G_1, we decided to specifically examine the time required for cells to progress through G_0/G_1 phase by blocking cells at mitotic prometaphase (G_2/M) with nocodazole (282) and monitor their progression through the cell cycle. Nocodazole, a microtubule inhibitor, disrupts microtubule formation and results in accumulation of cells at the onset of metaphase (217, 283, 284).

We chose to use L-428 (Amin) cells because the knockdowns showed the greatest defect in G_0/G_1 (**Figure 3.5B**). We were able to block the majority of cells (~70-80%) at G_2/M in all the cell lines, but there was still a proportion (~20%) of cells that were in G_0/G_1 or S phase at the start of experiment (**Figure 3.8A**). We chose not to extend the length of blocking or increase the concentration of nocodazole because this has been shown to cause permanent cellular damage and spontaneous apoptosis in other cell types (282, 285). After 12 hours post release, the majority of cells had accumulated at G_0/G_1 phase (70-80%). We observed the knockdown cells required a longer time for the same amount of cells to progress to S phase. For example, it took 24 hours for ~30% of control cells to accumulate in S phase whereas 36 hours was required for the same percentage of knockdown cells

to enter S phase (**Figure 3.8A**). We then quantified the percentage of cells in each cell cycle stage at different time points after release from four different experiments. We found that c-Jun/JunB knockdown cells had a significantly larger population of G_0/G_1 cells 24 hours post-release accompanied by a smaller proportion of S phase cells compared to control shRNA-expressing cells (**Figure 3.8B**) In addition, we observed a 1.5- to 2-fold increase in the percentage of G_2/M cells in c-Jun/JunB shRNA-expressing cells after 12 hours release suggesting the knockdown cells required longer time to get out of G_2/M (**Figure 3.8B**). Thus the data suggest a delay in G_0/G_1 or the G_1/S transition in c-Jun/JunB shRNA-expressing cells which was consistent with previous observations (**Figure 3.5B**).

Figure 3.8

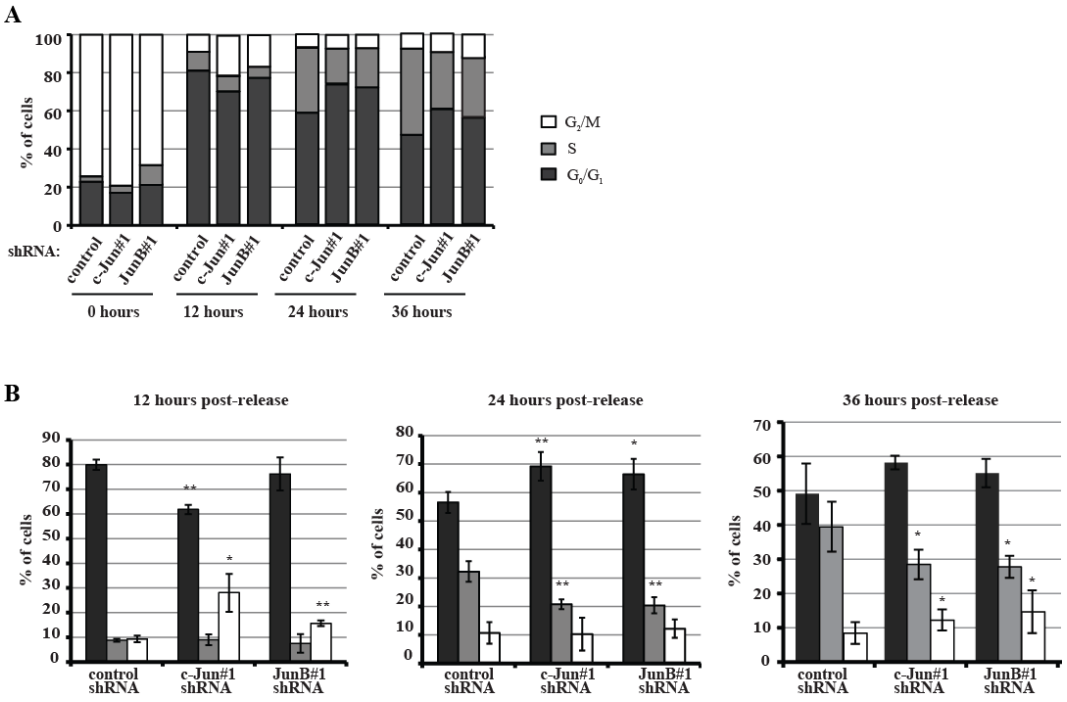

Figure 3.8 - Cell cycle dysregulation in c-Jun and JunB knockdown L-428 (Amin) cells following nocodozole block at G_2/M

A. Representative BrdU/7-AAD co-staining experiment from four independent experiments demonstrating the percentage of L-428 (Amin) cells expressing control, c-Jun, or JunB shRNA at the indicated times after release from nocodazole block **B.** Average and standard deviation of four independent experiments described in **A.** showing the cell cycle distribution at 12, 24 or 36 hours post release from nocodazole block. For **B**, *p* values were obtained by performing independent, two-tailed *t* tests comparing the c-Jun/JunB knock-down cells at each stage of the cell cycle with corresponding control shRNA-expressing cells. * $p<0.05$, ** $p<0.01$, *** $p<0.001$. Note: these data were generated using L-428 (Amin) cells.

3.10 Knocking down c-Jun or JunB impaired L-428 tumour cell growth *in vivo*

To further investigate c-Jun/JunB function in tumour formation and tumour growth, we examined cHL tumour growth in immunocompromised mice. We used L-428 (Amin) cells that were infected with an shRNA vector conferring resistance to G418 as a selection marker for mice experiments because the knockdown cell lines demonstrated a more stable knockdown than cells infected with shRNAs conferring puromycin resistance. The newly infected L-428 (Amin) cells were examined for their c-Jun and JunB protein expression prior to injection (**Figure 3.9A**). Both c-Jun and JunB shRNA-expressing cells demonstrated a reduction in their corresponding protein levels. Mice were injected with these cells and tumour growth was examined. When the majority of the control group reached experimental end-point (~58 days), we harvested the tumours from all mice and observed significantly larger tumours from mice injected with control shRNA-expressing cells compared to mice injected with c-Jun/JunB shRNA-expressing cells (**Figure 3.9B**). In addition, tumour length and width were measured at the end point and tumour volume was calculated. Statistical analysis showed that c-Jun and JunB shRNA-expressing cells generated smaller tumours (**Figure 3.9B)**. Moreover, tumour weight was measured and we observed a significant reduction in tumour weight (~80%) in tumours formed by c-Jun or JunB shRNA-expressing cells when compared to tumours formed by control shRNA-expressing cells (**Figure 3.9C**). Therefore, c-Jun and JunB not only promote cHL cell line proliferation in vitro, they are also important for cHL tumour growth *in vivo*.

Figure 3.9

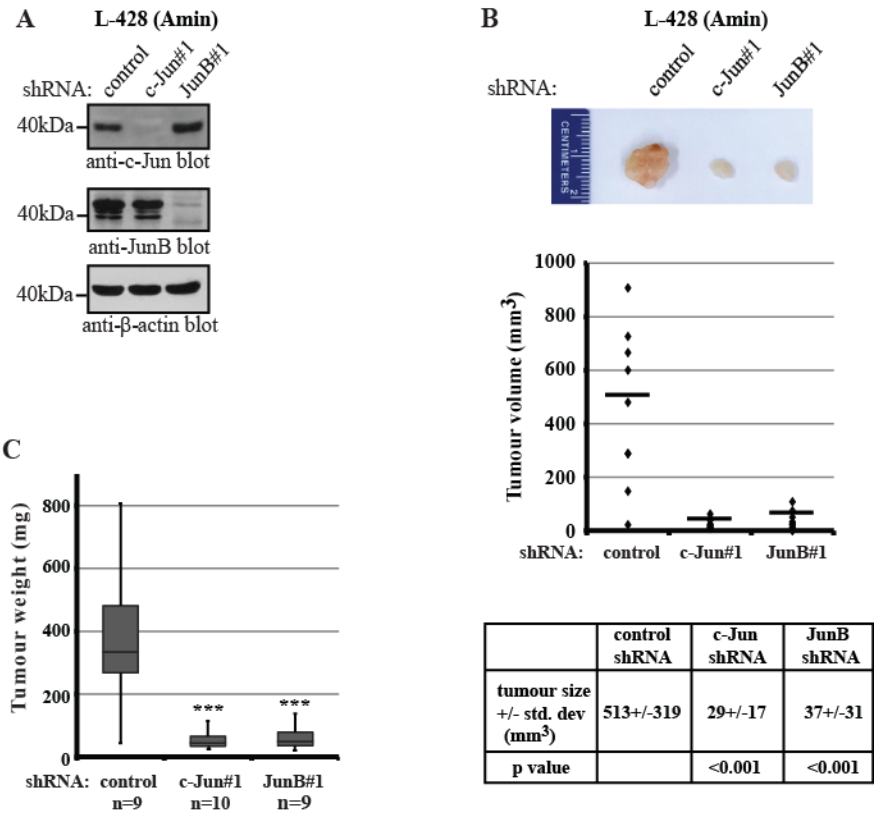

	control shRNA	c-Jun shRNA	JunB shRNA
tumour size +/- std. dev (mm^3)	513+/-319	29+/-17	37+/-31
p value		<0.001	<0.001

Figure 3.9 - c-Jun and JunB knockdown impairs the ability of the L-428 (Amin) cHL cell line to form tumours in immunocompromised mice.

A. Western blots showing the degree of c-Jun and JunB silencing in L-428 (Amin) cells expressing the indicated shRNAs. Molecular mass markers are indicated to the left of blots. The anti-β-actin blot serves as a loading control. **B.** Ten mice were injected with each of the shRNA-expressing cell lines shown in **A.** At the end point (fifty-nine days after injection), mice were euthanized and tumours were harvested. The picture shows a representative median sized tumour from each of the groups, and the dot plot shows the raw data for each of the tumour groups. The average and standard deviation of each group is listed in the table below with the corresponding

p values comparing c-Jun/JunB shRNA-expressing tumour size with control shRNA-expressing tumours. **C**. Whisker-box plot showing the weight (in mg) of tumours isolated from mice described in **B.** The results shown in this figure are representative of two independent experiments. Note: at end point, we had nine mice in the control and JunB shRNA groups because one mouse in the control shRNA group was euthanized prior to day 59 due to an unacceptable large tumour and we could not find the tumour in one mouse in the JunB shRNA group. *p* values were obtained by performing independent, two-tailed *t* tests comparing the volume (**B**) or weight (**C**) of tumours formed by c-Jun/JunB knockdown cells compared to control shRNA-expressing cells. *** $p<0.001$. Note: the data were generated using L-428 (Amin) cells

3.11 c-Jun and JunB double knockdown cells had a similar slow growth rate as single knockdown cells

Finally, we wanted to examine the effect of knocking down both c-Jun and JunB genes on cHL growth rate. We generated L-428 double knockdown cell lines using shRNA-containing vectors with G418 and puromycin resistance markers and examined c-Jun and JunB protein levels by western blotting (**Figure 3.10A**). We then performed growth curve assays to look at the effect of knocking down these proteins on growth rate. Interestingly, the double knockdown cells exhibited a similar slow growth phenotype as c-Jun/JunB single knockdown cells (**Figure 3.10B**). We also used the Resazurin-based viability assay (286) to quantify the number of live cells at later days in the growth curve and observed a similar reduction in the number of live cells in c-Jun/JunB double shRNA-expressing cells (**Figure 3.10C**). Statistical analysis showed that all the knockdown cells had significantly reduced cell numbers compared to control cells, but there was no statistically significant difference between the double and single knockdown cells (**Figure 3.10D & E**). Therefore, based on these results, c-Jun and JunB double knockdown cells had a comparable growth defect to single knockdown cells.

Figure 3.10

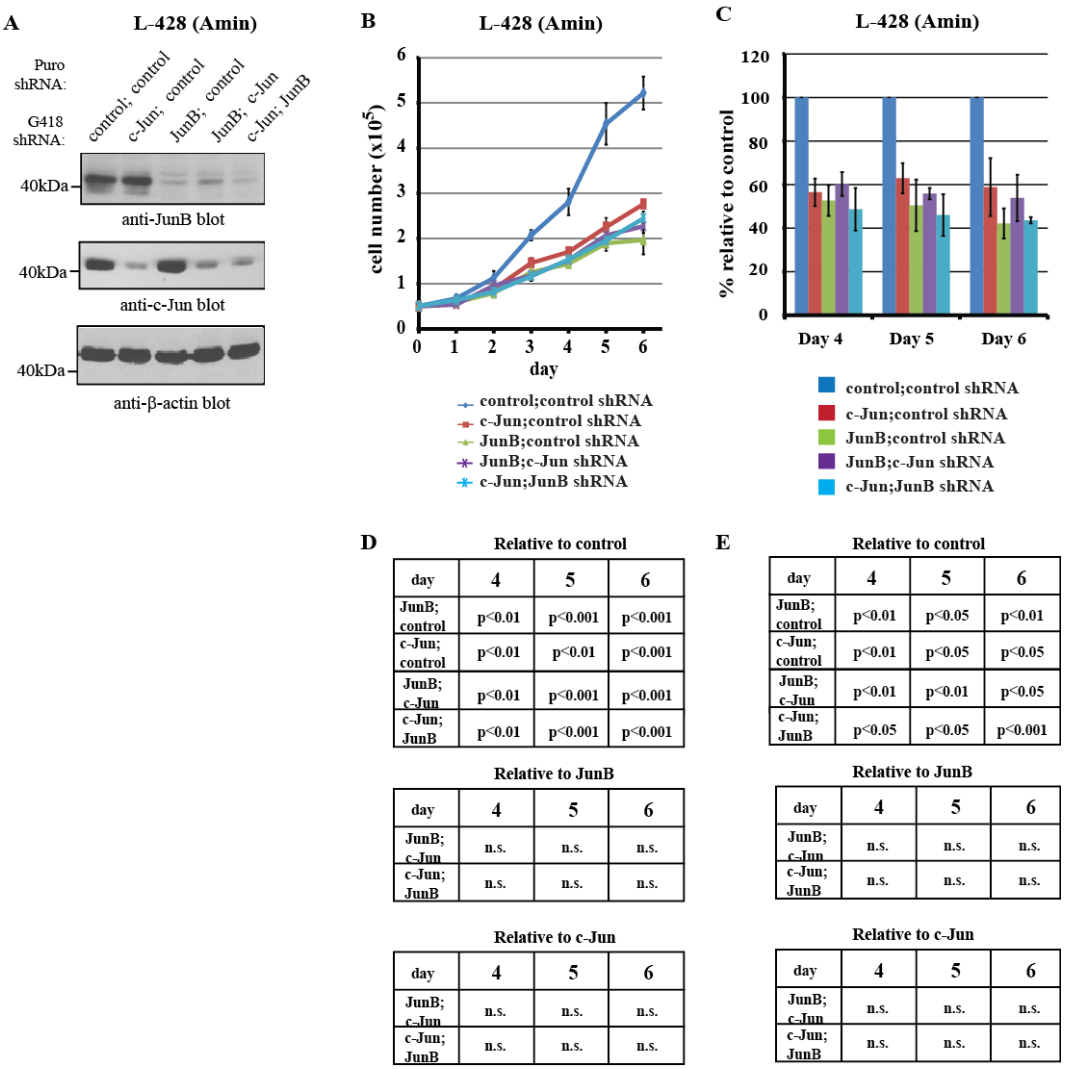

D

Relative to control

day	4	5	6
JunB; control	p<0.01	p<0.001	p<0.001
c-Jun; control	p<0.01	p<0.01	p<0.001
JunB; c-Jun	p<0.01	p<0.001	p<0.001
c-Jun; JunB	p<0.01	p<0.001	p<0.001

Relative to JunB

day	4	5	6
JunB; c-Jun	n.s.	n.s.	n.s.
c-Jun; JunB	n.s.	n.s.	n.s.

Relative to c-Jun

day	4	5	6
JunB; c-Jun	n.s.	n.s.	n.s.
c-Jun; JunB	n.s.	n.s.	n.s.

E

Relative to control

day	4	5	6
JunB; control	p<0.01	p<0.05	p<0.01
c-Jun; control	p<0.01	p<0.05	p<0.05
JunB; c-Jun	p<0.01	p<0.01	p<0.05
c-Jun; JunB	p<0.05	p<0.05	p<0.001

Relative to JunB

day	4	5	6
JunB; c-Jun	n.s.	n.s.	n.s.
c-Jun; JunB	n.s.	n.s.	n.s.

Relative to c-Jun

day	4	5	6
JunB; c-Jun	n.s.	n.s.	n.s.
c-Jun; JunB	n.s.	n.s.	n.s.

Figure 3.10 - Examining the growth defect in L-428 (Amin) double knockdown cells

(**A**) c-Jun and JunB protein levels were examined by western blotting in control shRNA-expressing cells, single c-Jun and JunB knockdown cells, and double knockdown cell lines. Note: each cell line is indicated by the two shRNAs used, separated by a semicolon. The anti-β-actin blot serves as loading control and the molecular mass markers are to the left of the blots. Growth rate was examined by

(**B**) live cell counting using Trypan blue exclusion and (**C**) Resazurin-based viability assay. For **B** and **C,** the data are the average and standard deviation of 3 independent experiments. The *p* values listed in the tables in **D** and **E** represent independent, two-tailed *t* tests (**D**) and paired two tail *t*-test (**E**) comparing knockdown cell lines to control cells, double knockdown cells with JunB single knockdown cells, and double knockdown cell lines with c-Jun single knockdown cells. Note: **D** represents *p* values for the growth curves in **B,** and **E** represents *p* values for the Resazurin assay in **C**. All experiments in **Figure 3.10** were from the same initial population of cells and were performed using L-428 (Amin) cells.

3.12 c-Jun was up-regulated in JunB knockdown cells over time

One interesting observation we had in our shRNA-mediated knockdown cell lines was that the c-Jun level was modestly up-regulated in KM-H2 JunB shRNA expressing cells (**Figure 3.2D**). To examine this phenotype further, we collected L-428 (Amin) and KM-H2 cell lysates from the same infection at two different time points and examined c-Jun and JunB expression levels over time. We observed a consistent trend in JunB knockdown cells where c-Jun levels gradually increased over time in L-428 (Amin) cells (**Figure 3.11A**). This phenotype was highly variable in terms of the degree of up-regulation and the time required to observe this effect. Although KM-H2 JunB knockdown cells also demonstrated a modest up-regulation of c-Jun, this did not increase as much over time as the early and late stage cells showed a similar extent of up-regulation (**Figure 3.11B**). In contrast, we did not observe JunB up-regulation in the c-Jun knockdown cells.

Figure 3.11

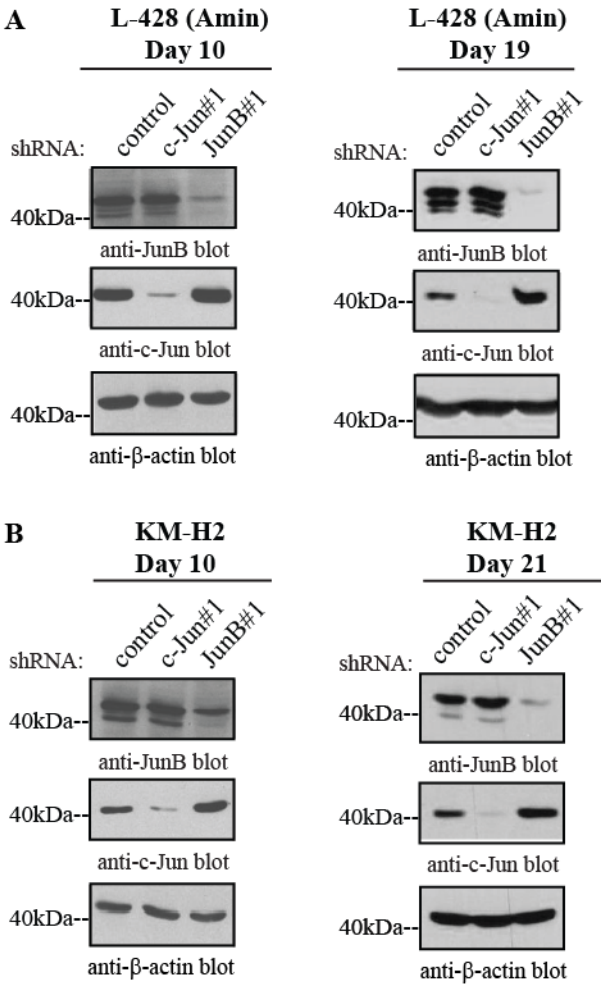

Figure 3.11 - Up-regulation of c-Jun in JunB shRNA-expressing cells.

Western blots showing c-Jun and JunB protein levels in L-428 (Amin) (**A**) and KM-H2 (**B**) cells. Samples were collected at different time points post selection and was indicated on the top of each blot. The anti-β-actin blot serves as loading control and molecular mass markers are indicated to the left of the blots. Note: The degree of c-Jun up-regulation was variable amongst different infections and these blots were chosen to represent an intermediate degree of up-regulation amongst at least three sample sets.

3.13 Discussion

3.13.1 Summary of findings

In this study, we investigated the role of c-Jun and JunB in regulating HRS cell proliferation and apoptosis by specifically knocking down these genes using shRNAs targeting the *c-Jun* and *JunB* mRNAs. In all the cHL cell lines examined, we observed a reduced growth rate and an approximate 2-fold longer doubling time in c-Jun/JunB knockdown cells (**Figures 3.2**) with minimal effect on spontaneous apoptosis rates (**Figure 3.4**). One exception was L-540 cells where we observed a 10% increase in apoptosis rate in c-Jun/JunB knockdown cells (**Figure 3.4C**). To further characterize the growth defect, we estimated the duration of each stage of cell cycle and found that both c-Jun and JunB knockdowns exhibited a similar defect on the cell cycle with an extended G_0/G_1 phase. This phenotype was common to all four cHL cell lines examined (**Figure 3.5**). In addition, L-428 (DSMZ), KM-H2 and L-540 cells also exhibited a moderately prolonged G_2/M phase (**Figure 3.5**). The growth defect and deregulated cell cycle were confirmed with another c-Jun/JunB shRNA (**Figure 3.3 & 3.6**). Furthermore, we showed that L-428 (Amin) c-Jun/JunB shRNA-expressing cells formed smaller tumours *in vivo* (**Figure 3.9**). Taken together, we demonstrated that the c-Jun and JunB transcription factors are important in cHL cell line proliferation and tumour growth and both AP-1 proteins contribute to cHL proliferation in a similar manner within cell lines. In addition, we determined that the major cause of the longer doubling time observed in all knockdown cells was due to a significantly longer G_0/G_1 phase. In contrast to previous studies (130, 256), this is the first study to discriminate the contribution of c-Jun and JunB in cHL proliferation and apoptosis. .

3.13.2 Comparing our cell cycle results with published data and future directions for unveiling the cell cycle defect associated with c-Jun/JunB knockdown.

Previously, the Leventaki group published that JNK promotes cHL tumour cell proliferation (256). Specifically, they showed that inhibition of JNK activity using the JNK inhibitor, SP600125, resulted in a G_2/M arrest in L-1236 and L-428 cells as judged by a 2-fold increase in the G_2/M population and a complete inhibition of growth of cell colonies. Consistent with their published data, we also observed a 2-fold increase in G_2/M population in our L-428 (DSMZ) knockdown cells in addition to a modest decrease in S phase (**Figure 3.5A**). However, this blockage was not common to all cHL cell lines as we did not observe this G_2/M block in KM-H2 or L-540 cells (**Figure 3.5 C-D**). We further estimated the time required to pass through each stage of cell cycle using the doubling time and the cell cycle distribution profile. Instead of a G_2/M arrest, we found that the primary defect is a prolonged G_0/G_1 and this phenotype was common to all four cell lines examined. There are at least two possible reasons for the different conclusions of our study with Leventaki's study. One reason comes from the inhibitor SP600125, which had been previously shown to inhibit other molecules such as CDK2 (287, 288) which is known to regulate the G_2/M phase (117, 212). Thus, the much more severe defect in G_2/M observed by Leventaki's group could be the result of inhibiting these molecules whereas we only investigate c-Jun effect. Another reason is our experimental methods used for quantification of cell cycle distribution, which could contribute to the different percentages obtained in untreated cells from these

two studies. While we used BrdU/7-AAD to discriminate the stages of the cell cycle, Leventaki's group used propidium iodide staining to quantify the stages.

One question that remains to be resolved is whether the extended G_0/G_1 is due to a delay in G_1 or cells entering G_0 because in our study, we could not differentiate cells in G_0 from G_1 phase. To discriminate the two phases, we could use flow cytometry analysis to examine cycle specific proteins such as Ki-67 (289). Ki-67 is expressed in all phases of cell cycle except during G_0 phase (290) and immunohistochemistry studies showed its expression level is relatively high in cHL patient samples (291, 292). Also, there is some evidence suggesting inhibition of c-Jun led to a reversible entry into a G_0-like state in cycling cells (208). Therefore, it is possible that the higher proportion of G_0/G_1 cells in the knockdown cell lines was the result of increased numbers of cells in G_0 phase.

3.13.3 Limitations of study and unresolved issues

We also observed a similar growth defect in L-428 c-Jun/JunB double knockdown cells as the c-Jun and JunB single knockdown cells (**Figure 3.10**). We postulate that we did not observe a further reduction in the growth rate in the double knockdowns cells because the cells had already reached a minimal growth rate in the single knockdowns. Other possibilities such as redundancy between c-Jun and JunB will be discussed in detail in **Section 5.5**. However, although we did not see a further reduction in growth rate from the growth curve, we can not exclude the possibility that double knockdown cells have a greater proliferation defect because of the limitation of our approach and assay which may not be able to measure further reduction in growth rate in the double knockdown cells. Therefore, a much

more sensitive method such as BrdU/7-AAD labelled proliferation assay should be used instead. We did not perform cell cycle analysis because we could not obtain enough cells to perform before restoration of c-Jun or JunB occurred. Moreover, since these cells were grown in media containing two drugs (G418 and puromycin), they grew much slower than cells used in previous experiments (compare growth rates in **Figure 3.2F** and **3.10B**). Thus, to reduce the time required for finishing selection, we could use a lentiviral vector containing both shRNAs to generate double knockdown cells (293) so we have more time for other biological experiments.

In our study, we used a shRNA-mediated gene silencing approach to specifically knockdown c-Jun and JunB to look at their function individually. This method is a good way to differentiate the relative contribution of c-Jun and JunB in cHL proliferation; however, there are several caveats associated with our stable knockdown cell lines. For example, we observed an up-regulation of c-Jun protein levels in KM-H2 and L-428 (Amin) JunB shRNA-expressing cells (**Figure 3.2D and 3.11)** and this phenotype was more prominent in L-428 (Amin) cells grown for longer periods of time (compare **Figure 3.11A** early and later stages). This phenotype was observed by another group when using JunB shRNA that led to an up-regulation in c-Jun protein in 3T3-immortalized mouse fibroblasts (294). The authors of this study postulated that this elevated c-Jun protein levels could be due to the relief of competition by JunB on the c-Jun promoter. Specifically, JunB normally can interfere with c-Jun transactivation by competing for the promoter site (176, 182). Thus knocking down JunB leads to better access of c-Jun to its own

promoter and hence increases c-Jun transcription. However, we do not have mRNA data corresponding to the later stages to confirm this hypothesis because we focused our experiments at early stages to rule out any compensatory effect of c-Jun. Interestingly, we did not observe a similar up-regulation of JunB protein in the c-Jun shRNA-expressing cell lines. Thus, in our cHL cell lines, c-Jun expression appears to be induced in response to the loss of JunB but not the other way around. Similar to the induction of c-Jun, we also observed a gradual restoration of both JunB and c-Jun protein in the knockdown cell lines but restoration of c-Jun was faster. Therefore, for our study, experiments were performed at an early stage post-selection to limit the effect of c-Jun induction and restoration.

Another caveat of our shRNA approach is the potential of selecting for cells that undergo alterations in order to tolerate c-Jun/JunB knockdown. Although we tried to conduct our experiments as early as possible to limit the chances of selecting cells that could tolerate the loss of c-Jun/JunB, we still need to take this into account when analyzing data. For example, we showed that c-Jun and JunB have no effect on apoptosis in L-428 and KM-H2 cells (**Figure 3.4A-B, D**); however, this conclusion can only be drawn from our model system because we intentionally selected for cells that could survive and proliferate over time. c-Jun and JunB may still have effect on apoptosis but these cells were lost during selection period before we performed our experiment. Nonetheless, we believe the effect is minor because for all the infections we performed, we did not observe a vast population of cells that were undergoing apoptosis post selection.

Another pitfall of our experiments is the lack of a second distinct JunB shRNA that can effectively knockdown JunB. The two JunB shRNAs are not totally distinct shRNA because JunB#6 shRNA overlaps with JunB#1 shRNA (**Appendix 1**), so it is not surprising that the growth and cell cycle defects were similar with the two shRNAs (compare **Figure 3.2** and **3.3**, **3.5** and **3.6**). Because these two shRNAs overlap, we cannot rule out that our observed phenotypes are due to the off-targeting of the shRNAs. Thus we need to find another shRNA to resolve this issue. If not, we need to add JunB cDNA into JunB#1 shRNA-expressing cells to see if we can rescue the phenotype. These alternative approaches will be discussed in detail in Chapter 5 (Section **5.4**).

In our study, we used two L-428 cells from two different sources and observed some differences in their growth rate (**Figure 3.2A & B**) and cell cycle distribution (**Figure 3.5A & B**). However, given our analyses (**Figure 3.7**) we are confident that the two L-428 cells are derived from same origin. Moreover, the fact that both L-428 knockdown cells exhibited a delay in G_0/G_1 (Tables in **Figure 3.5 A-B**) further supports that c-Jun and JunB affect G_0/G_1 progression in cHL. However, given that L-428 (Amin) cells showed LOH at three loci (**Figure 3.7D**) and our inability to amplify ELMO-SLC3OA1 fusion gene (**Figure 3.7A & C**), there are definitely some differences between the two cells. Thus, the experiments which were performed only on L-428 (Amin) cells (**Figure 3.8-3.11**) need to be repeated in the future on L-428 (DSMZ) to provide a more conclusive understanding of c-Jun and JunB function in L-428 cell cycle regulation and tumour growth *in vivo*.

5.13.4 Conclusions

In conclusion, using shRNA-mediated gene knockdown approach, we were able to show that both c-Jun and JunB promote cHL cell line proliferation in vitro and in vivo. Moreover, they function similarly within cell lines primarily by altering the cell cycle at G_0/G_1. However, we would need to have another JunB shRNA to confirm the JunB-regulated proliferation phenotype.

CHAPTER 4: EXAMINING CHANGES IN TRANSCRIPTIONAL PROFILE IN C-JUN AND JUNB KNOCKDOWN CHL CELL LINES BY MICROARRAY STUDIES

4.1 Introduction

cHL is characterized by aberrant expression of c-Jun and JunB and strong AP-1 activity. In Chapter 3, we showed that c-Jun and JunB promote cHL cell proliferation and tumour growth. In this chapter, we wanted to determine what genes and other cellular activities they regulate in cHL. Previous work had identified some AP-1-regulated genes in cHL. For example, AP-1 activity in L-428 cells has been demonstrated to promote the expression of the G_1 regulator, cyclin D2, and the proto-oncogene, c-met (130). Also, the c-Jun upstream regulator, JNK, has been shown to influence the expression of $p21^{Cip1}$ in KM-H2 cells (256). Furthermore, JunB promotes the expression of CD30 (259, 260), which activates many cellular pathways including the MEK/ERK pathway and the NFκB pathway to enhance HRS cell proliferation and inhibit apoptosis (90, 91, 99). Several studies have also revealed a potential role for c-Jun and JunB in maintaining the immunosuppressive environment of cHL. For example, they promote the expression of PD-L1 in cHL, which contributes to the escape of HRS cells from immune attack by inhibiting CTL activation (88, 265). c-Jun had also been shown to influence the expression of Galectin-1, which contributes to the immunosuppressive microenvironment by promoting the secretion of Th2 cytokines and increases the relative abundance of Tregs (82, 83, 264). In addition, AP-1 signalling had also been demonstrated to partially influence the production of LTA, a molecule secreted by HRS cells to regulate the recruitment of naïve CD4 T cells (267).

Since AP-1 sites are commonly found across the human genome (295), we hypothesized there were many more unknown downstream transcriptional targets of c-Jun and JunB in cHL. More importantly, we wanted to compare how gene expression was altered in c-Jun and JunB knockdown cells. Our analysis so far implied that c-Jun and JunB promote cHL proliferation by primarily facilitating the progression through the G_0/G_1 phase (Chapter 3). We hypothesized that c-Jun and JunB influence the expression of additional genes involved in cHL pathogenesis. Moreover, because c-Jun and JunB knockdowns shared a similar proliferation defect within cell lines, we postulated that c-Jun and JunB may share some transcriptional targets within each cell line. Therefore, in this chapter, we performed cDNA microarrays to identify differentially expressed genes in c-Jun and JunB knockdown cells, validated the mRNA and protein expression changes of several targets, and classified their cellular activities to better understand c-Jun and JunB function in cHL.

4.2 c-Jun/JunB-dependent gene profiling in L-428 (Amin) and KM-H2 cells

To identify additional c-Jun/JunB-regulated targets in cHL cell lines, gene expression profiling was performed on cHL cell lines. RNA from c-Jun#1 shRNA, JunB#1 shRNA and a non-targeting control shRNA-expressing cells were sent to the ATAGC microarray facility (University of Alberta) where they were converted to aRNA and subjected to affymetrix oligo microarray analysis (**Figure 4.1**). This experiment was performed on L-428 (Amin) and KM-H2 cells. We chose to use two cell lines to determine whether there were common targets between cHL cell

lines. We also used four sets of samples containing two (KM-H2) and three (L-428 (Amin)) independent infections in the microarray analysis as described in **Section 2.10.1** to increase our confidence in identifying genes that were regulated by c-Jun/JunB.

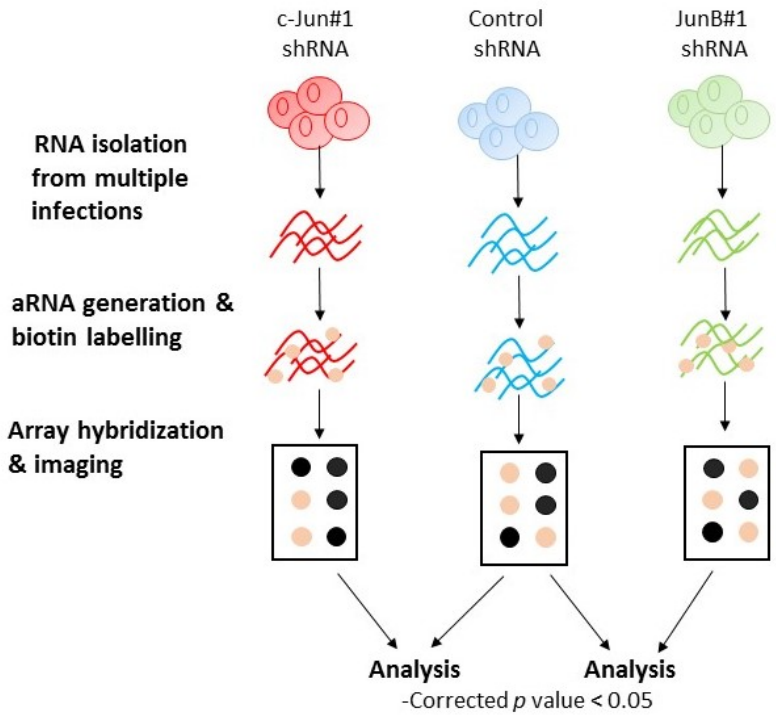

Figure 4.1 – Microarray analysis procedure

Four sets of RNAs from each of L-428 (Amin) or KM-H2 cells were sent to the ATAGC facility (University of Alberta) where mRNAs were converted to aRNAs and labelled with biotin. The samples were fragmented and then hybridized to affymetrix® GeneChip arrays and stained with Streptavidin-Phycoerythrin (SAPE) on GeneChip fluidic station 450 to obtain the basal gene expression levels. For each sample set, the expression value of each gene in c-Jun/JunB shRNA-expressing cells was compared to control shRNA-expressing cells and a moderate *t* test was performed. *p* values were corrected by the Benjamini-Hochberg method and all genes with a corrected *p* (*p* (corr)) value <0.05 were considered significant and were used for further analysis.

The number of genes found that were differentially expressed in c-Jun/JunB knockdown cells are listed in **Figure 4.2** and the genes with a fold change >1.5 are listed in **Appendix 4**. There were twice as many genes identified in KM-H2 cell line as in L-428 (Amin) cells. A total of 467 JunB-regulated genes and 176 c-Jun-regulated genes were found to be significantly different from control cells with a fold change >1.5 and p (corr) <0.05 in both cell lines. Interestingly, we observed more up-regulated genes than down-regulated genes following c-Jun or JunB knockdown with 313 up- vs 159 down-regulated genes in JunB shRNA-expressing cells and 121 up- vs. 55 down-regulated genes in c-Jun shRNA-expressing cells (**Figure 4.2**). In addition, we found more JunB-regulated genes than c-Jun-regulated genes in both L-428 (Amin) and KM-H2 cells.

Figure 4.2

A

L-428	JunB			c-Jun		
	Total	Up	Down	Total	Up	Down
>1	333	205	129	56	29	27
>1.5	235	150	85	51	27	24
>2.0	96	68	28	19	13	6

KM-H2	JunB			c-Jun		
	Total	Up	Down	Total	Up	Down
>1	564	287	277	293	157	136
>1.5	249	165	84	131	95	36
>2.0	72	58	14	40	39	1

Figure 4.2 – Identification of genes with altered expression in c-Jun and JunB shRNA–expressing cHL cell lines.

The numbers of genes in c-Jun and JunB shRNA-expressing L-428 (Amin) (left) or KM-H2 (right) cells with a significant *p* value (*p (corr)* <0.05) and altered expression (>1, >1.5 and >2-fold change) relative to control shRNA–expressing cells is shown.

4.3 c-Jun and JunB share many common dysregulated genes within each cell line

In order to compare the transcriptional profile of c-Jun and JunB, we generated Venn diagrams showing the common genes regulated by both c-Jun and JunB in each cell line (**Figure 4.3A**) as well as the number of dysregulated genes in common between the two cell lines (**Figure 4.3B**). We observed that 20-30% of the differentially expressed genes in c-Jun shRNA-expressing cells were also changed in JunB knockdown cells within the same cell line (**Figure 4.3A**). However, only ~10% genes were dysregulated by c-Jun or JunB in both cell lines (**Figure 4.3B**). Thus in cHL, c-Jun and JunB may regulate different genes in the two cHL cell lines but within the same cell line, c-Jun and JunB share many common targets. In addition, we observed an overlap between c-Jun-regulated genes in KM-H2 cells and JunB-regulated genes in L-428 (Amin) cells (**Figure 4.3C; right panel**).

Figure 4.3

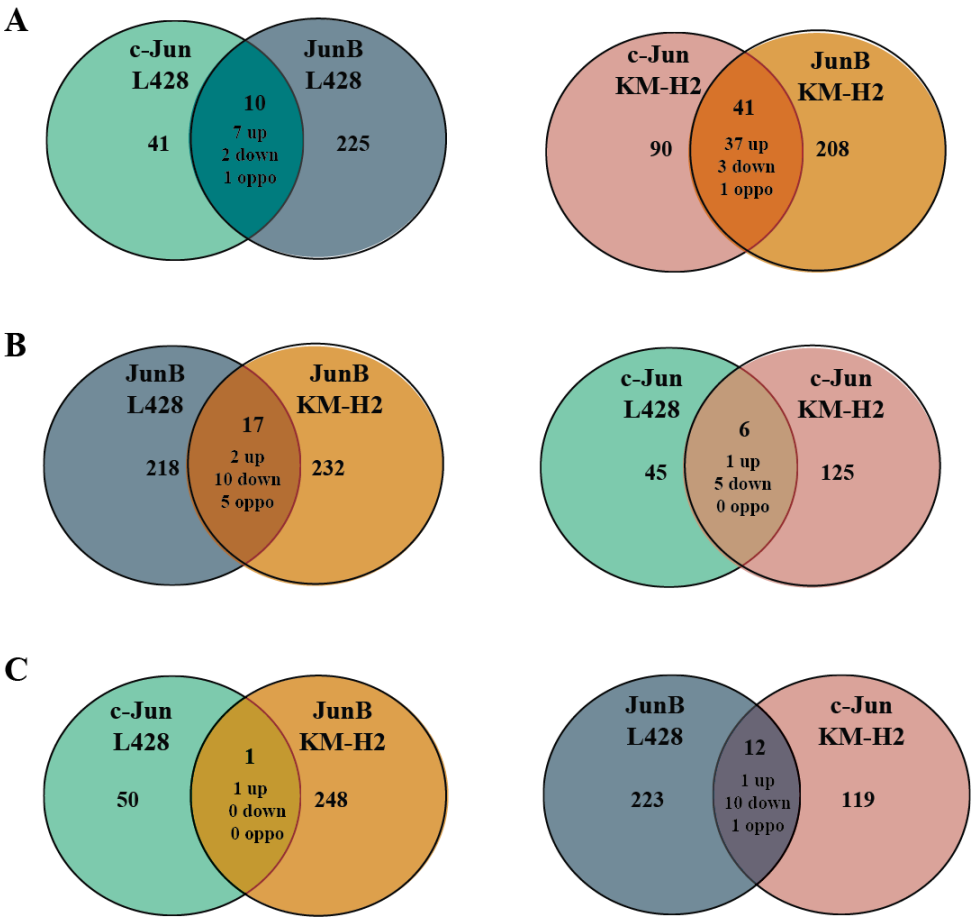

Figure 4.3 – Analyzing common targets with Venn diagrams

Venn diagrams showing the overlap in differentially expressed genes (>1.5 fold-change) between JunB and c-Jun (**A**) and L-428 (Amin) and KM-H2 cells **(B)**. **C.** overlap of L-428 (Amin) c-Jun with KM-H2 JunB (left) or L-428 (Amin) JunB with KM-H2 c-Jun (right). "Up" refers to genes whose expression was up-regulated in knockdown cells; "down", refers to genes whose expression was down-regulated in knockdown cells; "oppo" refers to genes that were up-regulated in one cell line but down-regulated in the other cell line. A list of the names of overlapping genes in each category and their fold change are shown in **Appendix 5**.

4.4 Functional analysis of differentially expressed genes

We then utilized Gene Ontology (GO) (296) information to get a better understanding of the molecular function and biological processes these genes are involved in. GO annotation of the identified genes was analyzed using the DAVID functional annotation (279) tool to identify enriched functional-related gene clusters in c-Jun or JunB knockdown cells (**Appendix 6**). Because we only identified a few c-Jun-regulated genes (51 in L-428 and 131 in KM-H2), we decided to combine JunB- and c-Jun-regulated genes when doing functional annotation to look at common AP-1 functions in cHL. The top five categories based on enrichment score are listed in **Table 4.1** and a complete list of all genes in the top ten clusters are listed in **Appendix 6**. Analysis showed that genes involved in wounding/inflammatory response, homeostasis, apoptosis and proliferation were among the most enriched clusters in biological process and lipid binding and transcription factor activity were the top hits for the molecular function category.

Table 4.1: Gene ontology analysis of differentially expressed genes

A: Functional Classification by Biological Pathways

Annotation Cluster #1 (54 hits)

Enrichment Score: 6.17

GO ID#	name	Count	*p*-value	Benjamini
GO:0009611	response to wounding	42	3.3E-08	4.1E-05
GO:0006954	inflammatory response	28	2.1E-06	1.3E-03

Annotation Cluster #2 (41 hits)

Enrichment Score: 3.59

GO ID#	name	Count	*p*-value	Benjamini
GO:0042592	homeostatic process	41	3.7E-04	2.8E-02
GO:0006875	cellular metal ion homeostasis	19	2.9E-05	6.0E-03

Annotation Cluster #3 (58 hits)

Enrichment Score: 2.36

GO ID#	name	Count	*p*-value	Benjamini
GO:0042981	Regulation of apoptosis	43	3.9E-04	2.8E-02
GO:0043065	Positive regulation of apoptosis	26	1.5E-03	6.6E-02

Annotation Cluster #4 (52 hits)

Enrichment Score: 2.28

GO ID#	name	Count	*p*-value	Benjamini
GO:0008284	positive regulation of proliferation	32	3.3E-06	1.6E-03
GO:0050670	regulation of lymphocyte proliferation	11	2.0E-04	2.1E-02

Annotation Cluster #5 (32 hits)

Enrichment Score: 2.28

GO ID#	name	Count	*p*-value	Benjamini
GO:0001775	cell activation	24	2.5E-05	5.0E-03
GO:0045321	leukocyte activation	21	4.9E-05	8.1E-03

B: Functional Classification by Molecular Function

Annotation Cluster #1 (32 hits)
Enrichment Score: 3.39

GO ID#	name	Count	*p*-value	Benjamini
GO:0008289	Lipid binding	32	2.2E-05	1.5E-02
GO:0035091	Phosphoinositide binding	11	9.7E-04	1.0E-01

Annotation Cluster #2 (6 hits)
Enrichment Score: 2.14

GO ID#	name	Count	*p*-value	Benjamini
GO:0016504	peptidase activator activity	6	5.6E-04	7.1E-02
GO:0008656	caspase activator activity	4	1.2E-02	5.1E-01

Annotation Cluster #3 (73 hits)
Enrichment Score: 2.00

GO ID#	name	Count	*p*-value	Benjamini
GO:0043565	sequence-specific DNA binding	35	5.1E-04	8.1E-02
GO:0003700	transcription factor activity	48	1.3E-03	1.1E-01

Annotation Cluster #4 (32 hits)
Enrichment Score: 2.00

GO ID#	name	Count	*p*-value	Benjamini
GO:0008092	cytoskeletal protein binding	31	4.0E-04	1.2E-01

Annotation Cluster #5 (12 hits)
Enrichment Score: 1.75

GO ID#	name	Count	*p*-value	Benjamini
GO:0004725	Protein tyrosine phosphatase activity	11	1.3E-03	1.0E-01

Table 4.1 - Functional annotation of c-Jun and JunB altered genes

Gene Ontology (GO) was performed using DAVID (278) to identify biological processes (**A**) and molecular functions (**B**) enriched amongst genes with differential expression in c-Jun/JunB shRNA-expressing cells ($\geqslant$1.5-fold change). For this analysis, c-Jun and JunB differentially expressed genes identified in both cell lines were combined. The top 5 annotation clusters based on enrichment score identified

are shown and listed according to their cluster enrichment score. One or two representative categories within each cluster are shown. The *p* values associated with each annotation terms represent one tailed Fisher Exact Probability value measured by Fisher Exact Test and the Benjamini values refer to the corrected *p* values using the Benjamini-Hochberg method to control false discovery rate.

4.5 Examining selected down-regulated genes

A total of eight down-regulated genes were selected for validation of mRNA by qRT-PCR. Seven of which were down-regulated in JunB shRNA-expressing cells and one was down-regulated in c-Jun shRNA-expressing cells. qRT-PCR results were consistent with the microarray data and showed these genes were down-regulated in JunB shRNA-expressing cells (**Figure 4.4A).** We also checked the expression of these genes in JunB#6 shRNA-expressing cells and found their expression were also down-regulated. One gene (eIF3J) was a common c-Jun regulated gene in both L-428 (Amin) and KM-H2 cells. We performed qRT-PCR to validate the expression level in our cells and we saw a consistent down-regulation in c-Jun#1 shRNA-expressing cells (**Figure 4.4C).** In addition, three of the genes were also shown to be down-regulated at protein level by western blotting (**Figure 4.4B & D).** Out of the eight down-regulated genes, only one (TIAM1) showed inconsistency with our qRT-PCR result. Thus, most of the down-regulated genes we examined could be confirmed to be down-regulated at the mRNA level and some at the protein level. In addition, both JunB#1 and #6 shRNA-expressing cells showed similar down-regulation of these selected genes.

Figure 4.4

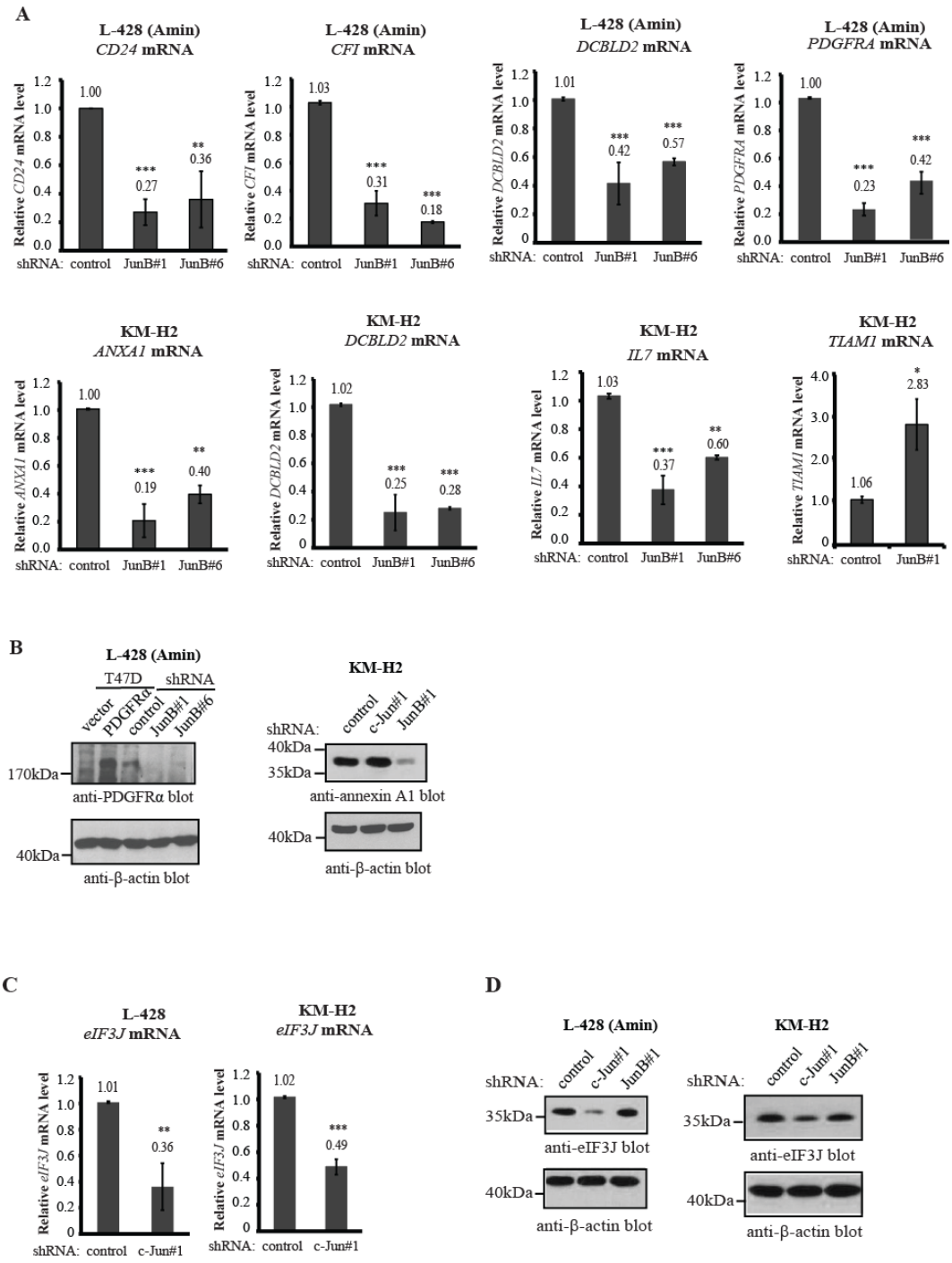
A
L-428 (Amin)
CD24 mRNA
Relative CD24 mRNA level
1.00
0.27
0.36
shRNA: control JunB#1 JunB#6
L-428 (Amin)
CFI mRNA
Relative CFI mRNA level
1.03
0.31
0.18
shRNA: control JunB#1 JunB#6
L-428 (Amin)
DCBLD2 mRNA
Relative DCBLD2 mRNA level
1.01
0.42
0.57
shRNA: control JunB#1 JunB#6
L-428 (Amin)
PDGFRA mRNA
Relative PDGFRA mRNA level
1.00
0.23
0.42
shRNA: control JunB#1 JunB#6
KM-H2
ANXA1 mRNA
Relative ANXA1 mRNA level
1.00
0.19
0.40
shRNA: control JunB#1 JunB#6
KM-H2
DCBLD2 mRNA
Relative DCBLD2 mRNA level
1.02
0.25
0.28
shRNA: control JunB#1 JunB#6
KM-H2
IL7 mRNA
Relative IL7 mRNA level
1.03
0.37
0.60
shRNA: control JunB#1 JunB#6
KM-H2
TIAM1 mRNA
Relative TIAM1 mRNA level
1.06
2.83
shRNA: control JunB#1
B
L-428 (Amin)
T47D
shRNA
vector
PDGFRα
control
JunB#1
JunB#6
170kDa
anti-PDGFRα blot
40kDa
anti-β-actin blot
KM-H2
shRNA:
control
c-Jun#1
JunB#1
40kDa
35kDa
anti-annexin A1 blot
40kDa
anti-β-actin blot
C
L-428
eIF3J mRNA
Relative eIF3J mRNA level
1.01
0.36
shRNA: control c-Jun#1
KM-H2
eIF3J mRNA
Relative eIF3J mRNA level
1.02
0.49
shRNA: control c-Jun#1
D
L-428 (Amin)
shRNA:
control
c-Jun#1
JunB#1
35kDa
anti-eIF3J blot
40kDa
anti-β-actin blot
KM-H2
shRNA:
control
c-Jun#1
JunB#1
35kDa
anti-eIF3J blot
40kDa
anti-β-actin blot

Figure 4.4 - Validation of selected down-regulated genes.

Selected down-regulated genes that were differentially expressed in JunB (**A & B**) or c-Jun (**C & D**) knockdown cells were examined at the mRNA and protein levels. qRT-PCR (**A**) and western blotting (**B**) experiments confirming the down-regulation of indicated genes in JunB shRNA-expressing cells. **C-D**, genes regulated by c-Jun were examined at the mRNA (**C**) and protein level (**D**) in c-Jun#1 shRNA-expressing cells. Results represent the average and standard deviation of four (JunB#1, c-Jun#1) and three (JunB#6) independent experiments performed on mRNA consisting of at least two separate infections. *p* values were obtained by performing paired, two-tailed *t* tests comparing c-Jun/JunB shRNA–expressing cells to cells expressing control shRNA. * $p<0.05$, ** $p<0.01$, *** $p<0.001$. For **B** and **D**, data are representative results from at least two independent experiments. Molecular mass markers are shown on the left of the blots and the anti-β-actin blot serves as loading control.

4.6 Examining selected up-regulated genes

We selected six up-regulated genes for validation with four of them being regulated by both c-Jun and JunB (CD52, CDKN1A ($p21^{Cip1}$), GBP1, SELL). We first performed qRT-PCR on these genes and showed a similar regulation in the corresponding c-Jun/JunB shRNA-expressing cells to the microarray data (**Figure 4.5A & C)**. We also checked the JunB-regulated genes in JunB#6 shRNA-expressing cells and found a similar up-regulation of these genes in JunB knockdown cells. Moreover, we examined the protein levels of some of the targets by western blotting and found that protein expression was also up-regulated in the corresponding cell lines (**Figure 4.5B & D)**. Furthermore, CD48 was examined at the protein level by flow cytometry (**Figure 4.5E**). Consistent with the microarray data, CD48 expression was found to be up-regulated in the two JunB shRNA-expressing cells associated with a significantly higher percentage of cells with higher CD48 expression. Interestingly, control cells showed two distinct CD48 expression levels. In summary, 13 of 14 differentially expressed genes identified in the microarrays were tested and found to be similarly regulated by qRT-PCR (**Table 4.2**).

Figure 4.5

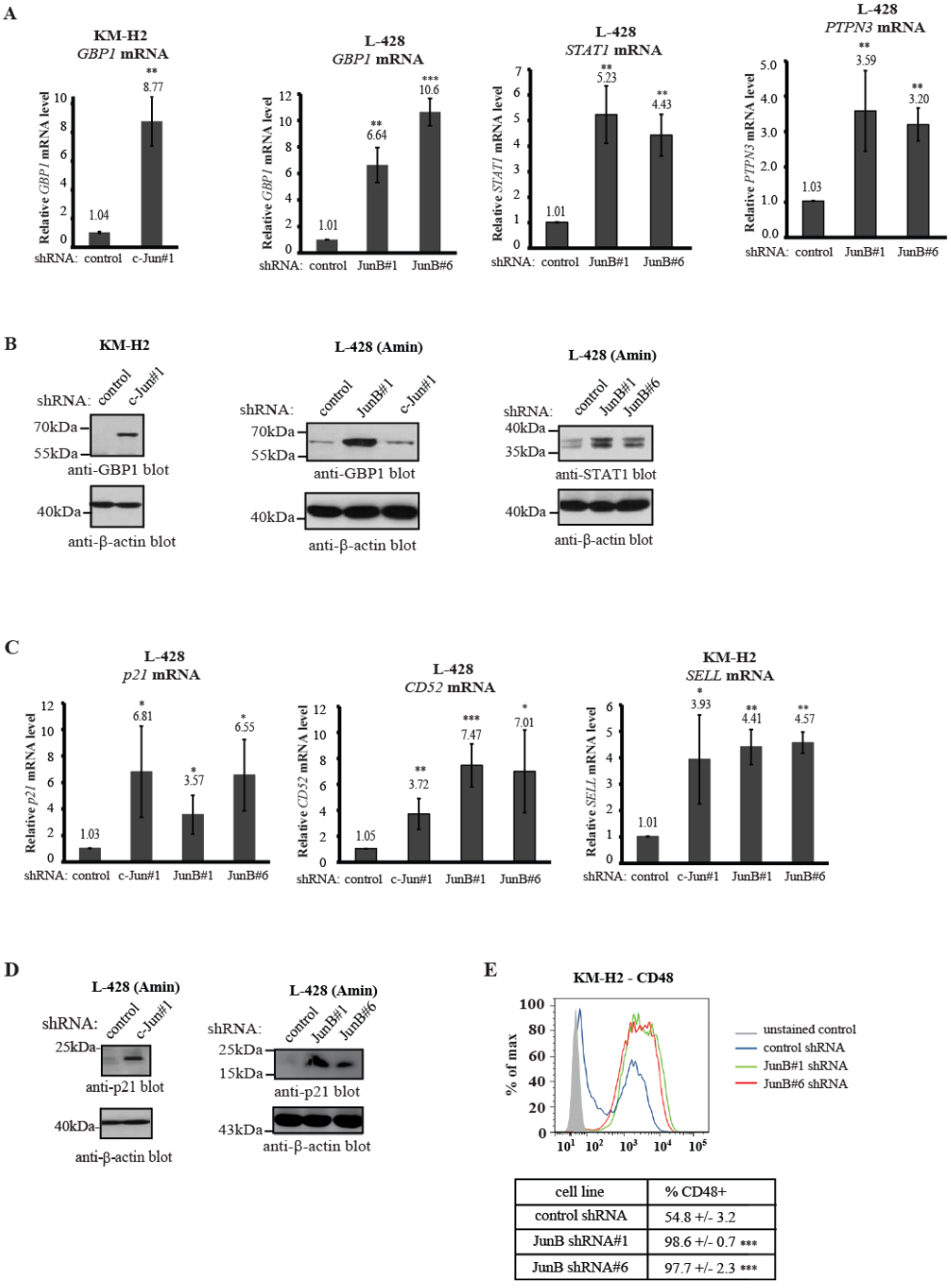

cell line	% CD48+
control shRNA	54.8 +/- 3.2
JunB shRNA#1	98.6 +/- 0.7 ***
JunB shRNA#6	97.7 +/- 2.3 ***

Figure 4.5 - Validation of up-regulated genes.

A-B up-regulated genes in either c-Jun or JunB knockdown cells. qRT-PCR (**A**) and western blotting (**B**) experiments examining the expression level of up-regulated genes in c-Jun or JunB shRNA-expressing cells. **C-D**, genes regulated by both c-Jun and JunB within the same cell line were examined at the mRNA (**C**) and protein levels (**D**) in c-Jun/JunB shRNA-expressing cells. The data represent the average and standard deviation of four (c-Jun/JunB#1 shRNA) and three (JunB#6 shRNA) independent experiments from at least two separate infections. *p* values were obtained by performing paired, two-tailed *t* tests comparing c-Jun/JunB shRNA–expressing cells to cells expressing control shRNA. * $p<0.05$, ** $p<0.01$, *** $p<0.001$. Representative western blots were chosen from at least three different experiments. Molecular mass markers are shown on the left of the blots and the anti-β-actin blot serves as loading control. **E**. CD48 surface expression measured by flow cytometry. One of three representative profiles is shown and the table below indicates the average and standard deviation of three independent experiments. The *p* values next to the number represent independent two-tailed *t* tests comparing JunB#1 and #6 shRNA–expressing cells to cells expressing control shRNA. *** $p<0.001$

Table 4.2: Summary of fold change of selected genes from microarray and qRT-PCR experiments.

Dysregulated genes in cHL			
Gene name	common name	fold change (microarray)	fold change (qRT-PCR)
down-regulated genes			
ANXA1	Annexin A1	-3.45 (JunB; KM-H2)	-5.00 (JunB; KM-H2)
CD24	CD24	-3.5 (JunB; L-428)	-3.70 (JunB;L-428)
CFI	Complement factor I	-2.53 (JunB; L-428)	-3.22 (JunB; L-428)
DCBLD2	Discoidin	-2.48 (JunB; L-428) -3.07 (JunB; KM-H2)	-2.38 (JunB; L-428) -4.00 (JunB; KM-H2)
EIF3J	Eukaryotic initiation factor 3J	-2.35 (c-Jun; L-428) -2.08 (c-Jun; KM-H2)	-2.78 (c-Jun; L-428) -2.04(c-Jun; KM-H2)
IL7	Interleukin 7	-1.78 (JunB; KM-H2)	-2.70 (JunB; KM-H2)
PDGFRA	Platelet-derived growth factor receptor alpha	-4.98 (JunB; L-428)	-4.00 (JunB; L-428)
TIAM1	T-cell lymphoma invasion and metastasis 1	-1.98 (JunB; KM-H2)	2.89 (JunB; KM-H2)
up-regulated genes			
CD52	CD52	7.08 (JunB; L-428) 2.41 (c-Jun; L-428)	7.47 (JunB; L-428) 3.72 (c-Jun; L-428)
CDKN1A (p21)	cyclin-dependent kinase inhibitor 1A (p21, Cip1)	1.66 (JunB; L-428) 1.82(c-Jun; L-428)	3.57 (JunB; L-428) 6.81 (c-Jun; L-428)
GBP1	granulate binding protein 1, interferon-inducible	5.1 (c-Jun; KM-H2) 6.4 (JunB; L-428)	8.77 (c-Jun, KM-H2) 6.64 (JunB; L-428)
SELL	Selectin L (CD62L)	3.84 (JunB; KM-H2) 2.93 (c-Jun; KM-H2)	4.41 (JunB; KM-H2) 3.39 (c-Jun; KM-H2)
STAT1	signal transducer and activator of transcription 1	3.35 (JunB; L-428)	5.23 (JunB; L-428)
PTPN3	Protein tyrosine phosphatase non-receptor type 3	2.85 (JunB; L-428)	3.59 (JunB; L-428)

Table 4.2 - Summary of fold change of selected genes from microarray and qRT-PCR experiments.

Table showing the genes that were examined at the mRNA level by qRT-PCR and the corresponding fold change obtained by microarray. Note: (JunB; L-428) refers to the fold change in JunB#1 shRNA-expressing L-428 (Amin) cells. The number in the qRT-PCR column is the average of four independent experiments. These genes have had their mRNA levels examined in at least three independent samples from at least two independent infections.

4.7 Examining c-Jun-regulated genes in c-Jun#4 knockdown cells

For all JunB-regulated genes, we were able to confirm changes in the expression of both mRNA and protein level with two shRNAs (**Figure 4.4-4.5**). We went on to examine the expression of some of c-Jun-regulated genes in c-Jun#4 shRNA-expressing cells (Experiments performed together with graduate student Joyce Wu, and Dr. Robert Ingham). eIF3J demonstrated a down-regulation in both c-Jun#1 and c-Jun#4 shRNA-expressing cells in at least four (L-428) and two (KM-H2) different sample sets (**compare Figure 4.6A** and **4.4C-D**). However, $p21^{Cip1}$ was regulated differently in the two c-Jun shRNA-expressing cells. While c-Jun#1 knockdown cells showed up-regulation of $p21^{Cip1}$ mRNA and protein levels (**Figure 4.5C-D**), c-Jun#4 knockdown cells demonstrated a down-regulation of $p21^{Cip1}$ protein levels (**Figure 4.6A**) and mRNA levels (**Figure 4.6B**). Therefore, the two c-Jun shRNAs differed in $p21^{Cip1}$ regulation and we need to find another good c-Jun shRNA to determine $p21^{Cip1}$ regulation in c-Jun knockdown cells.

Figure 4.6

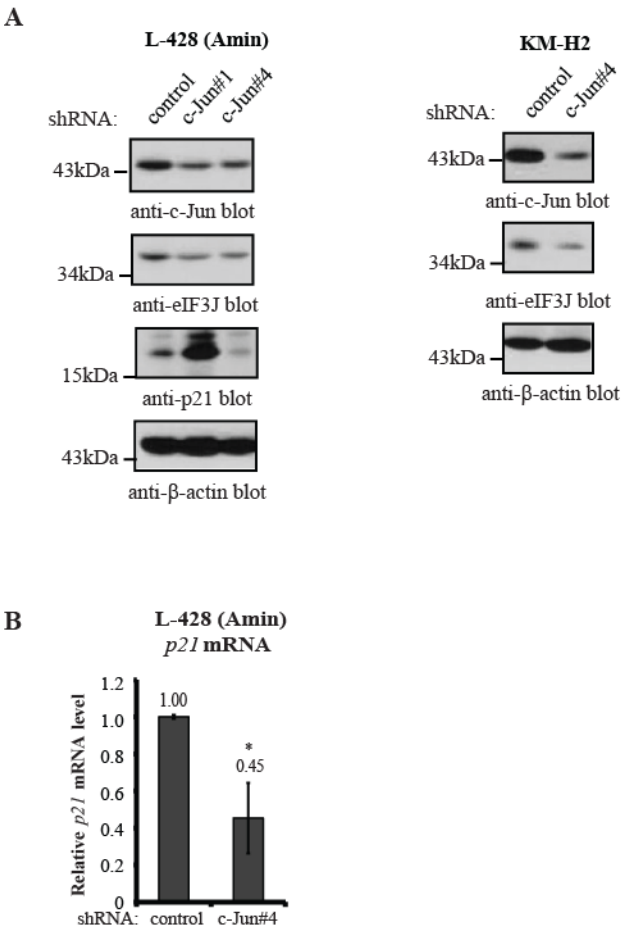

Figure 4.6 – Examining c-Jun targets in c-Jun shRNA #4 knockdown cells

A. western blots showing c-Jun, eIF3J and $p21^{Cip1}$ protein levels in c-Jun#4 shRNA-expressing cells. Data represent four (L-428) and two (KM-H2) independent infections. Molecular mass markers are shown on the left of the blots and the anti-β-actin blot serves as loading control. **B**. qRT-PCR showing the mRNA level of $p21^{Cip1}$ in L-428 c-Jun#4 knockdown cells. Data represent three independent experiments from three separate infections. * $p<0.05$

4.8 L-428 (Amin) targets were similarly regulated in L-428 (DSMZ) cells

We also examined whether the targets we identified and confirmed in L-428 (Amin) cells were also regulated in a similar way in L-428 (DSMZ) cells. We performed western blotting on four L-428 targets in four different experiments from four independent infections of L-428 (DSMZ) cells. Of the four targets, GBP-1, STAT1 are JunB-regulated targets (**Figure 4.5A-B**), eIF3J is a c-Jun target (**Figure 4.4C-D**) and $p21^{Cip1}$ is regulated by both c-Jun and JunB (**Figure 4.5C-D**). Western blots showed a consistent regulation of these gene expression in L-428 (DSMZ) cells (**Figure 4.7**). Therefore, the targets identified in L-428 (Amin) cells are also regulated by c-Jun/JunB in a similar manner in L-428 (DSMZ) cells (**compare Figure 4.4-4.5 to 4.7**).

Figure 4.7

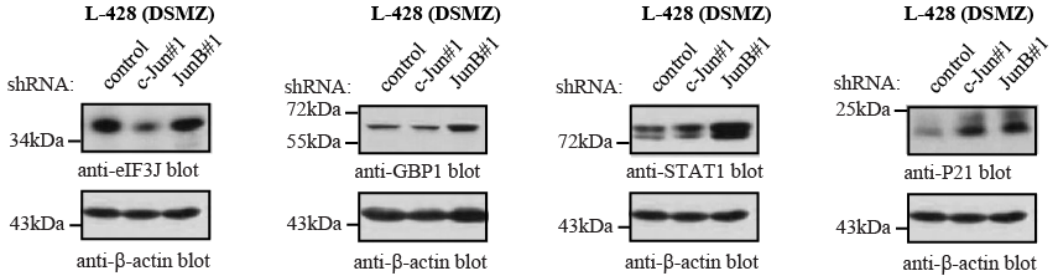

Figure 4.7 – Examining targets in L-428 (DSMZ) cells

Western blots showing protein levels of four targets (eIF3J, GBP1, STAT1, $p21^{Cip1}$) in L-428 (DSMZ) knockdown cells. Results are representative of four different sample sets from four independent infections. Molecular mass markers are shown on the left of the blots and the anti-β-actin blot serves as loading control.

4.9 Discussion

4.9.1 Summary of findings

We identified ~800 genes to be differentially expressed in c-Jun/JunB knockdown cells with more up-regulated genes identified than down-regulated genes (**Figure 4.2**). Furthermore, we found many common dysregulated genes between c-Jun and JunB within the same cell line, with half of c-Jun regulated genes overlapping with JunB-regulated genes in the same cell line (**Figure 4.3A**). The high degree of overlapping genes between c-Jun and JunB suggests the two proteins may share similar cellular functions in the same cell line and supports our previous observation of a similar cell cycle defects associated with knocking down c-Jun or JunB (Chapter 3). In contrast, we found fewer c-Jun or JunB regulated genes that were common between cell lines than we expected (**Figure 4.3B**), indicating that their cellular function may vary amongst different cHL cell lines.

One interesting observation was that c-Jun in KM-H2 cells and JunB in L-428 cells shared many common genes (**Figure 4.3C; right panel**). Given c-Jun and JunB shared many common targets in KM-H2 cells (**Figure 4.3A; right panel**), it is likely that JunB in L-428 cells has more similar functions with both c-Jun and JunB in KM-H2 cells. c-Jun on the other hand, may have different cellular functions in L-428 cells than in other cell types. Another possible reason for this observation could be due to the low number of genes discovered in L-428 c-Jun knockdown cells (51 total), which limits the probability of having similar genes with other cell lines. Moreover, by qRT-PCR we were able to confirm the expression of most (13/14) selected targets in our knockdown cells (**Figure 4.4-4.5**, **Table 4.2**). In

addition, all JunB-regulated genes tested were found to be affected similarly in two JunB shRNA-expressing cells (**Figure 4.4-4.5**).

4.9.2 Inconsistency of $p21^{Cip1}$ regulation with different c-Jun shRNAs

In contrast to the similar regulations found in the two JunB shRNA-expressing cells, we found one c-Jun target $p21^{Cip1}$, was differentially regulated in two c-Jun shRNA-expressing cells. In particular, we did not see an up-regulation in $p21^{Cip1}$ expression from the c-Jun#4 shRNA-expressing cells (Compare **Figure 4.5C** and **4.6B**). The discrepancy between the two shRNAs could be a result of one shRNA targeting some additional genes that interfere with the regulation of $p21^{Cip1}$. At this point we can not confidently say $p21^{Cip1}$ is affected when knocking down c-Jun in L-428 cells. To confirm that $p21^{Cip1}$ and other c-Jun targets we identified are truly c-Jun-regulated genes, a third shRNA needs to be used to resolve this inconsistency. This issue will be discussed in detail in Chapter 5.

4.9.3 GO annotation reveals many important c-Jun/JunB function in cHL pathogenesis

Despite the fact we need to confirm the expression of c-Jun-regulated genes with another shRNA, the genes we identified are valuable for understanding c-Jun and JunB function in cHL. Thus, we went on to analyze the biological and molecular functions of these genes using the DAVID online tool. From the DAVID ontology cluster analysis, we found that the most enriched cluster is response to wounding/inflammatory response **(Table 4.1)**. Also, out of the top ten gene ontology annotations (**Table 4.1, Appendix 6**), four are involved in inflammation and immune regulation. This is not surprising as inflammation is an important

aspect of cHL pathogenesis (132) and HRS cells depend on other immune cells for growth and survival signals. Many genes found in these clusters have been shown to either inhibit cytotoxic T cell and NK cell mediated killing (CD48 (297), CLEC2B (298, 299)), or are involved in attracting regulatory T cells or T helper cells (IL7 (53, 107)). For example, CD48 is a ligand of the NK cell activating receptor 2B4, which when interacting with CD48 on HRS cells could induce apoptosis of tumour cells (300). Thus, it is not surprising that the tumour cells would want to down-regulate CD48 expression. Interestingly, we found CD48 expression is consistently up-regulated in JunB knockdown cells of both ALK+ ALCL and KM-H2 cHL cell lines (Joyce Wu, unpublished results and **Appendix 4**). Moreover, similar to the microarray result, which showed CD48 expression was increased by ~5-fold upon JunB knockdown in KM-H2 cells (**Appendix 4)**, we were able to show a similar up-regulation of CD48 at protein level by flow cytometry in two JunB shRNA-expressing cells (**Figure 4.5E**). Previously CD48 had been shown to be down-regulated in acute myeloid leukemia, which leads to reduced NK cell cytotoxicity (301). Thus we think in cHL, the suppression of CD48 expression on tumour cells may also serve as a mechanism of NK cell evasion and its repression is JunB dependent. In addition, IL-7 mRNA transcripts are frequently observed in cHL cell lines (107). IL7 production by HRS cells has been shown to induce the production of Treg cells and is important in establishing Th2 dominant tumour environment (53). We identified IL-7 as a JunB-regulated gene in KM-H2 (-1.8-fold change) (**Appendix 4)** and we confirmed this finding by qRT-PCR (**Figure 4.4A**). Thus, cHL cell lines may produce high amount of IL-7 as a way to

help establish immune tolerant environment and this up-regulation is JunB dependent. One remaining question is whether these genes we found in our inflammatory clusters have biological function in cHL pathogenesis. Future work should be focus on examine their biological function in cHL. I will discuss about IL-7 and CD48 in detail in Chapter 5.

Some of the genes we identified are not consistent with our model and the biology of cHL. For example, CCL22 was identified to be up-regulated in c-Jun knockdown cells (3.83-fold, **Appendix 4**); but it is known to be highly expressed in primary HRS cells and cHL cell lines (97, 103) and is important in recruitment and induction of Th2 and Treg cells (52, 302, 303). Thus, we would expect it to be down-regulated in shRNA-expressing cells. At this point, we don't know the basal level of CCL22 in our cHL cell lines and whether the increases in protein level in the knockdown cells have any biological effects. Nonetheless, these clusters and categories provide an overview of some important functions of c-Jun and JunB in cHL.

Another remaining question is whether these targets are direct transcriptional targets or not. Since c-Jun and JunB are transcriptional activators (176, 182), we think most of the up-regulated genes in our knockdown cells are indirect targets. Thus, further validation of the transcriptional regulation should be done to examine which of these genes are direct transcriptional targets of c-Jun and JunB. We could perform ChIP to show direct transcriptional regulation.

4.9.4 Limitations of GO annotation and microarray approaches

One problem we faced when doing GO annotations using DAVID software was the limited output number of genes and the low enrichment score when we analyzed c-Jun-regulated genes alone because of the low total number of genes (51 in L-428 and 131 in KM-H2). The same problem occurred when we tried to analyze c-Jun- and JunB-regulated genes in L-428 cells. Therefore we combined c-Jun- and JunB-regulated genes in both cell lines when doing the functional annotation to look at c-Jun and JunB function in cHL. However, although we included all 615 genes in our analysis, the number of genes that fall in the categories were much lower than the input number. Thus, the results likely incompletely represent the cellular functions of c-Jun and JunB because some important categories could be left out from analysis if the number of differentially expressed genes in these categories was too low.

Another limitation of our microarray experiments is the potential of getting genes involved in innate immunity due to the shRNAs. Several studies showed shRNAs, like siRNAs can be immunogenic and can result in non-specific stimulation of the interferon response through activation of Toll-like receptors (304, 305). This can complicate the interpretation of our microarray data because these anti-viral genes, although their expression may depend on c-Jun or JunB, may not be biological relevant to cHL. In our microarray list, we discovered many immune response related genes such as IFNγ, IRF1, TLR3, etc. (**Appendices 4&6; clusters 9-10**). At this point we do not know whether these genes are involved in shaping the cHL microenvironment or they are simply an artifact of shRNA-stimulation.

Since inflammation is a key feature of cHL pathogenesis, it makes the discrimination of the two effects even harder. One possible way to solve this problem is to compare the expression levels of these genes in our control shRNA-expressing cells with non-transduced parental cells. If the basal level of these genes are changed in control shRNA-expressing cells, then we should omit these genes from our target gene list because they are probably due to shRNA-mediated innate immune stimulation.

4.9.4 Some previously known c-Jun/JunB targets are missing from our microarray results

Besides analyzing our gene list, we also examined the targets that were previously identified by other groups in our microarray data. c-Jun and JunB had been shown to regulate genes (PD-L1 (265), Galectin-1 (83), and LTA (267)) to support an immune tolerant environment. However, we only detected Galectin-1 (LGALS1) in our microarray list in KM-H2 JunB knockdown cells with a fold change of -1.5 (**Appendix 4**). We did not find PD-L1 or LTA on our list. To check whether they were false negatives, we could perform qRT-PCR to check their mRNA level or use flow cytometry to check their protein expression in our knockdown cell lines. Moreover, LTA may be regulated by other kinases because the group used the JNK inhibitor, SP600125, to study the expression change of LTA in cHL. As discussed previously (Section **3.13.2**), SP600125 can have off-targeting effect as it can inhibit other kinases (268, 270, 287, 288). In addition, we also did not find CD30, which had been established to be a JunB regulated gene in cHL (259, 260), in our JunB-regulated gene list. Thus, our microarray experiments may not

give a full measurement of c-Jun and JunB transcriptional profile and we may have missed some important genes.

4.9.5 Conclusion

In conclusion, we identified several c-Jun- and JunB-regulated genes in the KM-H2 and L-428 cell lines. Gene ontology analysis showed that they regulate a variety of cellular pathways such as wounding/inflammatory response, proliferation, apoptosis and immune regulation which are likely important in cHL pathogenesis. Moreover, we found the two proteins share many downstream targets in the same cell line. One limitation of this study is the fact that we do not have a second shRNA to confirm the genes we found are truly c-Jun/JunB dependent.

CHAPTER 5: GENERAL DISCUSSION AND FUTURE DIRECTIONS

5.1 Summary of findings

In this study, we showed both c-Jun and JunB support cHL cell lines proliferation (**Figure 3.2--3.6**) and tumour growth (**Figure 3.9**). Moreover, cell cycle studies unveiled the growth defect associated with knocking down c-Jun or JunB was largely due to a delay in G_0/G_1 progression (**Figure 3.5**). Besides proliferation, we also examined c-Jun and JunB transcriptional profiles in two cHL cell lines in order to gain a better understanding of the function of these two AP-1 proteins in cHL (Chapter 4). We found the two AP-1 transcription factors regulate numerous genes involved in diverse biological processes such as wounding/inflammatory response, cellular homeostasis, proliferation and apoptosis (**Table 4.1, Appendix 6**). For some of these genes, we were able to confirm the change of expression at the mRNA and protein levels (**Figures 4.5-4.6**) in c-Jun/JunB knockdown cells.

5.2 Potential targets involved in the delay in G_0/G_1 progression in cHL knockdown cells

We observed a major defect in G_0/G_1 in c-Jun/JunB shRNA-expressing cells (**Figure 3.5, 3.6**). One unanswered question from this study is how knockdown of c-Jun and JunB results in this extended G_0/G_1 in HRS cells. Several studies showed that HRS cells display deregulation of the genes involved in the promoting G_1/S and G_2/M checkpoints (117, 122, 292). Our microarray showed several target genes involved in cell cycle regulation, particularly in the G_1 to S transition. One of which is $p21^{Cip1}$, an important negative regulator of the G_1 to S transition by binding to and inhibiting the activity of cyclinD-CDK4/6 (215, 306). Animal studies further supports a role of $p21^{Cip1}$ as tumour suppressor, as $p21^{Cip1-/-}$ mice develop

spontaneous tumours (307), and together with other tumour suppressors, correlates with many human neoplasm poor prognosis such as colorectal (308-310), cervical(311), and breast cancer(312). Our microarray data showed $p21^{Cip1}$ was up-regulated in both L-428 c-Jun and JunB knockdown cells (**Appendix 4**) and we were able to confirm the up-regulation of $p21^{Cip1}$ expression at the mRNA and protein expression in the corresponding knockdown cells by qRT-PCR and western blotting, respectively (**Figure 4.5C-D, 4.7**). Therefore, it would be interesting to know whether the up-regulation of $p21^{Cip1}$ contributes to the slow growth phenotype in c-Jun or JunB knockdown cells. To test this, we could reduce $p21^{Cip1}$ expression in c-Jun/JunB knockdown cells using siRNA or inhibit $p21^{Cip1}$ activity using pharmacological inhibitors such as UC2288 (313) to see whether the knockdown cells can recover from the growth defect.

Besides $p21^{Cip1}$, the G_0/G_1 delay observed in our knockdown cells could be due to the dysregulation of other G_0/G_1 regulators. Some of these G_0/G_1 or G_1/S regulatory molecules in our microarray are BTG2 (314-316), BCL6 (317-319), HES1 (320, 321) which were shown to regulate G_0/G_1 in other cell types. Among them, BTG2 is a tumour suppressor and it was found to be up-regulated (2-fold) in L-428 JunB knockdown cells; whereas BCL6 (-1.8-fold) and HES1 (-1.7-fold) were shown to have growth promoting activity and were down-regulated in KM-H2 JunB knockdown cells (**Appendix 4**). It remains to be determined whether these molecules have a cell cycle regulatory role in cHL. We think the growth defect observed in the knockdown cells is due to multiple factors. One reason for that is we observed a slow growth rate in c-Jun#4 shRNA-expressing cells (**Figure 3.3B)**

even though $p21^{Cip1}$ was down-regulated in these cells (**Figure 4.6B-C**), which suggests there must be other players responsible for the reduced proliferation in the c-Jun#4 knockdown cells. Another reason is that $p21^{Cip1}$ was not found in KM-H2 microarray list. This could be a false negative result, which requires further investigation in the KM-H2 knockdown cells by qRT-PCR. Nonetheless, we think $p21^{Cip1}$ may be responsible in part for the growth inhibitory effect of c-Jun/JunB suppression in L-428 cells. Additional targets (BTG2, BCL6, HES1) remain for further investigation on whether their deregulation is involved in growth defect to unveil the molecular mechanism of the impaired G_0/G_1 phase in c-Jun/JunB knockdown cells.

5.3 Comparing the function of c-Jun and JunB in regulating proliferation and apoptosis amongst other CD30 positive lymphomas

Since c-Jun and JunB are overexpressed in other CD30+ lymphomas including ALK+ ALCL, ALK- ALCL, CD30+ DLBCL (250, 255), it is plausible that these two transcription factors share similar functions in promoting tumour proliferation as in cHL. Much of the work had been focused on ALK+ ALCL, which demonstrated a role for JunB in promoting the proliferation of ALK+ ALCL cell lines ((251) and unpublished observation by Joyce Wu and Dr. Robert Ingham). Using a siRNA-mediated gene silencing approach, the growth defect in several ALK+ALCL cell lines following JunB knockdown was mainly associated with G_1/S and G_2/M cell cycle delay (195, 251). In addition our lab using shRNA approach showed a similar G_0/G_1 extension in ALK+ ALCL cell lines when JunB was knocked down (unpublished data by Joyce Wu and Dr. Robert Ingham). The

cell cycle defect associated with JunB knockdown in ALK+ALCL cell lines was similar to the four cHL c-Jun/JunB knockdown cell lines we investigated which all exhibited a major G_1/S delay or prolonged G_0/G_1 phase with a modest G_2/M extension in some knockdown cell lines (**Figure 3.5**). Recently, it was demonstrated that JunB expression positively correlates with the expression of several positive cell cycle molecules such as cyclin A, cyclin B1 and cyclin E in DLBCL tissue samples (241). In addition, Blonska's group showed knocking down both JunB and c-Jun reduced DLBCL cell proliferation and tumour growth; however, this study did not differentiate the effect of JunB from c-Jun. Nonetheless, these results provided some insights into JunB function in DLBCL. Therefore, JunB may control cell cycle progression at G_0/G_1 and G_1/S in other CD30+ lymphomas and there may be a common mechanism of JunB-regulated tumour proliferation in all CD30+ lymphomas. Future work should expand to examine the role of JunB in the cell cycle regulation of other CD30+ lymphomas.

However, c-Jun function in ALK+ ALCL has been controversial. While some studies suggested c-Jun promotes the cell cycle progression in ALK+ ALCL through regulating molecules such as $p21^{Cip1}$, cyclin A and D3 (280), others including our lab, showed c-Jun had no proliferation function in ALK+ ALCL cell lines following c-Jun knockdown ((195) and unpublished observation by Joyce Wu and Dr. Robert Ingham). Thus, whether c-Jun has a common function in cell cycle progression amongst the CD30+ lymphomas needs further investigation. For us we need a second c-Jun shRNA to confirm that c-Jun is not involved in ALK+ ALCL cell proliferation.

We did not observe a role in apoptosis regulation for c-Jun and JunB in L-428 and KM-H2 cHL cell lines (**Figure 3.4**). However, Atsaves *et al.* demonstrated that silencing JunB sensitized ALK+ALCL cells to etoposide-induced apoptosis (251). Thus the elevated level of JunB in tumour cells may function to confer resistance to chemotherapy. It would be interesting to examine if JunB has similar effect in cHL or other CD30+ lymphomas, which could provide another therapeutic approach to increase the effectiveness of standard chemotherapy. Particularly it would be interesting to examine L-540 cells which demonstrated a moderate induction of apoptosis following c-Jun/JunB knockdown (**Figure 3.4C**).

5.4 Future work to solve the shRNA problems

The seed sequence recognized by JunB#6 shRNA partially overlaps with JunB#1 shRNA (**Appendix 1**), so the proliferation defect (**Figure 3.2, 3.5**) and genes identified in the microarrays (**Figure 4.2**, **Appendix 4**) in JunB#1 knockdown cells could not be confirmed to be JunB dependent unless we can show a similar phenotype with another JunB shRNA that targets a different region of *JunB*. Also, cells expressing c-Jun#1 and c-Jun#4 shRNAs showed inconsistent regulation of $p21^{Cip1}$ mRNA and protein expression (compare **Figure 4.5 C-D** with **Figure 4.6**); although these two shRNAs target completely different regions of *JUN* (**Appendix 1**). Moreover, despite the different expression of $p21^{Cip1}$ in the two c-Jun knockdown cells, we observed a similar cell cycle defect (extended G_0/G_1). However, we did see a slight increase (~10%) of G_2/M proportion in c-Jun #4 shRNA-expressing cells compared to c-Jun#1 shRNA-expressing cells (compare **Figure 3.5B** and **3.6A**) which could be a result of $p21^{Cip1}$ difference. However, we

do not know whether this subtle difference in G_2/M is enough to be due to the differential regulation of $p21^{Cip1}$. To solve these problems, we were trying to identify additional JunB and c-Jun shRNAs that give a good knockdown level (**Appendix 2**). We tried six additional JunB shRNAs and found two which (JunB#3 & JunB#5) appear to work somewhat in L-428 cells but not KM-H2 and L-540 cells (**Appendix 2**). However, this experiment was only performed once so we need to repeat these experiments with a different infection. If we can consistently knockdown JunB in L-428 cells using either JunB#3 or JunB#5 shRNAs, we could repeat experiments (**Figures 3.2, 3.5, and 4.4-4.5**) to examine whether the growth defects and the changes in the expression of selected target genes associated with reduced JunB levels were consistent with JunB#1 shRNA-expressing cells. We also have several additional c-Jun shRNAs that we could try to obtain another c-Jun knockdown cell line to examine c-Jun effect on proliferation and target regulation to see if a consistent phenotype is associated with reduced c-Jun level.

To ensure the phenotypes are c-Jun/JunB mediated, we could also overexpress c-Jun or JunB in the corresponding c-Jun#1/JunB#1 shRNA-expressing cells to see whether we can rescue the phenotypes. Specifically, we would transfect a vector containing either c-Jun or JunB gene with a GFP gene. We would repeat experiments in **Figures 3.2, 3.4-3.5 and 4.4-4.5** to see if we could rescue the phenotypes. The GFP is used to gate on transfected cells so we can concentrate on c-Jun/JunB-overexpressing cells. We would expect that by overexpressing c-Jun or JunB in the #1 shRNA-expressing cells, the cells would reverse the proliferation suppression associated with c-Jun/JunB knockdown and restore the expression

level of target genes. In reconciling the regulation of $p21^{Cip1}$ by c-Jun, because both c-Jun shRNAs may have off-targeting effect, we can examine whether the change in $p21^{Cip1}$ expression in the two different knockdown cells is reduced upon introduction of c-Jun cDNA. In regard to the same growth phenotype observed in two c-Jun knockdown cells with different $p21^{Cip1}$ expression, at this point we can not determine the exact mechanism of c-Jun-mediated cell cycle defect. However, if we see a consistent rescue of the proliferation phenotype in both c-Jun#1 and c-Jun#4 knockdown cells, we will be confident that the cell cycle defect is c-Jun dependent, although the mechanism may differ.

If both methods do not work in our cHL cell lines, we can use other methods to silence c-Jun or JunB expression such as siRNA-mediated knockdown or CRISPR-mediated gene knockout. Previously, we tried to knockdown c-Jun and JunB with siRNAs using electroporation but this method did not work on cHL cell lines as we did not observe a reduced c-Jun/JunB protein level following siRNA transfection (**Appendix 7**). In the future, we could use Nucleofector™ technology instead to increase the transfection efficiency and to see whether we can knockdown c-Jun or JunB with siRNAs. Another alternative to generating knockdown cell lines is to knockout the genes using CRISPR technology, which our lab is currently working on (Joyce Wu, Jared Pelkey-Cooper and Dr Robert Ingham; unpublished work).

5.5 Redundancy between c-Jun and JunB in cHL cell lines

One interesting observation we had was that knocking down c-Jun and JunB within cell lines resulted in a similar alteration in cell growth (**Figure 3.2**, **3.9**), apoptosis

(**Figure 3.4**), and cell cycle defect (**Figure 3.5**). Moreover, c-Jun and JunB knockdown cell lines shared many differentially expressed genes within cell lines (**Figure 4.3A**). Furthermore, previous research using ChIP demonstrated common transcriptional targets of c-Jun and JunB, such as PD-L1 in cHL (265) and PDFGRB in ALK+ ALCL (322). These results suggested that the two AP-1 proteins may have redundant functions. To further investigate the functional relationship between c-Jun and JunB, we generated double knockdown cell lines and examined their growth. Interestingly, we found that knocking down both c-Jun and JunB did not lead to synergistic anti-proliferative effect since the double knockdown cells showed a similar growth rate as the single knockdown cells (**Figure 3.10**).

There are two simple models for the reduced growth rate in the c-Jun and JunB knockdown cells. Firstly, c-Jun and JunB may be completely functionally redundant in cHL with respect to the genes that that control G_0/G_1 phase progression (Model 1) (**Figure 5.1**). This is supported by our microarray data which showed many common genes whose expression was similarly changed in c-Jun and JunB knockdown cells within cell lines (**Figure 4.3A, Appendix 5**). In particular, $p21^{Cip1}$ up-regulation in c-Jun and JunB L-428 knockdown cells would support Model 1. This model would suggest that the overall phenotype is dictated by the total level of both proteins. In other words, in the context of cell proliferation, the cells require a minimum level of total c-Jun/JunB activity, irregardless of the specific protein. Another possible explanation is that the two proteins are not functional redundant and they regulate different pathways involved in proliferation (Model 2, **Figure**

5.1). From our microarray results, we identified numerous genes involved in proliferation that were regulated by only one AP-1 protein (e.g. BTG2, HES1, BCL6; **Appendix 6**, Cluster 3).

To test which model is more likely to explain the growth phenotype, we could overexpress c-Jun in JunB knockdown cells or *vice versa* to see if we can rescue the growth defect in the single knockdown cells. If we see restoration of growth, then the two proteins are more likely to have redundant functions in proliferation and Model 1 would be the possible explanation for the growth phenotype. One the other hand, if we do not see restoration of growth rate in c-Jun-overexpressing JunB knockdown cells, then it suggests Model 2 is more likely the mechanism by which c-Jun and JunB regulation of proliferation. Based on the data we have, we think the two proteins are more likely to be partially redundant (Model 2) since we identified more proliferation-related genes outside the overlapping region of **Figure 4.3A**. In addition, we did not observe an increase in growth rate in the later stage JunB knockdown cells when c-Jun was up-regulated. This observation suggests c-Jun can not rescue the JunB shRNA-mediated growth defect in cHL cells and further supports Model 2.

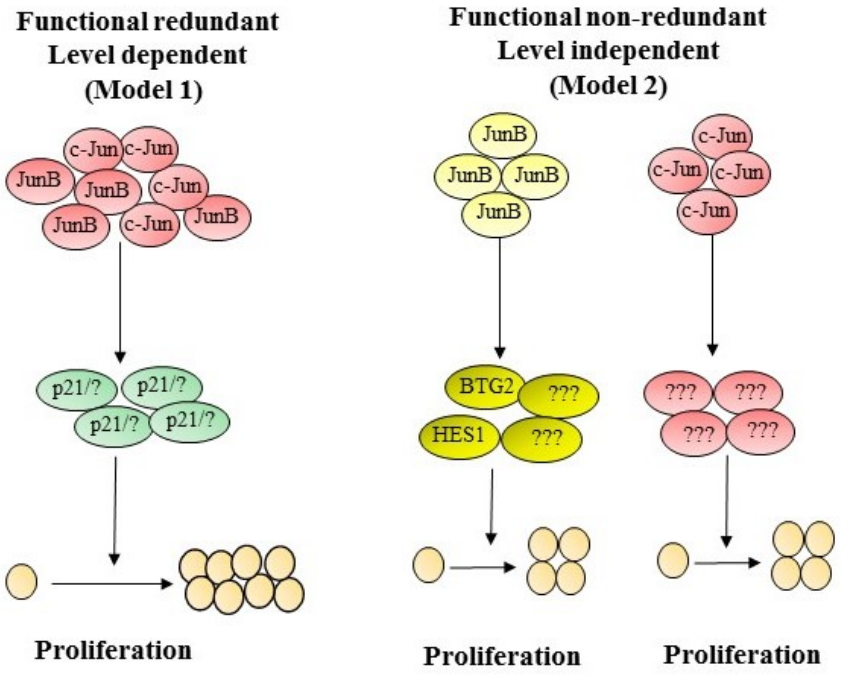

Figure 5.1 - Possible Models for how c-Jun and JunB could regulate cHL proliferation

Diagram shows two different models for how c-Jun and JunB could regulate cell proliferation. c-Jun and JunB could be completely functional redundant (Model 1) by regulation the same genes (eg. $p21^{Cip1}$or other unknown targets) that promote the proliferation of cHL. The growth rate depends on the total level of c-Jun and JunB. On the other hand, c-Jun and JunB may regulate distinct sets of molecular targets and each downstream pathway is required for cHL proliferation (Model 2). The growth rate in this model is dependent on the total activity of both pathways.

5.6 Future directions for examining c-Jun/JunB-regulated candidate genes identified by microarray and their application to clinical studies

In our microarray study, we identified hundreds of c-Jun/JunB regulated genes that are involved in various cellular pathways including inflammation, homeostasis, proliferation, apoptosis, and lymphocyte activation (**Appendix 6**). Some of the targets genes that would be interesting to follow up with were briefly discussed in Section **4.9.3**. For example, IL-7, which was identified to be promoted by JunB in KM-H2 cells had been demonstrated to play a role in the proliferation of HRS cells and promotes Treg proliferation and differentiation (53, 54). It would be interesting to know whether knocking down JunB could exert similar effect on the recruitment of Tregs. To test whether IL-7 plays a role in regulating Treg proliferation and differentiation, we could co-culture KM-H2 control or JunB knockdown cells with naïve T cells in the presence or absence of IL-7 blocking antibody and examine proliferation (CFSE assay) and differentiation into Tregs (CD25, Foxp3 staining). In addition, we could perform transwell assays to examine whether knockdown of JunB has an effect on Treg recruitment to HRS cells. An IL-7 blocking antibody will be used to ensure the effect is IL-7 mediated.

In addition to IL-7, JunB was identified to influence several surface molecules such as CD48 to potentially help tumour cells escape the recognition and killing mediated by CTL and NK cells (300, 301). It remains to be determined whether suppression of CD48 by JunB would result in reduced NK-mediated killing by performing NK cytotoxicity assays using control and JunB shRNA-expressing cHL cell lines in the presence and absence of a CD48 blocking antibody.

It remains to be determined whether there is a correlation between c-Jun or JunB expression and the expression of microarray targets in patient samples and whether the expression of these targets in cHL are distinctly different from other B cell lymphomas or other hematopoietic malignancies, which could serve as a biomarker for cHL. For example, BTG2 which was an up-regulated gene in the JunB knockdown cells and may contribute to the delay in G_0/G_1 (314, 316) (discussed in Section **5.2**). BTG2 was reported to be repressed in primary HRS cells compared to other B cell non-Hodgkin lymphomas (323). Therefore, we would expect up-regulated genes identified in knockdown cells to show minimal expression in HRS cells compared to other lymphomas and that down-regulated genes might be expressed at higher levels in HRS cells than other lymphomas. Nonetheless, before we pursue any individual targets further, we need to confirm these targets are c-Jun- or JunB-regulated genes with another shRNA or by rescuing the phenotype with cDNAs.

From our microarray data, we observed only a small number of common c-Jun/JunB-regulated genes overlapping between L-428 and KM-H2 cell lines (**Figure 4.3B**). This was not surprising because the two cell lines are derived from different subtypes and a previous microarray study showed that L-428 cells showed the least relatedness with KM-H2 cells amongst tested four cHL cell lines (39). Future work should start by examining these genes in other cHL cell lines such as L-540 and expand to other CD30+ lymphomas to see if they are common c-Jun or JunB regulated genes. Until now, CD30 was the only gene found to be regulated by JunB in both ALK+ ALCL and cHL cell lines (260). Given cHL was found to be

more closely to ALCL than other B cell lymphomas based on microarray analysis (324), it would be interesting to know whether c-Jun and JunB share common downstream targets other than CD30 between these two lymphomas and those genes could give more insights on the general molecular function of c-Jun and JunB in lymphomas. One example is the CD48 molecule we found whose expression was minimal in ALK+ ALCL cells and was up-regulated in JunB knockdown cell lines (Joyce Wu; unpublished data).

5.7 Conclusions

This thesis described the importance of the two AP-1 transcription factors, c-Jun and JunB, in regulating cHL tumour cell proliferation and revealed genes directly/indirectly regulated by c-Jun/JunB in two cHL cell lines. Specially, we showed a role for each protein in cHL proliferation and revealed a common defect in G_0/G_1 when c-Jun or JunB was knocked down. Furthermore, we identified numerous gene targets that are either directly or indirectly regulated by c-Jun and JunB in cHL and provided some potential therapeutic targets for future work. However, we need to examine whether these phenotypes hold true with a second shRNA or cDNA rescue, or CRISPR/Cas9 gene targeting before we can firmly conclude these findings are c-Jun/JunB dependent. Nonetheless, our data provide important insights into the specific roles of the two aberrantly expressed proteins, c-Jun and JunB, in the pathogenesis of cHL.

REFERENCES

1. Hodgkin. (1832) On some Morbid Appearances of the Absorbent Glands and Spleen. *Med Chir Trans* **17**, 68-114
2. Geller, S. A., and Taylor, C. R. (2013) Thomas Hodgkin: the "man" and "his disease": humani nihil a se alienum putabit (nothing human was foreign to him). *Virchows Arch* **463**, 353-365
3. Engert, A., and Younes, A. *Hodgkin lymphoma : a comprehensive overview*
4. Swerdlow, S. H., International Agency for Research on Cancer., and World Health Organization. (2008) *WHO classification of tumours of haematopoietic and lymphoid tissues*, International Agency for Research on Cancer, Lyon, France
5. Kuppers, R., Engert, A., and Hansmann, M. L. (2012) Hodgkin lymphoma. *J Clin Invest* **122**, 3439-3447
6. Statistics, C. C. S. s. A. C. o. C. (2014) Canadian Cancer Statistics 2014. Canadian Cancer Society, Toronto, ON
7. Hjalgrim, H., and Engels, E. A. (2008) Infectious aetiology of Hodgkin and non-Hodgkin lymphomas: a review of the epidemiological evidence. *J Intern Med* **264**, 537-548
8. Jaffe, E. S., Harris, N. L., Stein, H., and Isaacson, P. G. (2008) Classification of lymphoid neoplasms: the microscope as a tool for disease discovery. *Blood* **112**, 4384-4399
9. Kuppers, R. (2009) The biology of Hodgkin's lymphoma. *Nat Rev Cancer* **9**, 15-27
10. Ansell, S. M. (2012) Hodgkin lymphoma: 2012 update on diagnosis, risk-stratification, and management. *Am J Hematol* **87**, 1096-1103
11. Engert, A., Plutschow, A., Eich, H. T., Lohri, A., Dorken, B., Borchmann, P., Berger, B., Greil, R., Willborn, K. C., Wilhelm, M., Debus, J., Eble, M. J., Sokler, M., Ho, A., Rank, A., Ganser, A., Trumper, L., Bokemeyer, C., Kirchner, H., Schubert, J., Kral, Z., Fuchs, M., Muller-Hermelink, H. K., Muller, R. P., and Diehl, V. (2010) Reduced treatment intensity in patients with early-stage Hodgkin's lymphoma. *N Engl J Med* **363**, 640-652
12. van der Kaaij, M. A., Heutte, N., Meijnders, P., Abeilard-Lemoisson, E., Spina, M., Moser, E. C., Allgeier, A., Meulemans, B., Simons, A. H., Lugtenburg, P. J., Aleman, B. M., Noordijk, E. M., Ferme, C., Thomas, J., Stamatoullas, A., Fruchart, C., Brice, P., Gaillard, I., Bologna, S., Ong, F., Eghbali, H., Doorduijn, J. K., Morschhauser, F., Sebban, C., Roesink, J. M., Bouteloup, M., Van Hoof, A., Raemaekers, J. M., Henry-Amar, M., and Kluin-Nelemans, H. C. (2012) Premature ovarian failure and fertility in long-term survivors of Hodgkin's lymphoma: a European Organisation for Research and Treatment of Cancer Lymphoma Group and Groupe d'Etude des Lymphomes de l'Adulte Cohort Study. *J Clin Oncol* **30**, 291-299
13. Swerdlow, A. J., Higgins, C. D., Smith, P., Cunningham, D., Hancock, B. W., Horwich, A., Hoskin, P. J., Lister, T. A., Radford, J. A., Rohatiner, A. Z., and Linch, D. C. (2011) Second cancer risk after chemotherapy for Hodgkin's lymphoma: a collaborative British cohort study. *J Clin Oncol* **29**, 4096-4104
14. American Cancer Society. (2014) Hodgkin Disease. Vol. 2016
15. Stein, H., Delsol, G., Pileri, S.A., Weiss, L.M., Poppema, S., Jaffe, E.S. (2008) Classical Hodgkin lymphoma, introduction. In *WHO Series on Histological and Genetic Typing of Human Tumours* (Swerdlow S.H., C. E., Harris N.L., Jaffe E.S., Pileri S.A., Stein H., Thiele J., Vardiman, J.W., ed), International Agency for Research on Cancer (IARC), Lyon

16. Matsuki, E., and Younes, A. (2015) Lymphomagenesis in Hodgkin lymphoma. *Semin Cancer Biol*
17. Kuppers, R., and Hansmann, M. L. (2005) The Hodgkin and Reed/Sternberg cell. *Int J Biochem Cell Biol* **37**, 511-517
18. Takahashi, H., Hideshima, K., Kawazoe, K., Tsuda, N., Fujita, S., Shibata, Y., Okabe, H., and Yamabe, S. (1995) Immunophenotypes of Reed-Sternberg cells and their variants: a study of 68 cases of Hodgkin's disease. *Tohoku J Exp Med* **177**, 193-211
19. van den Berg, A., Visser, L., and Poppema, S. (1999) High expression of the CC chemokine TARC in Reed-Sternberg cells. A possible explanation for the characteristic T-cell infiltratein Hodgkin's lymphoma. *Am J Pathol* **154**, 1685-1691
20. Oudejans, J. J., Kummer, J. A., Jiwa, M., van der Valk, P., Ossenkoppele, G. J., Kluin, P. M., Kluin-Nelemans, J. C., and Meijer, C. J. (1996) Granzyme B expression in Reed-Sternberg cells of Hodgkin's disease. *Am J Pathol* **148**, 233-240
21. Foss, H. D., Reusch, R., Demel, G., Lenz, G., Anagnostopoulos, I., Hummel, M., and Stein, H. (1999) Frequent expression of the B-cell-specific activator protein in Reed-Sternberg cells of classical Hodgkin's disease provides further evidence for its B-cell origin. *Blood* **94**, 3108-3113
22. Schmid, C., Pan, L., Diss, T., and Isaacson, P. G. (1991) Expression of B-cell antigens by Hodgkin's and Reed-Sternberg cells. *Am J Pathol* **139**, 701-707
23. Kuppers, R., and Rajewsky, K. (1998) The origin of Hodgkin and Reed/Sternberg cells in Hodgkin's disease. *Annu Rev Immunol* **16**, 471-493
24. Kanzler, H., Kuppers, R., Hansmann, M. L., and Rajewsky, K. (1996) Hodgkin and Reed-Sternberg cells in Hodgkin's disease represent the outgrowth of a dominant tumor clone derived from (crippled) germinal center B cells. *J Exp Med* **184**, 1495-1505
25. Marafioti, T., Hummel, M., Foss, H. D., Laumen, H., Korbjuhn, P., Anagnostopoulos, I., Lammert, H., Demel, G., Theil, J., Wirth, T., and Stein, H. (2000) Hodgkin and reed-sternberg cells represent an expansion of a single clone originating from a germinal center B-cell with functional immunoglobulin gene rearrangements but defective immunoglobulin transcription. *Blood* **95**, 1443-1450
26. Kuppers, R., Rajewsky, K., Zhao, M., Simons, G., Laumann, R., Fischer, R., and Hansmann, M. L. (1994) Hodgkin disease: Hodgkin and Reed-Sternberg cells picked from histological sections show clonal immunoglobulin gene rearrangements and appear to be derived from B cells at various stages of development. *Proc Natl Acad Sci U S A* **91**, 10962-10966
27. Muschen, M., Rajewsky, K., Brauninger, A., Baur, A. S., Oudejans, J. J., Roers, A., Hansmann, M. L., and Kuppers, R. (2000) Rare occurrence of classical Hodgkin's disease as a T cell lymphoma. *J Exp Med* **191**, 387-394
28. Seitz, V., Hummel, M., Marafioti, T., Anagnostopoulos, I., Assaf, C., and Stein, H. (2000) Detection of clonal T-cell receptor gamma-chain gene rearrangements in Reed-Sternberg cells of classic Hodgkin disease. *Blood* **95**, 3020-3024
29. Hoffman, R. (2013) Hematology basic principles and practice. pp. 1 online resource (xxxi, 2343 p.), Saunders/Elsevier, Philadelphia, PA

30. Sinkovics, J. G. (1991) Hodgkin's disease revisited: Reed-Sternberg cells as natural hybridomas. *Crit Rev Immunol* **11**, 33-63
31. Pringle, J. H., Shaw, J. A., Gillies, A., and Lauder, I. (1997) Numerical chromosomal aberrations in Hodgkin's disease detected by in situ hybridisation on routine paraffin sections. *J Clin Pathol* **50**, 553-558
32. Weber-Matthiesen, K., Deerberg, J., Poetsch, M., Grote, W., and Schlegelberger, B. (1995) Numerical chromosome aberrations are present within the CD30+ Hodgkin and Reed-Sternberg cells in 100% of analyzed cases of Hodgkin's disease. *Blood* **86**, 1464-1468
33. Kuppers, R., Brauninger, A., Muschen, M., Distler, V., Hansmann, M. L., and Rajewsky, K. (2001) Evidence that Hodgkin and Reed-Sternberg cells in Hodgkin disease do not represent cell fusions. *Blood* **97**, 818-821
34. Rengstl, B., Newrzela, S., Heinrich, T., Weiser, C., Thalheimer, F. B., Schmid, F., Warner, K., Hartmann, S., Schroeder, T., Kuppers, R., Rieger, M. A., and Hansmann, M. L. (2013) Incomplete cytokinesis and re-fusion of small mononucleated Hodgkin cells lead to giant multinucleated Reed-Sternberg cells. *Proc Natl Acad Sci U S A* **110**, 20729-20734
35. Wu, T. C., Mann, R. B., Charache, P., Hayward, S. D., Staal, S., Lambe, B. C., and Ambinder, R. F. (1990) Detection of EBV gene expression in Reed-Sternberg cells of Hodgkin's disease. *Int J Cancer* **46**, 801-804
36. Niedobitek, G., Kremmer, E., Herbst, H., Whitehead, L., Dawson, C. W., Niedobitek, E., von Ostau, C., Rooney, N., Grasser, F. A., and Young, L. S. (1997) Immunohistochemical detection of the Epstein-Barr virus-encoded latent membrane protein 2A in Hodgkin's disease and infectious mononucleosis. *Blood* **90**, 1664-1672
37. Pallesen, G., Hamilton-Dutoit, S. J., Rowe, M., and Young, L. S. (1991) Expression of Epstein-Barr virus latent gene products in tumour cells of Hodgkin's disease. *Lancet* **337**, 320-322
38. Flavell, K. J., and Murray, P. G. (2000) Hodgkin's disease and the Epstein-Barr virus. *Mol Pathol* **53**, 262-269
39. Kuppers, R., Klein, U., Schwering, I., Distler, V., Brauninger, A., Cattoretti, G., Tu, Y., Stolovitzky, G. A., Califano, A., Hansmann, M. L., and Dalla-Favera, R. (2003) Identification of Hodgkin and Reed-Sternberg cell-specific genes by gene expression profiling. *J Clin Invest* **111**, 529-537
40. Kuppers, R. (2012) New insights in the biology of Hodgkin lymphoma. *Hematology Am Soc Hematol Educ Program* **2012**, 328-334
41. Doerr, J. R., Malone, C. S., Fike, F. M., Gordon, M. S., Soghomonian, S. V., Thomas, R. K., Tao, Q., Murray, P. G., Diehl, V., Teitell, M. A., and Wall, R. (2005) Patterned CpG methylation of silenced B cell gene promoters in classical Hodgkin lymphoma-derived and primary effusion lymphoma cell lines. *J Mol Biol* **350**, 631-640
42. Ushmorov, A., Leithauser, F., Sakk, O., Weinhausel, A., Popov, S. W., Moller, P., and Wirth, T. (2006) Epigenetic processes play a major role in B-cell-specific gene silencing in classical Hodgkin lymphoma. *Blood* **107**, 2493-2500
43. Schwering, I., Brauninger, A., Klein, U., Jungnickel, B., Tinguely, M., Diehl, V., Hansmann, M. L., Dalla-Favera, R., Rajewsky, K., and Kuppers, R. (2003) Loss of the B-lineage-specific gene expression program in Hodgkin and Reed-Sternberg cells of Hodgkin lymphoma. *Blood* **101**, 1505-1512

44. Torlakovic, E., Tierens, A., Dang, H. D., and Delabie, J. (2001) The transcription factor PU.1, necessary for B-cell development is expressed in lymphocyte predominance, but not classical Hodgkin's disease. *Am J Pathol* **159**, 1807-1814
45. Re, D., Muschen, M., Ahmadi, T., Wickenhauser, C., Staratschek-Jox, A., Holtick, U., Diehl, V., and Wolf, J. (2001) Oct-2 and Bob-1 deficiency in Hodgkin and Reed Sternberg cells. *Cancer Res* **61**, 2080-2084
46. Stein, H., Marafioti, T., Foss, H. D., Laumen, H., Hummel, M., Anagnostopoulos, I., Wirth, T., Demel, G., and Falini, B. (2001) Down-regulation of BOB.1/OBF.1 and Oct2 in classical Hodgkin disease but not in lymphocyte predominant Hodgkin disease correlates with immunoglobulin transcription. *Blood* **97**, 496-501
47. Jundt, F., Anagnostopoulos, I., Forster, R., Mathas, S., Stein, H., and Dorken, B. (2002) Activated Notch1 signaling promotes tumor cell proliferation and survival in Hodgkin and anaplastic large cell lymphoma. *Blood* **99**, 3398-3403
48. Jundt, F., Acikgoz, O., Kwon, S. H., Schwarzer, R., Anagnostopoulos, I., Wiesner, B., Mathas, S., Hummel, M., Stein, H., Reichardt, H. M., and Dorken, B. (2008) Aberrant expression of Notch1 interferes with the B-lymphoid phenotype of neoplastic B cells in classical Hodgkin lymphoma. *Leukemia* **22**, 1587-1594
49. Lam, K. P., Kuhn, R., and Rajewsky, K. (1997) In vivo ablation of surface immunoglobulin on mature B cells by inducible gene targeting results in rapid cell death. *Cell* **90**, 1073-1083
50. Liu, Y., Sattarzadeh, A., Diepstra, A., Visser, L., and van den Berg, A. (2014) The microenvironment in classical Hodgkin lymphoma: an actively shaped and essential tumor component. *Semin Cancer Biol* **24**, 15-22
51. Vermeer, M. H., Dukers, D. F., ten Berge, R. L., Bloemena, E., Wu, L., Vos, W., de Vries, E., Tensen, C. P., Meijer, C. J., and Willemze, R. (2002) Differential expression of thymus and activation regulated chemokine and its receptor CCR4 in nodal and cutaneous anaplastic large-cell lymphomas and Hodgkin's disease. *Mod Pathol* **15**, 838-844
52. Ishida, T., Ishii, T., Inagaki, A., Yano, H., Komatsu, H., Iida, S., Inagaki, H., and Ueda, R. (2006) Specific recruitment of CC chemokine receptor 4-positive regulatory T cells in Hodgkin lymphoma fosters immune privilege. *Cancer Res* **66**, 5716-5722
53. Cattaruzza, L., Gloghini, A., Olivo, K., Di Francia, R., Lorenzon, D., De Filippi, R., Carbone, A., Colombatti, A., Pinto, A., and Aldinucci, D. (2009) Functional coexpression of Interleukin (IL)-7 and its receptor (IL-7R) on Hodgkin and Reed-Sternberg cells: Involvement of IL-7 in tumor cell growth and microenvironmental interactions of Hodgkin's lymphoma. *Int J Cancer* **125**, 1092-1101
54. Tanijiri, T., Shimizu, T., Uehira, K., Yokoi, T., Amuro, H., Sugimoto, H., Torii, Y., Tajima, K., Ito, T., Amakawa, R., and Fukuhara, S. (2007) Hodgkin's reed-sternberg cell line (KM-H2) promotes a bidirectional differentiation of CD4+CD25+Foxp3+ T cells and CD4+ cytotoxic T lymphocytes from CD4+ naive T cells. *J Leukoc Biol* **82**, 576-584
55. Marshall, N. A., Christie, L. E., Munro, L. R., Culligan, D. J., Johnston, P. W., Barker, R. N., and Vickers, M. A. (2004) Immunosuppressive regulatory T cells are abundant in the reactive lymphocytes of Hodgkin lymphoma. *Blood* **103**, 1755-1762

56. Ho, W. T., Pang, W. L., Chong, S. M., Castella, A., Al-Salam, S., Tan, T. E., Moh, M. C., Koh, L. K., Gan, S. U., Cheng, C. K., and Schwarz, H. (2013) Expression of CD137 on Hodgkin and Reed-Sternberg cells inhibits T-cell activation by eliminating CD137 ligand expression. *Cancer Res* **73**, 652-661
57. Herbst, H., Foss, H. D., Samol, J., Araujo, I., Klotzbach, H., Krause, H., Agathanggelou, A., Niedobitek, G., and Stein, H. (1996) Frequent expression of interleukin-10 by Epstein-Barr virus-harboring tumor cells of Hodgkin's disease. *Blood* **87**, 2918-2929
58. Hsu, S. M., Lin, J., Xie, S. S., Hsu, P. L., and Rich, S. (1993) Abundant expression of transforming growth factor-beta 1 and -beta 2 by Hodgkin's Reed-Sternberg cells and by reactive T lymphocytes in Hodgkin's disease. *Hum Pathol* **24**, 249-255
59. Kadin, M. E., Agnarsson, B. A., Ellingsworth, L. R., and Newcom, S. R. (1990) Immunohistochemical evidence of a role for transforming growth factor beta in the pathogenesis of nodular sclerosing Hodgkin's disease. *Am J Pathol* **136**, 1209-1214
60. Poppema, S., Potters, M., Visser, L., and van den Berg, A. M. (1998) Immune escape mechanisms in Hodgkin's disease. *Ann Oncol* **9 Suppl 5**, S21-24
61. Steidl, C., Lee, T., Shah, S. P., Farinha, P., Han, G., Nayar, T., Delaney, A., Jones, S. J., Iqbal, J., Weisenburger, D. D., Bast, M. A., Rosenwald, A., Muller-Hermelink, H. K., Rimsza, L. M., Campo, E., Delabie, J., Braziel, R. M., Cook, J. R., Tubbs, R. R., Jaffe, E. S., Lenz, G., Connors, J. M., Staudt, L. M., Chan, W. C., and Gascoyne, R. D. (2010) Tumor-associated macrophages and survival in classic Hodgkin's lymphoma. *N Engl J Med* **362**, 875-885
62. Tan, K. L., Scott, D. W., Hong, F., Kahl, B. S., Fisher, R. I., Bartlett, N. L., Advani, R. H., Buckstein, R., Rimsza, L. M., Connors, J. M., Steidl, C., Gordon, L. I., Horning, S. J., and Gascoyne, R. D. (2012) Tumor-associated macrophages predict inferior outcomes in classic Hodgkin lymphoma: a correlative study from the E2496 Intergroup trial. *Blood* **120**, 3280-3287
63. Tudor, C. S., Bruns, H., Daniel, C., Distel, L. V., Hartmann, A., Gerbitz, A., and Buettner, M. J. (2014) Macrophages and dendritic cells as actors in the immune reaction of classical Hodgkin lymphoma. *PLoS One* **9**, e114345
64. Ma, Y., Visser, L., Roelofsen, H., de Vries, M., Diepstra, A., van Imhoff, G., van der Wal, T., Luinge, M., Alvarez-Llamas, G., Vos, H., Poppema, S., Vonk, R., and van den Berg, A. (2008) Proteomics analysis of Hodgkin lymphoma: identification of new players involved in the cross-talk between HRS cells and infiltrating lymphocytes. *Blood* **111**, 2339-2346
65. Abe, R., Peng, T., Sailors, J., Bucala, R., and Metz, C. N. (2001) Regulation of the CTL response by macrophage migration inhibitory factor. *J Immunol* **166**, 747-753
66. Alvaro, T., Lejeune, M., Salvado, M. T., Bosch, R., Garcia, J. F., Jaen, J., Banham, A. H., Roncador, G., Montalban, C., and Piris, M. A. (2005) Outcome in Hodgkin's lymphoma can be predicted from the presence of accompanying cytotoxic and regulatory T cells. *Clin Cancer Res* **11**, 1467-1473
67. Greaves, P., Clear, A., Owen, A., Iqbal, S., Lee, A., Matthews, J., Wilson, A., Calaminici, M., and Gribben, J. G. (2013) Defining characteristics of classical Hodgkin lymphoma microenvironment T-helper cells. *Blood* **122**, 2856-2863

68. Chetaille, B., Bertucci, F., Finetti, P., Esterni, B., Stamatoullas, A., Picquenot, J. M., Copin, M. C., Morschhauser, F., Casasnovas, O., Petrella, T., Molina, T., Vekhoff, A., Feugier, P., Bouabdallah, R., Birnbaum, D., Olive, D., and Xerri, L. (2009) Molecular profiling of classical Hodgkin lymphoma tissues uncovers variations in the tumor microenvironment and correlations with EBV infection and outcome. *Blood* **113**, 2765-3775
69. Diepstra, A., van Imhoff, G. W., Karim-Kos, H. E., van den Berg, A., te Meerman, G. J., Niens, M., Nolte, I. M., Bastiaannet, E., Schaapveld, M., Vellenga, E., and Poppema, S. (2007) HLA class II expression by Hodgkin Reed-Sternberg cells is an independent prognostic factor in classical Hodgkin's lymphoma. *J Clin Oncol* **25**, 3101-3108
70. Steidl, C., Shah, S. P., Woolcock, B. W., Rui, L., Kawahara, M., Farinha, P., Johnson, N. A., Zhao, Y., Telenius, A., Neriah, S. B., McPherson, A., Meissner, B., Okoye, U. C., Diepstra, A., van den Berg, A., Sun, M., Leung, G., Jones, S. J., Connors, J. M., Huntsman, D. G., Savage, K. J., Rimsza, L. M., Horsman, D. E., Staudt, L. M., Steidl, U., Marra, M. A., and Gascoyne, R. D. (2011) MHC class II transactivator CIITA is a recurrent gene fusion partner in lymphoid cancers. *Nature* **471**, 377-381
71. Reiners, K. S., Kessler, J., Sauer, M., Rothe, A., Hansen, H. P., Reusch, U., Hucke, C., Kohl, U., Durkop, H., Engert, A., and von Strandmann, E. P. (2013) Rescue of impaired NK cell activity in hodgkin lymphoma with bispecific antibodies in vitro and in patients. *Mol Ther* **21**, 895-903
72. Van den Berg, A., Visser, L., Eberwine, J., Dadvand, L., and Poppema, S. (2000) Frequent lack of translation of antigen presentation-associated molecules MHC class I, CD1a and Beta(2)-microglobulin in Reed-Sternberg cells. *Int J Cancer* **86**, 548-552
73. Diepstra, A., Poppema, S., Boot, M., Visser, L., Nolte, I. M., Niens, M., Te Meerman, G. J., and van den Berg, A. (2008) HLA-G protein expression as a potential immune escape mechanism in classical Hodgkin's lymphoma. *Tissue Antigens* **71**, 219-226
74. Pogge von Strandmann, E., Simhadri, V. R., von Tresckow, B., Sasse, S., Reiners, K. S., Hansen, H. P., Rothe, A., Boll, B., Simhadri, V. L., Borchmann, P., McKinnon, P. J., Hallek, M., and Engert, A. (2007) Human leukocyte antigen-B-associated transcript 3 is released from tumor cells and engages the NKp30 receptor on natural killer cells. *Immunity* **27**, 965-974
75. Zocchi, M. R., Catellani, S., Canevali, P., Tavella, S., Garuti, A., Villaggio, B., Zunino, A., Gobbi, M., Fraternali-Orcioni, G., Kunkl, A., Ravetti, J. L., Boero, S., Musso, A., and Poggi, A. (2012) High ERp5/ADAM10 expression in lymph node microenvironment and impaired NKG2D ligands recognition in Hodgkin lymphomas. *Blood* **119**, 1479-1489
76. Dasgupta, S., Bhattacharya-Chatterjee, M., O'Malley, B. W., Jr., and Chatterjee, S. K. (2005) Inhibition of NK cell activity through TGF-beta 1 by down-regulation of NKG2D in a murine model of head and neck cancer. *J Immunol* **175**, 5541-5550
77. Lee, J. C., Lee, K. M., Kim, D. W., and Heo, D. S. (2004) Elevated TGF-beta1 secretion and down-modulation of NKG2D underlies impaired NK cytotoxicity in cancer patients. *J Immunol* **172**, 7335-7340

78. Verbeke, C. S., Wenthe, U., Grobholz, R., and Zentgraf, H. (2001) Fas ligand expression in Hodgkin lymphoma. *Am J Surg Pathol* **25**, 388-394
79. Kim, L. H., Eow, G. I., Peh, S. C., and Poppema, S. (2003) The role of CD30, CD40 and CD95 in the regulation of proliferation and apoptosis in classical Hodgkin's lymphoma. *Pathology* **35**, 428-435
80. Dotti, G., Savoldo, B., Pule, M., Straathof, K. C., Biagi, E., Yvon, E., Vigouroux, S., Brenner, M. K., and Rooney, C. M. (2005) Human cytotoxic T lymphocytes with reduced sensitivity to Fas-induced apoptosis. *Blood* **105**, 4677-4684
81. Gandhi, M. K., Lambley, E., Duraiswamy, J., Dua, U., Smith, C., Elliott, S., Gill, D., Marlton, P., Seymour, J., and Khanna, R. (2006) Expression of LAG-3 by tumor-infiltrating lymphocytes is coincident with the suppression of latent membrane antigen-specific CD8+ T-cell function in Hodgkin lymphoma patients. *Blood* **108**, 2280-2289
82. Gandhi, M. K., Moll, G., Smith, C., Dua, U., Lambley, E., Ramuz, O., Gill, D., Marlton, P., Seymour, J. F., and Khanna, R. (2007) Galectin-1 mediated suppression of Epstein-Barr virus specific T-cell immunity in classic Hodgkin lymphoma. *Blood* **110**, 1326-1329
83. Juszczynski, P., Ouyang, J., Monti, S., Rodig, S. J., Takeyama, K., Abramson, J., Chen, W., Kutok, J. L., Rabinovich, G. A., and Shipp, M. A. (2007) The AP1-dependent secretion of galectin-1 by Reed Sternberg cells fosters immune privilege in classical Hodgkin lymphoma. *Proc Natl Acad Sci U S A* **104**, 13134-13139
84. Keir, M. E., Butte, M. J., Freeman, G. J., and Sharpe, A. H. (2008) PD-1 and its ligands in tolerance and immunity. *Annu Rev Immunol* **26**, 677-704
85. Parry, R. V., Chemnitz, J. M., Frauwirth, K. A., Lanfranco, A. R., Braunstein, I., Kobayashi, S. V., Linsley, P. S., Thompson, C. B., and Riley, J. L. (2005) CTLA-4 and PD-1 receptors inhibit T-cell activation by distinct mechanisms. *Mol Cell Biol* **25**, 9543-9553
86. Yokosuka, T., Takamatsu, M., Kobayashi-Imanishi, W., Hashimoto-Tane, A., Azuma, M., and Saito, T. (2012) Programmed cell death 1 forms negative costimulatory microclusters that directly inhibit T cell receptor signaling by recruiting phosphatase SHP2. *J Exp Med* **209**, 1201-1217
87. Dong, H., Strome, S. E., Salomao, D. R., Tamura, H., Hirano, F., Flies, D. B., Roche, P. C., Lu, J., Zhu, G., Tamada, K., Lennon, V. A., Celis, E., and Chen, L. (2002) Tumor-associated B7-H1 promotes T-cell apoptosis: a potential mechanism of immune evasion. *Nat Med* **8**, 793-800
88. Yamamoto, R., Nishikori, M., Kitawaki, T., Sakai, T., Hishizawa, M., Tashima, M., Kondo, T., Ohmori, K., Kurata, M., Hayashi, T., and Uchiyama, T. (2008) PD-1-PD-1 ligand interaction contributes to immunosuppressive microenvironment of Hodgkin lymphoma. *Blood* **111**, 3220-3224
89. Ansell, S. M., Lesokhin, A. M., Borrello, I., Halwani, A., Scott, E. C., Gutierrez, M., Schuster, S. J., Millenson, M. M., Cattry, D., Freeman, G. J., Rodig, S. J., Chapuy, B., Ligon, A. H., Zhu, L., Grosso, J. F., Kim, S. Y., Timmerman, J. M., Shipp, M. A., and Armand, P. (2015) PD-1 blockade with nivolumab in relapsed or refractory Hodgkin's lymphoma. *N Engl J Med* **372**, 311-319
90. Molin, D., Fischer, M., Xiang, Z., Larsson, U., Harvima, I., Venge, P., Nilsson, K., Sundstrom, C., Enblad, G., and Nilsson, G. (2001) Mast cells express functional

CD30 ligand and are the predominant CD30L-positive cells in Hodgkin's disease. *Br J Haematol* **114**, 616-623

91. Pinto, A., Aldinucci, D., Gloghini, A., Zagonel, V., Degan, M., Improta, S., Juzbasic, S., Todesco, M., Perin, V., Gattei, V., Herrmann, F., Gruss, H. J., and Carbone, A. (1996) Human eosinophils express functional CD30 ligand and stimulate proliferation of a Hodgkin's disease cell line. *Blood* **88**, 3299-3305
92. Carbone, A., Gloghini, A., Gattei, V., Aldinucci, D., Degan, M., De Paoli, P., Zagonel, V., and Pinto, A. (1995) Expression of functional CD40 antigen on Reed-Sternberg cells and Hodgkin's disease cell lines. *Blood* **85**, 780-789
93. Carbone, A., Gloghini, A., Gruss, H. J., and Pinto, A. (1995) CD40 ligand is constitutively expressed in a subset of T cell lymphomas and on the microenvironmental reactive T cells of follicular lymphomas and Hodgkin's disease. *Am J Pathol* **147**, 912-922
94. Gruss, H. J., Hirschstein, D., Wright, B., Ulrich, D., Caligiuri, M. A., Barcos, M., Strockbine, L., Armitage, R. J., and Dower, S. K. (1994) Expression and function of CD40 on Hodgkin and Reed-Sternberg cells and the possible relevance for Hodgkin's disease. *Blood* **84**, 2305-2314
95. Hedvat, C. V., Jaffe, E. S., Qin, J., Filippa, D. A., Cordon-Cardo, C., Tosato, G., Nimer, S. D., and Teruya-Feldstein, J. (2001) Macrophage-derived chemokine expression in classical Hodgkin's lymphoma: application of tissue microarrays. *Mod Pathol* **14**, 1270-1276
96. Aldinucci, D., Lorenzon, D., Cattaruzza, L., Pinto, A., Gloghini, A., Carbone, A., and Colombatti, A. (2008) Expression of CCR5 receptors on Reed-Sternberg cells and Hodgkin lymphoma cell lines: involvement of CCL5/Rantes in tumor cell growth and microenvironmental interactions. *Int J Cancer* **122**, 769-776
97. Hanamoto, H., Nakayama, T., Miyazato, H., Takegawa, S., Hieshima, K., Tatsumi, Y., Kanamaru, A., and Yoshie, O. (2004) Expression of CCL28 by Reed-Sternberg cells defines a major subtype of classical Hodgkin's disease with frequent infiltration of eosinophils and/or plasma cells. *Am J Pathol* **164**, 997-1006
98. Jundt, F., Anagnostopoulos, I., Bommert, K., Emmerich, F., Muller, G., Foss, H. D., Royer, H. D., Stein, H., and Dorken, B. (1999) Hodgkin/Reed-Sternberg cells induce fibroblasts to secrete eotaxin, a potent chemoattractant for T cells and eosinophils. *Blood* **94**, 2065-2071
99. Gruss, H. J., Ulrich, D., Dower, S. K., Herrmann, F., and Brach, M. A. (1996) Activation of Hodgkin cells via the CD30 receptor induces autocrine secretion of interleukin-6 engaging the NF-kappabeta transcription factor. *Blood* **87**, 2443-2449
100. Zheng, B., Fiumara, P., Li, Y. V., Georgakis, G., Snell, V., Younes, M., Vauthey, J. N., Carbone, A., and Younes, A. (2003) MEK/ERK pathway is aberrantly active in Hodgkin disease: a signaling pathway shared by CD30, CD40, and RANK that regulates cell proliferation and survival. *Blood* **102**, 1019-1027
101. Foss, H. D., Herbst, H., Gottstein, S., Demel, G., Araujo, I., and Stein, H. (1996) Interleukin-8 in Hodgkin's disease. Preferential expression by reactive cells and association with neutrophil density. *Am J Pathol* **148**, 1229-1236
102. Khnykin, D., Troen, G., Berner, J. M., and Delabie, J. (2006) The expression of fibroblast growth factors and their receptors in Hodgkin's lymphoma. *J Pathol* **208**, 431-438

103. Niens, M., Visser, L., Nolte, I. M., van der Steege, G., Diepstra, A., Cordano, P., Jarrett, R. F., Te Meerman, G. J., Poppema, S., and van den Berg, A. (2008) Serum chemokine levels in Hodgkin lymphoma patients: highly increased levels of CCL17 and CCL22. *Br J Haematol* **140**, 527-536
104. Renne, C., Minner, S., Kuppers, R., Hansmann, M. L., and Brauninger, A. (2008) Autocrine NGFbeta/TRKA signalling is an important survival factor for Hodgkin lymphoma derived cell lines. *Leuk Res* **32**, 163-167
105. Renne, C., Willenbrock, K., Kuppers, R., Hansmann, M. L., and Brauninger, A. (2005) Autocrine- and paracrine-activated receptor tyrosine kinases in classic Hodgkin lymphoma. *Blood* **105**, 4051-4059
106. Teofili, L., Di Febo, A. L., Pierconti, F., Maggiano, N., Bendandi, M., Rutella, S., Cingolani, A., Di Renzo, N., Musto, P., Pileri, S., Leone, G., and Larocca, L. M. (2001) Expression of the c-met proto-oncogene and its ligand, hepatocyte growth factor, in Hodgkin disease. *Blood* **97**, 1063-1069
107. Foss, H. D., Hummel, M., Gottstein, S., Ziemann, K., Falini, B., Herbst, H., and Stein, H. (1995) Frequent expression of IL-7 gene transcripts in tumor cells of classical Hodgkin's disease. *Am J Pathol* **146**, 33-39
108. Glimelius, I., Edstrom, A., Amini, R. M., Fischer, M., Nilsson, G., Sundstrom, C., Enblad, G., and Molin, D. (2006) IL-9 expression contributes to the cellular composition in Hodgkin lymphoma. *Eur J Haematol* **76**, 278-283
109. Ullrich, K., Blumenthal-Barby, F., Lamprecht, B., Kochert, K., Lenze, D., Hummel, M., Mathas, S., Dorken, B., and Janz, M. (2015) The IL-15 cytokine system provides growth and survival signals in Hodgkin lymphoma and enhances the inflammatory phenotype of HRS cells. *Leukemia* **29**, 1213-1218
110. Kapp, U., Yeh, W. C., Patterson, B., Elia, A. J., Kagi, D., Ho, A., Hessel, A., Tipsword, M., Williams, A., Mirtsos, C., Itie, A., Moyle, M., and Mak, T. W. (1999) Interleukin 13 is secreted by and stimulates the growth of Hodgkin and Reed-Sternberg cells. *J Exp Med* **189**, 1939-1946
111. Trieu, Y., Wen, X. Y., Skinnider, B. F., Bray, M. R., Li, Z., Claudio, J. O., Masih-Khan, E., Zhu, Y. X., Trudel, S., McCart, J. A., Mak, T. W., and Stewart, A. K. (2004) Soluble interleukin-13Ralpha2 decoy receptor inhibits Hodgkin's lymphoma growth in vitro and in vivo. *Cancer Res* **64**, 3271-3275
112. Maggio, E. M., Van Den Berg, A., de Jong, D., Diepstra, A., and Poppema, S. (2003) Low frequency of FAS mutations in Reed-Sternberg cells of Hodgkin's lymphoma. *Am J Pathol* **162**, 29-35
113. Muschen, M., Re, D., Brauninger, A., Wolf, J., Hansmann, M. L., Diehl, V., Kuppers, R., and Rajewsky, K. (2000) Somatic mutations of the CD95 gene in Hodgkin and Reed-Sternberg cells. *Cancer Res* **60**, 5640-5643
114. Thomas, R. K., Schmitz, R., Harttrampf, A. C., Abdil-Hadi, A., Wickenhauser, C., Distler, V., Hansmann, M. L., Schultze, J. L., Kuppers, R., and Wolf, J. (2005) Apoptosis-resistant phenotype of classical Hodgkin's lymphoma is not mediated by somatic mutations within genes encoding members of the death-inducing signaling complex (DISC). *Leukemia* **19**, 1079-1082
115. Mathas, S., Lietz, A., Anagnostopoulos, I., Hummel, F., Wiesner, B., Janz, M., Jundt, F., Hirsch, B., Johrens-Leder, K., Vornlocher, H. P., Bommert, K., Stein, H., and Dorken, B. (2004) c-FLIP mediates resistance of Hodgkin/Reed-Sternberg cells to death receptor-induced apoptosis. *J Exp Med* **199**, 1041-1052

116. Dutton, A., O'Neil, J. D., Milner, A. E., Reynolds, G. M., Starczynski, J., Crocker, J., Young, L. S., and Murray, P. G. (2004) Expression of the cellular FLICE-inhibitory protein (c-FLIP) protects Hodgkin's lymphoma cells from autonomous Fas-mediated death. *Proc Natl Acad Sci U S A* **101**, 6611-6616
117. Garcia, J. F., Camacho, F. I., Morente, M., Fraga, M., Montalban, C., Alvaro, T., Bellas, C., Castano, A., Diez, A., Flores, T., Martin, C., Martinez, M. A., Mazorra, F., Menarguez, J., Mestre, M. J., Mollejo, M., Saez, A. I., Sanchez, L., and Piris, M. A. (2003) Hodgkin and Reed-Sternberg cells harbor alterations in the major tumor suppressor pathways and cell-cycle checkpoints: analyses using tissue microarrays. *Blood* **101**, 681-689
118. Bai, M., Papoudou-Bai, A., Kitsoulis, P., Horianopoulos, N., Kamina, S., Agnantis, N. J., and Kanavaros, P. (2005) Cell cycle and apoptosis deregulation in classical Hodgkin lymphomas. *In Vivo* **19**, 439-453
119. Chu, W. S., Aguilera, N. S., Wei, M. Q., and Abbondanzo, S. L. (1999) Antiapoptotic marker Bcl-X(L), expression on Reed-Sternberg cells of Hodgkin's disease using a novel monoclonal marker, YTH-2H12. *Hum Pathol* **30**, 1065-1070
120. Kashkar, H., Haefs, C., Shin, H., Hamilton-Dutoit, S. J., Salvesen, G. S., Kronke, M., and Jurgensmeier, J. M. (2003) XIAP-mediated caspase inhibition in Hodgkin's lymphoma-derived B cells. *J Exp Med* **198**, 341-347
121. Feuerborn, A., Moritz, C., Von Bonin, F., Dobbelstein, M., Trumper, L., Sturzenhofecker, B., and Kube, D. (2006) Dysfunctional p53 deletion mutants in cell lines derived from Hodgkin's lymphoma. *Leuk Lymphoma* **47**, 1932-1940
122. Garcia, J. F., Villuendas, R., Sanchez-Beato, M., Sanchez-Aguilera, A., Sanchez, L., Prieto, I., and Piris, M. A. (2002) Nucleolar p14(ARF) overexpression in Reed-Sternberg cells in Hodgkin's lymphoma: absence of p14(ARF)/Hdm2 complexes is associated with expression of alternatively spliced Hdm2 transcripts. *Am J Pathol* **160**, 569-578
123. Janz, M., Stuhmer, T., Vassilev, L. T., and Bargou, R. C. (2007) Pharmacologic activation of p53-dependent and p53-independent apoptotic pathways in Hodgkin/Reed-Sternberg cells. *Leukemia* **21**, 772-779
124. Drakos, E., Thomaides, A., Medeiros, L. J., Li, J., Leventaki, V., Konopleva, M., Andreeff, M., and Rassidakis, G. Z. (2007) Inhibition of p53-murine double minute 2 interaction by nutlin-3A stabilizes p53 and induces cell cycle arrest and apoptosis in Hodgkin lymphoma. *Clin Cancer Res* **13**, 3380-3387
125. Agostinelli, C., and Pileri, S. (2014) Pathobiology of hodgkin lymphoma. *Mediterr J Hematol Infect Dis* **6**, e2014040
126. Bargou, R. C., Emmerich, F., Krappmann, D., Bommert, K., Mapara, M. Y., Arnold, W., Royer, H. D., Grinstein, E., Greiner, A., Scheidereit, C., and Dorken, B. (1997) Constitutive nuclear factor-kappaB-RelA activation is required for proliferation and survival of Hodgkin's disease tumor cells. *J Clin Invest* **100**, 2961-2969
127. Cochet, O., Frelin, C., Peyron, J. F., and Imbert, V. (2006) Constitutive activation of STAT proteins in the HDLM-2 and L540 Hodgkin lymphoma-derived cell lines supports cell survival. *Cell Signal* **18**, 449-455
128. Georgakis, G. V., Li, Y., Rassidakis, G. Z., Medeiros, L. J., Mills, G. B., and Younes, A. (2006) Inhibition of the phosphatidylinositol-3 kinase/Akt promotes G1 cell cycle arrest and apoptosis in Hodgkin lymphoma. *Br J Haematol* **132**, 503-511
129. Dutton, A., Reynolds, G. M., Dawson, C. W., Young, L. S., and Murray, P. G. (2005) Constitutive activation of phosphatidyl-inositide 3 kinase contributes to

the survival of Hodgkin's lymphoma cells through a mechanism involving Akt kinase and mTOR. *J Pathol* **205**, 498-506
130. Mathas, S., Hinz, M., Anagnostopoulos, I., Krappmann, D., Lietz, A., Jundt, F., Bommert, K., Mechta-Grigoriou, F., Stein, H., Dorken, B., and Scheidereit, C. (2002) Aberrantly expressed c-Jun and JunB are a hallmark of Hodgkin lymphoma cells, stimulate proliferation and synergize with NF-kappa B. *Embo J* **21**, 4104-4113
131. Perkins, N. D., and Gilmore, T. D. (2006) Good cop, bad cop: the different faces of NF-kappaB. *Cell Death Differ* **13**, 759-772
132. Aldinucci, D., Gloghini, A., Pinto, A., De Filippi, R., and Carbone, A. (2010) The classical Hodgkin's lymphoma microenvironment and its role in promoting tumour growth and immune escape. *J Pathol* **221**, 248-263
133. Huen, D. S., Henderson, S. A., Croom-Carter, D., and Rowe, M. (1995) The Epstein-Barr virus latent membrane protein-1 (LMP1) mediates activation of NF-kappa B and cell surface phenotype via two effector regions in its carboxy-terminal cytoplasmic domain. *Oncogene* **10**, 549-560
134. Herrero, J. A., Mathew, P., and Paya, C. V. (1995) LMP-1 activates NF-kappa B by targeting the inhibitory molecule I kappa B alpha. *J Virol* **69**, 2168-2174
135. Mitchell, T., and Sugden, B. (1995) Stimulation of NF-kappa B-mediated transcription by mutant derivatives of the latent membrane protein of Epstein-Barr virus. *J Virol* **69**, 2968-2976
136. Jacobs, M. D., and Harrison, S. C. (1998) Structure of an IkappaBalpha/NF-kappaB complex. *Cell* **95**, 749-758
137. Joos, S., Menz, C. K., Wrobel, G., Siebert, R., Gesk, S., Ohl, S., Mechtersheimer, G., Trumper, L., Moller, P., Lichter, P., and Barth, T. F. (2002) Classical Hodgkin lymphoma is characterized by recurrent copy number gains of the short arm of chromosome 2. *Blood* **99**, 1381-1387
138. Martin-Subero, J. I., Gesk, S., Harder, L., Sonoki, T., Tucker, P. W., Schlegelberger, B., Grote, W., Novo, F. J., Calasanz, M. J., Hansmann, M. L., Dyer, M. J., and Siebert, R. (2002) Recurrent involvement of the REL and BCL11A loci in classical Hodgkin lymphoma. *Blood* **99**, 1474-1477
139. Cabannes, E., Khan, G., Aillet, F., Jarrett, R. F., and Hay, R. T. (1999) Mutations in the IkBa gene in Hodgkin's disease suggest a tumour suppressor role for IkappaBalpha. *Oncogene* **18**, 3063-3070
140. Jungnickel, B., Staratschek-Jox, A., Brauninger, A., Spieker, T., Wolf, J., Diehl, V., Hansmann, M. L., Rajewsky, K., and Kuppers, R. (2000) Clonal deleterious mutations in the IkappaBalpha gene in the malignant cells in Hodgkin's lymphoma. *J Exp Med* **191**, 395-402
141. Kato, M., Sanada, M., Kato, I., Sato, Y., Takita, J., Takeuchi, K., Niwa, A., Chen, Y., Nakazaki, K., Nomoto, J., Asakura, Y., Muto, S., Tamura, A., Iio, M., Akatsuka, Y., Hayashi, Y., Mori, H., Igarashi, T., Kurokawa, M., Chiba, S., Mori, S., Ishikawa, Y., Okamoto, K., Tobinai, K., Nakagama, H., Nakahata, T., Yoshino, T., Kobayashi, Y., and Ogawa, S. (2009) Frequent inactivation of A20 in B-cell lymphomas. *Nature* **459**, 712-716
142. Schmitz, R., Hansmann, M. L., Bohle, V., Martin-Subero, J. I., Hartmann, S., Mechtersheimer, G., Klapper, W., Vater, I., Giefing, M., Gesk, S., Stanelle, J., Siebert, R., and Kuppers, R. (2009) TNFAIP3 (A20) is a tumor suppressor gene in

Hodgkin lymphoma and primary mediastinal B cell lymphoma. *J Exp Med* **206**, 981-989
143. Shembade, N., Ma, A., and Harhaj, E. W. (2010) Inhibition of NF-kappaB signaling by A20 through disruption of ubiquitin enzyme complexes. *Science* **327**, 1135-1139
144. Wertz, I. E., O'Rourke, K. M., Zhou, H., Eby, M., Aravind, L., Seshagiri, S., Wu, P., Wiesmann, C., Baker, R., Boone, D. L., Ma, A., Koonin, E. V., and Dixit, V. M. (2004) De-ubiquitination and ubiquitin ligase domains of A20 downregulate NF-kappaB signalling. *Nature* **430**, 694-699
145. Diaz, T., Navarro, A., Ferrer, G., Gel, B., Gaya, A., Artells, R., Bellosillo, B., Garcia-Garcia, M., Serrano, S., Martinez, A., and Monzo, M. (2011) Lestaurtinib inhibition of the Jak/STAT signaling pathway in hodgkin lymphoma inhibits proliferation and induces apoptosis. *PLoS One* **6**, e18856
146. Murray, P. J. (2007) The JAK-STAT signaling pathway: input and output integration. *J Immunol* **178**, 2623-2629
147. Van Roosbroeck, K., Cox, L., Tousseyn, T., Lahortiga, I., Gielen, O., Cauwelier, B., De Paepe, P., Verhoef, G., Marynen, P., Vandenberghe, P., De Wolf-Peeters, C., Cools, J., and Wlodarska, I. (2011) JAK2 rearrangements, including the novel SEC31A-JAK2 fusion, are recurrent in classical Hodgkin lymphoma. *Blood* **117**, 4056-4064
148. Knoops, L., Hornakova, T., Royer, Y., Constantinescu, S. N., and Renauld, J. C. (2008) JAK kinases overexpression promotes in vitro cell transformation. *Oncogene* **27**, 1511-1519
149. Joos, S., Kupper, M., Ohl, S., von Bonin, F., Mechtersheimer, G., Bentz, M., Marynen, P., Moller, P., Pfreundschuh, M., Trumper, L., and Lichter, P. (2000) Genomic imbalances including amplification of the tyrosine kinase gene JAK2 in CD30+ Hodgkin cells. *Cancer Res* **60**, 549-552
150. Navarro, A., Diaz, T., Martinez, A., Gaya, A., Pons, A., Gel, B., Codony, C., Ferrer, G., Martinez, C., Montserrat, E., and Monzo, M. (2009) Regulation of JAK2 by miR-135a: prognostic impact in classic Hodgkin lymphoma. *Blood* **114**, 2945-2951
151. Hao, Y., Chapuy, B., Monti, S., Sun, H. H., Rodig, S. J., and Shipp, M. A. (2014) Selective JAK2 inhibition specifically decreases Hodgkin lymphoma and mediastinal large B-cell lymphoma growth in vitro and in vivo. *Clin Cancer Res* **20**, 2674-2683
152. Baus, D., and Pfitzner, E. (2006) Specific function of STAT3, SOCS1, and SOCS3 in the regulation of proliferation and survival of classical Hodgkin lymphoma cells. *Int J Cancer* **118**, 1404-1413
153. Kube, D., Holtick, U., Vockerodt, M., Ahmadi, T., Haier, B., Behrmann, I., Heinrich, P. C., Diehl, V., and Tesch, H. (2001) STAT3 is constitutively activated in Hodgkin cell lines. *Blood* **98**, 762-770
154. Skinnider, B. F., Elia, A. J., Gascoyne, R. D., Patterson, B., Trumper, L., Kapp, U., and Mak, T. W. (2002) Signal transducer and activator of transcription 6 is frequently activated in Hodgkin and Reed-Sternberg cells of Hodgkin lymphoma. *Blood* **99**, 618-626
155. Scheeren, F. A., Diehl, S. A., Smit, L. A., Beaumont, T., Naspetti, M., Bende, R. J., Blom, B., Karube, K., Ohshima, K., van Noesel, C. J., and Spits, H. (2008) IL-21 is

expressed in Hodgkin lymphoma and activates STAT5: evidence that activated STAT5 is required for Hodgkin lymphomagenesis. *Blood* **111**, 4706-4715
156. Holtick, U., Vockerodt, M., Pinkert, D., Schoof, N., Sturzenhofecker, B., Kussebi, N., Lauber, K., Wesselborg, S., Loffler, D., Horn, F., Trumper, L., and Kube, D. (2005) STAT3 is essential for Hodgkin lymphoma cell proliferation and is a target of tyrphostin AG17 which confers sensitization for apoptosis. *Leukemia* **19**, 936-944
157. Buglio, D., Georgakis, G. V., Hanabuchi, S., Arima, K., Khaskhely, N. M., Liu, Y. J., and Younes, A. (2008) Vorinostat inhibits STAT6-mediated TH2 cytokine and TARC production and induces cell death in Hodgkin lymphoma cell lines. *Blood* **112**, 1424-1433
158. Krebs, D. L., and Hilton, D. J. (2000) SOCS: physiological suppressors of cytokine signaling. *J Cell Sci* **113 (Pt 16)**, 2813-2819
159. Weniger, M. A., Melzner, I., Menz, C. K., Wegener, S., Bucur, A. J., Dorsch, K., Mattfeldt, T., Barth, T. F., and Moller, P. (2006) Mutations of the tumor suppressor gene SOCS-1 in classical Hodgkin lymphoma are frequent and associated with nuclear phospho-STAT5 accumulation. *Oncogene* **25**, 2679-2684
160. Kleppe, M., Tousseyn, T., Geissinger, E., Kalender Atak, Z., Aerts, S., Rosenwald, A., Wlodarska, I., and Cools, J. (2011) Mutation analysis of the tyrosine phosphatase PTPN2 in Hodgkin's lymphoma and T-cell non-Hodgkin's lymphoma. *Haematologica* **96**, 1723-1727
161. Schmitz, R., Stanelle, J., Hansmann, M. L., and Kuppers, R. (2009) Pathogenesis of classical and lymphocyte-predominant Hodgkin lymphoma. *Annu Rev Pathol* **4**, 151-174
162. Shaulian, E., and Karin, M. (2002) AP-1 as a regulator of cell life and death. *Nat Cell Biol* **4**, E131-136
163. Shaulian, E., and Karin, M. (2001) AP-1 in cell proliferation and survival. *Oncogene* **20**, 2390-2400
164. Wagner, E. F., and Eferl, R. (2005) Fos/AP-1 proteins in bone and the immune system. *Immunol Rev* **208**, 126-140
165. Angel, P., Imagawa, M., Chiu, R., Stein, B., Imbra, R. J., Rahmsdorf, H. J., Jonat, C., Herrlich, P., and Karin, M. (1987) Phorbol ester-inducible genes contain a common cis element recognized by a TPA-modulated trans-acting factor. *Cell* **49**, 729-739
166. Eferl, R., and Wagner, E. F. (2003) AP-1: a double-edged sword in tumorigenesis. *Nat Rev Cancer* **3**, 859-868
167. Eychene, A., Rocques, N., and Pouponnot, C. (2008) A new MAFia in cancer. *Nat Rev Cancer* **8**, 683-693
168. Angel, P., and Karin, M. (1991) The role of Jun, Fos and the AP-1 complex in cell-proliferation and transformation. *Biochim Biophys Acta* **1072**, 129-157
169. Smith, S. E., Papavassiliou, A. G., and Bohmann, D. (1993) Different TRE-related elements are distinguished by sets of DNA-binding proteins with overlapping sequence specificity. *Nucleic Acids Res* **21**, 1581-1585
170. Hai, T., and Curran, T. (1991) Cross-family dimerization of transcription factors Fos/Jun and ATF/CREB alters DNA binding specificity. *Proc Natl Acad Sci U S A* **88**, 3720-3724

171. Halazonetis, T. D., Georgopoulos, K., Greenberg, M. E., and Leder, P. (1988) c-Jun dimerizes with itself and with c-Fos, forming complexes of different DNA binding affinities. *Cell* **55**, 917-924
172. Ryseck, R. P., and Bravo, R. (1991) c-JUN, JUN B, and JUN D differ in their binding affinities to AP-1 and CRE consensus sequences: effect of FOS proteins. *Oncogene* **6**, 533-542
173. Alani, R., Brown, P., Binetruy, B., Dosaka, H., Rosenberg, R. K., Angel, P., Karin, M., and Birrer, M. J. (1991) The transactivating domain of the c-Jun proto-oncoprotein is required for cotransformation of rat embryo cells. *Mol Cell Biol* **11**, 6286-6295
174. Metz, R., Kouzarides, T., and Bravo, R. (1994) A C-terminal domain in FosB, absent in FosB/SF and Fra-1, which is able to interact with the TATA binding protein, is required for altered cell growth. *EMBO J* **13**, 3832-3842
175. O'Shea, E. K., Rutkowski, R., Stafford, W. F., 3rd, and Kim, P. S. (1989) Preferential heterodimer formation by isolated leucine zippers from fos and jun. *Science* **245**, 646-648
176. Deng, T., and Karin, M. (1993) JunB differs from c-Jun in its DNA-binding and dimerization domains, and represses c-Jun by formation of inactive heterodimers. *Genes Dev* **7**, 479-490
177. Derijard, B., Hibi, M., Wu, I. H., Barrett, T., Su, B., Deng, T., Karin, M., and Davis, R. J. (1994) JNK1: a protein kinase stimulated by UV light and Ha-Ras that binds and phosphorylates the c-Jun activation domain. *Cell* **76**, 1025-1037
178. Binetruy, B., Smeal, T., and Karin, M. (1991) Ha-Ras augments c-Jun activity and stimulates phosphorylation of its activation domain. *Nature* **351**, 122-127
179. Pulverer, B. J., Kyriakis, J. M., Avruch, J., Nikolakaki, E., and Woodgett, J. R. (1991) Phosphorylation of c-jun mediated by MAP kinases. *Nature* **353**, 670-674
180. Devary, Y., Gottlieb, R. A., Smeal, T., and Karin, M. (1992) The mammalian ultraviolet response is triggered by activation of Src tyrosine kinases. *Cell* **71**, 1081-1091
181. Bannister, A. J., Oehler, T., Wilhelm, D., Angel, P., and Kouzarides, T. (1995) Stimulation of c-Jun activity by CBP: c-Jun residues Ser63/73 are required for CBP induced stimulation in vivo and CBP binding in vitro. *Oncogene* **11**, 2509-2514
182. Chiu, R., Angel, P., and Karin, M. (1989) Jun-B differs in its biological properties from, and is a negative regulator of, c-Jun. *Cell* **59**, 979-986
183. Smeal, T., Binetruy, B., Mercola, D. A., Birrer, M., and Karin, M. (1991) Oncogenic and transcriptional cooperation with Ha-Ras requires phosphorylation of c-Jun on serines 63 and 73. *Nature* **354**, 494-496
184. Arias, J., Alberts, A. S., Brindle, P., Claret, F. X., Smeal, T., Karin, M., Feramisco, J., and Montminy, M. (1994) Activation of cAMP and mitogen responsive genes relies on a common nuclear factor. *Nature* **370**, 226-229
185. Bakiri, L., Lallemand, D., Bossy-Wetzel, E., and Yaniv, M. (2000) Cell cycle-dependent variations in c-Jun and JunB phosphorylation: a role in the control of cyclin D1 expression. *EMBO J* **19**, 2056-2068
186. Schutte, J., Viallet, J., Nau, M., Segal, S., Fedorko, J., and Minna, J. (1989) jun-B inhibits and c-fos stimulates the transforming and trans-activating activities of c-jun. *Cell* **59**, 987-997

187. Li, B., Tournier, C., Davis, R. J., and Flavell, R. A. (1999) Regulation of IL-4 expression by the transcription factor JunB during T helper cell differentiation. *EMBO J* **18**, 420-432
188. Ghosh, S., Ashcraft, K., Jahid, M. J., April, C., Ghajar, C. M., Ruan, J., Wang, H., Foster, M., Hughes, D. C., Ramirez, A. G., Huang, T., Fan, J. B., Hu, Y., and Li, R. (2013) Regulation of adipose oestrogen output by mechanical stress. *Nat Commun* **4**, 1821
189. Garaude, J., Farras, R., Bossis, G., Charni, S., Piechaczyk, M., Hipskind, R. A., and Villalba, M. (2008) SUMOylation regulates the transcriptional activity of JunB in T lymphocytes. *J Immunol* **180**, 5983-5990
190. Angel, P., Hattori, K., Smeal, T., and Karin, M. (1988) The jun proto-oncogene is positively autoregulated by its product, Jun/AP-1. *Cell* **55**, 875-885
191. Hicks, M. J., Hu, Q., Macrae, E., and DeWille, J. (2015) Mitogen-activated protein kinase signaling controls basal and oncostatin M-mediated JUNB gene expression. *Mol Cell Biochem* **403**, 115-124
192. Reunanen, N., Li, S. P., Ahonen, M., Foschi, M., Han, J., and Kahari, V. M. (2002) Activation of p38 alpha MAPK enhances collagenase-1 (matrix metalloproteinase (MMP)-1) and stromelysin-1 (MMP-3) expression by mRNA stabilization. *J Biol Chem* **277**, 32360-32368
193. Watanabe, M., Itoh, K., Togano, T., Kadin, M. E., Watanabe, T., Higashihara, M., and Horie, R. (2012) Ets-1 activates overexpression of JunB and CD30 in Hodgkin's lymphoma and anaplastic large-cell lymphoma. *Am J Pathol* **180**, 831-838
194. Watanabe, M., Sasaki, M., Itoh, K., Higashihara, M., Umezawa, K., Kadin, M. E., Abraham, L. J., Watanabe, T., and Horie, R. (2005) JunB induced by constitutive CD30-extracellular signal-regulated kinase 1/2 mitogen-activated protein kinase signaling activates the CD30 promoter in anaplastic large cell lymphoma and reed-sternberg cells of Hodgkin lymphoma. *Cancer Res* **65**, 7628-7634
195. Staber, P. B., Vesely, P., Haq, N., Ott, R. G., Funato, K., Bambach, I., Fuchs, C., Schauer, S., Linkesch, W., Hrzenjak, A., Dirks, W. G., Sexl, V., Bergler, H., Kadin, M. E., Sternberg, D. W., Kenner, L., and Hoefler, G. (2007) The oncoprotein NPM-ALK of anaplastic large-cell lymphoma induces JUNB transcription via ERK1/2 and JunB translation via mTOR signaling. *Blood* **110**, 3374-3383
196. Nateri, A. S., Riera-Sans, L., Da Costa, C., and Behrens, A. (2004) The ubiquitin ligase SCFFbw7 antagonizes apoptotic JNK signaling. *Science* **303**, 1374-1378
197. Wei, W., Jin, J., Schlisio, S., Harper, J. W., and Kaelin, W. G., Jr. (2005) The v-Jun point mutation allows c-Jun to escape GSK3-dependent recognition and destruction by the Fbw7 ubiquitin ligase. *Cancer Cell* **8**, 25-33
198. Fang, D., and Kerppola, T. K. (2004) Ubiquitin-mediated fluorescence complementation reveals that Jun ubiquitinated by Itch/AIP4 is localized to lysosomes. *Proc Natl Acad Sci U S A* **101**, 14782-14787
199. Gao, M., Labuda, T., Xia, Y., Gallagher, E., Fang, D., Liu, Y. C., and Karin, M. (2004) Jun turnover is controlled through JNK-dependent phosphorylation of the E3 ligase Itch. *Science* **306**, 271-275
200. Migliorini, D., Bogaerts, S., Defever, D., Vyas, R., Denecker, G., Radaelli, E., Zwolinska, A., Depaepe, V., Hochepied, T., Skarnes, W. C., and Marine, J. C. (2011) Cop1 constitutively regulates c-Jun protein stability and functions as a tumor suppressor in mice. *J Clin Invest* **121**, 1329-1343

201. Wertz, I. E., O'Rourke, K. M., Zhang, Z., Dornan, D., Arnott, D., Deshaies, R. J., and Dixit, V. M. (2004) Human De-etiolated-1 regulates c-Jun by assembling a CUL4A ubiquitin ligase. *Science* **303**, 1371-1374
202. Zhang, H., and Xing, L. (2013) Ubiquitin e3 ligase itch negatively regulates osteoblast differentiation from mesenchymal progenitor cells. *Stem Cells* **31**, 1574-1583
203. Fang, D., Elly, C., Gao, B., Fang, N., Altman, Y., Joazeiro, C., Hunter, T., Copeland, N., Jenkins, N., and Liu, Y. C. (2002) Dysregulation of T lymphocyte function in itchy mice: a role for Itch in TH2 differentiation. *Nat Immunol* **3**, 281-287
204. Zhao, L., Huang, J., Guo, R., Wang, Y., Chen, D., and Xing, L. (2010) Smurf1 inhibits mesenchymal stem cell proliferation and differentiation into osteoblasts through JunB degradation. *J Bone Miner Res* **25**, 1246-1256
205. Barila, D., Mangano, R., Gonfloni, S., Kretzschmar, J., Moro, M., Bohmann, D., and Superti-Furga, G. (2000) A nuclear tyrosine phosphorylation circuit: c-Jun as an activator and substrate of c-Abl and JNK. *EMBO J* **19**, 273-281
206. Johnson, R. S., van Lingen, B., Papaioannou, V. E., and Spiegelman, B. M. (1993) A null mutation at the c-jun locus causes embryonic lethality and retarded cell growth in culture. *Genes Dev* **7**, 1309-1317
207. Kovary, K., and Bravo, R. (1991) The jun and fos protein families are both required for cell cycle progression in fibroblasts. *Mol Cell Biol* **11**, 4466-4472
208. Smith, M. J., and Prochownik, E. V. (1992) Inhibition of c-jun causes reversible proliferative arrest and withdrawal from the cell cycle. *Blood* **79**, 2107-2115
209. Pfarr, C. M., Mechta, F., Spyrou, G., Lallemand, D., Carillo, S., and Yaniv, M. (1994) Mouse JunD negatively regulates fibroblast growth and antagonizes transformation by ras. *Cell* **76**, 747-760
210. Wisdom, R., Johnson, R. S., and Moore, C. (1999) c-Jun regulates cell cycle progression and apoptosis by distinct mechanisms. *EMBO J* **18**, 188-197
211. Bertoli, C., Skotheim, J. M., and de Bruin, R. A. (2013) Control of cell cycle transcription during G1 and S phases. *Nat Rev Mol Cell Biol* **14**, 518-528
212. Malumbres, M., and Barbacid, M. (2009) Cell cycle, CDKs and cancer: a changing paradigm. *Nat Rev Cancer* **9**, 153-166
213. Resnitzky, D., Gossen, M., Bujard, H., and Reed, S. I. (1994) Acceleration of the G1/S phase transition by expression of cyclins D1 and E with an inducible system. *Mol Cell Biol* **14**, 1669-1679
214. Albanese, C., Johnson, J., Watanabe, G., Eklund, N., Vu, D., Arnold, A., and Pestell, R. G. (1995) Transforming p21ras mutants and c-Ets-2 activate the cyclin D1 promoter through distinguishable regions. *J Biol Chem* **270**, 23589-23597
215. Niculescu, A. B., 3rd, Chen, X., Smeets, M., Hengst, L., Prives, C., and Reed, S. I. (1998) Effects of p21(Cip1/Waf1) at both the G1/S and the G2/M cell cycle transitions: pRb is a critical determinant in blocking DNA replication and in preventing endoreduplication. *Mol Cell Biol* **18**, 629-643
216. Abbas, T., and Dutta, A. (2009) p21 in cancer: intricate networks and multiple activities. *Nat Rev Cancer* **9**, 400-414
217. Blajeski, A. L., Phan, V. A., Kottke, T. J., and Kaufmann, S. H. (2002) G(1) and G(2) cell-cycle arrest following microtubule depolymerization in human breast cancer cells. *J Clin Invest* **110**, 91-99
218. Shaulian, E. (2010) AP-1--The Jun proteins: Oncogenes or tumor suppressors in disguise? *Cell Signal* **22**, 894-899

219. Wang, C. H., Tsao, Y. P., Chen, H. J., Chen, H. L., Wang, H. W., and Chen, S. L. (2000) Transcriptional repression of p21((Waf1/Cip1/Sdi1)) gene by c-jun through Sp1 site. *Biochem Biophys Res Commun* **270**, 303-310
220. Kolomeichuk, S. N., Bene, A., Upreti, M., Dennis, R. A., Lyle, C. S., Rajasekaran, M., and Chambers, T. C. (2008) Induction of apoptosis by vinblastine via c-Jun autoamplification and p53-independent down-regulation of p21WAF1/CIP1. *Mol Pharmacol* **73**, 128-136
221. Hennigan, R. F., and Stambrook, P. J. (2001) Dominant negative c-jun inhibits activation of the cyclin D1 and cyclin E kinase complexes. *Mol Biol Cell* **12**, 2352-2363
222. Saha, M. N., Jiang, H., Yang, Y., Zhu, X., Wang, X., Schimmer, A. D., Qiu, L., and Chang, H. (2012) Targeting p53 via JNK pathway: a novel role of RITA for apoptotic signaling in multiple myeloma. *PLoS One* **7**, e30215
223. Schreiber, M., Kolbus, A., Piu, F., Szabowski, A., Mohle-Steinlein, U., Tian, J., Karin, M., Angel, P., and Wagner, E. F. (1999) Control of cell cycle progression by c-Jun is p53 dependent. *Genes Dev* **13**, 607-619
224. Levine, A. J. (1997) p53, the cellular gatekeeper for growth and division. *Cell* **88**, 323-331
225. el-Deiry, W. S., Tokino, T., Velculescu, V. E., Levy, D. B., Parsons, R., Trent, J. M., Lin, D., Mercer, W. E., Kinzler, K. W., and Vogelstein, B. (1993) WAF1, a potential mediator of p53 tumor suppression. *Cell* **75**, 817-825
226. Kardassis, D., Papakosta, P., Pardali, K., and Moustakas, A. (1999) c-Jun transactivates the promoter of the human p21(WAF1/Cip1) gene by acting as a superactivator of the ubiquitous transcription factor Sp1. *J Biol Chem* **274**, 29572-29581
227. Eferl, R., Ricci, R., Kenner, L., Zenz, R., David, J. P., Rath, M., and Wagner, E. F. (2003) Liver tumor development. c-Jun antagonizes the proapoptotic activity of p53. *Cell* **112**, 181-192
228. Bossy-Wetzel, E., Bakiri, L., and Yaniv, M. (1997) Induction of apoptosis by the transcription factor c-Jun. *EMBO J* **16**, 1695-1709
229. Schutte, J., Minna, J. D., and Birrer, M. J. (1989) Deregulated expression of human c-jun transforms primary rat embryo cells in cooperation with an activated c-Ha-ras gene and transforms rat-1a cells as a single gene. *Proc Natl Acad Sci U S A* **86**, 2257-2261
230. Johnson, R., Spiegelman, B., Hanahan, D., and Wisdom, R. (1996) Cellular transformation and malignancy induced by ras require c-jun. *Mol Cell Biol* **16**, 4504-4511
231. Lloyd, A., Yancheva, N., and Wasylyk, B. (1991) Transformation suppressor activity of a Jun transcription factor lacking its activation domain. *Nature* **352**, 635-638
232. Suzuki, T., Murakami, M., Onai, N., Fukuda, E., Hashimoto, Y., Sonobe, M. H., Kameda, T., Ichinose, M., Miki, K., and Iba, H. (1994) Analysis of AP-1 function in cellular transformation pathways. *J Virol* **68**, 3527-3535
233. Young, M. R., Li, J. J., Rincon, M., Flavell, R. A., Sathyanarayana, B. K., Hunziker, R., and Colburn, N. (1999) Transgenic mice demonstrate AP-1 (activator protein-1) transactivation is required for tumor promotion. *Proc Natl Acad Sci U S A* **96**, 9827-9832

234. Watts, R. G., Ben-Ari, E. T., Bernstein, L. R., Birrer, M. J., Winterstein, D., Wendel, E., and Colburn, N. H. (1995) c-jun and multistage carcinogenesis: association of overexpression of introduced c-jun with progression toward a neoplastic endpoint in mouse JB6 cells sensitive to tumor promoter-induced transformation. *Mol Carcinog* **13**, 27-36
235. Domann, F. E., Levy, J. P., Birrer, M. J., and Bowden, G. T. (1994) Stable expression of a c-JUN deletion mutant in two malignant mouse epidermal cell lines blocks tumor formation in nude mice. *Cell Growth Differ* **5**, 9-16
236. Zenz, R., Scheuch, H., Martin, P., Frank, C., Eferl, R., Kenner, L., Sibilia, M., and Wagner, E. F. (2003) c-Jun regulates eyelid closure and skin tumor development through EGFR signaling. *Dev Cell* **4**, 879-889
237. Nateri, A. S., Spencer-Dene, B., and Behrens, A. (2005) Interaction of phosphorylated c-Jun with TCF4 regulates intestinal cancer development. *Nature* **437**, 281-285
238. Vleugel, M. M., Greijer, A. E., Bos, R., van der Wall, E., and van Diest, P. J. (2006) c-Jun activation is associated with proliferation and angiogenesis in invasive breast cancer. *Hum Pathol* **37**, 668-674
239. Smith, L. M., Wise, S. C., Hendricks, D. T., Sabichi, A. L., Bos, T., Reddy, P., Brown, P. H., and Birrer, M. J. (1999) cJun overexpression in MCF-7 breast cancer cells produces a tumorigenic, invasive and hormone resistant phenotype. *Oncogene* **18**, 6063-6070
240. Blonska, M., Zhu, Y., Chuang, H. H., You, M. J., Kunkalla, K., Vega, F., and Lin, X. (2015) Jun-regulated genes promote interaction of diffuse large B-cell lymphoma with the microenvironment. *Blood* **125**, 981-991
241. Papoudou-Bai, A., Goussia, A., Batistatou, A., Stefanou, D., Malamou-Mitsi, V., and Kanavaros, P. (2015) The expression levels of JunB, JunD and p-c-Jun are positively correlated with tumor cell proliferation in diffuse large B-cell lymphomas. *Leuk Lymphoma*, 1-8
242. Passegue, E., Jochum, W., Schorpp-Kistner, M., Mohle-Steinlein, U., and Wagner, E. F. (2001) Chronic myeloid leukemia with increased granulocyte progenitors in mice lacking junB expression in the myeloid lineage. *Cell* **104**, 21-32
243. Passegue, E., Wagner, E. F., and Weissman, I. L. (2004) JunB deficiency leads to a myeloproliferative disorder arising from hematopoietic stem cells. *Cell* **119**, 431-443
244. Thomsen, M. K., Bakiri, L., Hasenfuss, S. C., Wu, H., Morente, M., and Wagner, E. F. (2015) Loss of JUNB/AP-1 promotes invasive prostate cancer. *Cell Death Differ* **22**, 574-582
245. Passegue, E., and Wagner, E. F. (2000) JunB suppresses cell proliferation by transcriptional activation of p16(INK4a) expression. *EMBO J* **19**, 2969-2979
246. Andrecht, S., Kolbus, A., Hartenstein, B., Angel, P., and Schorpp-Kistner, M. (2002) Cell cycle promoting activity of JunB through cyclin A activation. *J Biol Chem* **277**, 35961-35968
247. Yamaguchi, N., Yuki, R., Kubota, S., Aoyama, K., Kuga, T., Hashimoto, Y., Tomonaga, T., and Yamaguchi, N. (2015) c-Abl-mediated tyrosine phosphorylation of JunB is required for Adriamycin-induced expression of p21. *The Biochemical journal* **471**, 67-77

248. Passegue, E., Jochum, W., Behrens, A., Ricci, R., and Wagner, E. F. (2002) JunB can substitute for Jun in mouse development and cell proliferation. *Nat Genet* **30**, 158-166
249. Schorpp-Kistner, M., Wang, Z. Q., Angel, P., and Wagner, E. F. (1999) JunB is essential for mammalian placentation. *EMBO J* **18**, 934-948
250. Rassidakis, G. Z., Thomaides, A., Atwell, C., Ford, R., Jones, D., Claret, F. X., and Medeiros, L. J. (2005) JunB expression is a common feature of CD30+ lymphomas and lymphomatoid papulosis. *Mod Pathol* **18**, 1365-1370
251. Atsaves, V., Lekakis, L., Drakos, E., Leventaki, V., Ghaderi, M., Baltatzis, G. E., Chioureas, D., Jones, D., Feretzaki, M., Liakou, C., Panayiotidis, P., Gorgoulis, V., Patsouris, E., Medeiros, L. J., Claret, F. X., and Rassidakis, G. Z. (2014) The oncogenic JUNB/CD30 axis contributes to cell cycle deregulation in ALK+ anaplastic large cell lymphoma. *Br J Haematol* **167**, 514-523
252. Szremska, A. P., Kenner, L., Weisz, E., Ott, R. G., Passegue, E., Artwohl, M., Freissmuth, M., Stoxreiter, R., Theussl, H. C., Parzer, S. B., Moriggl, R., Wagner, E. F., and Sexl, V. (2003) JunB inhibits proliferation and transformation in B-lymphoid cells. *Blood* **102**, 4159-4165
253. Ott, R. G., Simma, O., Kollmann, K., Weisz, E., Zebedin, E. M., Schorpp-Kistner, M., Heller, G., Zochbauer, S., Wagner, E. F., Freissmuth, M., and Sexl, V. (2007) JunB is a gatekeeper for B-lymphoid leukemia. *Oncogene* **26**, 4863-4871
254. Yang, M. Y., Liu, T. C., Chang, J. G., Lin, P. M., and Lin, S. F. (2003) JunB gene expression is inactivated by methylation in chronic myeloid leukemia. *Blood* **101**, 3205-3211
255. Drakos, E., Leventaki, V., Schlette, E. J., Jones, D., Lin, P., Medeiros, L. J., and Rassidakis, G. Z. (2007) c-Jun expression and activation are restricted to CD30+ lymphoproliferative disorders. *Am J Surg Pathol* **31**, 447-453
256. Leventaki, V., Drakos, E., Karanikou, M., Psatha, K., Lin, P., Schlette, E., Eliopoulos, A., Vassilakopoulos, T. P., Papadaki, H., Patsouris, E., Medeiros, L. J., and Rassidakis, G. Z. (2014) c-JUN N-terminal kinase (JNK) is activated and contributes to tumor cell proliferation in classical Hodgkin lymphoma. *Hum Pathol* **45**, 565-572
257. Horie, R., Higashihara, M., and Watanabe, T. (2003) Hodgkin's lymphoma and CD30 signal transduction. *Int J Hematol* **77**, 37-47
258. Hartmann, S., Martin-Subero, J. I., Gesk, S., Husken, J., Giefing, M., Nagel, I., Riemke, J., Chott, A., Klapper, W., Parrens, M., Merlio, J. P., Kuppers, R., Brauninger, A., Siebert, R., and Hansmann, M. L. (2008) Detection of genomic imbalances in microdissected Hodgkin and Reed-Sternberg cells of classical Hodgkin's lymphoma by array-based comparative genomic hybridization. *Haematologica* **93**, 1318-1326
259. Watanabe, M., Ogawa, Y., Ito, K., Higashihara, M., Kadin, M. E., Abraham, L. J., Watanabe, T., and Horie, R. (2003) AP-1 mediated relief of repressive activity of the CD30 promoter microsatellite in Hodgkin and Reed-Sternberg cells. *Am J Pathol* **163**, 633-641
260. Watanabe, M., Ogawa, Y., Itoh, K., Koiwa, T., Kadin, M. E., Watanabe, T., Okayasu, I., Higashihara, M., and Horie, R. (2008) Hypomethylation of CD30 CpG islands with aberrant JunB expression drives CD30 induction in Hodgkin lymphoma and anaplastic large cell lymphoma. *Lab Invest* **88**, 48-57

261. Olive, M., Krylov, D., Echlin, D. R., Gardner, K., Taparowsky, E., and Vinson, C. (1997) A dominant negative to activation protein-1 (AP1) that abolishes DNA binding and inhibits oncogenesis. *J Biol Chem* **272**, 18586-18594
262. Bogoyevitch, M. A., and Kobe, B. (2006) Uses for JNK: the many and varied substrates of the c-Jun N-terminal kinases. *Microbiol Mol Biol Rev* **70**, 1061-1095
263. Gururajan, M., Chui, R., Karuppannan, A. K., Ke, J., Jennings, C. D., and Bondada, S. (2005) c-Jun N-terminal kinase (JNK) is required for survival and proliferation of B-lymphoma cells. *Blood* **106**, 1382-1391
264. Rodig, S. J., Ouyang, J., Juszczynski, P., Currie, T., Law, K., Neuberg, D. S., Rabinovich, G. A., Shipp, M. A., and Kutok, J. L. (2008) AP1-dependent galectin-1 expression delineates classical hodgkin and anaplastic large cell lymphomas from other lymphoid malignancies with shared molecular features. *Clin Cancer Res* **14**, 3338-3344
265. Green, M. R., Rodig, S., Juszczynski, P., Ouyang, J., Sinha, P., O'Donnell, E., Neuberg, D., and Shipp, M. A. (2012) Constitutive AP-1 activity and EBV infection induce PD-L1 in Hodgkin lymphomas and posttransplant lymphoproliferative disorders: implications for targeted therapy. *Clin Cancer Res* **18**, 1611-1618
266. Green, M. R., Monti, S., Rodig, S. J., Juszczynski, P., Currie, T., O'Donnell, E., Chapuy, B., Takeyama, K., Neuberg, D., Golub, T. R., Kutok, J. L., and Shipp, M. A. (2010) Integrative analysis reveals selective 9p24.1 amplification, increased PD-1 ligand expression, and further induction via JAK2 in nodular sclerosing Hodgkin lymphoma and primary mediastinal large B-cell lymphoma. *Blood* **116**, 3268-3277
267. Fhu, C. W., Graham, A. M., Yap, C. T., Al-Salam, S., Castella, A., Chong, S. M., and Lim, Y. C. (2014) Reed-Sternberg cell-derived lymphotoxin-alpha activates endothelial cells to enhance T-cell recruitment in classical Hodgkin lymphoma. *Blood* **124**, 2973-2982
268. Ito, M., Kitamura, H., Kikuguchi, C., Hase, K., Ohno, H., and Ohara, O. (2011) SP600125 inhibits cap-dependent translation independently of the c-Jun N-terminal kinase pathway. *Cell Struct Funct* **36**, 27-33
269. Moon, D. O., Kim, M. O., Choi, Y. H., Kim, N. D., Chang, J. H., and Kim, G. Y. (2008) Bcl-2 overexpression attenuates SP600125-induced apoptosis in human leukemia U937 cells. *Cancer Lett* **264**, 316-325
270. Tanemura, S., Momose, H., Shimizu, N., Kitagawa, D., Seo, J., Yamasaki, T., Nakagawa, K., Kajiho, H., Penninger, J. M., Katada, T., and Nishina, H. (2009) Blockage by SP600125 of Fcepsilon receptor-induced degranulation and cytokine gene expression in mast cells is mediated through inhibition of phosphatidylinositol 3-kinase signalling pathway. *J Biochem* **145**, 345-354
271. Drexler, H. G., and Minowada, J. (1992) Hodgkin's disease derived cell lines: a review. *Hum Cell* **5**, 42-53
272. Livak, K. J., and Schmittgen, T. D. (2001) Analysis of relative gene expression data using real-time quantitative PCR and the 2(-Delta Delta C(T)) Method. *Methods* **25**, 402-408
273. Korzynska, A., Zychowicz, M. (2008) A Method of Estimation of the Cell Doubling Time on Basis of the Cell Culture Monitoring Data. *Biocybernetics and Biomedical Engineering* **28**, 75-82

274. Solovei, I., Schermelleh, L., Albeiz, H., Cremer, T. (2006) Detection of Cell Cycle Stages *in situ* in Growing Cell Populations. In *Cell biology : a laboratory handbook* (Celis, J. E., ed) Vol. 1 p. 293, Elsevier Academic, Amsterdam ; Boston
275. Tomayko, M. M., and Reynolds, C. P. (1989) Determination of subcutaneous tumor size in athymic (nude) mice. *Cancer chemotherapy and pharmacology* **24**, 148-154
276. Euhus, D. M., Hudd, C., LaRegina, M. C., and Johnson, F. E. (1986) Tumor measurement in the nude mouse. *J Surg Oncol* **31**, 229-234
277. Jensen, M. M., Jorgensen, J. T., Binderup, T., and Kjaer, A. (2008) Tumor volume in subcutaneous mouse xenografts measured by microCT is more accurate and reproducible than determined by 18F-FDG-microPET or external caliper. *BMC Med Imaging* **8**, 16
278. Huang da, W., Sherman, B. T., and Lempicki, R. A. (2009) Systematic and integrative analysis of large gene lists using DAVID bioinformatics resources. *Nat Protoc* **4**, 44-57
279. Huang da, W., Sherman, B. T., and Lempicki, R. A. (2009) Bioinformatics enrichment tools: paths toward the comprehensive functional analysis of large gene lists. *Nucleic Acids Res* **37**, 1-13
280. Leventaki, V., Drakos, E., Medeiros, L. J., Lim, M. S., Elenitoba-Johnson, K. S., Claret, F. X., and Rassidakis, G. Z. (2007) NPM-ALK oncogenic kinase promotes cell-cycle progression through activation of JNK/cJun signaling in anaplastic large-cell lymphoma. *Blood* **110**, 1621-1630
281. Solovei, I., Schermelleh, L., Albiez, H., and Cremer, T. (2006) Chapter 35 - Detection of Cell Cycle Stages in situ in Growing Cell Populations. In *Cell Biology (Third Edition)* (Celis, J. E., ed) pp. 291-299, Academic Press, Burlington
282. Jordan, M. A., Thrower, D., and Wilson, L. (1992) Effects of vinblastine, podophyllotoxin and nocodazole on mitotic spindles. Implications for the role of microtubule dynamics in mitosis. *J Cell Sci* **102 (Pt 3)**, 401-416
283. Choi, H. J., Fukui, M., and Zhu, B. T. (2011) Role of cyclin B1/Cdc2 up-regulation in the development of mitotic prometaphase arrest in human breast cancer cells treated with nocodazole. *PLoS One* **6**, e24312
284. Jordan, M. A., and Wilson, L. (1998) Microtubules and actin filaments: dynamic targets for cancer chemotherapy. *Curr Opin Cell Biol* **10**, 123-130
285. Hong, F. D., Chen, J., Donovan, S., Schneider, N., and Nisen, P. D. (1999) Taxol, vincristine or nocodazole induces lethality in G1-checkpoint-defective human astrocytoma U373MG cells by triggering hyperploid progression. *Carcinogenesis* **20**, 1161-1168
286. Czekanska, E. M. (2011) Assessment of cell proliferation with resazurin-based fluorescent dye. *Methods Mol Biol* **740**, 27-32
287. Fabian, M. A., Biggs, W. H., 3rd, Treiber, D. K., Atteridge, C. E., Azimioara, M. D., Benedetti, M. G., Carter, T. A., Ciceri, P., Edeen, P. T., Floyd, M., Ford, J. M., Galvin, M., Gerlach, J. L., Grotzfeld, R. M., Herrgard, S., Insko, D. E., Insko, M. A., Lai, A. G., Lelias, J. M., Mehta, S. A., Milanov, Z. V., Velasco, A. M., Wodicka, L. M., Patel, H. K., Zarrinkar, P. P., and Lockhart, D. J. (2005) A small molecule-kinase interaction map for clinical kinase inhibitors. *Nat Biotechnol* **23**, 329-336
288. Bain, J., Plater, L., Elliott, M., Shpiro, N., Hastie, C. J., McLauchlan, H., Klevernic, I., Arthur, J. S., Alessi, D. R., and Cohen, P. (2007) The selectivity of protein kinase inhibitors: a further update. *Biochem J* **408**, 297-315

289. Vignon, C., Debeissat, C., Georget, M. T., Bouscary, D., Gyan, E., Rosset, P., and Herault, O. (2013) Flow cytometric quantification of all phases of the cell cycle and apoptosis in a two-color fluorescence plot. *PLoS One* **8**, e68425
290. Schluter, C., Duchrow, M., Wohlenberg, C., Becker, M. H., Key, G., Flad, H. D., and Gerdes, J. (1993) The cell proliferation-associated antigen of antibody Ki-67: a very large, ubiquitous nuclear protein with numerous repeated elements, representing a new kind of cell cycle-maintaining proteins. *J Cell Biol* **123**, 513-522
291. Morente, M. M., Piris, M. A., Abraira, V., Acevedo, A., Aguilera, B., Bellas, C., Fraga, M., Garcia-Del-Moral, R., Gomez-Marcos, F., Menarguez, J., Oliva, H., Sanchez-Beato, M., and Montalban, C. (1997) Adverse clinical outcome in Hodgkin's disease is associated with loss of retinoblastoma protein expression, high Ki67 proliferation index, and absence of Epstein-Barr virus-latent membrane protein 1 expression. *Blood* **90**, 2429-2436
292. Kanavaros, P., Stefanaki, K., Vlachonikolis, J., Eliopoulos, G., Kakolyris, S., Rontogianni, D., Gorgoulis, V., and Georgoulias, V. (2000) Expression of p53, p21/waf1, bcl-2, bax, Rb and Ki67 proteins in Hodgkin's lymphomas. *Histol Histopathol* **15**, 445-453
293. Xu, X. M., Yoo, M. H., Carlson, B. A., Gladyshev, V. N., and Hatfield, D. L. (2009) Simultaneous knockdown of the expression of two genes using multiple shRNAs and subsequent knock-in of their expression. *Nat Protoc* **4**, 1338-1348
294. Gurzov, E. N., Bakiri, L., Alfaro, J. M., Wagner, E. F., and Izquierdo, M. (2008) Targeting c-Jun and JunB proteins as potential anticancer cell therapy. *Oncogene* **27**, 641-652
295. Zhou, H., Zarubin, T., Ji, Z., Min, Z., Zhu, W., Downey, J. S., Lin, S., and Han, J. (2005) Frequency and distribution of AP-1 sites in the human genome. *DNA Res* **12**, 139-150
296. Ashburner, M., Ball, C. A., Blake, J. A., Botstein, D., Butler, H., Cherry, J. M., Davis, A. P., Dolinski, K., Dwight, S. S., Eppig, J. T., Harris, M. A., Hill, D. P., Issel-Tarver, L., Kasarskis, A., Lewis, S., Matese, J. C., Richardson, J. E., Ringwald, M., Rubin, G. M., and Sherlock, G. (2000) Gene ontology: tool for the unification of biology. The Gene Ontology Consortium. *Nat Genet* **25**, 25-29
297. Elishmereni, M., and Levi-Schaffer, F. (2011) CD48: A co-stimulatory receptor of immunity. *Int J Biochem Cell Biol* **43**, 25-28
298. Thomas, M., Boname, J. M., Field, S., Nejentsev, S., Salio, M., Cerundolo, V., Wills, M., and Lehner, P. J. (2008) Down-regulation of NKG2D and NKp80 ligands by Kaposi's sarcoma-associated herpesvirus K5 protects against NK cell cytotoxicity. *Proc Natl Acad Sci U S A* **105**, 1656-1661
299. Welte, S., Kuttruff, S., Waldhauer, I., and Steinle, A. (2006) Mutual activation of natural killer cells and monocytes mediated by NKp80-AICL interaction. *Nat Immunol* **7**, 1334-1342
300. Brown, M. H., Boles, K., van der Merwe, P. A., Kumar, V., Mathew, P. A., and Barclay, A. N. (1998) 2B4, the natural killer and T cell immunoglobulin superfamily surface protein, is a ligand for CD48. *J Exp Med* **188**, 2083-2090
301. Elias, S., Yamin, R., Golomb, L., Tsukerman, P., Stanietsky-Kaynan, N., Ben-Yehuda, D., and Mandelboim, O. (2014) Immune evasion by oncogenic proteins of acute myeloid leukemia. *Blood* **123**, 1535-1543

302. Gobert, M., Treilleux, I., Bendriss-Vermare, N., Bachelot, T., Goddard-Leon, S., Arfi, V., Biota, C., Doffin, A. C., Durand, I., Olive, D., Perez, S., Pasqual, N., Faure, C., Ray-Coquard, I., Puisieux, A., Caux, C., Blay, J. Y., and Menetrier-Caux, C. (2009) Regulatory T cells recruited through CCL22/CCR4 are selectively activated in lymphoid infiltrates surrounding primary breast tumors and lead to an adverse clinical outcome. *Cancer Res* **69**, 2000-2009
303. Li, Y. Q., Liu, F. F., Zhang, X. M., Guo, X. J., Ren, M. J., and Fu, L. (2013) Tumor secretion of CCL22 activates intratumoral Treg infiltration and is independent prognostic predictor of breast cancer. *PLoS One* **8**, e76379
304. Rao, D. D., Vorhies, J. S., Senzer, N., and Nemunaitis, J. (2009) siRNA vs. shRNA: similarities and differences. *Adv Drug Deliv Rev* **61**, 746-759
305. Jackson, A. L., and Linsley, P. S. (2010) Recognizing and avoiding siRNA off-target effects for target identification and therapeutic application. *Nat Rev Drug Discov* **9**, 57-67
306. Brugarolas, J., Moberg, K., Boyd, S. D., Taya, Y., Jacks, T., and Lees, J. A. (1999) Inhibition of cyclin-dependent kinase 2 by p21 is necessary for retinoblastoma protein-mediated G1 arrest after gamma-irradiation. *Proc Natl Acad Sci U S A* **96**, 1002-1007
307. Martin-Caballero, J., Flores, J. M., Garcia-Palencia, P., and Serrano, M. (2001) Tumor susceptibility of p21(Waf1/Cip1)-deficient mice. *Cancer Res* **61**, 6234-6238
308. Bukholm, I. K., and Nesland, J. M. (2000) Protein expression of p53, p21 (WAF1/CIP1), bcl-2, Bax, cyclin D1 and pRb in human colon carcinomas. *Virchows Arch* **436**, 224-228
309. Edmonston, T. B., Cuesta, K. H., Burkholder, S., Barusevicius, A., Rose, D., Kovatich, A. J., Boman, B., Fry, R., Fishel, R., and Palazzo, J. P. (2000) Colorectal carcinomas with high microsatellite instability: defining a distinct immunologic and molecular entity with respect to prognostic markers. *Hum Pathol* **31**, 1506-1514
310. Ogino, S., Kawasaki, T., Kirkner, G. J., Ogawa, A., Dorfman, I., Loda, M., and Fuchs, C. S. (2006) Down-regulation of p21 (CDKN1A/CIP1) is inversely associated with microsatellite instability and CpG island methylator phenotype (CIMP) in colorectal cancer. *J Pathol* **210**, 147-154
311. Lu, X., Toki, T., Konishi, I., Nikaido, T., and Fujii, S. (1998) Expression of p21WAF1/CIP1 in adenocarcinoma of the uterine cervix: a possible immunohistochemical marker of a favorable prognosis. *Cancer* **82**, 2409-2417
312. Balbin, M., Hannon, G. J., Pendas, A. M., Ferrando, A. A., Vizoso, F., Fueyo, A., and Lopez-Otin, C. (1996) Functional analysis of a p21WAF1,CIP1,SDI1 mutant (Arg94 --> Trp) identified in a human breast carcinoma. Evidence that the mutation impairs the ability of p21 to inhibit cyclin-dependent kinases. *J Biol Chem* **271**, 15782-15786
313. Wettersten, H. I., Hee Hwang, S., Li, C., Shiu, E. Y., Wecksler, A. T., Hammock, B. D., and Weiss, R. H. (2013) A novel p21 attenuator which is structurally related to sorafenib. *Cancer Biol Ther* **14**, 278-285
314. Hu, X., Xing, L., Jiao, Y., Xu, J., Wang, X., Han, A., and Yu, J. (2013) BTG2 overexpression increases the radiosensitivity of breast cancer cells in vitro and in vivo. *Oncol Res* **20**, 457-465

315. Lim, I. K., Lee, M. S., Ryu, M. S., Park, T. J., Fujiki, H., Eguchi, H., and Paik, W. K. (1998) Induction of growth inhibition of 293 cells by downregulation of the cyclin E and cyclin-dependent kinase 4 proteins due to overexpression of TIS21. *Mol Carcinog* **23**, 25-35
316. Guardavaccaro, D., Corrente, G., Covone, F., Micheli, L., D'Agnano, I., Starace, G., Caruso, M., and Tirone, F. (2000) Arrest of G(1)-S progression by the p53-inducible gene PC3 is Rb dependent and relies on the inhibition of cyclin D1 transcription. *Mol Cell Biol* **20**, 1797-1815
317. Hurtz, C., Hatzi, K., Cerchietti, L., Braig, M., Park, E., Kim, Y. M., Herzog, S., Ramezani-Rad, P., Jumaa, H., Muller, M. C., Hofmann, W. K., Hochhaus, A., Ye, B. H., Agarwal, A., Druker, B. J., Shah, N. P., Melnick, A. M., and Muschen, M. (2011) BCL6-mediated repression of p53 is critical for leukemia stem cell survival in chronic myeloid leukemia. *J Exp Med* **208**, 2163-2174
318. Phan, R. T., Saito, M., Basso, K., Niu, H., and Dalla-Favera, R. (2005) BCL6 interacts with the transcription factor Miz-1 to suppress the cyclin-dependent kinase inhibitor p21 and cell cycle arrest in germinal center B cells. *Nat Immunol* **6**, 1054-1060
319. Wang, Y. Q., Xu, M. D., Weng, W. W., Wei, P., Yang, Y. S., and Du, X. (2015) BCL6 is a negative prognostic factor and exhibits pro-oncogenic activity in ovarian cancer. *Am J Cancer Res* **5**, 255-266
320. Monahan, P., Rybak, S., and Raetzman, L. T. (2009) The notch target gene HES1 regulates cell cycle inhibitor expression in the developing pituitary. *Endocrinology* **150**, 4386-4394
321. Murata, K., Hattori, M., Hirai, N., Shinozuka, Y., Hirata, H., Kageyama, R., Sakai, T., and Minato, N. (2005) Hes1 directly controls cell proliferation through the transcriptional repression of p27Kip1. *Mol Cell Biol* **25**, 4262-4271
322. Laimer, D., Dolznig, H., Kollmann, K., Vesely, P. W., Schlederer, M., Merkel, O., Schiefer, A. I., Hassler, M. R., Heider, S., Amenitsch, L., Thallinger, C., Staber, P. B., Simonitsch-Klupp, I., Artaker, M., Lagger, S., Turner, S. D., Pileri, S., Piccaluga, P. P., Valent, P., Messana, K., Landra, I., Weichhart, T., Knapp, S., Shehata, M., Todaro, M., Sexl, V., Hofler, G., Piva, R., Medico, E., Ruggeri, B. A., Cheng, M., Eferl, R., Egger, G., Penninger, J. M., Jaeger, U., Moriggl, R., Inghirami, G., and Kenner, L. (2012) PDGFR blockade is a rational and effective therapy for NPM-ALK-driven lymphomas. *Nat Med* **18**, 1699-1704
323. Tiacci, E., Doring, C., Brune, V., van Noesel, C. J., Klapper, W., Mechtersheimer, G., Falini, B., Kuppers, R., and Hansmann, M. L. (2012) Analyzing primary Hodgkin and Reed-Sternberg cells to capture the molecular and cellular pathogenesis of classical Hodgkin lymphoma. *Blood* **120**, 4609-4620
324. Willenbrock, K., Kuppers, R., Renne, C., Brune, V., Eckerle, S., Weidmann, E., Brauninger, A., and Hansmann, M. L. (2006) Common features and differences in the transcriptome of large cell anaplastic lymphoma and classical Hodgkin's lymphoma. *Haematologica* **91**, 596-604

APPENDICES

Appendix 1: c-Jun and JunB shRNA targeting sequence

```
   1 GAGCGGCCAG GCCAGCCTCG GAGCCAGCAG GGAGCTGGGA GCTGGGGGAA ACGACGCCAG
  61 GAAAGCTATC GCGCCAGAGA GGGCGACGGG GGCTCGGGAA GCCTGACAGG GCTTTTGCGC
 121 ACAGCTGCCG GCTGGCTGCT ACCCGCCCGC GCCAGCCCCC GAGAACGCGC GACCAGGCAC
 181 CCAGTCCGGT CACCGCAGCG GAGAGCTCGC CGCTCGCTGC AGCGAGGCCC GGAGCGGCCC
 241 CGCAGGGACC CTCCCCAGAC CGCCTGGGCC GCCCGGATGT GCACTAAAAT GGAACAGCCC
 301 TTCTACCACG ACGACTCATA CACAGCTACG GGATACGGCC GGGCCCCTGG TGGCCTCTCT
 361 CTACACGACT ACAAACTCCT GAAACCGAGC CTGGCGGTCA ACCTGGCCGA CCCCTACCGG
 421 AGTCTCAAAG CGCCTGGGGC TCGCGGACCC GGCCCAGAGG GCGGCGGTGG CGGCAGCTAC
 481 TTTTCTGGTC AGGGCTCGGA CACCGGCGCG TCTCTCAAGC TCGCCTCTTC GGAGCTGGAA
 541 CGCCTGATTG TCCCCAACAG CAACGGCGTG ATCACGACGA CGCCTACACC CCCGGGACAG
 601 TACTTTTACC CCCGCGGGGG TGGCAGCGGT GGAGGTGCAG GGGGCGCAGG GGGCGGCGTC
 661 ACCGAGGAGC AGGAGGGCTT CGCCGACGGC TTTGTCAAAG CCCTGGACGA TCTGCACAAG
 721 ATGAACCACG TGACACCCCC CAACGTGTCC CTGGGCGCTA CCGGGGGGCC CCCGGCTGGG
 781 CCCGGGGGCG TCTACGCCGG CCCGGAGCCA CCTCCCGTTT ACACCAACCT CAGCAGCTAC
 841 TCCCCAGCCT CTGCGTCCTC GGGAGGCGCC GGGGCTGCCG TCGGGACCGG GAGCTCGTAC
 901 CCGACGACCA CCATCAGCTA CCTCCCACAC GCGCCGCCCT TCGCCGGTGG CCACCCGGCG
 961 CAGCTGGGCT TGGGCCGCGG CGCCTCCACC TTCAAGGAGG AACCGCAGAC CGTGCCGGAG
1021 GCGCGCAGCC GGGACGCCAC GCCGCCGGTG TCCCCCATCA ACATGGAAGA CCAAGAGCGC
1081 ATCAAAGTGG AGCGCAAGCG GCTGCGGAAC CGGCTGGCGG CCACCAAGTG CCGGAAGCGG
1141 AAGCTGGAGC GCATCGCGCG CCTGGAGGAC AAGGTGAAGA CGCTCAAGGC CGAGAACGCG
1201 GGGCTGTCGA GTACCGCCGG CCTCCTCCGG GAGCAGGTGG CCCAGCTCAA ACAGAAGGTC
1261 ATGACCCACG TCAGCAACGG CTGTCAGCTG CTGCTTGGGG TCAAGGGACA CGCCTTCTGA
1321 ACGTCCCCTG CCCCTTTACG GACACCCCCT CGCTTGGACG GCTGGGCACA CGCCTCCCAC
1381 TGGGGTCCAG GGAGCAGGCG GTGGGCACCC ACCCTGGGAC CTAGGGGCGC CGCAAACCAC
1441 ACTGGACTCC GGCCCTCCTA CCCTGCGCCC AGTCCTTCCA CCTCGACGTT TACAAGCCCC
1501 CCCTTCCACT TTTTTTTGTA TGTTTTTTTT CTGCTGGAAA CAGACTCGAT TCATATTGAA
1561 TATAATATAT TTGTGTATTT AACAGGGAGG GGAAGAGGGG GCGATCGCGG CGGAGCTGGC
1621 CCCGCCGCCT GGTACTCAAG CCCGCGGGGA CATTGGGAAG GGGACCCCCG CCCCCTGCCC
1681 TCCCCTCTCT GCACCGTACT GTGGAAAAGA AACACGCACT TAGTCTCTAA AGAGTTTATT
1741 TTAAGACGTG TTTGTGTTTG TGTGTGTTTG TTCTTTTTAT TGAATCTATT TAAGTAAAAA
1801 AAAAATTGGT TCTTTAAAAA AAAAAAAAAA AA
```

Figure A1a– JunB shRNA targeting sequence map

Figure shows the mRNA sequence for *JunB* and the coding sequence is underlined. The two JunB shRNA sequences can be found in **Table 2.1**. JunB#1 shRNA targeting sequence is red and underlined and the JunB#6 shRNA targeting sequence is highlighted in green. Both shRNAs target the 3' untranslated region of JunB mRNA.

GACATCATGGGCTATTTTTAGGGGTTGACTGGTAGCAGATAAGTGTTGAGCTCGGGCTGGATAA
GGGCTCAGAGTTGCACTGAGTGTGGCTGAAGCAGCGAGGCGGGAGTGGAGGTGCGCGGAGTCAG
GCAGACAGACAGACACAGCCAGCCAGCCAGGTCGGCAGTATAGTCCGAACTGCAAATCTTATTT
TCTTTTCACCTTCTCTCTAACTGCCCAGAGCTAGCGCCTGTGGCTCCCGGGCTGGTGTTTCGGG
AGTGTCCAGAGAGCCTGGTCTCCAGCCGCCCCCGGGAGGAGAGCCCTGCTGCCCAGGCGCTGTT
GACAGCGGCGGAAAGCAGCGGTACCCACGCGCCCGCCGGGGGAAGTCGGCGAGCGGCTGCAGCA
GCAAAGAACTTTCCCGGCTGGGAGGACCGGAGACAAGTGGCAGAGTCCCGGAGCGAACTTTTGC
AAGCCTTTCCTGCGTCTTAGGCTTCTCCACGGCGGTAAAGACCAGAAGGCGGCGGAGAGCCACG
CAAGAGAAGAAGGACGTGCGCTCAGCTTCGCTCGCACCGGTTGTTGAACTTGGGCGAGCGCGAG
CCGCGGCTGCCGGGCGCCCCCTCCCCCTAGCAGCGGAGGAGGGGACAAGTCGTCGGAGTCCGGG
CGGCCAAGACCCGCCGCCGGCCGGCCACTGCAGGGTCCGCACTGATCCGCTCCGCGGGGAGAGC
CGCTGCTCTGGGAAGTGAGTTCGCCTGCGGACTCCGAGGAACCGCTGCGCCCGAAGAGCGCTCA
GTGAGTGACCGCGACTTTTCAAAGCCGGGTAGCGCGCGCGAGTCGACAAGTAAGAGTGCGGGAG
GCATCTTAATTAACCCTGCGCTCCCTGGAGCGAGCTGGTGAGGAGGGCGCAGCGGGGACGACAG
CCAGCGGGTGCGTGCGCTCTTAGAGAAACTTTCCCTGTCAAAGGCTCCGGGGGGCGCGGGTGTC
CCCCGCTTGCCAGAGCCCTGTTGCGGCCCCGAAACTTGTGCGCGCAGCCCAAACTAACCTCACG
TGAAGTGACGGACTGTTCTATGACTGCAAAGATGGAAACGACCTTCTATGACGATGCCCTCAAC
GCCTCGTTCCTCCCGTCCGAGAGCGGACCTTATGGCTACAGTAACCCCAAGATCCTGAAACAGA
GCATGACCCTGAACCTGGCCGACCCAGTGGGGAGCCTGAAGCCGCACCTCCGCGCCAAGAACTC
GGACCTCCTCACCTCGCCCGACGTGGGGCTGCTCAAGCTGGCGTCGCCCGAGCTGGAGCGCCTG
ATAATCCAGTCCAGCAACGGGCACATCACCACCACGCCGACCCCCACCCAGTTCCTGTGCCCCA
AGAACGTGACAGATGAGCAGGAGGGCTTCGCCGAGGGCTTCGTGCGCGCCCTGGCCGAACTGCA
CAGCCAGAACACGCTGCCCAGCGTCACGTCGGCGGCGCAGCCGGTCAACGGGGCAGGCATGGTG
GCTCCCGCGGTAGCCTCGGTGGCAGGGGGCAGCGGCAGCGGCGGCTTCAGCGCCAGCCTGCACA
GCGAGCCGCCGGTCTACGCAAACCTCAGCAACTTCAACCCAGGCGCGCTGAGCAGCGGCGGCGG
GGCGCCCTCCTACGGCGCGGCCGGCCTGGCCTTTCCCGCGCAACCCCAGCAGCAGCAGCAGCCG
CCGCACCACCTGCCCCAGCAGATGCCCGTGCAGCACCCGCGGCTGCAGGCCCTGAAGGAGGAGC
CTCAGACAGTGCCCGAGATGCCCGGCGAGACACCGCCCCTGTCCCCCATCGACATGGAGTCCCA
GGAGCGGATCAAGGCGGAGAGGAAGCGCATGAGGAACCGCATCGCTGCCTCCAAGTGCCGAAAA
AGGAAGCTGGAGAGAATCGCCCGGCTGGAGGAAAAAGTGAAAACCTTGAAAGCTCAGAACTCGG
AGCTGGCGTCCACGGCCAACATGCTCAGGGAACAGGTGGCACAGCTTAAACAGAAAGTCATGAA
CCACGTTAACAGTGGGTGCCAACTCATGCTAACGCAGCAGTTGCAAACATTTTGAAGAGAGACC
GTCGGGGGCTGAGGGGCAACGAAGAAAAAAAATAACACAGAGAGACAGACTTGAGAACTTGACA
AGTTGCGACGGAGAGAAAAAAGAAGTGTCCGAGAACTAAAGCCAAGGGTATCCAAGTTGGACTG
GGTTGCGTCCTGACGGCGCCCCCAGTGTGCACGAGTGGGAAGGACTTGGCGCGCCCTCCCTTGG
CGTGGAGCCAGGGAGCGGCCGCCTGCGGGCTGCCCCGCTTTGCGGACGGGCTGTCCCCGCGCGA
ACGGAACGTTGGACTTTTCGTTAACATTCAGACCAAGAACTGCATGGACCTAACATTCGATCTC
ATTCAGTATTAAGGGGGAGGGGGAGGGGGTTACAAACTGCAATAGAGACTGTAGATTGCTTCTG
TAGTACTCCTTAAGAACACAAAGCGGGGGGAGGGTTGGGGAGGGGCGGCAGGAGGGAGGTTTGT
GAGAGCGAGGCTGAGCCTACAGATGAACTCTTTCTGGCCTGCCTTCGTTAACTGTGTATGTACA
TATATATATTTTTTAATTTGATGAAAGCTGATTACTGTCAATAAACAGCTTCATGCCTTTGTAA
GTTATTTCTTGTTTGTTTGTTTGGGTATCCTGCCCAGTGTTGTTTGTAAATAAGAGATTTGGAG
CACTCTGAGTTTACCATTTGTAATAAAGTATATAATTTTTTTATGTTTTGTTTCTGAAAATTCC
AGAAAGGATATTTAAGAAAATACAATAAACTATTGGAAAGTACTCCCCTAACCTCTTTTCTGCA
TCATCTGTAGATACTAGCTATCTAGGTGGAGTTGAAAGAGTTAAGAATGTCGATTAAAATCACT
CTCAGTGCTTCTTACTATTAAGCAGTAAAAACTGTTCTCTATTAGACTTTAGAAATAAATGTAC
CTGATGTACCTGATGCTATGGTCAGGTTATACTCCTCCTCCCCCAGCTATCTATATGGAATTGC
TTACCAAAGGATAGTGCGATGTTTCAGGAGGCTGGAGGAAGGGGGGTTGCAGTGGAGAGGGACA
GCCCACTGAGAAGTCAAACATTTCAAAGTTTGGATTGTATCAAGTGGCATGTGCTGTGACCATT
TATAATGTTAGTAGAAATTTTACAATAGGTGCTTATTCTCAAAGCAGGAATTGGTGGCAGATTT
TACAAAAGATGTATCCTTCCAATTTGGAATCTTCTCTTTGACAATTCCTAGATAAAAAGATGGC
CTTTGCTTATGAATATTTATAACAGCATTCTTGTCACAATAAATGTATTCAAATACCAAAAAAA
AAAAAAAAAA

Figure A1b – c-Jun shRNA targeting sequence map

Figure shows the mRNA sequence for *Jun* and the coding sequence is underlined. The two c-Jun shRNA sequences can be found in **Table 2.1**. The c-Jun#1 shRNA targeting sequence is highlighted in green and targets the 3' untranslated region of c-Jun mRNA. The c-Jun#4 shRNA targeting sequence is highlighted in yellow and targets the coding sequence.

Appendix 2: Additional shRNA tested

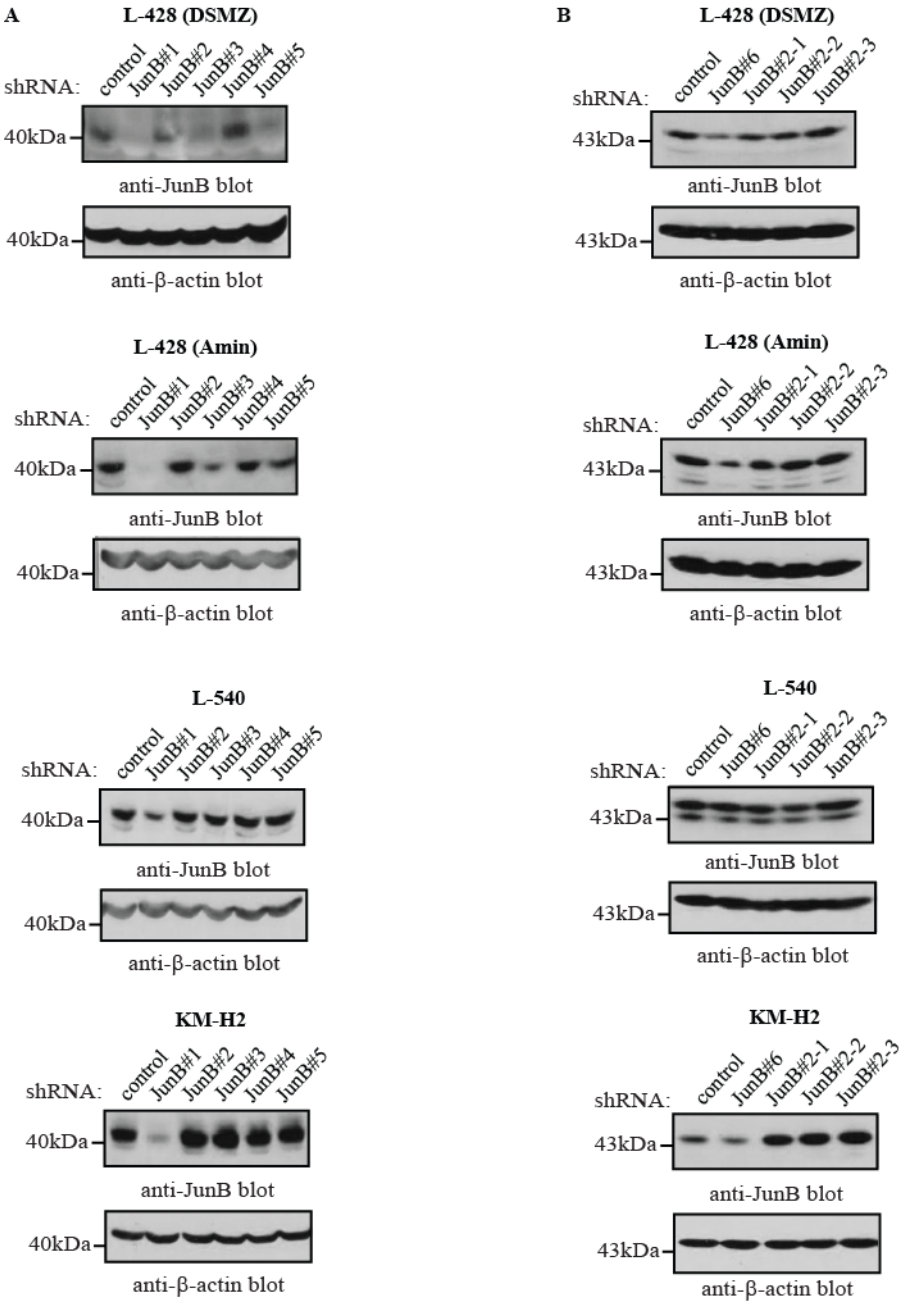

Figure A2 – additional JunB shRNA tested

Western blots showing the degree of JunB silencing in all four cHL cells expressing the JunB#2, #3, #4, #5 (**A**) and JunB #2-1, #2-2 and #2-3 shRNAs (**B**). JunB #1 and #6 shRNAs were used as a positive control for silencing JunB expression. Molecular mass markers are indicated on the left of blots. The anti-β-actin blot serves as a loading control. All data in this figure was generated from one infection and the experiment was performed once.

Appendix 3: STR report

The Centre for Applied GenomicsCell line authentication report

Genetic Analysis Facility

The Centre for Applied Genomics

The Hospital for Sick Children

Peter Gilgan Centre for Research and Learning 686 Bay St.,

Toronto, ON, Canada M5G 0A4

Date of report: February 10, 2016

Description of service: DNA for two samples labelled "L-428 (new)" and "L-428 (old)" were submitted to the TCAG Genetic Analysis Facility for STR profiling using Promega's GenePrint® 10 System (part B9510).

Results:

Sample name	L-428 (new)		L-428 (old)		Comment
Marker	Allele 1	Allele 2	Allele 1	Allele 2	
Amelogenin	X	X	X	X	Match
CSF1PO	10	13	10	10	Consistent with LOH
D13S317	14	14	14	14	Match
D16S539	11	12	11	11	Consistent with LOH
D21S11	31.2	31.2	31.2	31.2	Match
D5S818	11	12	11	11	Consistent with LOH
D7S820	11	11	11	11	Match
THO1	7	9.3	7	9.3	Match
TPOX	8	9	8	9	Match
vWA	15	15	15	15	Match

Conclusions:

The DNA (STR) profile for sample "L-428 (new)" is a 100% match to the profile listed for L-428 (http://strdb.cogcell.org). Sample "L-428 (new)" and "L-428 (old)" are identical at 7/10 loci and consistent at 3/10 loci under an assumption of loss of heterozygosity (LOH) in line "L-428 (old)". It is highly probable that "L-428 (new)" and "L-428 (old)" are derived from the same individual.

Disclaimers:

TCAG offers STR Analysis testing for research purposes only. The genotype data presented is TCAG staff's best attempt at interpretation given TCAG's limited knowledge of the project. It is highly recommended the raw data be viewed to ascertain quality and confidence in the genotype calls made.

Report generated by: Tara Paton, PhD – Facility Manager, TCAG Genetic Analysis Facility

Appendix 4: Complete list of differentially expressed genes (>1.5-fold change)

L-428 – JunB-regulated genes

Probe set ID	Corrected *p* value	Fold change	Gene symbol	Entrez Gene #
11752930_a_at	0.00475086	8.611936	GBP1	2633
11717580_a_at	0.002285257	7.084145	CD52	1043
11723069_at	0.012028287	6.248702	GABBR1 /// UBD	10537 /// 2550
11730947_at	0.023815557	5.453097	IFNG	3458
11752869_s_at	0.002285257	5.1056685	CEBPD	1052
11762406_s_at	0.011307783	4.9603763	GBP2	2634
11733439_a_at	0.009076601	4.82238	GBP5	115362
11764263_s_at	0.001633697	4.545227	TRPV3	162514
11735869_s_at	0.028490076	4.244945	TRIM64 /// TRIM64B /// TRIM64C	120146 /// 642446 /// 646754
11732538_at	0.018853867	3.9457445	TBX21	30009
11740288_a_at	0.005909528	3.945635	CHRNA1	1134
11741911_a_at	0.001633697	3.8900592	GBP3	2635
11717873_x_at	0.007616849	3.8584945	IRF8	3394
11731193_at	0.013763558	3.5743403	UNC13C	440279
11733952_at	0.023434987	3.5703495	GBP4	115361
11758708_s_at	0.003506825	3.5193408	PRAMEF1 /// PRAMEF13 /// PRAMEF14 /// PRAMEF2	400736 /// 65121 /// 65122 /// 729528
AFFX-HUMISGF3A/M97935_MA_at	0.006665857	3.4211125	STAT1 /// STAT1	6772
11758420_s_at	0.001633697	3.3670537	TRIM43 /// TRIM43B	129868 /// 653192
11726689_a_at	0.009953444	3.3547213	STAT1	6772
11741324_s_at	0.030531071	3.281614	TRIM51 /// TRIM51EP /// TRIM51GP /// TRIM51HP	120824 /// 399940 /// 440041 /// 84767
11732870_a_at	0.001648696	3.148249	CASP1	834
11748907_a_at	0.004509646	3.0901022	RARRES3	5920
11741830_s_at	0.010250964	3.0748658	LOC729974 /// RFPL4A	342931 /// 729974
11737390_at	0.007770187	3.0564973	ZSCAN4	201516
11744434_a_at	0.032712653	3.011702	PARP9	83666
11731181_a_at	0.028751856	2.9028823	EPSTI1	94240
11729899_a_at	7.42E-04	2.9014664	C4BPB	725

Probe set ID	Corrected *p* value	Fold change	Gene symbol	Entrez Gene #
11740364_a_at	0.002285257	2.8517904	PTPN3	5774
11718982_s_at	0.03604339	2.8197427	CCL4 /// CCL4L1 /// CCL4L2	388372 /// 6351 /// 9560
11717562_x_at	0.024905264	2.8125653	DTX3L	151636
11723669_s_at	0.005495473	2.8032763	SEMA3C	10512
11758180_s_at	0.024905264	2.6565142	LOC100128551 /// ZDHHC14	100128551 /// 79683
11745070_x_at	0.02600996	2.6546535	LOC440040	440040
11735772_s_at	0.03364459	2.6394618	LOC440040 /// TRIM48 /// TRIM49DP /// TRIM49L1	399939 /// 440040 /// 729384 /// 79097
11717863_a_at	0.01541695	2.6191206	DUSP5	1847
11735773_x_at	0.034730013	2.609373	TRIM48	79097
11722221_at	0.018853867	2.5974202	BFSP2	8419
11724381_at	0.043255176	2.5814254	FAM65B	9750
11730365_at	0.028202225	2.5796828	AMPD1	270
11741153_a_at	0.03349264	2.4742374	NCF2	4688
11721302_a_at	0.008078662	2.4652843	CLEC2B	9976
11755350_a_at	0.034730013	2.4310915	XIRP1	165904
11755214_a_at	0.006690874	2.417367	TMTC1	83857
11737618_at	0.025818618	2.4098587	RFPL4B	442247
11716734_at	0.024905264	2.3697765	IRF1	3659
11723823_a_at	0.016100753	2.3616009	MYO5C	55930
11730907_a_at	0.01426256	2.3196502	ABCB1	5243
11720669_at	0.036555212	2.3003309	KAT2B	8850
11735035_a_at	0.001566752	2.2887592	GCET2	257144
11730457_a_at	0.006690874	2.245885	AIM2	9447
11752387_a_at	0.002948745	2.2387953	ETS1	2113
11755417_a_at	3.97E-04	2.2120805	KIAA0922	23240
11751606_x_at	0.006690874	2.1920545	SP140	11262
11747666_a_at	0.008365662	2.1912584	WARS	7453
11756806_a_at	0.011858982	2.1895514	ISG20	3669
11734783_at	0.033200994	2.1717591	CLIC2	1193
11726201_a_at	0.020560762	2.1207328	OAS2	4939
11719902_a_at	7.42E-04	2.0944033	PHF11	51131
11743352_s_at	0.0371839	2.0892718	COBLL1	22837
11759889_a_at	0.008456832	2.087772	BCL2L11	10018
11724883_a_at	0.036555212	2.0674474	HAPLN3	145864
11733305_a_at	0.03498743	2.0599816	TFAP2B	7021
11745538_a_at	0.03747921	2.0513408	MAP7D2	256714
11715615_at	0.002285257	2.0414402	BTG2	7832
11721996_a_at	0.011307783	2.0196187	PARP14	54625
11728240_s_at	0.03882441	2.0151553	RRAGD	58528

Probe set ID	Corrected *p* value	Fold change	Gene symbol	Entrez Gene #
11721430_a_at	0.025010796	2.0063705	SYBU	55638
11718908_s_at	0.016100753	2.0063396	CHST2	9435
11733698_s_at	0.028965862	2.0029426	SGK1	6446
11729769_a_at	0.017450217	1.997516	CD38	952
11751548_a_at	0.003502065	1.9926015	C10orf10	11067
11731755_a_at	0.014383511	1.990859	SYTL2	54843
11758500_s_at	0.014383511	1.9727751	TMEM140	55281
11729330_a_at	8.79E-04	1.9497979	EPB41L4B	54566
11724117_x_at	0.040153425	1.9424797	SAMD9L	219285
11736295_at	0.009618892	1.9277328	FGFBP3	143282
11721566_s_at	0.037318725	1.9249321	KBTBD11	9920
11723975_x_at	0.025632491	1.9186437	APOL3	80833
11728274_a_at	0.003506825	1.8993875	PMP22	5376
11720994_x_at	0.048851784	1.8925732	CCL3	6348
11747631_x_at	0.048998173	1.8888212	XAF1	54739
11750661_a_at	0.017450217	1.8845248	RGS22	26166
11720618_s_at	0.007598499	1.8700417	TRIM9	114088
11742267_s_at	0.027257424	1.8625101	PRAMEF24 /// PRAMEF7 /// PRAMEF8	391002 /// 441871 /// 729516
11731896_a_at	0.01492306	1.8568056	TNFSF4	7292
11730371_a_at	0.008456832	1.8462144	EIF4E3	317649
11754368_a_at	0.039678805	1.8410885	FBN1	2200
11730729_a_at	0.043584358	1.8276542	TAP1	6890
11715757_a_at	0.016313417	1.8262594	RGS2	5997
11718048_a_at	0.014834358	1.8162009	GLRX	2745
11720611_a_at	0.003506825	1.8056927	NAP1L5	266812
11741742_at	0.012781304	1.7945869	LEUTX	342900
11727072_at	0.04768399	1.7919807	ENPP6	133121
11723947_a_at	0.03807648	1.7908658	ACSL5	51703
11737791_s_at	0.012881474	1.784277	APOL1 /// APOL2	23780 /// 8542
11734285_x_at	0.027504407	1.7799088	CSAG2 /// CSAG3	389903 /// 728461
11747264_a_at	0.03328441	1.7763156	BCAS1	8537
11736761_at	0.025818618	1.7605652	CARD16	114769
11719588_a_at	0.028912978	1.7537677	OAS1	4938
11737914_at	0.013487919	1.7526957	GPR15	2838
11752528_a_at	0.03328441	1.7523713	RASGRP1	10125
11744005_at	0.007067103	1.7507555	PHLDA2	7262
11733919_s_at	0.013089397	1.7469949	SERTAD2	9792
11725255_a_at	0.033560086	1.7239478	IL15	3600
11759895_at	0.032511007	1.7229532	PCDH9	5101
11751299_a_at	0.011873323	1.7219921	APOL2	23780
11726965_a_at	0.020223912	1.7172605	L3MBTL3	84456

Probe set ID	Corrected *p* value	Fold change	Gene symbol	Entrez Gene #
11730608_at	0.014834358	1.7162693	HNF4G	3174
11745189_a_at	0.027881432	1.7121694	APOL1	8542
11739823_a_at	0.015456768	1.7079858	CPNE8	144402
11726392_at	0.013763558	1.6902951	GIMAP2	26157
11720746_s_at	0.008941465	1.6782757	BCL6	604
11747448_x_at	0.01426256	1.6718695	BTN3A2	11118
11764149_s_at	0.034787707	1.6663517	DUSP16	80824
11733385_a_at	0.002948745	1.6656975	TMEM182	130827
11726281_x_at	0.006971222	1.6654581	BCR	613
11749980_x_at	0.045409217	1.6636711	HOPX	84525
11715388_s_at	0.024145182	1.6632433	CDKN1A	1026
11755831_a_at	0.032549918	1.6552432	WDR63	126820
11743846_s_at	0.017170567	1.6550328	CFH /// CFHR1	3075 /// 3078
11746292_a_at	0.01426256	1.6286167	CPOX	1371
11745820_s_at	0.044879343	1.6152539	PLAGL1	5325
11755758_s_at	0.023434987	1.6133684	NLRC5	84166
11733115_a_at	0.003215974	1.6113476	CA2	760
11719492_s_at	0.022374453	1.6085476	IFI35	3430
11721994_s_at	0.017210176	1.59889	UBE2L6	9246
11730683_a_at	0.032712653	1.597319	TSHR	7253
11749564_a_at	0.04317917	1.590377	EFEMP1	2202
11757712_a_at	0.034173917	1.5857276	L3MBTL4	91133
11745839_a_at	0.023815557	1.5745522	C9orf3 /// LOC100507319	100507319 /// 84909
11720372_at	0.028965862	1.5610555	TESC	54997
11722514_a_at	0.003502065	1.5587133	IDNK	414328
11719227_x_at	0.036021557	1.5541878	KCNN4	3783
11743036_s_at	0.018690454	1.5470476	SAT1	6303
11749693_a_at	0.030270798	1.5442348	ARHGAP17	55114
11730739_a_at	0.026259398	1.5441853	PDLIM4	8572
11737511_a_at	0.012843357	1.5370005	SP100	6672
11760819_x_at	0.036648184	1.5335134	IGHG1 /// IGHV4-31	28396 /// 3500
11754330_a_at	0.015053015	1.5323263	IRF2	3660
11725746_a_at	0.025632491	1.531408	PITPNC1	26207
11742186_a_at	0.020559072	1.5306722	TMOD2	29767
11723854_at	0.03882441	1.5270703	SAMD9	54809
11744702_a_at	0.019410346	1.5257999	KCNMA1	3778
11740429_s_at	0.03609424	1.5247201	XRN1	54464
11745727_a_at	0.013801761	1.5243225	TCF12	6938
11727325_a_at	0.01541695	1.5212523	GFI1	2672
11732415_s_at	0.028202225	1.5163107	TIAM1	7074
11729281_s_at	0.02974962	1.5123862	PTP4A3	11156
11727473_at	0.023434987	1.50862	CLC	1178
11745715_a_at	0.047504537	1.5050827	CAV1	857

Probe set ID	Corrected *p* value	Fold change	Gene symbol	Entrez Gene #
11742215_s_at	0.006514233	1.5025399	APP	351
11719773_s_at	0.014160823	-1.500413	C5orf24	134553
11725232_at	0.020560762	-1.5013574	ATP8B2	57198
11716165_a_at	0.027504407	-1.5025121	LOC100505828 /// MGST3	100505828 /// 4259
11731095_x_at	0.041570466	-1.5044233	TRAF3IP1	26146
11720637_x_at	0.020223912	-1.5065131	CXADR	1525
11727145_s_at	0.039357197	-1.5131031	KLF11	8462
11737839_a_at	0.024145182	-1.518247	MBOAT7	79143
11728709_a_at	0.021812668	-1.5195783	EMP2	2013
11727044_a_at	0.009800388	-1.5201159	TMEM173	340061
11724464_a_at	0.012071028	-1.5210276	ANLN	54443
11742766_a_at	0.020338967	-1.5317978	DENND5A	23258
11727397_s_at	0.03814133	-1.5331177	CTNNA1	1495
11741738_x_at	0.003506825	-1.5382915	C3orf33	285315
11718936_s_at	0.017989522	-1.5412585	MMD	23531
11743721_at	0.016313417	-1.5486437	LGALS1	3956
11740602_s_at	0.028912978	-1.5520856	APH1B	83464
11743626_s_at	0.008676252	-1.5566385	LGR4	55366
11727052_at	0.004391244	-1.5637134	HOXB13	10481
11719691_x_at	0.01426256	-1.5676748	TWSG1	57045
11715822_s_at	0.007891362	-1.5705428	SYPL1	6856
11729176_at	0.014834358	-1.571919	KLHL4	56062
11723032_a_at	0.00475086	-1.5783986	PLP2	5355
11759416_x_at	0.025921825	-1.580319	HFE	3077
11740008_s_at	0.020560762	-1.5836561	CHRFAM7A /// CHRNA7	1139 /// 89832
11739885_s_at	0.03382704	-1.5927284	DOCK7	85440
11720566_at	0.036555212	-1.5968102	BCAT1	586
11743537_a_at	0.019739557	-1.6042305	DNAJC18	202052
11744618_a_at	0.034730013	-1.6075929	DUSP6	1848
11723633_s_at	0.013089397	-1.6231103	IRF2BPL	64207
11723768_a_at	0.016504625	-1.6236156	SNX24	28966
11759545_a_at	0.026259398	-1.6264231	PRMT2	3275
11741449_s_at	0.008456832	-1.6293415	CD99	4267
11717559_a_at	0.048998173	-1.6360307	ABLIM1	3983
11730080_x_at	0.012562775	-1.6390632	IL28RA	163702
11733454_a_at	0.028912978	-1.6438115	CCDC41	51134
11730290_x_at	0.048998173	-1.6449648	ARHGAP5	394
11757310_s_at	0.01426256	-1.6476974	TMEM98	26022
11734600_a_at	0.016313417	-1.6609393	PSIP1	11168
11736777_at	0.003268031	-1.6650794	CBLN1	869
11753913_a_at	0.025818618	-1.6716512	SSX2IP	117178
11723163_s_at	0.012843357	-1.6775154	NR3C2	4306
11720012_at	0.035974227	-1.6775951	JARID2	3720
11734235_a_at	0.012843357	-1.7064707	PLA2G12B	84647
11758854_at	0.001566752	-1.7070489	ATL3	25923

Probe set ID	Corrected *p* value	Fold change	Gene symbol	Entrez Gene #
11740213_a_at	0.027127314	-1.7071285	TBL1X	6907
11718140_a_at	0.014598119	-1.709518	EMP3	2014
11758147_s_at	0.042345755	-1.7131273	MAPK13	5603
11734507_s_at	0.014160823	-1.7151657	MECOM	2122
11743113_x_at	0.020223912	-1.7243689	S100A10	6281
11721097_at	0.012639815	-1.7531958	TMX1	81542
11756105_a_at	0.044136472	-1.7690954	BMPR2	659
11725861_a_at	0.03604339	-1.7891228	MYBL1	4603
11721362_a_at	7.42E-04	-1.8216735	MAP4K3	8491
11730857_at	0.008036695	-1.8694391	ZC2HC1A	51101
11748259_a_at	0.023434987	-1.8865303	CUEDC1	404093
11754314_a_at	0.022286316	-1.956522	TTC7B	145567
11743815_a_at	0.003506825	-1.9589393	S1PR1	1901
11726496_at	0.034730013	-2.047957	RYR2	6262
11757383_a_at	0.030103106	-2.054877	CTSH	1512
11715673_x_at	0.002285257	-2.0647616	JUNB	3726
11750609_a_at	6.46E-04	-2.1181617	ITSN1	6453
11763555_a_at	7.42E-04	-2.132625	SNX12	29934
11756078_a_at	0.02171102	-2.164062	ARHGEF37	389337
11721775_s_at	7.42E-04	-2.2221072	ASPH	444
11740369_x_at	0.002285257	-2.2342432	PDLIM5	10611
11735148_a_at	0.012562775	-2.245346	SOCS2	8835
11719247_at	0.003032898	-2.2992394	AIM1	202
11735271_a_at	0.021812668	-2.386039	GCNT1	2650
11753244_a_at	0.030531071	-2.4334898	BDNF	627
11736132_s_at	0.001633697	-2.4814296	DCBLD2	131566
11742791_at	0.002259239	-2.4969897	ATP6AP1L /// FLJ41309	645079 /// 92270
11753068_a_at	0.006181299	-2.5302453	CFI	3426
11724145_a_at	0.012071028	-2.690906	SLC37A1	54020
11744735_a_at	0.039455395	-2.732549	TMEM200A	114801
11752745_x_at	0.005261277	-2.806189	LGMN	5641
11729864_at	0.003506825	-2.8179202	MYBPC2	4606
11759295_at	0.025308628	-2.8536243	EHF	26298
11735077_a_at	0.012073387	-2.902818	CYP2C18	1562
11719160_at	0.025010796	-2.9169145	RAPH1	65059
11726762_at	7.42E-04	-3.3136203	SLCO3A1	28232
11715918_s_at	0.00354163	-3.5143437	CD24	100133941
11748647_a_at	0.032267556	-3.664662	PTPRR	5801
11733091_a_at	0.02317602	-4.5961523	TSPAN8	7103
11760753_a_at	0.010838163	-5.714992	PDGFRA	5156
11758048_s_at	1.05E-05	-7.28522	THRB	7068

L-428 – c-Jun-regulated genes				
Probe set ID	**Corrected *p* value**	**Fold change**	**Gene symbol**	**Entrez Gene #**
11730365_at	0.001385844	4.3576155	AMPD1	270
11731706_at	0.040694267	3.8298585	CCL22	6367
11729899_a_at	0.019851973	3.1738627	C4BPB	725
11754429_a_at	0.04850015	2.5132415	LAMA2	3908
11717581_s_at	0.019851973	2.4064975	CD52	1043
11755214_a_at	0.019851973	2.3890345	TMTC1	83857
11757153_x_at	0.019851973	2.3404448	SNHG12 /// SNORA16A /// SNORA44 /// SNORA61	677825 /// 677838 /// 692073 /// 85028
11758873_a_at	0.013234993	2.3271275	HPSE	10855
11719164_a_at	0.04867641	2.2811408	CLCN5	1184
11739232_x_at	0.029011155	2.2762287	RASSF2	9770
11723048_at	0.046554685	2.103136	CX3CR1	1524
11739506_a_at	0.028778838	2.070551	LONRF2	164832
11728515_a_at	0.040694267	2.0430446	SP140	11262
11756243_a_at	0.046106465	1.8235096	DAPP1	27071
11715388_s_at	0.046106465	1.8167628	CDKN1A	1026
11743589_at	0.019640965	1.7860966	SNX29	92017
11720099_s_at	0.046554685	1.781147	CEP70	80321
11741184_a_at	0.032129325	1.7636828	AMPD3	272
11734657_s_at	0.040694267	1.7479519	SLC2A14 /// SLC2A3	144195 /// 6515
11730683_a_at	0.026385698	1.72389	TSHR	7253
11749461_a_at	0.04392429	1.630621	CDH11	1009
11742020_a_at	0.032129325	1.6191757	INPP4A	3631
11720871_s_at	0.019851973	1.6168927	PDE7A	5150
11723936_a_at	0.0444082	1.6034131	SNX1	6642
11729575_a_at	0.041982405	1.5542227	XBP1	7494
11727211_a_at	0.032242794	1.5427747	HEATR5B	54497
11741102_a_at	0.029011155	1.5139431	PTPN22	26191
11738526_a_at	0.046106465	-1.5313451	GFM2	84340
11758064_s_at	0.041982405	-1.5526116	FZD8	8325
11715837_a_at	0.045529563	-1.5543573	HEXB	3074
11734967_a_at	0.034219477	-1.578793	THEMIS	387357
11763696_s_at	0.019851973	-1.5895928	NIPA2	81614
11723707_a_at	0.032129325	-1.6289096	AIFM2	84883
11729201_at	0.034219477	-1.6483282	C6orf120	387263
11722232_a_at	0.049968343	-1.657445	PCP4	5121
11727682_at	0.03305523	-1.6743557	ACVR2B	93
11722796_a_at	0.019640965	-1.6756119	MAPK6	5597
11741059_s_at	0.0476668	-1.6824589	SATB1	6304
11755592_s_at	0.019640965	-1.7013644	DNAJC24	120526
11740008_s_at	0.019851973	-1.7077419	CHRFAM7A /// CHRNA7	1139 /// 89832

Probe set ID	Corrected *p* value	Fold change	Gene symbol	Entrez Gene #
11744581_a_at	0.0444082	-1.7546525	KHDRBS3	10656
11731560_at	0.019851973	-1.82818	FAM89A	375061
11744005_at	0.032129325	-1.8372054	PHLDA2	7262
11757558_s_at	0.014411251	-1.9171059	LONRF1	91694
11728499_x_at	0.032129325	-2.0422723	SVIL	6840
11719628_a_at	0.009243077	-2.1333344	HDHD1	8226
11723838_at	0.046106465	-2.1371784	GATA6	2627
11740213_a_at	0.03477498	-2.1920378	TBL1X	6907
11724275_s_at	0.015305555	-2.2102022	TMEM158	25907
11759022_s_at	0.037208773	-2.2433522	ELK3	2004
11725637_a_at	0.001385844	-2.353245	EIF3J	8669

KM-H2 – JunB-regulated genes

Probe set ID	Corrected *p* value	Fold change	Gene symbol	Entrez Gene #
11729972_at	0.008381084	27.438988	CYP4Z1	199974
11725910_a_at	3.20E-04	8.401869	COL4A6	1288
11737833_at	0.011216905	8.083577	IL12B	3593
11753121_s_at	0.016292684	7.2067356	CYP4Z1 /// CYP4Z2P	163720 /// 199974
11758087_s_at	0.013131246	6.6991367	DPYS	1807
11718492_at	4.11E-04	6.5970097	SLC1A2	6506
11720819_s_at	1.91E-04	6.1932445	CXCL12	6387
11746506_a_at	0.015116785	5.678038	SPP1	6696
11718181_s_at	0.001281328	4.783559	FERMT2	10979
11728523_a_at	7.68E-04	4.685484	MYCL1	4610
11735937_a_at	1.97E-04	4.481185	CD48	962
11725598_a_at	2.07E-04	4.3162956	SULT1C2	6819
11738356_s_at	8.17E-04	3.894974	OR4N2 /// OR4N3P	390429 /// 390539
11735157_at	0.002206217	3.8914313	CYSLTR1	10800
11720167_at	2.46E-05	3.8396156	SELL	6402
11730484_at	0.001273012	3.7329798	PTGER3	5733
11734567_a_at	9.91E-04	3.3779018	RASGRP2	10235
11723940_at	0.024762778	3.1809094	GKN1	56287
11736958_at	0.003149467	3.0682578	TNFSF15	9966
11715164_s_at	2.30E-04	3.0072677	IGLL3P	91353
11763550_x_at	1.13E-04	2.960531	IGK@ /// IGKC /// LOC100294406	100294406 /// 3514 /// 50802
11739880_a_at	0.006721429	2.9152808	GLIS3	169792
11741418_a_at	0.008381084	2.9017627	KCNQ1	3784
11724768_s_at	5.45E-04	2.8322093	FCGR2A /// FCGR2C	2212 /// 9103
11761671_a_at	0.024762778	2.8262975	ETV7	51513
11745359_a_at	0.004733916	2.815379	MLIP	90523
11742961_s_at	0.012399554	2.7402527	FAM43A	131583
11727947_at	0.032461397	2.7359133	MEGF6	1953
11749587_x_at	0.003516338	2.6922076	FCGR2A	2212
11722470_x_at	4.34E-04	2.681416	ACSL6 /// LOC100505572	100505572 /// 23305
11742738_a_at	0.003149467	2.572569	BBS9	27241
11756978_a_at	0.004833958	2.5526671	KCNN2	3781
11734162_a_at	0.012863846	2.5261023	TFEC	22797
11740996_a_at	1.91E-04	2.5172203	SPAG6	9576
11734215_x_at	0.004160842	2.3424609	MPP7	143098
11744669_a_at	0.028341401	2.3393466	LINC00158	54072
11734339_at	0.016111018	2.3389401	POU3F1	5453

Probe set ID	Corrected *p* value	Fold change	Gene symbol	Entrez Gene #
11735710_s_at	0.006441491	2.2658656	SAMSN1	64092
11736871_s_at	0.014789936	2.2584987	TRPC6	7225
11728469_a_at	0.022441333	2.2214	BTBD11	121551
11732351_at	0.002542615	2.2160804	HGF	3082
11756545_a_at	0.025664976	2.1970878	GKN2	200504
11748761_a_at	0.009006026	2.1960437	KLF5	688
11723272_at	0.016529024	2.1846359	FEM1C	56929
11720300_a_at	0.016116368	2.1600246	SLA	6503
11756590_a_at	4.74E-04	2.1334853	KMO	8564
11733284_x_at	0.04800842	2.1292713	MYBPC1	4604
11726536_at	0.018026687	2.1216671	CYP1A1	1543
11731880_at	0.003331499	2.0987573	NLRP1	22861
11722312_a_at	0.040761076	2.0978432	CLDN18	51208
11726796_a_at	1.97E-04	2.0854435	NEXN	91624
11757367_s_at	0.005157541	2.075097	HSPA6 /// HSPA7	3310 /// 3311
11741899_s_at	0.003409233	2.0476239	FCGR2B	2213
11731554_a_at	0.03549235	2.0432243	SYNPO2	171024
11722054_a_at	0.025383327	2.036131	CYP4X1	260293
11730650_at	0.032612864	2.0178592	ANO3	63982
11715346_at	0.02362418	2.0100915	EBI3	10148
11732466_a_at	0.005318988	2.0065317	CXCL11	6373
11721511_at	6.40E-04	1.9957211	NUS1	116150
11718927_a_at	0.008381084	1.9953319	ARID5B	84159
11716987_a_at	0.006121277	1.9852449	HMGCS1	3157
11759347_x_at	0.010435135	1.9799331	TXK	7294
11720982_s_at	0.001703062	1.9723696	PTK2B	2185
11730704_s_at	0.001499456	1.9634854	OR51E2	81285
11722128_at	9.94E-04	1.9536916	FAM102B	284611
11716063_at	0.014789936	1.9475989	TNC	3371
11732403_a_at	0.014789936	1.9426229	OGFRL1	79627
11740507_a_at	0.010489685	1.941164	ARHGAP26	23092
11758488_s_at	0.041204635	1.9357828	SPATA16	83893
11716697_at	0.009858931	1.9351751	FABP4	2167
11730401_a_at	0.002594768	1.9339602	RASGRF1	5923
11717760_a_at	6.06E-04	1.9294807	GMFG	9535
11735084_s_at	0.009002909	1.9074168	FREM2	341640
11716048_at	0.006441491	1.9015797	TRIB1	10221
11756496_a_at	0.03475444	1.8930186	SERPINA6	866
11760819_x_at	4.34E-04	1.8809872	IGHG1 /// IGHV4-31	28396 /// 3500
11742368_x_at	0.007402171	1.8784001	OR4N2	390429
11756080_s_at	0.010820235	1.8782543	NUS1 /// NUS1P3	11049 /// 116150
11739809_at	0.024369668	1.8690481	TMEM156	80008

Probe set ID	Corrected *p* value	Fold change	Gene symbol	Entrez Gene #
11722991_a_at	0.011389782	1.8507655	DMD	1756
11740117_a_at	0.008342474	1.8501936	RNF24	11237
11760929_x_at	0.014644671	1.845844	IGHG1 /// IGHM	28396 /// 3500
11737967_at	9.03E-04	1.8293172	C15orf54	400360
11723553_at	0.041063428	1.8244036	F5	2153
11716338_a_at	0.046919912	1.8208145	INSIG1	3638
11761958_s_at	0.012853901	1.8146071	YME1L1	10730
11733549_at	0.011230206	1.802692	TEC	7006
11758901_at	0.026899086	1.8006603	RIPK2	8767
11747143_x_at	0.004733916	1.7802495	ACSL6	23305
11750231_x_at	0.019749807	1.7757127	IGHG1 /// IGHG3 /// IGHM /// IGHV4-31	28396 /// 3500 /// 3502 /// 3507
11724271_a_at	0.021083469	1.7604755	HLF	3131
11763307_s_at	0.003418272	1.7598222	NFATC2	4773
11740092_x_at	0.025383327	1.7591208	MSMO1	6307
11737911_a_at	0.021083469	1.7478185	GPR84	53831
11726272_a_at	0.017151307	1.7466496	ATP1B1	481
11739605_a_at	0.014789936	1.743663	CCDC88A	55704
11718198_at	0.034355402	1.7424393	LHFP	10186
11728935_at	0.00852639	1.7249093	C11orf41	25758
11748120_a_at	0.009002909	1.7211455	LCP2	3937
11744481_s_at	0.025765033	1.7211375	OPN3	23596
11724007_s_at	0.008650568	1.720836	ENTPD1	953
11747262_s_at	0.040061478	1.7173735	RRAS2	22800
11737993_s_at	0.010929152	1.7167776	DST /// LOC100652766	100652766 /// 667
11740318_s_at	0.011422882	1.7142951	KCNJ3	3760
11719869_a_at	0.027340809	1.7130344	MYCN	4613
11720695_at	0.014315561	1.7037121	C1orf54	79630
11724820_a_at	0.027414367	1.7011462	NEK6	10783
11757179_x_at	0.031423483	1.7007133	RPL4 /// SNORD16 /// SNORD18A /// SNORD18B /// SNORD18C	595097 /// 595098 /// 595099 /// 595100 /// 6124
11737831_a_at	0.001703062	1.6905665	FNBP1L	54874
11715274_x_at	0.042542987	1.689698	TPM2	7169
11742813_at	0.003264919	1.684433	SEMA6A	57556
11759082_at	0.022891741	1.6774094	DCT	1638
11763394_a_at	0.005744751	1.6655648	LOC100505946	100505946
11723188_s_at	0.005294527	1.6578137	ADAM19	8728
11731258_at	0.03274003	1.651859	TMEM170B	100103407
11727116_a_at	0.012001242	1.6499623	PLA1A	51365

Probe set ID	Corrected *p* value	Fold change	Gene symbol	Entrez Gene #
11747033_at	0.016222563	1.6462598	MGC34800	162137
11733080_a_at	0.021900358	1.6375791	POT1	25913
11740449_a_at	0.035983145	1.6292757	CCDC147	159686
11722146_s_at	0.005953073	1.6292375	PAIP2B	400961
11719147_at	0.028595185	1.628036	FAM117A	81558
11723824_s_at	6.06E-04	1.6180924	MYO5C	55930
11736424_a_at	0.04189196	1.6162419	STARD4	134429
11736632_at	0.04661029	1.6139822	APOBEC3H	164668
11719898_s_at	0.036136687	1.6131492	HBEGF	1839
11747725_a_at	0.032228377	1.6076387	STXBP6	29091
11753764_s_at	0.014233426	1.6066401	TNFRSF21	27242
11725013_at	0.04661029	1.5939195	MMACHC	25974
11719042_s_at	0.004869956	1.587265	ACSL4	2182
11731121_s_at	0.006441491	1.586408	VASH2	79805
11729566_a_at	0.009419476	1.5855143	GTDC1	79712
11756174_s_at	0.011621115	1.5848672	SCD	6319
11741727_a_at	0.004125858	1.5741016	NEDD1	121441
11739080_s_at	0.03062781	1.562127	DNAJB4	11080
11739068_a_at	0.015113121	1.5619835	KIFAP3	22920
11748808_a_at	9.39E-04	1.5615262	ARID3B	10620
11718448_at	0.02059877	1.5602431	SH3BGRL2	83699
11724554_s_at	0.002620494	1.559893	PCGF5	84333
11734316_a_at	0.007035546	1.5595105	WDR17	116966
11756471_a_at	0.04415159	1.5587493	MFSD2A	84879
11736544_at	0.017779129	1.5575118	MACC1	346389
11739383_a_at	0.010820235	1.5534544	IDI1	3422
11745789_a_at	0.018187694	1.5526773	TMEM135	65084
11757981_s_at	0.03429433	1.5519764	WASF3	10810
11753998_a_at	0.038824968	1.5487461	CD58	965
11715460_a_at	0.035913162	1.5485669	DHCR24	1718
11756302_x_at	0.04320308	1.5463109	CD37	951
11744351_a_at	0.02672482	1.5447932	LOC728392 /// NLRP1	22861 /// 728392
11757675_s_at	0.009480241	1.5418704	C16orf87	388272
11742431_a_at	0.01572228	1.5382838	DGKI	9162
11731202_a_at	0.011422882	1.5374131	AIM1L	55057
11725688_x_at	0.009002909	1.5335991	RHPN2	85415
11725568_a_at	0.04348303	1.5303696	ATP8A1	10396
11754336_s_at	0.040162142	1.5273776	DOCK1	1793
11721134_at	0.004160842	1.5200686	GFPT2	9945
11722563_x_at	0.030270064	1.5198536	CYP51A1 /// LRRD1	1595 /// 401387
11739054_a_at	0.003430348	1.5196401	PTPN6	5777
11756243_a_at	0.007121915	1.5175797	DAPP1	27071
11730176_x_at	0.003188066	1.5116615	C4orf3	401152

Probe set ID	Corrected *p* value	Fold change	Gene symbol	Entrez Gene #
11717271_a_at	0.003890329	1.5116205	PRAME	23532
11757509_x_at	0.03281541	1.5080136	RAB6A	5870
11755655_a_at	0.024762778	1.5066664	MICAL3	57553
11727237_a_at	0.017248247	1.5060511	UST	10090
11731901_a_at	0.03475444	1.5022221	SESN3	143686
11736897_x_at	0.010007126	-1.5004243	PRRG4	79056
11719160_at	0.004083997	-1.5066824	RAPH1	65059
11734336_x_at	0.005157541	-1.509856	SIGIRR	59307
11727022_at	0.042612545	-1.510671	TMEM64	169200
11749781_s_at	0.017315542	-1.5136969	BCAT1	586
11753399_x_at	0.004169032	-1.516213	ANXA2	302
11719641_at	0.024678657	-1.5305719	CDS1	1040
11751302_a_at	0.03135932	-1.5363784	TWF1	5756
11715537_x_at	0.002060638	-1.5369949	IDH2	3418
11736053_x_at	0.02266428	-1.537988	EEF1A1 /// LOC100653236	100653236 /// 1915
11721874_at	0.014789936	-1.5425942	IFIT2	3433
11718880_at	0.007227192	-1.552785	ZCCHC14	23174
11730296_a_at	0.006423217	-1.5538108	TLR3	7098
11739156_at	0.010820235	-1.5539187	TMX4	56255
11734340_a_at	0.027516356	-1.5566663	FAM124B	79843
11721775_s_at	0.009419476	-1.5569714	ASPH	444
11736582_a_at	0.016222563	-1.5582945	TRIM36	55521
11727400_a_at	0.025461102	-1.580969	GSTZ1	2954
11733784_at	0.04320308	-1.5813572	PPP2R1B	5519
11758194_s_at	0.044630766	-1.5840701	DPP4	1803
11716258_at	0.03549235	-1.5876533	RHEB	6009
11740465_at	0.018664269	-1.593908	GPR171	29909
11720731_a_at	0.001899156	-1.5965875	SUMF1	285362
11728466_a_at	0.009006026	-1.59837	GLDC	2731
11722182_a_at	0.0319562	-1.6016768	ATP6V1C1	528
11735341_s_at	0.007035546	-1.611337	TANC1	85461
11716698_s_at	0.013131246	-1.6124232	HBP1	26959
11734902_a_at	0.030834578	-1.6128373	CYP4V2	285440
11738844_a_at	0.012727122	-1.6138548	LOC100653217 /// NTM	100653217 /// 50863
11758137_s_at	0.006441491	-1.6175523	SPOPL	339745
11721528_at	0.014789936	-1.6196911	ZDHHC2	51201
11755935_a_at	0.011678087	-1.6264414	MYL5	4636
11739468_at	0.025461102	-1.6451181	TMEM87B	84910
11762445_a_at	0.022064758	-1.649331	C14orf182	283551
11741159_a_at	0.025517803	-1.6496913	EYA1	2138
11739654_at	0.00864035	-1.6497355	TNFRSF10A	8797
11729835_at	0.025664976	-1.6508373	EIF5A2	56648
11729861_x_at	0.019835375	-1.6659348	H6PD	9563
11716724_x_at	0.00737729	-1.6702517	DPY19L1	23333
11730404_at	0.035800364	-1.6860338	MEX3B	84206

Probe set ID	Corrected *p* value	Fold change	Gene symbol	Entrez Gene #
11758629_s_at	0.002542615	-1.6883101	SPTBN1	6711
11750609_a_at	0.003188066	-1.6888822	ITSN1	6453
11724776_at	0.011315669	-1.6904833	PGM2L1	283209
11716551_s_at	0.002070407	-1.6946152	HES1	3280
11728104_at	0.018187694	-1.6963995	HTR2B	3357
11758854_at	0.014315561	-1.7274168	ATL3	25923
11757679_s_at	0.009131637	-1.733052	SMAD5	4090
11756547_a_at	0.010954527	-1.7446233	CLU	1191
11739540_a_at	0.044630766	-1.7459258	PIK3R1	5295
11722088_s_at	0.033584658	-1.7464083	NR1D2	9975
11720746_s_at	0.014315561	-1.7662648	BCL6	604
11723424_at	0.021900358	-1.7723547	IFNAR1	3454
11717935_a_at	0.003149467	-1.7739887	ERMP1	79956
11735258_x_at	0.04173323	-1.7851081	IL7	3574
11743285_s_at	3.94E-04	-1.785857	GOLT1B	51026
11719257_s_at	0.031573985	-1.8013471	LRP6	4040
11730465_at	0.021926671	-1.804066	KCNJ2	3759
11725675_a_at	0.009419476	-1.8201611	RORA	6095
11716196_x_at	0.02672482	-1.8245834	ID1	3397
11721212_a_at	0.00534765	-1.8274561	THBS4	7060
11756105_a_at	0.010820235	-1.8349988	BMPR2	659
11759119_at	0.011216905	-1.8539332	TBCEL	219899
11725180_a_at	0.033584658	-1.8625828	RUNX2	860
11732415_s_at	0.003890329	-1.876182	TIAM1	7074
11736246_a_at	0.002708911	-1.8870915	AMIGO2	347902
11721099_at	0.049166538	-1.9101403	C3AR1	719
11718541_a_at	9.03E-04	-1.9184649	MTSS1	9788
11732898_at	0.012968406	-1.9237567	LIPI	149998
11721097_at	0.002708911	-1.926389	TMX1	81542
11730457_a_at	0.011389782	-1.9777663	AIM2	9447
11741049_s_at	0.014233426	-2.0377648	TMEM100	55273
11734313_at	4.73E-04	-2.0411196	OBSCN	84033
11725443_at	0.001827754	-2.0852299	TCEAL7	56849
11742984_a_at	0.003149467	-2.13965	EGFLAM	133584
11717559_a_at	0.001357193	-2.1492085	ABLIM1	3983
11761425_at	0.005549097	-2.2951639	GALNT11	63917
11758377_s_at	0.001499456	-2.439978	TLR1	7096
11731407_x_at	4.73E-04	-2.4980357	IFIT3	3437
11736761_at	0.03587059	-2.50315	CARD16	114769
11715673_x_at	1.91E-04	-2.516193	JUNB	3726
11763555_a_at	0.002030342	-2.602142	SNX12	29934
11748907_a_at	0.002542615	-2.6360712	RARRES3	5920
11736132_s_at	1.91E-04	-3.079634	DCBLD2	131566
11717514_a_at	3.14E-04	-3.4547262	ANXA1	301
11723814_s_at	5.55E-04	-3.6351664	ARHGAP29	9411

KM-H2 – c-Jun-regulated genes

Probe set ID	Corrected *p* value	Fold change	Gene symbol	Entrez Gene #
11726827_at	0.005313663	11.9382105	STAP1	26228
11726329_x_at	0.001363553	5.6624923	GBP1	2633
11723069_at	0.006173489	4.3637786	GABBR1 /// UBD	10537 /// 2550
11733950_at	0.008790884	4.2487826	GBP4	115361
11758087_s_at	0.015544553	3.9546907	DPYS	1807
11732084_a_at	0.006155024	3.6430738	TFEC	22797
11731584_a_at	0.006815743	3.4597552	FCRLA	84824
11744318_at	0.01091728	3.3736374	CCDC85A	114800
11725459_s_at	0.014201811	3.2412438	S100A7 /// S100A7A	338324 /// 6278
11757367_s_at	0.004752198	3.145322	HSPA6 /// HSPA7	3310 /// 3311
11720167_at	0.004750912	2.9329643	SELL	6402
11732466_a_at	0.021060567	2.9161463	CXCL11	6373
11724768_s_at	0.03684422	2.8259752	FCGR2A /// FCGR2C	2212 /// 9103
11749587_x_at	0.019188771	2.7915828	FCGR2A	2212
11735157_at	0.006602448	2.6041708	CYSLTR1	10800
11741911_a_at	0.004750912	2.5991747	GBP3	2635
11762406_s_at	0.005313663	2.5585454	GBP2	2634
11735224_a_at	0.005313663	2.4891355	KLRG1	10219
11741049_s_at	0.003776285	2.4753973	TMEM100	55273
11716132_a_at	0.023235394	2.448666	FSTL3	10272
11722054_a_at	0.021060567	2.4342685	CYP4X1	260293
11729761_at	0.045551844	2.4301717	PLA2G2D	26279
11722011_a_at	0.03684422	2.3952475	GIMAP4	55303
11737012_at	0.004553141	2.3827748	APLF	200558
11727881_at	0.011287882	2.3260777	BBS12	166379
11730484_at	0.026324632	2.2719805	PTGER3	5733
11734567_a_at	0.020084841	2.2164643	RASGRP2	10235
11730650_at	0.007807955	2.1906219	ANO3	63982
11758468_s_at	0.021060567	2.1602652	TSHZ2	128553
11758233_s_at	0.04835374	2.1473796	VNN1	8876
11723553_at	0.008293341	2.1459067	F5	2153
11743561_a_at	0.032499533	2.1396217	PTPRC	5788
11741899_s_at	0.005313663	2.0955439	FCGR2B	2213
11756978_a_at	0.029283324	2.0695326	KCNN2	3781
11730338_a_at	0.017747799	2.06411	SMAD6	4091
11757815_s_at	0.020044003	2.052542	METTL7A	25840
11725460_x_at	0.003776285	2.0343099	S100A7	6278
11727554_s_at	0.036547896	2.0307655	PKIB	5570
11757985_s_at	0.011287882	2.003753	PDE7B	27115

Probe set ID	Corrected *p* value	Fold change	Gene symbol	Entrez Gene #
11717858_a_at	0.01859705	1.9950682	CD37	951
11754474_a_at	0.03978821	1.9859641	PLEK	5341
11730704_s_at	9.63E-04	1.9525632	OR51E2	81285
11759287_at	0.008125707	1.9491535	DNAJB4	11080
11722469_a_at	0.034432553	1.9489293	ACSL6 /// LOC100505572	100505572 /// 23305
11735710_s_at	0.021585474	1.9399024	SAMSN1	64092
11723145_a_at	0.026182909	1.9377519	RANBP17	64901
11729232_s_at	0.009632714	1.9218451	KLF3	51274
11743406_x_at	0.029283324	1.9008608	C4orf34	201895
11715164_s_at	0.006155024	1.8807267	IGLL3P	91353
11732351_at	0.016267834	1.8702779	HGF	3082
11723699_s_at	0.03424919	1.8573126	OAS3	4940
11718949_a_at	0.017747799	1.8557533	MPP5	64398
11727223_a_at	0.02002393	1.8475525	CSGALNACT1	55790
11721302_a_at	0.011806974	1.8441671	CLEC2B	9976
11758488_s_at	0.0262126	1.8434767	SPATA16	83893
11720159_a_at	0.009280552	1.8399911	DENND3	22898
11733091_a_at	0.006509711	1.8237748	TSPAN8	7103
11718927_a_at	0.032542836	1.81838	ARID5B	84159
11735937_a_at	0.029283324	1.8037827	CD48	962
11728302_at	0.020084841	1.8016723	TGFA	7039
11741152_x_at	0.011110377	1.7958822	PLAGL1	5325
11750067_a_at	0.026182909	1.7880558	SPIB	6689
11725857_s_at	0.007807955	1.7656413	SLC2A13	114134
11724117_x_at	0.021060567	1.7507302	SAMD9L	219285
11725568_a_at	0.026182909	1.7360481	ATP8A1	10396
11763550_x_at	0.020292673	1.7332364	IGK@ /// IGKC /// LOC100294406	100294406 /// 3514 /// 50802
11758651_s_at	0.015066278	1.7174393	SH3GL3	6457
11730175_at	0.013762068	1.7117258	C4orf3	401152
11750740_a_at	0.016279606	1.7000911	ST3GAL5	8869
11720300_a_at	0.023235394	1.697482	SLA	6503
11744481_s_at	0.03684422	1.6960866	OPN3	23596
11757926_s_at	0.006155024	1.6928445	SLC9A9	285195
11736871_s_at	0.047035474	1.6866186	TRPC6	7225
11757793_s_at	0.040378932	1.6768728	TFPI	7035
11756896_a_at	0.020084841	1.6759015	COL6A6	131873
11724271_a_at	0.005353622	1.6683395	HLF	3131
11745535_a_at	0.047678698	1.6645346	CRB1	23418
11744572_a_at	0.015066278	1.6634676	KLF5	688
11733165_s_at	0.041280888	1.6618388	YIPF5	81555
11744195_at	0.04907001	1.6542981	FAT3	120114
11755686_a_at	0.010385592	1.653536	CPOX	1371

Probe set ID	Corrected *p* value	Fold change	Gene symbol	Entrez Gene #
11756912_a_at	0.03684422	1.6481669	AOX1	316
11725249_at	0.035872865	1.6462201	LY75	4065
11740134_a_at	0.011661301	1.6257238	CALD1	800
11751887_a_at	0.04907001	1.6197163	COL4A6	1288
11731193_at	0.012261071	1.6123832	UNC13C	440279
11750174_a_at	0.03187563	1.6117502	LOC645954	645954
11718735_at	0.03978821	1.6052271	PCMTD1	115294
11730401_a_at	0.009165928	1.5871506	RASGRF1	5923
11742067_s_at	0.04307449	1.5717839	LRRTM4	80059
11739054_a_at	0.020254651	1.5689728	PTPN6	5777
11729688_s_at	0.0242176	1.561744	LYRM7	90624
11740508_s_at	0.04809225	1.5573564	ARHGAP26	23092
11734316_a_at	0.006173489	1.5559312	WDR17	116966
11757961_s_at	0.01091728	1.5383642	MAGI2	9863
11749171_a_at	0.03458046	1.5344073	UPB1	51733
11734064_a_at	0.02558545	1.5070032	AMPD3	272
11759648_at	0.022157032	-1.5089669	CREB3L2	64764
11726590_at	0.036547896	-1.5098923	ELOVL4	6785
11756310_a_at	0.047035474	-1.5132802	NXT2	55916
11745907_at	0.044695064	-1.5155551	LOC729852	729852
11719257_s_at	0.03978821	-1.5237024	LRP6	4040
11749068_a_at	0.014201811	-1.5267886	C6orf211	79624
11717658_at	0.005408754	-1.5426329	CD109	135228
11727737_s_at	0.008712745	-1.5465502	AKAP7	9465
11729655_a_at	0.036647495	-1.5546831	SMAD2	4087
11756765_x_at	0.03978821	-1.554831	BCL2L13	23786
11731560_at	0.021060567	-1.5730873	FAM89A	375061
11729947_a_at	0.017755365	-1.5748941	TRMT10A	93587
11758931_a_at	0.02485138	-1.5946447	HEATR5A	25938
11732674_at	0.01299307	-1.5962677	C1orf53	388722
11728701_a_at	0.033950843	-1.6018118	CD55	1604
11725457_at	0.009165928	-1.6024536	FBXO33	254170
11743909_at	0.039035924	-1.6070213	ALG14	199857
11720080_at	0.0262126	-1.6084869	NTRK2	4915
11747128_a_at	0.048838556	-1.6267967	PHTF2	57157
11758491_s_at	0.005313663	-1.6273055	AGPS	8540
11744752_a_at	0.04809225	-1.6308398	GTF3C2	2976
11727682_at	0.00621134	-1.638878	ACVR2B	93
11723785_s_at	0.015240262	-1.6529186	LIMCH1	22998
11738626_a_at	0.0185275	-1.6648048	FOXP2	93986
11731577_a_at	0.045551844	-1.6766157	SLC22A1	6580
11719628_a_at	0.007018723	-1.6872011	HDHD1	8226
11734458_a_at	0.04809225	-1.7091733	FAM160B1	57700

Probe set ID	Corrected *p* value	Fold change	Gene symbol	Entrez Gene #
11742683_x_at	0.023235394	-1.7319468	HIST1H1C	3006
11751138_a_at	0.022839487	-1.7572113	USP46	64854
11734313_at	0.003776285	-1.7704911	OBSCN	84033
11721843_a_at	0.007666421	-1.8198025	ATL3	25923
11717419_a_at	0.005313663	-1.8440629	DNAL1	83544
11728049_s_at	0.006155024	-1.86706	HIST1H4A /// HIST1H4B /// HIST1H4C /// HIST1H4D /// HIST1H4E /// HIST1H4F /// HIST1H4H /// HIST1H4I /// HIST1H4J /// HIST1H4K /// HIST1H4L /// HIST2H4A /// HIST2H4B /// HIST4H4	121504 /// 554313 /// 8294 /// 8359 /// 8360 /// 8361 /// 8362 /// 8363 /// 8364 /// 8365 /// 8366 /// 8367 /// 8368 /// 8370
11752101_s_at	0.007610807	-1.9246788	EIF2S1	1965
11725637_a_at	0.004752198	-2.0823689	EIF3J	8669
11718397_s_at	0.034136143	-2.3140028	JUN	3725

Appendix 4 – Complete list of differentially expressed genes (>1.5-fold change).

Table of genes that were significantly altered in expression (≥1.5-fold change) in L-428 or KM-H2 cell lines when c-Jun or JunB was knocked-down. Fold change compares the expression of each gene in c-Jun/JunB shRNA-expressing cells to cells expressing control shRNA. Only one probe is shown for each gene. In cases where multiple probes for individual genes were present, probe with the greatest fold change was chosen.

Appendix 5: Common regulated genes

A: common c-Jun-regulated genes

Gene name	Alternative name	Fold change (KM-H2)	Fold change (L-428)
AMPD3		1.5070032 1.5004903	1.7636828
ACVR2B	ACTRIIB, ActR-IIB, HTX4	-1.638878	-1.6743557
EIF3J	EIF3S1, eIF3-alpha, eIF3-p35	-2.0823689	-2.353245
FAM89A	C1orf153	-1.5730873	-1.82818
HDHD1	DXF68S1E, FAM16AX, GS1A	-1.6872011 -1.6782507	-2.1333344 -1.8777279

B: common JunB-regulated genes

Gene name	Alternative name(s)	Fold change (KM-H2)	Fold change (L-428)
IGHG1 /// IGHG3 /// IGHM		1.845844 1.7757127 1.5987562	1.5335134
MYO5C		1.6180924	2.36160092.346913
ABLIM1	ABLIM, LIMAB1, LIMATIN, abLIM-1	-2.1492085 -1.9224327 -1.9001272 -1.3623247	-1.6360307 -1.4597598
ASPH	AAH, BAH, CASQ2BP1, FDLAB, HAAH, JCTN, junctin	-1.5569714	-2.2221072
ATL3	HSN1F	-1.7274168	-1.7070489
BCAT1	BCATC, BCT1, ECA39, MECA39, PNAS121, PP18	-1.5136969 -1.4588093 -1.2824342	-1.5968102 -1.4639204
BMPR2	BMPR-II, BMPR3, BMR2, BRK-3, POVD1, PPH1, T-ALK	-1.8349988 -1.5932338	-1.7690954 -1.5327047
DCBLD2	CLCP1, ESDN	-3.079634	-2.4814296
ITSN1	ITSN, SH3D1A, SH3P17	-1.6888822 -1.5089275 -1.3962718	-2.1181617 -1.8109685 -1.5756085 -1.4615881
RAPH1	ALS2CR18, ALS2CR9, LPD, PREL-2, PREL2, RMO1, RalGDS/AF-6	-1.5066824	-2.9169145 -2.5133736
SNX12		-2.602142	-2.132625

		-1.5187253	
Gene name	**Alternative name(s)**	**Fold change (KM-H2)**	**Fold change (L-428)**
TMX1	PDIA11, TMX, TXNDC, TXNDC1	-1.926389 -1.6189922	-1.7531958 -1.3068738
AIM2	PYHIN4	-1.9777663 -1.8441274	2.245885 2.0460415
BCL6	BCL5A, LAZ3, ZBTB27, ZNF51	-1.7662648	1.6782757 1.619385
CARD16	COP, COP1, PSEUDO-ICE	-2.50315	1.7605652
RARRES3	HRASLS4, HRSL4, PLA1/2-3, RIG1, TIG3	-2.6360712 -2.4580405	3.0901022 3.0297673
TIAM1		-1.876182	1.5163107

C: c-Jun (L-428) and JunB (KM-H2) overlapping genes

Gene name	**Alternative name(s)**	**Fold change (KM-H2)**	**Fold change (L-428)**	
DAPP1	Bam32	1.51758 1.442444 1.39048	1.82351	

D: c-Jun (KM-H2) and JunB (L-428) overlapping genes

Gene name	**Alternative name(s)**	**Fold change (KM-H2)**	**Fold change (L-428)**
CLEC2B	AICL, CLECSF2, HP10085, IFNRG1	1.844167	2.465284
CPOX	CPO, CPX, HCP	1.653536	1.628617 1.586561 1.373637
GABBR1	GABABR1-3, GB1, GPRC3A, dJ271M21.1.1, dJ271M21.1.2	4.363779	6.248702
GBP1		5.662492 5.141082 4.806957 4.322616 3.925417	8.611936 7.593415 7.031148 6.804356 6.222754
GBP2		2.558545 2.555178	4.960376 4.850102
GBP3		2.599175	3.890059
GBP4	Mpa2	4.248783 2.450829 2.424009 2.140274	3.57035 3.524718 3.489409 3.454461 2.881933

Gene name	Alternative name(s)	Fold change (KM-H2)	Fold change (L-428)
PLAGL1	LOT1, ZAC, ZAC1	1.795882	1.615254
SAMD9L	C7orf6, DRIF2, UEF1	1.75073	1.94248 1.930633
UNC13C		1.612383	3.57434 3.157699
ATL3	HSN1F	-1.8198	-1.70705
TSPAN8	CO-029, TM4SF3	1.823775	-4.59615

E: c-Jun and JunB overlapping genes in L-428 cells

Gene name	Alternative name(s)	Fold change (JunB)	Fold change (c-Jun)
AMPD1	MAD, MADA, MMDD	2.5796828	4.357616
C4BPB	C4BP	2.9014664	3.173863
CD52	CDW52	7.084145 5.2826447	2.406498
CDKN1A	CAP20, CDKN1, CIP1, MDA-6, P21, SDI1, WAF1, p21CIP1	1.6632433 1.357287	1.816763
SP140	LYSP100, LYSP100-A, LYSP100-B	2.1920545 2.164957 2.1444545 1.9184294	2.043045
TMTC1	ARG99, OLFA, TMTC1	2.417367	2.389035
TSHR	CHNG1, LGR3, hTSHR-I	1.597319	1.72389
CHRFAM7A /// CHRNA7	CHRNA7, CHRNA7-DR1, D-10	-1.5836561	-1.70774
TBL1X	EBI, SMAP55, TBL1	-1.7071285	-2.19204
PHLDA2	BRW1C, BWR1C, HLDA2, IPL,	1.7507555	-1.83721

F: c-Jun and JunB overlapping genes in KM-H2 cells

Gene name	Alternative name(s)	Fold change (JunB)	Fold change (c-Jun)
ACSL6 /// LOC100505572		2.681416 2.437208	1.948929
ANO3	DYT23; DYT24; TMEM16C; C11orf25; GENX-3947	2.017859	2.190622
ARID5B	DESRT; MRF-2; MRF2	1.995332 1.539145 1.492598	1.81838

Gene name	Alternative name(s)	Fold change (JunB)	Fold change (c-Jun)
ATP8A1	ATPIA; ATPP2; ATPASEII	1.53037	1.736048
C4orf3		1.511662 1.496042	1.711726 1.680213
CD37	GP52-40; TSPAN26	1.546311	1.995068 1.70971
CD48	BCM1; BLAST; BLAST1; SLAMF2; MEM-102	4.481185 3.046226	1.803783
COL4A6	DFNX6; DELXq22.3; CXDELq22.3	8.401869 8.335178 2.149108 1.750916 1.433989	1.619716
CXCL11	IP9; H174; IP-9; b-R1; I-TAC; SCYB11; SCYB9B	2.006532 1.908214 1.905426	2.916146 2.835914 2.807133
CYP4X1	CYP_a; CYPIVX1; A230025G20; Cyp4a28-ps	2.036131	2.434269
CYSLTR1	CYSLT1; CYSLTR; CYSLT1R; HMTMF81	3.891431 3.800872	2.604171
DNAJB4	DNAJW, DjB4, HLJ1	1.562127	1.949154 1.706269
DPYS	DHP, DHPase	6.699137	3.954691
F5	FVL, PCCF, RPRGL1, THPH2	1.824404 1.700309 1.658361	2.145907 2.133262 1.924131
FCGR2A	CD32, CD32A, CDw32, FCG2, FCGR21, FcGR, IGFR2, FCGR2A	2.692208 2.643511	2.791583 2.617593
FCGR2B	AI528646, CD32, F630109E10Rik, Fc[g]RII, FcgRII, Fcgr2, Fcgr2a, Fcr-2, Fcr-3, Ly-17, Ly-m20, LyM-1, Lym-1, fcRII	2.047624 2.017712 2.009119 1.768132	2.095544 2.092503 2.072625 1.773575
HGF	DFNB39, F-TCFB, HPTA, SF, HGF	2.21608 2.07192	1.870278
HLF	E230015K02Rik	1.760476	1.66834 1.352418
HSPA6 /// HSPA7	HSP70B	2.075097	3.145322
IGLL3P	16.1; IGLL3	3.007268	1.880727
KCNN2	KCa2.2, SK2, SKCA2, SKCa 2, hSK2	2.552667	2.069533

Gene name	Alternative name(s)	Fold change (JunB)	Fold change (c-Jun)
KLF5	BTEB2, CKLF, IKLF	2.196044 2.148523	1.663468 1.500682
OPN3	ECPN, PPP1R116	1.721138	1.696087
OR51E2	OR51E3P, OR52A2, PSGR	1.963485	1.952563
PTGER3	EP3, Pgerep3, Ptgerep3	3.73298 2.446449 2.405681 1.397475	2.271981 1.785531
PTPN6	HCP, HCPH, HPTP1C, PTP-1C, SH-PTP1, SHP-1, SHP-1L, SHP1	1.51964 1.405417	1.568973 1.487627
RASGRF1	AI844718, CDC25, CDC25Mm, Gnrp, Grf1, Grfbeta, P190-A, Ras-GRF1, p190, p190RhoGEF	1.93396 1.453919	1.587151
RASGRP2	CALDAG-GEFI, CDC25L	3.37790	2.216464
SAMSN1	HACS1, NASH1, SASH2, SH3D6B, SLy2	2.265866 2.01415	1.939902 1.741356
SELL	CD62L, LAM1, LECAM1, LEU8, LNHR, LSEL, LYAM1, PLNHR, TQ1	3.839616 2.986401	2.932964 2.039747
SLA	SLA1P, SLA	2.160025 2.121054	1.697482 1.6569
SPATA16	NYD-SP12, SPGF6	1.935783	1.843477
TFEC	TCFEC, TFE-C-L, TFECL, bHLHe34, hTFEC-L, TFEC	2.526102 2.480763 2.454052	3.643074 2.645584 2.486037
TRPC6	FSGS2, TRP6	2.258499	1.686619
WDR17		1.559511	1.555931
ATL3	HSN1F	-1.7274168	-1.8198
LRP6	ADCAD2	-1.8013471	-1.5237
OBSCN	ARHGEF30, UNC89	-2.0411196	-1.77049
TMEM100		-1.9819576 -2.0377648	2.475397 2.281343

Appendix 5 – Common regulated genes.

List of overlapping genes shown in the Venn diagrams in **Fig. 4.3.** Alternative names are provided and corresponding fold change in the indicated knock-down cell lines (relative to control shRNA-expressing cells) is shown.

Appendix 6: Gene Ontology analysis of differentially expressed genes

A: Functional Classification by Biological Pathways

Annotation Cluster #1 (54 hits)
Enrichment Score: 6.17

GO ID#	name	Count	*p*-value	Benjamini
GO:0009611	response to wounding	42	3.3E-08	4.1E-05
GO:0006954	inflammatory response	28	2.1E-06	1.3E-03

Gene Symbol	Gene name	Infla ?
ANXA1	annexin A1	*
AOX1	aldehyde oxidase 1	*
APOL2	apolipoprotein L, 2	*
APOL3	apolipoprotein L, 3	*
C3AR1	complement component 3a receptor 1	
C4BPB	complement component 4 binding protein, beta	*
CCL22	chemokine (C-C motif) ligand 22	*
CCL3	chemokine (C-C motif) ligand 3	*
CD24, CD24L4	CD24 molecule; CD24 molecule-like 4	*
CD55	CD55 molecule, decay accelerating factor for complement	*
CFI	complement factor I	*
CHST2	carbohydrate (N-acetylglucosamine-6-O) sulfotransferase 2	*
CLU	clusterin	*
CX3CR1	chemokine (C-X3-C motif) receptor 1	
CXCL11	chemokine (C-X-C motif) ligand 11	*
CYP1A1	cytochrome P450, family 1, subfamily A, polypeptide 1	
CYSLTR1	cysteinyl leukotriene receptor 1	*
DCBLD2	discoidin, CUB and LCCL domain containing 2	
ELK3	ELK3, ETS-domain protein (SRF accessory protein 2)	
ENTPD1	ectonucleoside triphosphate diphosphohydrolase 1	
F5	coagulation factor V (proaccelerin, labile factor)	
HBEGF	heparin-binding EGF-like growth factor	
HOXB13	homeobox B13	
IL15	interleukin 15	*
KLRG1	killer cell lectin-like receptor subfamily G, member 1	*
LY75, CD302	CD302 molecule; lymphocyte antigen 75	*
MECOM	ecotropic viral integration site 1	*
PDGFRA	platelet-derived growth factor receptor, alpha polypeptide	
PLA2G2D	phospholipase A2, group IID	*
PLEK	pleckstrin	
PTGER3	prostaglandin E receptor 3 (subtype EP3)	*
PTPN6	protein tyrosine phosphatase, non-receptor type 6	
RIPK2	receptor-interacting serine-threonine kinase 2	*
SIGIRR	single immunoglobulin and toll-interleukin 1 receptor (TIR) domain	*

SLC1A2	solute carrier family 1 (glial high affinity glutamate transporter), member 2	
SPP1	secreted phosphoprotein 1	*
TFPI	tissue factor pathway inhibitor (lipoprotein-associated coagulation inhibitor)	
TLR1	toll-like receptor 1	*
TLR3	toll-like receptor 3	*
TNC	tenascin C	
TNFSF4	tumor necrosis factor (ligand) superfamily, member 4	*
VNN1	vanin 1	*

Annotation Cluster #2 (41 hits)

Enrichment Score: 3.59

GO ID#	name	Count	*p*-value	Benjamini
GO:0042592	Homeostatic process	41	3.7E-04	2.8E-02
GO:0006875	Cellular metal ion homeostasis	19	2.9E-05	6.0E-03

Gene Symbol	Gene name	Ion?
APP	amyloid beta (A4) precursor protein	*
BCL2L11	BCL2-like 11 (apoptosis facilitator)	
BCL6	B-cell CLL/lymphoma 6	
C3AR1	complement component 3a receptor 1	*
CAV1	caveolin 1, caveolae protein, 22kDa	
CCL3	chemokine (C-C motif) ligand 3	*
CD24, CD24L4	CD24 molecule; CD24 molecule-like 4	*
CD38	CD38 molecule	*
CD52	CD52 molecule	*
CD55	CD55 molecule, decay accelerating factor for complement	*
CHRNA1	cholinergic receptor, nicotinic, alpha 1 (muscle)	
CXCL12	chemokine (C-X-C motif) ligand 12 (stromal cell-derived factor 1)	*
CYSLTR1	cysteinyl leukotriene receptor 1	*
DMD	dystrophin	
EIF5A2	eukaryotic translation initiation factor 5A2	
FABP4	fatty acid binding protein 4, adipocyte	
GLRX	glutaredoxin (thioltransferase)	
HEXB	hexosaminidase B (beta polypeptide)	*
HFE	hemochromatosis	
IFNG	interferon, gamma	
IL7	interleukin 7	
JUN	jun oncogene	
KCNMA1	potassium large conductance calcium-activated channel, subfamily M, alpha member 1	*
KCNN4	potassium intermediate/small conductance calcium-activated channel, subfamily N, member 4	

KCNQ1	potassium voltage-gated channel, KQT-like subfamily, member 1	
MECOM	ecotropic viral integration site 1	
NR3C2	nuclear receptor subfamily 3, group C, member 2	*
PMP22	peripheral myelin protein 22	
POT1	POT1 protection of telomeres 1 homolog (S. pombe)	
POU3F1	POU class 3 homeobox 1	
PTGER3	prostaglandin E receptor 3 (subtype EP3)	*
PTK2B	PTK2B protein tyrosine kinase 2 beta	*
PTPRC	protein tyrosine phosphatase, receptor type, C	*
RYR2	ryanodine receptor 2 (cardiac)	*
S1PR1	sphingosine-1-phosphate receptor 1	*
SLC9A9	solute carrier family 9 (sodium/hydrogen exchanger), member 9	
SMAD5	SMAD family member 5	
TMX1	thioredoxin-related transmembrane protein 1	
TMX4	thioredoxin-related transmembrane protein 4	
TRPC6	transient receptor potential cation channel, subfamily C, member 6	*
XIRP1	xin actin-binding repeat containing 1	

Annotation Cluster #3 (58 hits)

Enrichment Score: 2.36

GO ID#	name	Count	*p*-value	Benjamini
GO:0042981	Regulation of apoptosis	43	3.9E-04	2.8E-02
GO:0043065	Positive regulation of apoptosis	26	1.5E-03	6.6E-02

Gene Symbol	Gene name	Pos ?
AIFM2	apoptosis-inducing factor, mitochondrion-associated, 2	*
AMIGO2	adhesion molecule with Ig-like domain 2	
ANXA1	annexin A1	
APH1B	anterior pharynx defective 1 homolog B (C. elegans)	*
APP	amyloid beta (A4) precursor protein	*
BCL2L11	BCL2-like 11 (apoptosis facilitator)	*
BCL2L13	BCL2-like 13 (apoptosis facilitator)	*
BCL6	B-cell CLL/lymphoma 6	*
BDNF	brain-derived neurotrophic factor	
BTG2	BTG family, member 2	
CARD16	caspase recruitment domain family, member 16	
CASP1	caspase 1, apoptosis-related cysteine peptidase (interleukin 1, beta, convertase)	*
CD24, CD24L4	CD24 molecule; CD24 molecule-like 4	*
CD38	CD38 molecule	*
CDKN1A	cyclin-dependent kinase inhibitor 1A (p21, Cip1)	*
CLU	clusterin	

DHCR24	24-dehydrocholesterol reductase	
ETS1	v-ets erythroblastosis virus E26 oncogene homolog 1 (avian)	*
EYA1	eyes absent homolog 1 (Drosophila)	
HGF	hepatocyte growth factor (hepapoietin A; scatter factor)	
IFNG	interferon, gamma	*
IL12B	interleukin 12B (natural killer cell stimulatory factor 2, cytotoxic lymphocyte maturation factor 2, p40)	*
IL7	interleukin 7	
ITSN1	intersectin 1 (SH3 domain protein)	*
JUN	jun oncogene	*
KCNMA1	potassium large conductance calcium-activated channel, subfamily M, alpha member 1	*
LGALS1	lectin, galactoside-binding, soluble, 1	
NLRP1	NLR family, pyrin domain containing 1	*
OBSCN	obscurin, cytoskeletal calmodulin and titin-interacting RhoGEF	*
PLAGL1	pleiomorphic adenoma gene-like 1	*
PRAME	preferentially expressed antigen in melanoma	
PTPRC	protein tyrosine phosphatase, receptor type, C	*
RASGRF1	Ras protein-specific guanine nucleotide-releasing factor 1	*
RIPK2	receptor-interacting serine-threonine kinase 2	*
RYR2	ryanodine receptor 2 (cardiac)	*
SMAD6	SMAD family member 6	
SOCS2	suppressor of cytokine signaling 2	
STAT1	signal transducer and activator of transcription 1, 91kDa	*
TIAM1	T-cell lymphoma invasion and metastasis 1	*
TMX1	thioredoxin-related transmembrane protein 1	
TNFRSF10A	tumor necrosis factor receptor superfamily, member 10a	*
TNFSF15	tumor necrosis factor (ligand) superfamily, member 15	
VNN1	vanin 1	

Annotation Cluster #4 (52 hits)

Enrichment Score: 2.28

GO ID#	name	Count	*p*-value	Benjamini
GO:0008284	positive regulation of proliferation	32	3.3E-06	1.6E-03
GO:0050670	regulation of lymphocyte proliferation	11	2.0E-04	2.1E-02

Gene Symbol	Gene name	Lym?
ARHGAP5	Rho GTPase activating protein 5	
BCL6	B-cell CLL/lymphoma 6	*
CD24, CD24L4	CD24 molecule; CD24 molecule-like 4	*
CD38	CD38 molecule	*
CDKN1A	cyclin-dependent kinase inhibitor 1A (p21, Cip1)	*
CLU	clusterin	
EBI3	Epstein-Barr virus induced 3	*

EIF5A2	eukaryotic translation initiation factor 5A2	
FABP4	fatty acid binding protein 4, adipocyte	
FOXP2	forkhead box P2	
GKN1	gastrokine 1	
HBEGF	heparin-binding EGF-like growth factor	
HES1	hairy and enhancer of split 1, (Drosophila)	
IFNG	interferon, gamma	*
IL12B	interleukin 12B (natural killer cell stimulatory factor 2, cytotoxic lymphocyte maturation factor 2, p40)	*
IL15	interleukin 15	*
IL7	interleukin 7	*
JUN	jun oncogene	
KLF5	Kruppel-like factor 5 (intestinal)	
MYCN	v-myc myelocytomatosis viral related oncogene, neuroblastoma derived (avian)	
PDGFRA	platelet-derived growth factor receptor, alpha polypeptide	
PRAME	preferentially expressed antigen in melanoma	
PTK2B	PTK2B protein tyrosine kinase 2 beta	
PTPRC	protein tyrosine phosphatase, receptor type, C	*
RIPK2	receptor-interacting serine-threonine kinase 2	*
RUNX2	runt-related transcription factor 2	
S1PR1	sphingosine-1-phosphate receptor 1	
STAT1	signal transducer and activator of transcription 1, 91kDa	
TGFA	transforming growth factor, alpha	
TNFSF4	tumor necrosis factor (ligand) superfamily, member 4	
TSHR	thyroid stimulating hormone receptor	
VASH2	vasohibin 2	

Annotation Cluster #5 (32 hits)

Enrichment Score: 2.28

GO ID#	name	Count	*p*-value	Benjamini
GO:0001775	cell activation	24	2.5E-05	5.0E-03
GO:0045321	leukocyte activation	21	4.9E-05	8.1E-03

Gene Symbol	Gene name	Leuk ?
BCL6	B-cell CLL/lymphoma 6	*
CD24, CD24L4	CD24 molecule; CD24 molecule-like 4	*
CD48	CD48 molecule	*
CXCL12	chemokine (C-X-C motif) ligand 12 (stromal cell-derived factor 1)	*
DPP4	dipeptidyl-peptidase 4	*
ENTPD1	ectonucleoside triphosphate diphosphohydrolase 1	
IFNAR1	interferon (alpha, beta and omega) receptor 1	*
IL12B	interleukin 12B (natural killer cell stimulatory factor 2, cytotoxic lymphocyte maturation factor 2, p40)	*

IL15	interleukin 15	*
IL7	interleukin 7	*
IRF1	interferon regulatory factor 1	*
LCP2	lymphocyte cytosolic protein 2 (SH2 domain containing leukocyte protein of 76kDa)	*
PDGFRA	platelet-derived growth factor receptor, alpha polypeptide	
PIK3R1	phosphoinositide-3-kinase, regulatory subunit 1 (alpha)	*
PLEK	pleckstrin	
PTPN22	protein tyrosine phosphatase, non-receptor type 22 (lymphoid)	*
PTPRC	protein tyrosine phosphatase, receptor type, C	*
RIPK2	receptor-interacting serine-threonine kinase 2	*
THEMIS	thymocyte selection pathway associated	*
TLR1	toll-like receptor 1	*
TLR3	toll-like receptor 3	*
TMX1	thioredoxin-related transmembrane protein 1	*
TNFSF4	tumor necrosis factor (ligand) superfamily, member 4	*
TSHR	thyroid stimulating hormone receptor	*

Annotation Cluster #6 (13 hits)

Enrichment Score: 1.92

GO ID#	name	Count	*p*-value	Benjamini
GO:0042110	T cell activation	13	4.4E-04	2.9E-02
GO:0042098	T cell proliferation	5	8.4E-03	1.9E-01

Gene Symbol	Gene name	Proli ?
CD48	CD48 molecule	
CXCL12	chemokine (C-X-C motif) ligand 12 (stromal cell-derived factor 1)	*
DPP4	dipeptidyl-peptidase 4	
IFNAR1	interferon (alpha, beta and omega) receptor 1	
IL12B	interleukin 12B (natural killer cell stimulatory factor 2, cytotoxic lymphocyte maturation factor 2, p40)	
IL15	interleukin 15	*
IL7	interleukin 7	
IRF1	interferon regulatory factor 1	
PTPN22	protein tyrosine phosphatase, non-receptor type 22 (lymphoid)	
PTPRC	protein tyrosine phosphatase, receptor type, C	*
RIPK2	receptor-interacting serine-threonine kinase 2	*
THEMIS	thymocyte selection pathway associated	
TNFSF4	tumor necrosis factor (ligand) superfamily, member 4	*

Annotation Cluster #7 (15 hits)

Enrichment Score: 1.89

GO ID#	name	Count	*p*-value	Benjamini
GO:0048514	blood vessel morphogenesis	15	5.1E-03	1.5E-01
GO:0001525	angiogenesis	11	1.5E-02	2.3E-01

Gene Symbol	Gene name	Ang ?
ANXA2	annexin A2	*
CAV1	caveolin 1, caveolae protein, 22kDa	
CXCL12	chemokine (C-X-C motif) ligand 12 (stromal cell-derived factor 1)	*
ELK3	ELK3, ETS-domain protein (SRF accessory protein 2)	*
ID1	inhibitor of DNA binding 1, dominant negative helix-loop-helix protein	*
JUN	jun oncogene	*
JUNB	jun B proto-oncogene	
KLF5	Kruppel-like factor 5 (intestinal)	*
NTRK2	neurotrophic tyrosine kinase, receptor, type 2	
NUS1, LOC729148	nuclear undecaprenyl pyrophosphate synthase 1 pseudogene; nuclear undecaprenyl pyrophosphate synthase 1 homolog (S. cerevisiae)	*
PTK2B	PTK2B protein tyrosine kinase 2 beta	*
S100A7	S100 calcium binding protein A7	*
S1PR1	sphingosine-1-phosphate receptor 1	*
SEMA3C	sema domain, immunoglobulin domain (Ig), short basic domain, secreted, (semaphorin) 3C	
TGFA	transforming growth factor, alpha	

Annotation Cluster #8 (15 hits)

Enrichment Score: 1.83

GO ID#	name	Count	*p*-value	Benjamini
GO:0051270	regulation of cell motion	14	6.0E-03	1.6E-01
GO:0030335	positive regulation of cell migration	8	1.8E-02	2.6E-01

Gene Symbol	Gene name	pos?
ARHGAP5	Rho GTPase activating protein 5	*
BCL6	B-cell CLL/lymphoma 6	
CXCL12	chemokine (C-X-C motif) ligand 12 (stromal cell-derived factor 1)	*
ETS1	v-ets erythroblastosis virus E26 oncogene homolog 1 (avian)	
HBEGF	heparin-binding EGF-like growth factor	*
LAMA2	laminin, alpha 2	

LOC100133211, RRAS2	related RAS viral (r-ras) oncogene homolog 2; similar to related RAS viral (r-ras) oncogene homolog 2	*
NEXN	nexilin (F actin binding protein)	
PDGFRA	platelet-derived growth factor receptor, alpha polypeptide	*
PIK3R1	phosphoinositide-3-kinase, regulatory subunit 1 (alpha)	*
PTK2B	PTK2B protein tyrosine kinase 2 beta	*
S1PR1	sphingosine-1-phosphate receptor 1	*
SP100	SP100 nuclear antigen	
TRIB1	tribbles homolog 1 (Drosophila)	

Annotation Cluster #9 (19 hits)

Enrichment Score: 1.75

GO ID#	name	Count	*p*-value	Benjamini
GO:0050778	positive regulation of immune response	13	1.5E-03	6.7E-02
GO:0002764	immune response-regulating signal transduction	7	6.8E-03	1.7E-01

Gene Symbol	Gene name	Sig ?
C3AR1	complement component 3a receptor 1	*
C4BPB	complement component 4 binding protein, beta	
CD24L4, CD24	CD24 molecule; CD24 molecule-like 4	*
CD55	CD55 molecule, decay accelerating factor for complement (Cromer blood group)	
CFI	complement factor I	
CLU	clusterin	
IL12B	interleukin 12B (natural killer cell stimulatory factor 2, cytotoxic lymphocyte maturation factor 2, p40)	
IL15	interleukin 15	
PTPN22	protein tyrosine phosphatase, non-receptor type 22 (lymphoid)	*
PTPRC	protein tyrosine phosphatase, receptor type, C	*
RIPK2	receptor-interacting serine-threonine kinase 2	*
THEMIS	thymocyte selection pathway associated	*
TLR3	toll-like receptor 3	*

Annotation Cluster #10 (14 hits)

Enrichment Score: 1.74

GO ID#	name	Count	*p*-value	Benjamini
GO:0001817	regulation of cytokine production	14	3.5E-03	1.1E-01

GO:0032649	regulation of interferon-gamma production	5	1.2E-02	2.2E-01

Gene Symbol	Gene name	IFN?
BCL6	B-cell CLL/lymphoma 6	
CASP1	caspase 1, apoptosis-related cysteine peptidase (interleukin 1, beta, convertase)	
CD24L4, CD24	CD24 molecule; CD24 molecule-like 4	
EBI3	Epstein-Barr virus induced 3	*
IFNAR1	interferon (alpha, beta and omega) receptor 1	*
IFNG	interferon, gamma	
IL12B	interleukin 12B (natural killer cell stimulatory factor 2, cytotoxic lymphocyte maturation factor 2, p40)	*
IRF1	interferon regulatory factor 1	
RIPK2	receptor-interacting serine-threonine kinase 2	*
SIGIRR	single immunoglobulin and toll-interleukin 1 receptor (TIR) domain	
TLR1	toll-like receptor 1	
TLR3	toll-like receptor 3	*
TNFSF15	tumor necrosis factor (ligand) superfamily, member 15	
TNFSF4	tumor necrosis factor (ligand) superfamily, member 4	

B: Functional Classification by Molecular Function

Annotation Cluster #1 (32 hits)
Enrichment Score: 3.39

GO ID#	name	Count	*p*-value	Benjamini
GO:0008289	lipid binding	32	2.2E-05	1.5E-02
GO:0035091	phosphoinositide binding	11	9.7E-04	1.0E-01

Gene Symbol	Gene name	PIB?
ANXA1	annexin A1	
ANXA2	annexin A2	*
APOL1	apolipoprotein L, 1	
APOL2	apolipoprotein L, 2	
APOL3	apolipoprotein L, 3	
ARHGAP29	Rho GTPase activating protein 29	
CAV1	caveolin 1, caveolae protein, 22kDa	
CCDC88A	coiled-coil domain containing 88A	*
DAPP1	dual adaptor of phosphotyrosine and 3-phosphoinositides	
FABP4	fatty acid binding protein 4, adipocyte	
FNBP1L	formin binding protein 1-like	
HNF4G	hepatocyte nuclear factor 4, gamma	

NR3C2	nuclear receptor subfamily 3, group C, member 2	
PIK3R1	phosphoinositide-3-kinase, regulatory subunit 1 (alpha)	*
PITPNC1	phosphatidylinositol transfer protein, cytoplasmic 1	
PLEK	pleckstrin	*
RASGRP1	RAS guanyl releasing protein 1 (calcium and DAG-regulated)	
RASGRP2	RAS guanyl releasing protein 2 (calcium and DAG-regulated)	
S1PR1	sphingosine-1-phosphate receptor 1	
SELL	selectin L	
SERPINA6	serpin peptidase inhibitor, clade A (alpha-1 antiproteinase, antitrypsin), member 6	
SH3GL3	SH3-domain GRB2-like 3	
SNX1	sorting nexin 1	*
SNX12	sorting nexin 12	*
SNX24	sorting nexin 24	*
SNX29	sorting nexin 29	*
STARD4	StAR-related lipid transfer (START) domain containing 4	
SYTL2	synaptotagmin-like 2	*
TIAM1	T-cell lymphoma invasion and metastasis 1	
UNC13C	unc-13 homolog C (C. elegans)	
VNN1	vanin 1	*
ZCCHC14	zinc finger, CCHC domain containing 14	*

Annotation Cluster #2 (6 hits)

Enrichment Score: 2.14

GO ID#	name	Count	*p*-value	Benjamini
GO:0016504	peptidase activator activity	6	5.6E-04	7.1E-02
GO:0008656	caspase activator activity	4	1.2E-02	5.1E-01

Gene Symbol	Gene name	casp ?
APP	amyloid beta (A4) precursor protein	
BCL2L13	BCL2-like 13 (apoptosis facilitator)	*
CASP1	caspase 1, apoptosis-related cysteine peptidase (interleukin 1, beta, convertase)	*
CAV1	caveolin 1, caveolae protein, 22kDa	
NLRP1	NLR family, pyrin domain containing 1	*
TNFRSF10A	tumor necrosis factor receptor superfamily, member 10a	*

Annotation Cluster #3 (73 hits)

Enrichment Score: 2.00

GO ID#	name	Count	*p*-value	Benjamini
GO:0043565	sequence-specific DNA binding	35	5.1E-04	8.1E-02
GO:0003700	transcription factor activity	48	1.3E-03	1.1E-01

Gene Symbol	Gene name	DNA?
BCL6	B-cell CLL/lymphoma 6	*
CEBPD	CCAAT/enhancer binding protein (C/EBP), delta	*
CREB3L2	cAMP responsive element binding protein 3-like 2	*
EHF	ets homologous factor	*
ELK3	ELK3, ETS-domain protein (SRF accessory protein 2)	*
ETS1	v-ets erythroblastosis virus E26 oncogene homolog 1 (avian)	*
ETV7	ets variant 7	*
FOXP2	forkhead box P2	*
GATA6	GATA binding protein 6	*
GLIS3	GLIS family zinc finger 3	
HLF	hepatic leukemia factor	*
HNF4G	hepatocyte nuclear factor 4, gamma	*
HOPX	HOP homeobox	*
HOXB13	homeobox B13	*
IRF1	interferon regulatory factor 1	*
IRF2	interferon regulatory factor 2	
IRF8	interferon regulatory factor 8	*
JUN	jun oncogene	*
JUNB	jun B proto-oncogene	*
KLF11	Kruppel-like factor 11	
KLF3	Kruppel-like factor 3 (basic)	
KLF5	Kruppel-like factor 5 (intestinal)	
L3MBTL4	l(3)mbt-like 4 (Drosophila)	
LEUTX	leucine twenty homeobox	*
MECOM	ecotropic viral integration site 1	
MYCL1	v-myc myelocytomatosis viral oncogene homolog 1, lung carcinoma derived (avian)	
MYCN	v-myc myelocytomatosis viral related oncogene, neuroblastoma derived (avian)	
NFATC2	nuclear factor of activated T-cells, cytoplasmic, calcineurin-dependent 2	*
NR1D2	nuclear receptor subfamily 1, group D, member 2	*
NR3C2	nuclear receptor subfamily 3, group C, member 2	*
POU3F1	POU class 3 homeobox 1	*
RORA	RAR-related orphan receptor A	*
RUNX2	runt-related transcription factor 2	
SATB1	SATB homeobox 1	*
SMAD2	SMAD family member 2	*
SMAD5	SMAD family member 5	
SMAD6	SMAD family member 6	
SP140	SP140 nuclear body protein	
SPIB	Spi-B transcription factor (Spi-1/PU.1 related)	*
STAT1	signal transducer and activator of transcription 1, 91kDa	*
TBX21	T-box 21	
TCF12	transcription factor 12	*

TFAP2B	transcription factor AP-2 beta (activating enhancer binding protein 2 beta)	*
TFEC	transcription factor EC	
THRB	thyroid hormone receptor, beta (erythroblastic leukemia viral (v-erb-a) oncogene homolog 2, avian)	*
TSHZ2	teashirt zinc finger homeobox 2	*
XBP1	X-box binding protein 1	*
ZSCAN4	zinc finger and SCAN domain containing 4	

	sequence-specific DNA binding only genes	
Gene Symbol	**Gene name**	
GFI1	growth factor independent 1 transcription repressor	
POT1	POT1 protection of telomeres 1 homolog (S. pombe)	
TBL1X	transducin (beta)-like 1X-linked	

Annotation Cluster #4 (32 hits)

Enrichment Score: 2.00

GO ID#	name	Count	*p*-value	Benjamini
GO:0008092	cytoskeletal protein binding	31	4.0E-04	1.2E-01

Gene Symbol	Gene name
ABLIM1	actin binding LIM protein 1
ANLN	anillin, actin binding protein
ANXA2	annexin A2
BCL2L11	BCL2-like 11 (apoptosis facilitator)
CALD1	caldesmon 1
CCDC88A	coiled-coil domain containing 88A
CTNNA1	catenin (cadherin-associated protein), alpha 1, 102kDa
DMD	dystrophin
EPB41L4B	erythrocyte membrane protein band 4.1 like 4B
GMFG	glia maturation factor, gamma
KCNMA1	potassium large conductance calcium-activated channel, subfamily M, alpha member 1
KIFAP3	kinesin-associated protein 3
KLHL4	kelch-like 4 (Drosophila)
LIMCH1	LIM and calponin homology domains 1
MTSS1	metastasis suppressor 1
MYBPC1	myosin binding protein C, slow type
MYBPC2	myosin binding protein C, fast type
MYO5C	myosin VC

NEXN	nexilin (F actin binding protein)
OBSCN	obscurin, cytoskeletal calmodulin and titin-interacting RhoGEF
PDLIM5	PDZ and LIM domain 5
PTPN3	protein tyrosine phosphatase, non-receptor type 3
SPTBN1	spectrin, beta, non-erythrocytic 1
SSX2IP	synovial sarcoma, X breakpoint 2 interacting protein
SVIL	supervillin
SYNPO2	synaptopodin 2
TMOD2	tropomodulin 2 (neuronal)
TPM2	tropomyosin 2 (beta)
TWF1	twinfilin, actin-binding protein, homolog 1 (Drosophila)
WASF3	WAS protein family, member 3
XIRP1	xin actin-binding repeat containing 1

Annotation Cluster #5 (12 hits)

Enrichment Score: 1.75

GO ID#	name	Count	*p*-value	Benjamini
GO:0004725	protein tyrosine phosphatase activity	11	1.3E-03	1.0E-01

Gene Symbol	Gene name
DAPP1	dual adaptor of phosphotyrosine and 3-phosphoinositides
DUSP16	dual specificity phosphatase 16
DUSP5	dual specificity phosphatase 5
DUSP6	dual specificity phosphatase 6
EYA1	eyes absent homolog 1 (Drosophila)
PTP4A3	protein tyrosine phosphatase type IVA, member 3
PTPN22	protein tyrosine phosphatase, non-receptor type 22 (lymphoid)
PTPN3	protein tyrosine phosphatase, non-receptor type 3
PTPN6	protein tyrosine phosphatase, non-receptor type 6
PTPRC	protein tyrosine phosphatase, receptor type, C
PTPRR	protein tyrosine phosphatase, receptor type, R

Annotation Cluster #6 (26 hits)

Enrichment Score: 1.60

GO ID#	name	Count	*p*-value	Benjamini
GO:0019899	enzyme binding	26	1.9E-02	6.5E-01
GO:0019900	kinase binding	12	2.2E-02	6.5E-01

Gene Symbol	Gene name	Kin?
AKAP7	A kinase (PRKA) anchor protein 7	*
ANXA2	annexin A2	

CAV1	caveolin 1, caveolae protein, 22kDa	*
CCDC88A	coiled-coil domain containing 88A	*
CD24, CD24L4	CD24 molecule; CD24 molecule-like 4	*
CYP1A1	cytochrome P450, family 1, subfamily A, polypeptide 1	
DENND5A	DENN/MADD domain containing 5A	
DHCR24	24-dehydrocholesterol reductase	
DMD	dystrophin	
DOCK7	dedicator of cytokinesis 7	
KAT2B	K(lysine) acetyltransferase 2B	
MAGI2	membrane associated guanylate kinase, WW and PDZ domain containing 2	
NCF2	neutrophil cytosolic factor 2	
NLRP1	NLR family, pyrin domain containing 1	
PDLIM5	PDZ and LIM domain 5	*
PIK3R1	phosphoinositide-3-kinase, regulatory subunit 1 (alpha)	
PLEK	pleckstrin	*
POT1	POT1 protection of telomeres 1 homolog (S. pombe)	
PTK2B	PTK2B protein tyrosine kinase 2 beta	*
PTPRC	protein tyrosine phosphatase, receptor type, C	*
PTPRR	protein tyrosine phosphatase, receptor type, R	*
RYR2	ryanodine receptor 2 (cardiac)	*
SMAD2	SMAD family member 2	
SP100	SP100 nuclear antigen	*
SYTL2	synaptotagmin-like 2	
TRIB1	tribbles homolog 1 (Drosophila)	*

Annotation Cluster #7 (3 hits)

Enrichment Score: 1.17

GO ID#	name	Count	*p*-value	Benjamini
GO:0004467	long-chain-fatty-acid-CoA ligase activity	3	3.6E-02	7.5E-01

Gene Symbol	Gene name
ACSL4	acyl-CoA synthetase long-chain family member 4
ACSL5	acyl-CoA synthetase long-chain family member 5
ACSL6	acyl-CoA synthetase long-chain family member 6

Annotation Cluster #8 (20 hits)

Enrichment Score: 1.11

GO ID#	name	Count	*p*-value	Benjamini
GO:0005085	guanyl-nucleotide exchange factor activity	10	4.4E-02	7.3E-01
GO:0030695	GTPase regulator activity	20	4.3E-02	7.3E-01

Gene Symbol	Gene name	GEF?
ANXA2	annexin A2	
ARHGAP17	Rho GTPase activating protein 17	
ARHGAP26	Rho GTPase activating protein 26	
ARHGAP29	Rho GTPase activating protein 29	
ARHGAP5	Rho GTPase activating protein 5	
BCR	breakpoint cluster region	*
DENND5A	DENN/MADD domain containing 5A	
DOCK1	dedicator of cytokinesis 1	*
DOCK7	dedicator of cytokinesis 7	*
FLJ41603	FLJ41603 protein	*
ITSN1	intersectin 1 (SH3 domain protein)	*
JUN	jun oncogene	
MAP4K3	mitogen-activated protein kinase kinase kinase kinase 3	
OBSCN	obscurin, cytoskeletal calmodulin and titin-interacting RhoGEF	*
RASGRF1	Ras protein-specific guanine nucleotide-releasing factor 1	*
RASGRP1	RAS guanyl releasing protein 1 (calcium and DAG-regulated)	*
RASGRP2	RAS guanyl releasing protein 2 (calcium and DAG-regulated)	*
RGS2	regulator of G-protein signaling 2, 24kDa	
SYTL2	synaptotagmin-like 2	
TIAM1	T-cell lymphoma invasion and metastasis 1	*

Annotation Cluster #9 (16 hits)

Enrichment Score: 0.75

GO ID#	name	Count	*p*-value	Benjamini
GO:0070330	aromatase activity	4	4.0E-02	7.1E-01
GO:0009055	electron carrier activity	11	1.4E-01	8.7E-01

Gene Symbol	Gene name	Aro?
AOX1	aldehyde oxidase 1	
ASPH	aspartate beta-hydroxylase	
CYP1A1	cytochrome P450, family 1, subfamily A, polypeptide 1	*
CYP2C18	cytochrome P450, family 2, subfamily C, polypeptide 18	*
CYP4V2	cytochrome P450, family 4, subfamily V, polypeptide 2	
CYP4X1	cytochrome P450, family 4, subfamily X, polypeptide 1	*
CYP4Z1	cytochrome P450, family 4, subfamily Z, polypeptide 1	*
GLDC	glycine dehydrogenase (decarboxylating)	
GLRX	glutaredoxin (thioltransferase)	
KMO	kynurenine 3-monooxygenase (kynurenine 3-hydroxylase)	
NCF2	neutrophil cytosolic factor 2	

Annotation Cluster #10 (18 hits)

Enrichment Score: 0.66

GO ID#	name	Count	*p*-value	Benjamini
GO:0030244	carbohydrate binding	18	4.6E-02	7.2E-01

Gene Symbol	Gene name
AIM1	absent in melanoma 1
AIM1L	absent in melanoma 1-like
APP	amyloid beta (A4) precursor protein
CD24, CD24L4	CD24 molecule; CD24 molecule-like 4
CLC	Charcot-Leyden crystal protein
CLEC2B	C-type lectin domain family 2, member B
EGFLAM	EGF-like, fibronectin type III and laminin G domains
GALNT11	UDP-N-acetyl-alpha-D-galactosamine:polypeptide N-acetylgalactosaminyltransferase 11 (GalNAc-T11)
GFPT2	glutamine-fructose-6-phosphate transaminase 2
HAPLN3	hyaluronan and proteoglycan link protein 3
HBEGF	heparin-binding EGF-like growth factor
HEXB	hexosaminidase B (beta polypeptide)
KLRG1	killer cell lectin-like receptor subfamily G, member 1
LGALS1	lectin, galactoside-binding, soluble, 1
LY75, CD302	CD302 molecule; lymphocyte antigen 75
PTPRC	protein tyrosine phosphatase, receptor type, C
SELL	selectin L
THBS4	thrombospondin 4

Appendix 6 – Gene ontology analysis of differentially expressed genes.

Gene Ontology (GO) was performed using DAVID (278) to identify biological processes (**A**) and molecular functions (**B**) enriched amongst genes with altered expression in c-Jun/JunB shRNA-expressing cells (≥1.5-fold change). For this analysis, c-Jun and JunB differentially expressed genes identified in both cell lines were combined. The top 10 annotation clusters identified are shown and ranked according to their cluster enrichment score. Two representative categories

within each cluster are shown. The table below each cluster shows the grouped genes that fall in each category. For clusters with two categories listed, the genes in the table were from the category with the highest count number within each cluster and the third column indicates whether each gene fall into the second category. * refers to that specific gene that also appeared in the second category.

Appendix 7: Knockdown of c-Jun and JunB by siRNAs

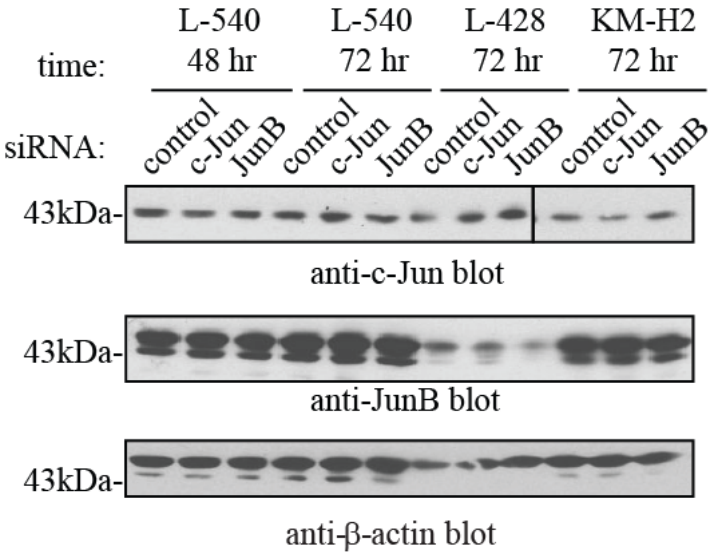

Appendix 7 – Knockdown of c-Jun and JunB with siRNAs

Western blots showing the degree of c-Jun and JunB silencing in three cHL cell lines transfected with a control and pooled c-Jun or JunB siRNAs using electroporation. Lysates were collected either 48 or 72 hours post transfection and is indicated on top of the blots. Molecular mass markers are indicated on the left of blots. The anti-β-actin blot serves as a loading control. Note: L-428 refers to L-428 (Amin) cells and the data in this figure represents at least two separate transfection experiments.